Preparation and Characterisation of Ionic Liquids and Investigations into their Potential use in the Absorption and Sequestration of Carbon Dioxide

A thesis submitted to the National University of Ireland in fulfillment of

the requirements for the degree of

Doctor of Philosophy

By

Wayne Daniel Fogarty, B.Sc.

NUI MAYNOOTH

Ollscoil na hÉireann Má Nuad

Department of Chemistry,
Faculty of Science and Engineering,
National University of Ireland Maynooth,
Maynooth,
Co. Kildare,
Ireland.

September 2013

Research Supervisors: Prof. Carmel Breslin and Dr. Denise Rooney

Head of Department: Dr. John Stephens

Table of Contents

Chapter 3:

Synthesis and Characterisation of Imidazolium Ionic Liquids

Chapter 4:

Synthesis and Characterisation of Phosphonium Ionic Liquids

Chapter 6:

Future Work

Appendix

Declaration of Authorship

I hereby certify that this thesis has not been submitted before, in whole or in part, to this or any other university for any degree and is, except where stated, the original work of the author.

Signed: _____ Date: _____

Wayne Daniel Fogarty, B.Sc.

Acknowledgments

Firstly I would like to thank my supervisors Prof. Carmel Breslin and Dr. Denise Rooney for their help and guidance over the last 4 years. They have been an absolute pleasure to work with and I am grateful that I was afforded the opportunity. In particular I would like to thank Denise for her patience, friendship, and advice without which I am sure this thesis wouldn't exist. A special thanks must also be given to Dr. Teresa Curtin in the University of Limerick and her two postgraduate students David Madden and Emma Daniels for allowing me use of their CO_2 absorption rig and the hours of training and company while there.

I would like to extend my sincere gratitude to both the current and former heads of the Chemistry Deapartment at NUI Maynooth, Dr John Stephens and Prof. John Lowry, as well as the chemistry department itself for providing both the opportunity and the facilities for this research could be conducted. Thanks must also be given to all the technical staff Ollie, MaryAnne, Barbara, Ria, Orla, Ken, Niamh, Donna, Anne, Carol, and Noel for their help during this time. I would also like to thank the EPA for financial assistance for the project

I could not write an acknowledgments section without thanking all the postgraduate student and postdoctoral staff (both past and present) in the Chemistry department for the great nights out and banter we have shared. In particular I would like to thank Louise for the endless cups of tea, chats, and for making me laugh due to her being the most easily frightened person in the country with the most hilarious screams, Orla for the house visits and movie nights, Laura for being as she would put it "awesome", and Emer for keeping me company during the morning coffees and keeping it real. The lads Pauraic and Dean must also be mentioned for the nights out in Maynooth, problem solving in work, and late night craic in the lab. Our trip to Alton towers was one of the highlights of the last 4 years and I am sure that with all of you I have a friend for life.

Away from the lab a mention must also be given to Mike, Clive, Laura B, and my oldest friend Marian for the many nights out, craic, and general wildness in Galway and Maynooth, which were at times a welcome distraction from the stress of the lab. A special thanks must also be given to Stephen (A.K.A Louis) for always giving me a laugh with the countless impersonations, bad jokes, and takeaway nights.

Finally, I would like to thank my family for all their support; Erica, Patrick, Stacey, and Shonagh, and in particular my parents Patrick and Jacqueline. It is because of their sacrifices, hardwork, love, and encouragement that I have made it to this point and although words of thanks may not do it justice, I will be forever grateful to them.

Dedication

Hannah Fogarty

Gone but never forgotten

I dedicate this to you

Thank You

Abbreviations

AAIL = amino acid ionic liquid

AMP = 2-amino-2-methyl-1-propanol

APMIM = 1-(3-aminopropyl)-3-methylimidazolium

Ar = Argon

ATR = Attenuated Total Reflection

BET = Brunauer–Emmett–Teller

BJH = Barrett-Joyner-Halenda

BMIM = 1-butyl-3-methylimidazolium

$CDCl_3$ = deuterated chloroform

COSY = correlation spectroscopy

d = doublet

DCA = dicyanamide

DEPT = Distortionless Enhancement by Polarisation Transfer

DMF = dimethylformamide

DMSO = dimethyl sulfoxide

DSC = Differential Scanning Calorimetry

dt = doublet of triplets

EDX = Energy Dispersive X-ray

EMIM = 1-ethyl-3-methylimidazolium

Endo = endothermic

ESI = electrospray ionisation

EtOH = ethanol

Exo = exothermic

GC = glassy carbon

HPLC = high performance liquid chromatography

h = hours

HSQC = Heteronuclear Single Quatum Coherence

IL = ionic liquid

IR = infra-red

J = coupling constant

m =multiplet

MEA = monoethanolamine

MeI = iodomethane

MeOH = methanol

NHE = Normal Hydrogen Electrode

NMR = Nuclear Magnetic Resonance

PEG = poyl(ethylene glycol)

PEI = polyethyleneimine

PES = polyethersulfone

ppm = parts per million

ppmv = parts per million volume

Pt = Platinum

pt = pseudo triplet

PTFE = poly(tetrafluorine ethylene)

PVDF = polyvinyldiene fluoride

q = quartet

rt = room temperature

RTIL = Room Temperature Ionic Liquid

s = singlet

SEM = Scanning Electron Microscopy

SILM = Supported Ionic Liquid Membrane

STP = Standard Temperature Pressure

t = time

t = triplet

Tf_2N^- = bis(triflimide)

TFA^- = trifluoroacetate

$TFMS^-$ = trifluoromethanesulfonate

T_g = glass transition temperature

TGA = Thermogravrimetric analysis

TGA-MS = Thermogravrimetric analysis – Mass Spectrometry

THF = tetrahydrofuran

T_m = melting point temperature

T_{onset} = onset of decomposition temperature

v/v = volume per volume

w/v = weight per volume

w/w = weight per weight

Abstract

The first area of the research presented in this thesis pertains to the synthesis and characterisation of novel ionic liquids. Three distinct categories of ionic liquids were synthesised, two of which are imidazolium based, with the latter category based on the phosphonium cations. The first category consist of cations which contain two *N*-heterocyclic rings and these are combined with a range of conventional anions such as bis(triflimide) and dicyanamide. The second category utilise the same cations but have amino acids as the anion in their carboxylate form, introducing NH_2 functionality into the ionic liquids and as such can be used in CO_2 absorption investigations. The last category of ionic liquids, are those which contain a phosphonium cation (trioctyl) quaternised with a number of groups containing different functionalities for different potential applications. In particular a pyrrole functionalised quaternary phosphonium salt was successfully polymerised. The novel ionic liquids were employed in two main areas of investigation.

Imidazolium ionic liquids containing conventional anions were immobilised onto a polymeric support, after which gases which are found in flue gas systems such as CO_2 and N_2, are passed through the membrane. The gases pass through at different rates due to the differing affinity of the liquids for the individual gases and as such separation of the gases is possible. These preliminary comparative permeability studies were confined to the first category of ionic liquids due to their lower viscosity and previous literature precedent of these anion types being used for these systems. Both single and binary ionic liquid systems were examined throughout the course of the investigation with the binary systems exhibiting some benefits in CO_2/N_2 selectivity.

Amino acid ionic liquids were immobilised onto a mesoporous silica (MCM-41) and their CO_2 absorption capability was investigated. These contained NH_2 functionality and as such are capable of CO_2 absorption through the formation of a carbamate species. The low volatility of the ionic liquids compared to amines, such as monoethanolamine (MEA), which are currently used in CO_2 gas capture technologies, make them an attractive area of research. A preliminary operational evaluation was conducted to examine anionic and cationic effects, as well as temperature and ionic liquid content of the impregnated MCM-41 silica.

Chapter 1:

Introduction

1.1 Climate change and global warming

Since the industrial revolution the human population has become heavily dependent on burning fossil fuels to provide our energy demands. However, one of the consequences of this is that atmospheric CO_2 levels have increased from pre-industrial revolution levels of 280 ppm to over 385 ppm.[1] It is argued that this increase in CO_2 levels has resulted in a 'greenhouse effect' and contributed to the observed average global temperature increase of 0.6 ^oC since the start of the 20th century.[1] The 'greenhouse effect' proposes that increased CO_2 levels result in excess heat being unable to escape the Earth's atmosphere, which is then reflected back towards the Earth's surface, resulting in an overall warming effect. The increase in the global temperature is a significant environmental problem and has resulted in damage to some of Earth's natural habitats due to melting of the ice caps and both the warming and rising of sea levels.[2] Governments are now aware of the potential threat society faces as a consequence of climate change, and this is evident by the enforcement of the Kyoto Protocol in 2005. This protocol is an international agreement, linked to the United Nations Framework Convention on Climate Change, which commits the participating countries to meet emission reduction targets. Due to the introduction of greener energy production on a mass scale still being in its infancy, mankind's dependence on fossils fuels seems unlikely to cease in the foreseeable future. Therefore in order for industrial countries to reduce their CO_2 emissions it is necessary to develop technologies which enable us to use fossil fuels in a way which either reduces or traps their emissions. Various approaches are currently being investigated, ranging from pre-combustion, oxy fuels, to post combustion based techniques.[3-5] Much attention has been focused on post-combustion based technology with the development of cheap, reusable and efficient systems, with the aim of trapping and separating CO_2 from other flue gases before being emitted from flues.[6-11] Many of these technologies can be integrated around pre-existing infrastructure with ease and in some cases not too much expense.[7]

1.2 CO_2 capture technologies

CO_2 capture technologies are based on two processes; 1) chemisorption i.e the material forms a covalent bond with the CO_2 or 2) the CO_2 forms non covalent interactions with the material and either dissolves in a liquid absorbent or is physisorbed on a solid adsorbent.[7,12,13]

1.2.1 Amine CO_2 absorbents

One of the most researched methods of CO_2 capture is the use of molecular solvents displaying amine functionality and these systems are already being utilized in industry. Amine CO_2 absorbents are an example of a chemisorption system. The chemical reaction involves one mole of CO_2 reacting with two moles of amine to form a carbamate and a quaternary ammonium ion as shown in Scheme 1.1.

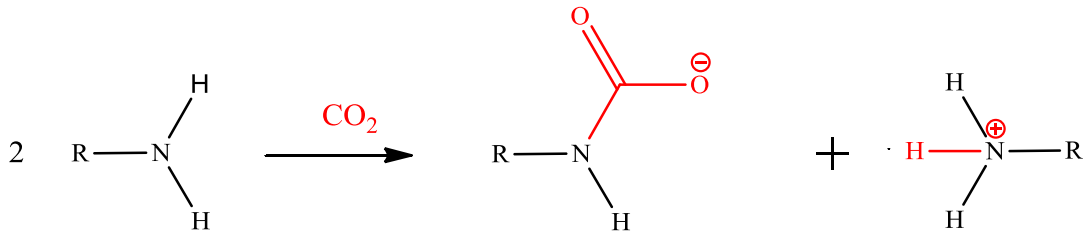

Scheme 1.1: The role of amine functionality in the chemical absorption of CO_2.

Amines have attracted much attention in this area due to their ability to selectively absorb CO_2 from most other flue gases.[14-16] Apart from this, they also exhibit low hydrocarbon solubility, high reactivity with CO_2, and are relatively inexpensive.[7] The most popular amine of choice is monoethanolamine (MEA) due to the cost and performance of this amine in CO_2 capture via chemical absorption.[6,7,17] The two main components of an amine scrubbing system are the absorber and the stripper.[3] Typically flue gases at a temperature of about 60 ^oC are channelled toward the amine solvent in the absorber where the chemical absorption of the CO_2 to the amine occurs. Then in the regenerator the amine solvent is heated to release the absorbed CO_2 where it is released in a concentrated form and stored. A schematic diagram of an amine scrubbing system is illustrated in Figure 1.1.

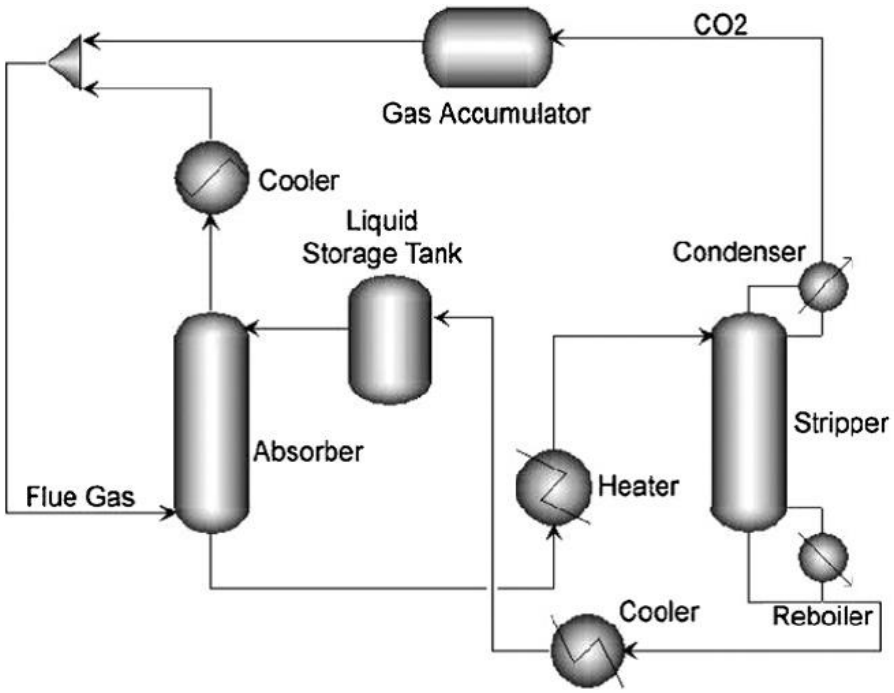

Figure 1.1: Illustration of typical amine scrubber plant for CO_2 capture.[18]

There are several problems with using amines, such as MEA, as CO_2 capture solvents. These include (a) high vapour pressure resulting in evaporation of solvent so there is a need to replenish amine stocks over time, (b) these amine systems require large energy inputs to remove the chemically absorbed species due to the stability of the carbamate species and as such can be an energy sinkhole with temperature of 100 - 140 ^oC required, and (c) the corrosive nature of these amine based solvents.[19-23] Much work has been completed on designing amines that require much less energy to regenerate them. One approach being sterically hindered amines such as 2-amino-2-methyl-1-propanol (AMP) which forms a less stable carbamate with CO_2 than MEA due to its bulkier groups.[16,24] This allows for the CO_2 to be desorbed at lower temperatures resulting in lower operational cost due to the lower energy requirements of the system.[20-23]

1.2.2 Ammonia CO_2 absorbents

Wet ammonia (NH_3) based scrubbing technology is similar to the amine technology mentioned above, both heavily relying on chemical absorption.[17] NH_3 may prove to be a wise choice due to its ability to also remove NO_x from flue gases.[25] There are two accepted routes by which the ammonia reacts with CO_2 which are described in Equation 1.1 and 1.2.[17]

$$2NH_{3\,(l)} + CO_{2\,(g)} + H_2O_{(l)} \rightleftharpoons (NH_4)_2CO_{3\,(s)} \qquad \text{(Equation 1.1)}$$

$$NH_{3\,(l)} + CO_{2\,(g)} + H_2O_{\,(l)} \rightleftharpoons NH_4HCO_{3\,(s)} \qquad \text{(Equation 1.2)}$$

Ammonia based scrubbers differ from conventional amine based systems in that they are not based on neat solvents. Ammonia concentration has been shown to have a large effect on the ability of the solution to absorb CO_2.[26] Diao *et al.* state that CO_2 capacity of the scrubber solvent decreases from 1.20 kg CO_2/ kg NH_3 at 7% (w/w) to 0.85 kg CO_2/ kg NH_3 at 35% (w/w).[26] One of the drawbacks of this system is the need for large amounts of solution to efficiently trap CO_2 from flue gases. Further significant disadvantages of the ammonia based system are the loss of the ammonia at elevated temperature and also the potential explosive results of the reaction between dry ammonia and CO_2.[25] Due to the operating temperature, (the temperature window is 20 - 30 ^oC), it is essential that flue gases be cooled from their current temperatures of 60 ^oC.[27] This requires more energy due to a cooling unit, making the NH_3 sorbents less energy efficient than their amine based counterparts.

1.2.3 Mesoporous silica CO_2 sorbents

A mesoporous silica is a type of silica synthesised from tetraethylorthosilicate using a template, and the first evidence of mesoporous silica originates as far back as 1970.[28] The result is a crystalline silica with nano size pores (pore diameter 2-50 nm), which are arranged in a uniform pattern, and have been used in a wide range of purposes such as catalysis, drug delivery and as sorbent materials for CO_2 gas.[29-37] There are several types of these mesoporous materials available with varying pores size, pore volume, and surface area. The most popular of these mesoporous materials are hexagonal structured MCM-41 (Mobil Composite of Matter 41 discovered in 1992), cubic structured MCM-48, and SBA-15 (Santa Barbara Amphorous 15), the latter, a silica also discovered by Mobil scientists in 1998 which contain much larger pore sizes (up to 30 nm) than its MCM-41 counterpart.[32,37-40] While these materials help address some of the problems associated with using organic solvents, there are some inherent disadvantages such as high manufacturing costs, and health concerns due to the possibility of these small particles entering the respiratory system. These have resulted in progress on using these

supports as CO_2 capture materials being slow but there is promise.[29,30,33,41] These materials demonstrate high thermal stability, large surface area, and it is relatively easy to functionalise their surface for a specific task.[29,33] In addition solvents can be impregnated into the mesoporous support potentially increasing the CO_2-philicity of the support.[42]

Two approaches have been investigated with respect to modifying mesoporous silicas to make CO_2 capture materials. The first is to utilise chemical absorption by functionalising the support with amine groups using the appropriate trimethoxysilane (Scheme 1.2).[31,41] From Scheme 1.2(a) it can be seen that hydroxyl groups present on the surface of the raw silica react with the incoming 3-aminopropyltrimethoxy silane, whereby the methoxy groups act as leaving groups to form methanol and allow the amine to be grafted onto the surface.[15] Once grafted the amine groups on the functionalised silica are then able to chemically bind to CO_2 as shown in Scheme 1.2(b). These functionalised mesoporous silicas also appear to have increased thermal stability in terms of volatility than their liquid amine counterparts. For example, SBA-15 has been modified with amine based trimethoxy silanes with varying chain length (Scheme 1.2) and no loss of amine from the support was observed up to 270 ^oC, in comparison to MEA which has a boiling point of 170 ^oC.[43] These materials have also shown to be recyclable with low energy requirements to regenerate the material.[41]

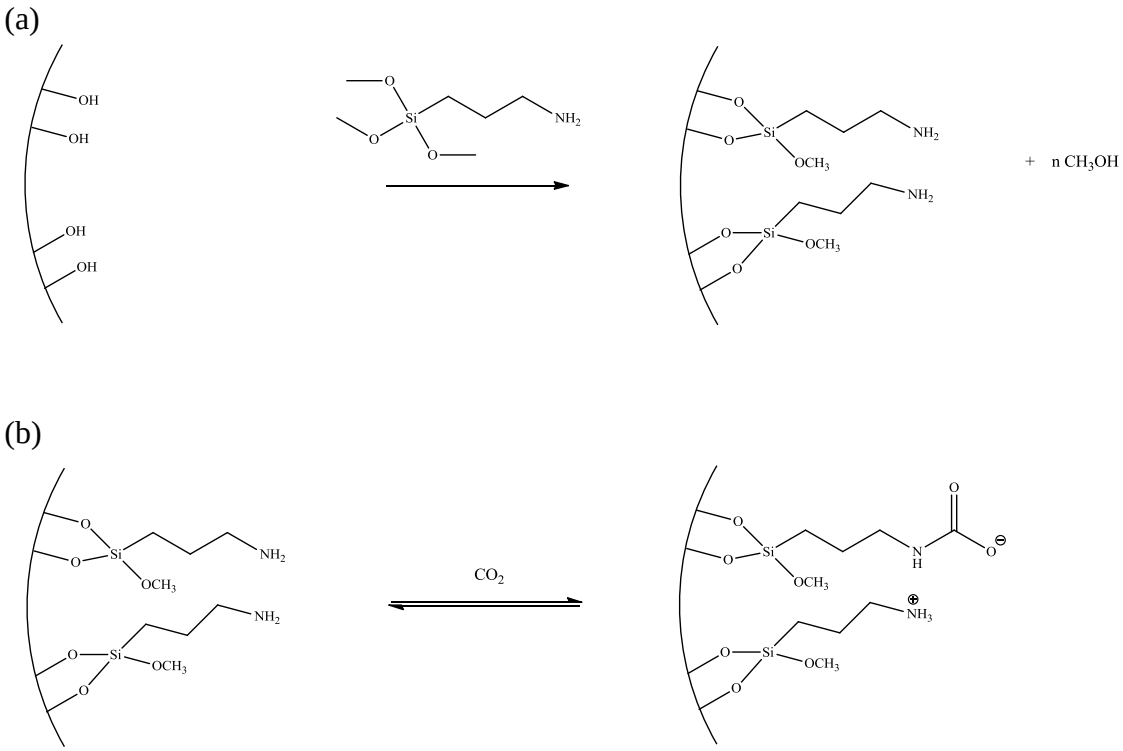

Scheme 1.2: Adsorption of CO_2 using silica modified with amine functionality.

An alternative approach to adding the amine to the support is the impregnation of the mesoporous material with an amine solvent.[29,44] Impregnation can occur via wet or dry impregnation. Wet impregnation of the amine occurs when the amine is dissolved in solvent and the mesoporous material is added and allowed to stir before the solvent is then removed to yield the impregnated material, whereas with dry impregnation no solvent is used and the amine is added directly to the mesoporous material. Wet impregnation is the preferred option due to ease of achieving a homogeneous spread of solvent throughout the support. This technique was first employed by Song *et al.* using a mesoporous silica MCM-41 impregnated with (PEI) (poly(ethyleneimine)) for CO_2 capture.[29] In this study they observed that the PEI started to decompose at lower temperatures in the support. Pure PEI had a decomposition temperature (T_{onset}) value of 150 ^oC with the PEI in the solid support exhibiting a T_{onset} value of 125 ^oC. However, at elevated temperatures, it was observed that the pure PEI had completely decomposed in comparison to that in the MCM-41 where 50% of the PEI remained. In addition, the solid support was shown to have a beneficial effect on CO_2 absorption capabilities of the PEI, obtaining a CO_2 adsorption capacity value of 112 mg/g adsorbent at 50% loading, a value higher than that shown for pure PEI (9 mg/g adsorbent).[29]

Later work completed on PEI with mesoporous silica also showed that increasing temperatures could have a beneficial effect on CO_2 uptake.[44] This study showed that low molecular weight (LMW) PEI/silica absorbed 116 mg/g adsorbent at room temperature and this increased to 166 mg/g adsorbent at 100 ^oC with an amine loading of 50%.[44] The researchers attributed the effect of higher temperature to a decrease in viscosity of the amine, resulting in greater access of CO_2 to the amine sites for chemical absorption. It was also noted in the same report that higher CO_2 absorption values were recorded with increased amine content up to a certain loading after which a decrease in CO_2 absorption was recorded. For example, at 70 ^oC a 50% loading of PEI on the silica resulted in 140 mg/g of CO_2 being absorbed whereas this value dropped to 135 mg/g at a 70% loading. It was proposed that at the higher amine loadings, the pores of the mesoporous material become blocked which restricts the movement of the incoming gas, rendering some amine sites inaccessible so that the material behaved more like bulk PEI.[44]

1.2.4 Zeolite CO_2 adsorbents

Zeolites are another example of mesoporous materials that have been of particular interest in the area of gas capture and separation technology.[11,13,45] Zeolites are composed of silicon atoms that are connected in a tetrahedral geometry to four other silicon or aluminium atoms through oxygen bonds.[11] The incorporation of aluminium into the framework results in negative charges on the zeolite, which are balanced by the presence of cations usually metal ions.[46] X and Y zeolites are some of the most widely investigated zeolites in the area of gas capture. X zeolites contain more aluminium atoms in their framework than Y zeolites and as such can contain a larger number of cations in the structure.[46] The charged areas of the X and Y zeolites are mainly confined to 3 areas of the mesoporous structure; 1) the sodalite cage, 2) the hexagonal ring inside the cage, and 3) the entrance of the supercage which are illustrated in Figure 1.2.[46]

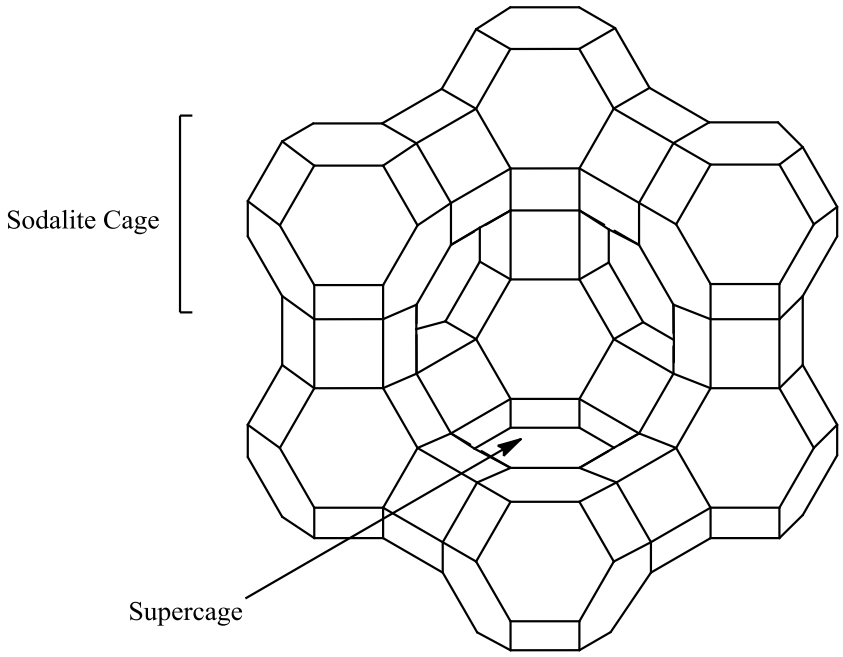

Figure 1.2: Illustration of the mesoporous structure of Zeolites

The mechanism of adsorption of CO_2 in zeolites is through electrostatic interactions. Studies on Group 1 metal zeolites have demonstrated that adsorption of the CO_2 occurs in two ways. The first occurs when CO_2 adsorbs to the metal ion by a ion-dipole interaction.[47] The second is an interaction whereby the CO_2 coordinates to either the Si or Al, and a metal cation.[48] This bi-coordination results in a much stronger interaction than that of the CO_2 to a single metal cation and thus pushes up regeneration temperatures, which is one of the main disadvantages of zeolites as CO_2 sorbents.[49] The metal cation can have a huge influence the physical properties of the zeolite. A number of studies have shown that increases in cation size leads to a decrease in the CO_2 capture capabilities due to blockage of the pores.[46] Walton *et al*. demonstrated that for X zeolite CO_2 capacities decreased in the following cation order; $Li^+ > Na^+ > K^+ > Rb^+ > Cs^+$.[46]

1.3 CO_2 separation technologies

The use of membranes to separate CO_2 from other flue gases is an area of great interest.[19,50-52] Membrane separation technology facilitates the isolation of CO_2 from benign flue gases after which it is stored. Three main approaches to membrane separation have been utilised. Approach one utilises the pore size of the membrane which can be matched to allow the selective passage of CO_2. Approach two involves the presence of functional groups on the membrane which can interact with the CO_2,[52]

while approach three involves impregnation of a solvent into the pores of the membrane, both of which are involved in the process of separation resulting in a hybrid system.[50,53] In general metallic, ceramic and carbon fiber membranes operate on approach 1, while polymeric membranes operate on approaches two and three.[7,52,54-56]

To obtain selectivity for CO_2 from a gas mixture, a driving force must be present to push/pull the flue gas through the membrane. In most research conducted this driving force has been in the form of vacuum and the stronger the vacuum applied the greater the driving force, which can result in increased separation values.[57] A simple schematic of the process is displayed in Figure 1.3 illustrating the mixed gas present on the feed side and the desired gas on the permeate side with small traces of the less permeable gas at a given time. In order to achieve a separation, a large difference in the permeability values for the respective gases must be observed. Those which display similar permeability values are theoretically inseparable.

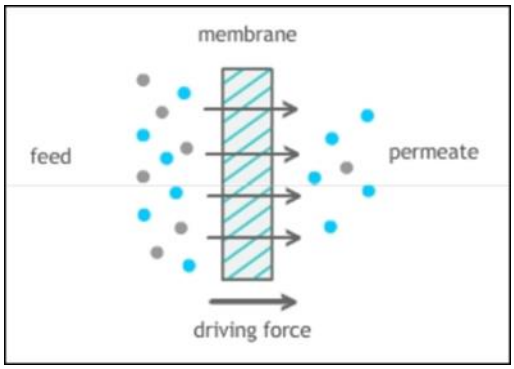

Figure 1.3: Illustration of the process by which gases behave in membrane separation technology at a given time.

As discussed above work has been performed on membranes which can selectively separate flue gases using a number of approaches. An example of a gas separation membrane system based on approach one was reported by He *et al.*[52] In this work they investigated the permeability of the different gases (H_2, CO_2, N_2, and CH_4) through a hollow carbon fibre membrane and it was observed that the permeability of the gases decreased as the kinetic diameter of the gas in question increased.[52] The following trend was observed; H_2 (2.98 Å) > CO_2 (3.30 Å) > N_2 (3.64 Å) > CH_4 (3.80 Å), indicating separation based on size. The researchers achieved a CO_2/N_2 separation of

13 at 30 °C and 15 at 50 °C.[52] An example of approach two was the use of polyimide-polyaniline membranes which contain amine functionality to achieve gas separation while research carried out by Teramoto *et al.* was based on approach three whereby polymeric membranes were impregnated with aqueous solutions of amines such as MEA and diethyleneamine to achieve CO_2/CH_4 separation.[50,58]

1.4 Combustion technologies to aid reducing CO_2 emissions

A complementary approach to the post-combustion technologies outlined in Section 1.2 and 1.3 is to alter the combustion process in order to reduce the number of types of gas emitted and so simplify the CO_2 absorption/separation processes, an example of which is Oxy-Fuel Combustion. In this combustion process the fuel is burned with nearly pure oxygen (95%) in combination with recycled flue gases.[59] It is imperative that the remaining 5% consists of recycled flue gases to prevent failure of the equipment which would result if combustion had taken place in pure oxygen due to the high temperatures that would be achieved.[60] The resulting post combustion gas is composed mainly of CO_2 with some water generated as a byproduct. This process avoids the dilution of the CO_2 with nitrogen as observed in post combustion techniques and allows the CO_2 to be easily purified and stored for future use.[61] A schematic diagram of an oxy-fuel combustion capture system is shown in Figure 1.4.

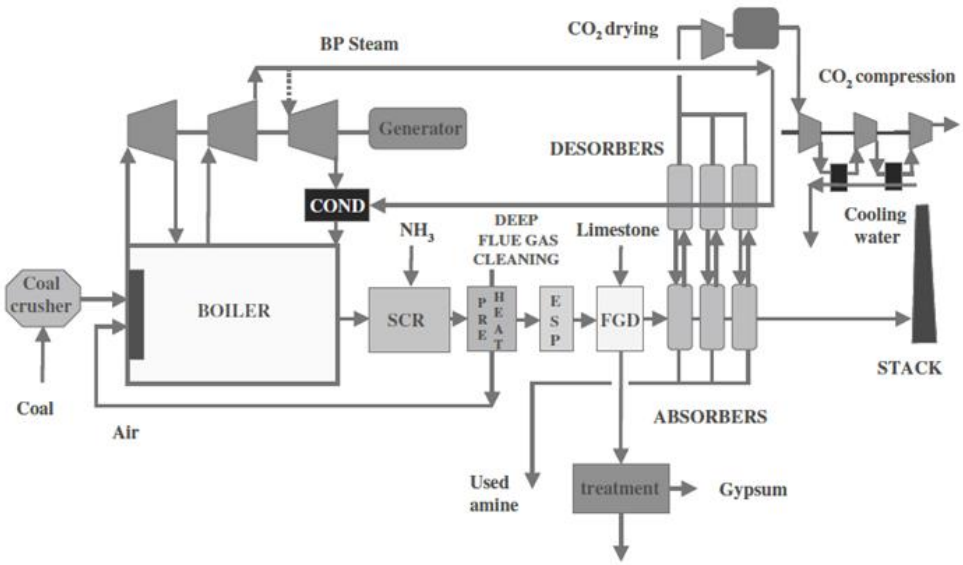

Figure 1.4: Schematic of oxy-combustion capture scheme.[61]

There are many advantages to oxy-fuel combustion systems such as high concentration of CO_2 and ease of purification of CO_2.[4] As with the post-combustion technologies mentioned previously, it would also be relatively straight forward to retrofit power plants with this technology. There is a concern that energy costs may be the downfall of oxy-fuel based technology due to the need to cool the recycled CO_2 to maintain temperature in the combustor, not to mention costs that would be incurred due to the need for large scale production of cryogenic oxygen.[62]

1.5 Introduction to ionic liquids

Currently there is a growing interest in developing ionic liquids as CO_2 absorption or separation materials due to their negligible vapour pressure and good thermal stability.[63-71] An ionic liquid is a salt composed of ions which are poorly coordinated, resulting in this class of chemical being in liquid form below 100 ^oC or in some cases at room temperature. Those that are liquid at room temperature are termed as Room Temperature Ionic Liquids (RTILs). Ionic liquids tend to consist of large, bulky, asymmetric organic cations such as *N,N*-dialkylimidazoliums, *N*-alkylpyridiniums, tetraalkylphosphoniums and anions such as halides, tetrafluroborates, and sulfonates as illustrated in Figure 1.5.[72]

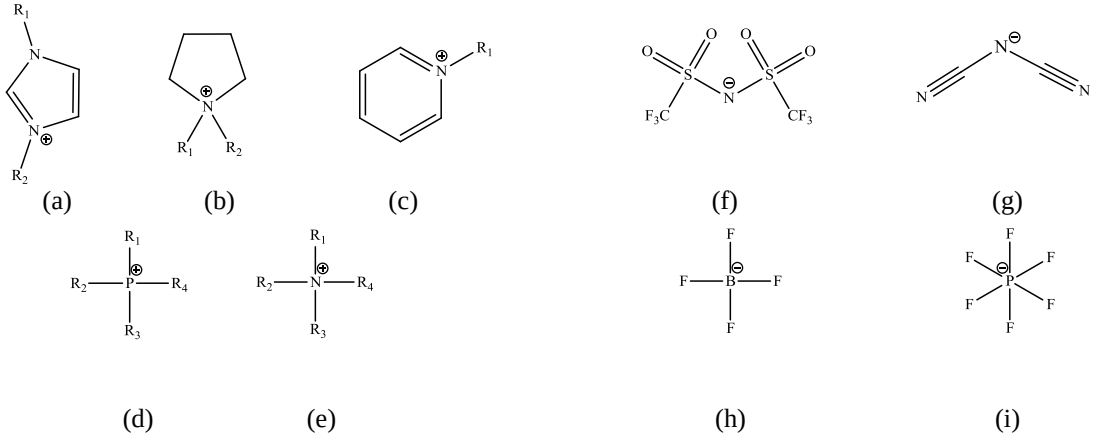

Figure 1.5: Representation of widely used cations and anions in ionic liquids: (a) *N,N*-di-alkylimidazolium, *N*-di-alkylpyrrolidinium, (c) *N*-alkylpyridinium, (d) tetra-alkylphosphonium, (e) tetra-alkylammonium, (f) bis(triflimide), (g) dicyanamide, (h) tetrafluoroborates, and (i) hexafluorophosphate

Ionic liquids were first discovered in 1914 by Paul Walden when he synthesised ethylammonium nitrate although at the time they were termed as molten salts.[73]

However, the potential of ionic liquids has only been explored over the last few decades after Wilkes and co-workers developed ionic liquids that were both air and moisture stable.[74] This has subsequently led to a huge interest in ionic liquids with a wide range of potential applications being investigated. These ionic liquids have many favourable properties such as low volatility, low toxicity, high viscosity, high ionic conductivity, low flammability, excellent thermal and chemical stability, and hydrogen bonding capability.[73,75] Ionic liquids can be divided into three sub categories: First-generation, second-generation, and third-generation ionic liquids.

First-generation ionic liquids are composed of large bulky asymmetric *N*-heterocycles chloride salts that are fused with haloaluminate(III).[74,76] These ionic liquids are highly sensitive to water and form hydroxoaluminate(III) species with the aluminium(III) chloride, resulting in decomposition of the liquid making them quite difficult to work with. The mixture of these ionic liquids with the haloaluminates generates various species depending on the ratios of the salts. This is highlighted in the reaction between 1-ethyl-3-methylimidazolium chloride [EMIM] Cl and aluminium chloride ($AlCl_3$) in Equations 1.3 - 1.5.[74,76]

$$[EMIM^+]\,Cl^- + AlCl_3 \rightleftharpoons [EMIM]^+\,[AlCl_4]^- \qquad \text{(Equation 1.3)}$$

$$[EMIM]^+\,[AlCl_4]^- + AlCl_3 \rightleftharpoons [EMIM]^+\,[Al_2Cl_7]^- \qquad \text{(Equation 1.4)}$$

$$[EMIM]^+\,[Al_2Cl_7]^- + AlCl_3 \rightleftharpoons [EMIM]^+\,[Al_3Cl_{10}]^- \qquad \text{(Equation 1.5)}$$

Second-generation ionic liquids which were first reported by Wilkes in 1992 are air and water stable and so can be used "on the bench" negating the need for a dry box and this increases their potential for use in several applications.[77] These consist of the *N*-heterocycle acting as the cation with simple inorganic and organic anions, such as tetrafluoroborates, hexafluorophosphates, and dicyanamides being the most common as shown in Figure 1.5. Although water stable, these ionic liquids due to their ionic nature do exhibit affinity towards water and are hygroscopic.

Third-generation ionic liquids are ionic liquids that feature chemical functionalities for the purpose of achieving a specific application.[8,9,78] Applications of third generation ionic liquids include metal extraction, CO_2 absorption, lubricants, solar cells and catalysts.[65,79-84] The incorporation of various functionalities of the liquids to achieve

various objectives has led to these ionic liquids being termed as "task specific" (Figure 1.6).

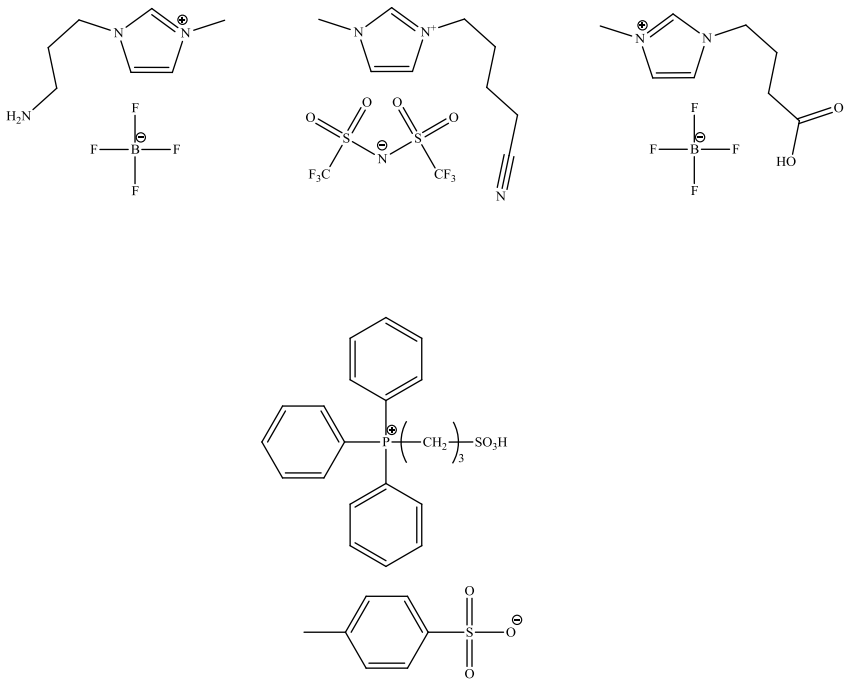

Figure 1.6: Examples of task specific ionic liquids (TSILs)

1.6 Synthesis of ionic liquids

A summary of the most common synthetic route to form second generation imidazole based ionic liquids is given in Scheme 1.1. The first step of this route is the alkylation of an imidazole moiety through the use of an alkylhalide in a molecular solvent such as ethanol, toluene or acetone.[83,85,86] This reaction proceeds via an S_N2 reaction positively charging the cation and the halide group which is a good leaving group becoming the anion. These salts are known as ionic liquid precursors, although if they melt at temperatures below 100 ^oC then they themselves are classified as ionic liquids. This synthetic route is also applicable to other ionic liquid cations such as the pyrroldinium, phosphonium, and pyridinium anions.[85,87,88]

Step 2 of Scheme 1.3 involves using these intermediate salts in a metathesis reaction, usually in water with the salt containing the desired anion. Exchange of the anion takes place resulting in the formation of an ionic liquid with the new anion and halide salt as a

byproduct. The ionic liquid precursor can be treated with an acid, which will also result in anion exchange and the formation of an acid byproduct.

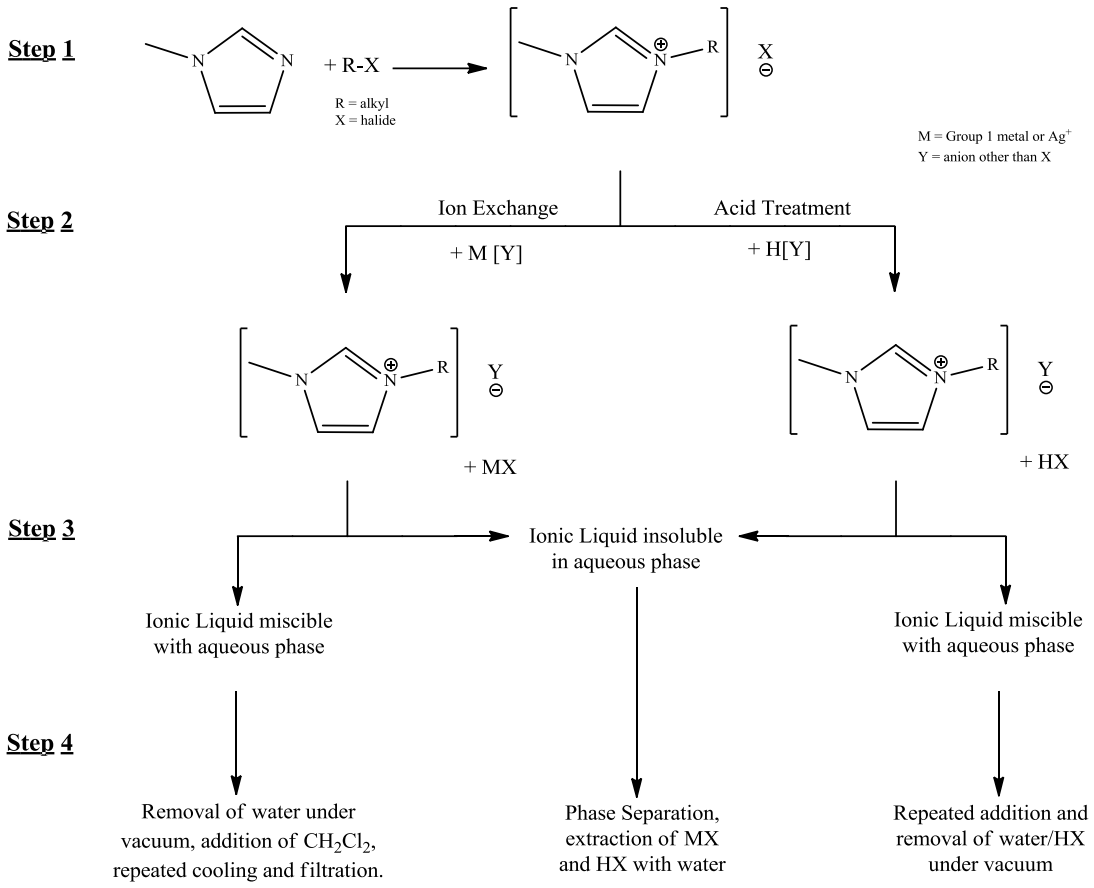

Scheme 1.3: Synthetic routes for the preparation of 2nd and 3rd generation ionic liquids.[75]

Ionic liquids can be either hydrophobic or hydrophilic, although the term hydrophobic is not entirely true as due to their ionic nature they will all absorb water. However this hydrophobicity can prove useful in terms of purification as illustrated in Step 3 of Scheme 1.3. Most of the common ionic liquid impurities such as the 1-methylimidazole precursor and sodium salts are readily water soluble and washing with water can remove these from the liquid. Those that are miscible with water must be purified via the addition of a chlorinated solvent and cooling to 0 ^{o}C to precipitate out any excess starting material or byproduct.[75] However, as demonstrated in Step 4 of Scheme 1.3, both types of ionic liquids are hygroscopic, therefore care must be taken to ensure that they remain dry.

In cases where salts which were required for the metathesis step with the desired anion are expensive or unavailable, alternative synthetic routes to those mentioned above are available. One such method involves using ion exchange resins (Scheme 1.4).[89,90] This process involves the formation of the ionic liquid halide precursor via the process described in the previous method. Once the ionic liquid precursor is formed, it is diluted down to a known concentration and passed through an OH^- functionalised ion exchange resin column. This changes the anion on the liquid to the OH^-, which is relatively unstable and so is immediately added dropwise to a solution of the desired organic acid (e.g. amino acid). The OH^- reacts with the acid resulting in deprotonation of the acid forming water as a byproduct. The conjugate base of the acid is anionic, which is then attracted to the positive charge of the imidazole derivative to form the new ionic liquid.

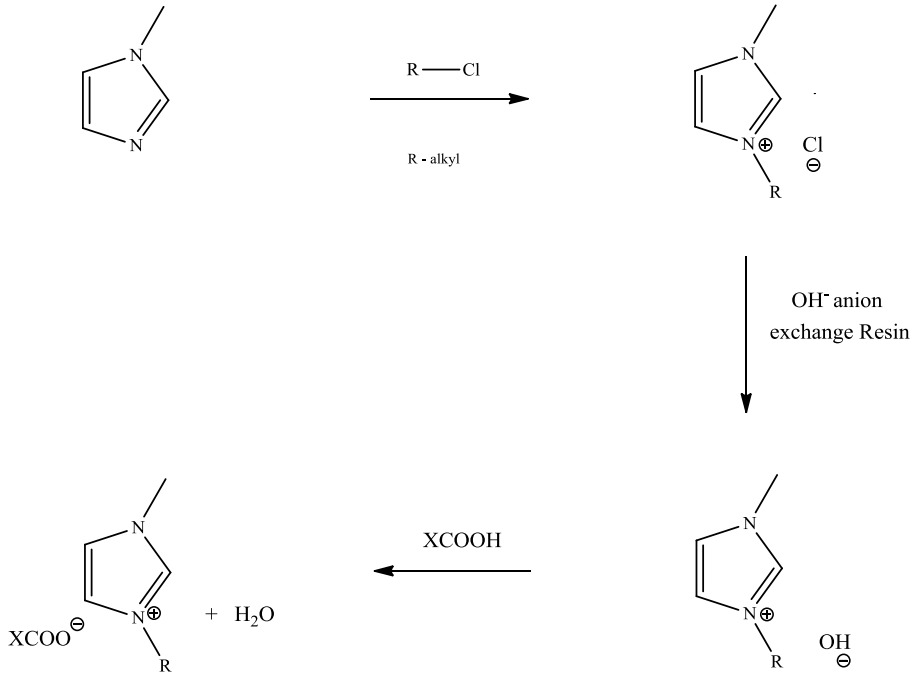

Scheme 1.4: Formation of ionic liquid using anion exchange resin.

A second alternative synthetic route involves the ionic liquids being prepared from their corresponding carbenes (Scheme 1.5).[91,92] This can only be achieved using 1,3-dialkyl imidazolium salts. The ionic liquid precursor is heated in a Kugelrohr apparatus in the presence of a base yielding the carbene which can be isolated via distillation. Addition of an acid yields ionic liquids which are effectively chloride free.

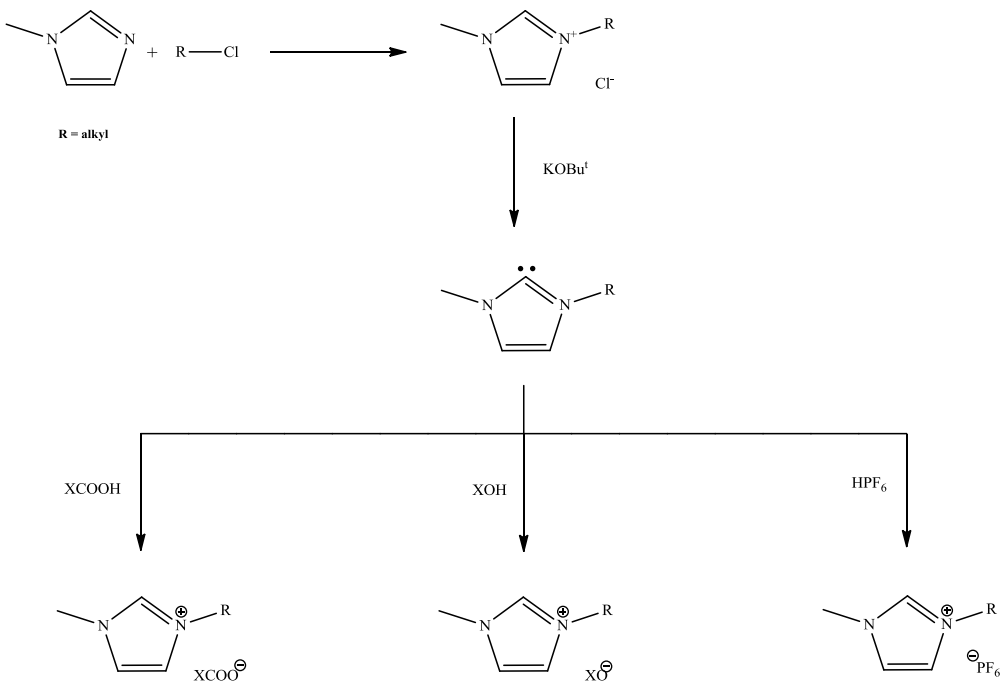

Scheme 1.5: Synthetic route of ionic liquid via carbene formation.

1.7 Melting points of ionic liquids

The nature of the crystal structure of an ionic liquid is critical for producing salts with low melting points. The Coulombic attraction or repulsion between the ions can be influenced by the ion-ion separation, the packing efficiency of the ions, and the product of the ionic charges. Coulombic interactions are not the only forces occurring in the crystalline lattice, with electron-electron and nucleus-nucleus repulsive forces between the ions also occurring.[93] These are known as the Born interactions. Taking both the Coulombic and Born interactions into account an expression can be derived to calculate the lattice energy. This is known as Born-Landé equation (Equation 1.6).[93]

$$E = \frac{-N_A M\, z^+ z^- e^2}{4\pi\varepsilon_0 r_0}\left(1 - \frac{1}{n}\right) \qquad \text{(Equation 1.6)}$$

where N_A is Avogadro's constant; M corresponds to the Madelung constant, z^+ and z^- are the ion charges, e is the elementary charge of an electron, ε_o relates to the permittivity of free space, n is the Born exponent and r_0 is the distance to the closest ion. The melting point of an ionic solid increases with increasing lattice energy.

In general, the structural features which influence the melting point of ionic liquids can be applied to the majority of cation species. However, most studies to determine factors

which control the melting points of ionic liquids focus on the imidazolium cation. As discussed in Section 1.5 ionic liquids are composed of asymmetric cations. This asymmetry prevents the ions from packing as tightly together as some of their sodium based counterparts increasing the distance (r_o) between the ions, resulting in weaker interactions between the ions. A comparison of the melting points of a series of imidazolium salts was carried out by Bonhote *et al.* in which they determined that the asymmetric cation always had a lower melting point that its symmetric analogue.[72] The difference in ionic packing is illustrated in Figure 1.7 with NaCl and an ionic liquid analogue, 1-butyl-3-methylimidazolium chloride [BMIM] Cl. Studies have shown that when anion sizes are increased the melting points of the ionic liquids decrease.[72] This is not surprising when looking at Equation 1.6 which states that the lattice energy of the salt is dependent on the distance between the charges and the Born exponent which is dependent on the size of the ion. Increasing the anion size increases the separation between z^+ and z^- which decreases the Coulombic interactions between the ions in the crystal lattice and it is this that results in the decrease of the melting points.[94,95] However, studies have stated that this explanation of ionic liquid melting points based solely on ion size must be treated with some care and is not fully sufficient in understanding the observed melting points.[96]

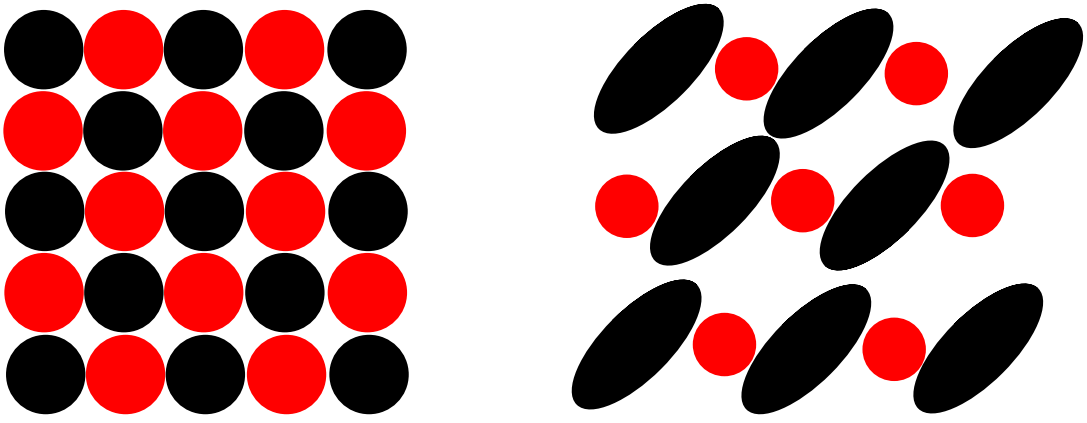

NaCl: m.p. 801 ^oC. [BMIM] Cl: m.p. 68 ^oC. [97]

Figure 1.7: Illustration of packing structure for NaCl and [BMIM] Cl.

Within a series of ionic liquids, small changes in the shape of uncharged covalent regions of ions can have an influence on melting points. For example, the length and stereochemistry of the alkyl substituents at the 1 and 3 positions of the imidazolium

cation can affect the melting point. Holbrey and Huddleston observed with the 1-alkyl-3-methylimidazolium cations, that as the chain length was increased the melting point of the ionic liquid decreased until the chain reached eight carbons in length.[64,98] This increase in melting point is generally noted when chain lengths approach n > 8, although this varies depending on the liquid in question. It is believed that this is the result of inter-chain hydrophobic packing effects. For example, it was found that using the tetrafluoroborate anion, when n = 4 a melting point of -88 ^{o}C was recorded, whereas when n = 10 the melting point was found to be approximately at room temperature.[64,98] Holbrey *et al.* illustrated the same trend using 1-alkyl-2-methylimidazolium tetrafluoroborates.[98] Upon examination of the glass transition (T_g) or the melting point (T_m) of the tetrafluoroborate liquids, they observed an initial increase when n = 2 with a T_m value of 103 ^{o}C before a sharp decrease with the n = 4 analogue having a T_g of -88 ^{o}C. When n = 6 a T_g value of -88 ^{o}C was observed before increasing again with the n = 12 analogue exhibiting a T_m of 21.4 ^{o}C.[98] Increased branching of the alkyl substituent also increases the melting points compared to its linear analogue due to changes in efficiency of the crystal packing as free rotation volume decreases and atom density increases.[95]

However, lengthening of alkyl chains does not always result in an increase in melting points. Studies on quaternary phosphonium and ammonium salts whereby the cationic charge is localised, have displayed decreasing melting points with increasing alkyl chain lengths.[99] This is due in part to the long alkyl chains shielding the cationic charge from the anionic charge interrupting hydrogen bonding, decreasing lattice energy, and also the long alkyl chains will have higher rotational degrees of freedom, preventing tight packing of the ions.

The strength of Coloumbic interactions can be reduced upon delocalisation of charges and this can also result in lower melting salts. This effect can be present in both the cation and anion.[72,100] The 1-alkyl-3-methylimidazolium based cations are the most widely used due to delocalisation of the positive charge around the *N*-heterocyclic ring, however delocalisation of charge can also occur on the anion. Scheme 1.6 below illustrates using resonance structures how the negative charge on the bis(triflimide) anion can be delocalised from the nitrogen atom through the sulfonyl groups.

Combining a 1-alkyl-3-methylimidazolium cation with this class of anion increases the likelihood that a liquid product would be formed, hence their popularity.

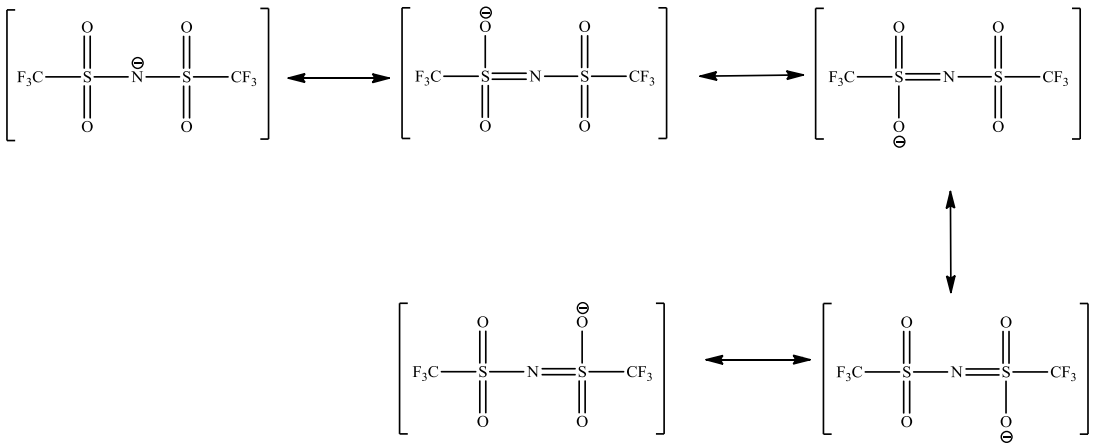

Scheme 1.6: Resonance structures of the bis(triflimide) anion.

It is well established that imidazolium based ionic liquids exhibit H-bonding between the C(2) H atom on the imidazolium ring and the anion.[91,101,102] It might be expected that by removing this H-bonding interaction through substituting an alkyl group at the C(2) position would lower the melting point but a number of researchers have observed the opposite effect.[96,72,101,103] For example, 1-ethyl-3-methylimidazolium bis(triflimide) has a melting point of -14.7 ^{o}C, while its methylated analogue, 1-ethyl-2,3-dimethylimidazolium bis(triflimide) has a melting point of 22 ^{o}C.[101] A number of theoretical studies have been carried out in an attempt to understand this phenomenon.[96,103] Hunt carried out *ab initio* calculations on gas phase ion pairs of 1-butyl-3-methylimidazolium chloride and 1-butyl-2,3-dimethylimidazolium chloride.[103] It was found that the loss in H-bonding is outweighed by a loss of entropy of the system. This occurs as there is a reduction in the number of stable ion-pair conformers as the freedom of rotation of the butyl chain is decreased due to the close proximity of the C(2) methyl group and there is now an energy preference for the anion to lie above or below the imidazolium ring instead of in front of it. Noack *at al.* carried out a study on 1-ethyl-3-methylimidazolium bis(triflimide) and 1-ethyl-2,3-dimethylimidazolium bis(triflimide) using IR, Raman and Nuclear Magnetic Resonance (NMR) spectroscopy.[101] They determined that the substitution of the H atom for a methyl group at the C(2) position of the imidazolium ring altered the electron density distribution across the cation. This altered the position and strength of the cation-anion interaction

and resulted in a more ordered, tighter packed molecular network with increased Coulombic but decreased Van der Waals interactions.

1.8 Thermal stability of ionic liquids

It is widely regarded that ionic liquids are thermally stable under high temperatures. The thermal stability of imidazolium ionic liquids is governed by the strength of the carbon-heteroatom bond and hydrogen bonding.[104] Although they are stable at elevated temperatures, prolonged use at elevated temperatures does lead to a gradual decomposition of the liquids.[105,106] When the liquids are exposed to these temperatures they are subject to pyrolysis unless no lower energy decomposition route is available. It has also been witnessed that increased substitution, in particular methylation at the C(2) position on the imidazole ring, leads to greater thermal stability of the liquids due to the removal of the acidic hydrogens.[95,107]

Work on 1,3-dialkylimidazolium halide salts have shown that they decompose via an E2 reaction.[106,108] Scheme 1.7 illustrates the pathway of decomposition of BMIM [Cl] proposed by Chan *et al*. using Thermogravimetric Analysis and Mass Spectrometry (TGA-MS). Dealkylation of the imidazole ring was observed which resulted in the formation of 1-methylimidazole, 1-butylimidazole and the corresponding alkyl halide. The alkyl halide then underwent further decomposition resulting in other alkyl halides and alkenes.

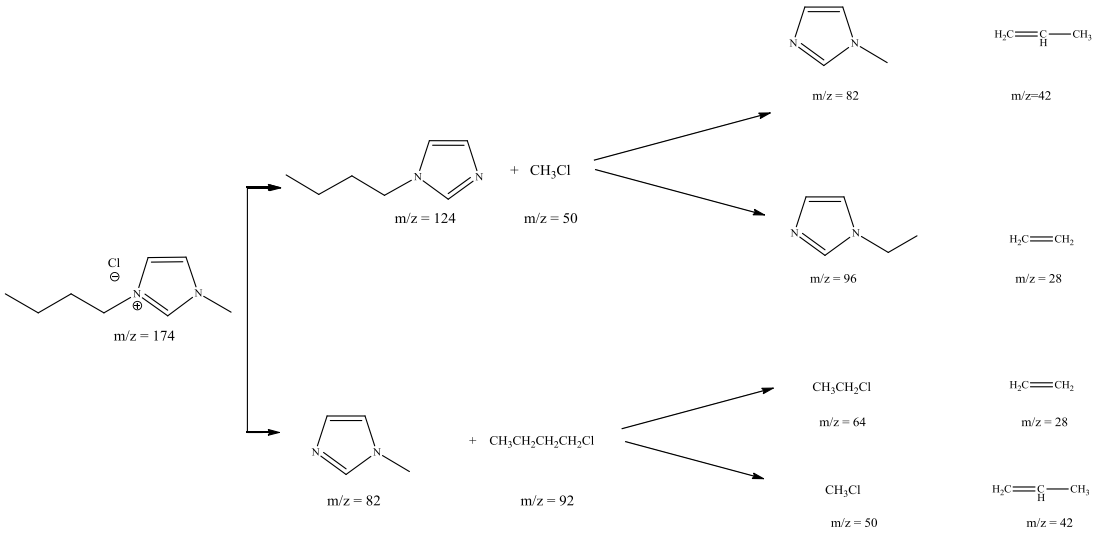

Scheme 1.7: Proposed decomposition pathway of 1-butyl-3-methylimidazolium chloride.

Alkylation of the anion followed by degradation of the cation is not the only method by which these liquids can decompose. Baranyai *et al.* studied ionic liquids with two anions, bis(trifluoromethanesulfonyl)amide and bis(methanesulfonyl)amide and examined their routes of decomposition.[109] They found that once decomposition had occurred, the non-fluorinated anion showed a similar route of decomposition to that found by Chan *et al.* indicating an reverse S_N2 reaction with alkylation of the amide.[108] However, when they examined the fluorinated anion they found no alkylation of the amide could be found and results suggested alkylation of the imidazole ring occurred at the C(2) position, indicating an alternative route of decomposition. They hypothesised that this occurred as a result of the poor nucleophilicity of the anion which conferred greater stability to the ionic liquid.[109]

It has been noted that many ionic liquids often differ in appearance due to the temperature at which they were prepared.[75] In general, during synthesis it is important to keep the reaction temperature and any work-up temperatures below 80 ^oC to prevent discolouration of the salts. It has been hypothesised that this colour is a direct result of impurities due to thermal degradation although efforts to detect these by NMR and other techniques have been unsuccessful.[110]

Phosphonium salts are known to decompose via a route different to that of the imidazolium salts, yielding trialkylphosphine oxide and alkane species.[111] Typically the quaternary phosphonium salts exhibit higher decomposition temperatures than the imidazolium salts albeit this thermal stability is dependent on the choice of anion.[87,112] For example, work by Bradaric *et al.* on phosphonium ionic liquids found that TGA-MS profiles of trihexyl(tetradecyl)phosphonium tetrafluoroborates indicated a thermal stability in excess of 350 ^oC.[87] More recently work on tetradecyl(trihexyl)phosphonium bis(triflimide) ionic liquids also exhibited similar degradation products with species such as $P(CH_2)_3$ (mass 73), $P(CH_2)_4$ (mass 87), $P(CH_2CH_2)_3$ (mass 115), and $CH_2{=}P(CH_2CH_2)_3$ (mass 129) recorded by mass spectrometry indicating the degradation of these phosphonium cations to trialkylphosphine species and smaller quaternary phosphonium cations.[113] Smaller fragments (CH_3, C_2H_5, C_3H_7, C_4H_9, C_5H_{11}, C_6H_{13}, C_7H_{15} (mass 15, 29, 43, 57, 71, 85, 99)) which originated from the alkyl chains were also detected.[113]

1.9 Viscosity of ionic liquids

In general ionic liquids tend to be more viscous than molecular solvents with values more comparable to oils. This higher viscosity has been attributed to the ability of ionic liquids to hydrogen bond, Coulombic attractions, and to a lesser extent Van der Waals interactions.[72] The viscosity is governed by similar factors to those which control their melting points (Section 1.7), and it is often observed that ionic liquids which have a high melting point also have a higher viscosity.[72] Studies have shown that the viscosity of the ionic liquids is strongly dependant on the nature of the anion present, with imidazolium based ionic liquids having exhibited the following viscosity trend Tf_2N^- < $CF_3CO_2^-$ < $CF_3SO_3^-$ < BF_4^- < PF_6^- which can be explained by anion size, and cation-anion interactions (in particular hydrogen bonding).[114] The viscosity is strongly dependant on temperature, generally decreasing with increasing temperature.[115-117]

Substitution of the imidazole ring can have a large effect on the viscosity of the liquids.[72] Bonhote *et al.* examined the 1-alkyl-3-methylimidazolium cation combined with the bis(triflimide) anion which showed a viscosity of 44 mPa.s at room temperature for the methyl form, which decreased for the ethyl form, with a value of 34 mPa.s, due to greater degrees of conformational freedom for the alkyl chain and lack of symmetry.[72] Both these factors will increase the entropy of the system and reduce the close packing of the ions reducing the Coulombic attraction forces and H-bonding between the anion and cation. However the viscosity was observed to increase again for the butyl form with a value of 52 mPa.s recorded.[72] The increase in viscosity upon lengthening of the chain occurred due to increased Van der Waals interactions and increased ion size reducing its mobility. As such it is a logical extension to deduce that the highly viscous nature of long chained phosphonium ionic liquids (liked the ones synthesised as part of this current study) is a consequence of Van der Waals interactions, in combination with the long alkyl chains increasing ion size. Introducing branching into the side chain also increases viscosity. In work presented on 1-methyl-3-alkylimidazolium bis(triflimide) salts, due to reduced rotational freedom, with the isobutyl form exhibiting a viscosity reading of 84 mPa.s.[72]

It was found that methylation of the imidazole ring at the C(2) position did not have the desired effect of lowering the viscosity by disrupting hydrogen bonding. However, this

finding is consistent with the observations made on the effect alkylation of the imidazole ring at the C2 position on melting points, and is attributed to an increase in the π-π stacking and methyl - π stacking interactions present on the imidazole ring.[72] As mentioned in Section 1.7, methylation at the C2 position hinders the rotational freedom of the alkyl chains attached to the nitrogen atoms of the imidazole ring which allows for tighter packing of the anions. The tighter packing of the anions increases Coloumbic interactions, reduces the mobility of the ions and results in higher viscosity values.[101]

With ionic liquids there are many discrepancies over published viscosity values. For example, reported values determined for the viscosity of one of the most common ionic liquids 1-butyl-3-methylimidazolium tetrafluoroborate [BMIM][BF_4], differ substantially from 65.2 mPa.s to 91.4 mPa.s.[75,117] Water, organic solvents, and chloride content are the main sources of error.[75] Seddon *et al*. added known concentrations of chloride to the liquids (Table 1.1) and compared the resulting viscosities.[75] All the ionic liquids studied exhibited a notable increase in their viscosity upon increases in their chloride content. The main source of chloride impurities originated from the alkylation step (Scheme 1.3 Step 1) and as such has led the development of halide free synthesis via the use of sulfonyl ethers and the use of silver salts during metathesis to remove soluble chloride.[75]

Table 1.1: Comparison of the viscosity of chloride contaminated and low chloride content batches of ionic liquids at 20 °C.[75]

Ionic Liquid	$[Cl^-]$ / mol Kg^{-1}	η / mPa.s
[C_2mim][BF_4]	0.01	66.5
	1.8	92.4
[C_4mim][BF_4]	0.01	154
	0.5	201
[C_4mim][NO_3][a]	0.02	67
	1.7	222.7
[C_8mim][NO_3]	0.01	1238
	2.2	8465

[a] at 45 °C.

1.10 Ionic liquids applied to CO_2 capture and separation technologies

Over the last few decades RTILs have been proposed as alternative CO_2 sorbent and separation materials for industrial applications.[118] There are several factors which influence the solubility of CO_2 in ionic liquids. These include the nature of the anion, the nature of the cation, functional groups on the ionic liquid, viscosity, temperature, and gas pressure.[119-123] As for the traditional CO_2 sorbent materials outlined in Section 1.2, there are two mechanisms by which ionic liquids can absorb CO_2, physical absorption and chemical absorption.[65,83,122]

1.10.1 Ionic liquid CO_2 absorbents

1.10.1.1 Physical absorption of CO_2 in ionic liquids

In order to explain physical absorption in ionic liquids, it is important to look at the packing structure. In Section 1.7 it was stated that ionic liquids consist of large bulky organic cations that inhibit effective packing of the ions producing gaps in the structure. When gases such as CO_2, are applied to the ionic liquid at high pressure, the gas is forced into these gaps where they are held by weak non - covalent forces of attraction. Blanchard *et al.* considered this to be one of the reasons why CO_2 is so soluble in ionic liquids due to their work on supercritical CO_2 and ionic liquids where no change in the liquids volume was observed indicating that the CO_2 was present in the void inter-ion spaces.[124] This is illustrated in Figure 1.8.

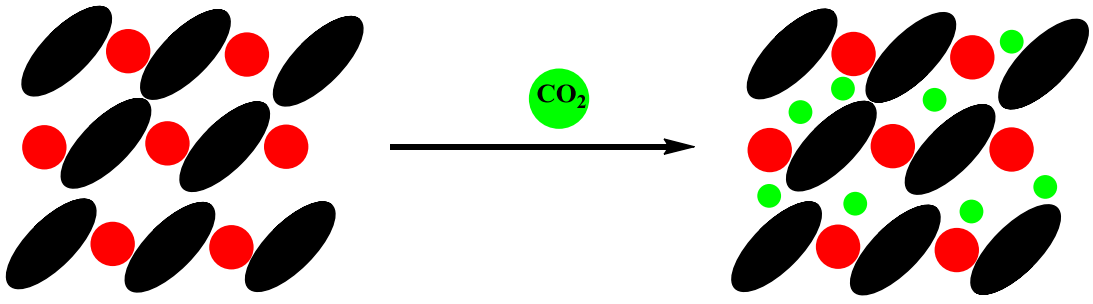

Figure 1.8: Illustration of crystal lattice structure of ionic liquids to demonstrate physical absorption of gases.

Studies of the physical absorption of CO_2 into ionic liquids have shown that the choice of anion appears to be one of the major contributors to the CO_2-philicity of ionic

liquids, and this has been demonstrated using experimental, spectroscopic, and simulation methods.[125,126] Kazarian *et al.* used ATR-IR spectroscopy to examine CO_2 dissolved in two ionic liquids [BMIM]BF_4 and [BMIM]PF_6.[126] They observed that the band rising from the bending mode of CO_2, was split into a doublet. Moreover, the degree of splitting of the band was notably different between the two samples. Earlier work completed by the same research group using Lewis bases and CO_2 demonstrated that the interaction between the two did result in splitting of the IR band arising from the CO_2 bending mode.[127] Therefore they proposed that the BF_4^- and PF_6^- anions can act as weak Lewis bases. Moreover, they hypothesised that the two ions were interacting with the CO_2 in a similar manner, with the extent of the splitting of the CO_2 IR bend band indicated the strength of these interactions.

Solubility measurement of CO_2 in ionic liquids also demonstrates the importance of anion selection for absorption studies. Solubility studies based on the [BMIM] cation with a variety of anions showed that the CO_2 uptake of the liquids under identical conditions increases in the following order; $[NO_3^-] < [DCA^-] < [BF_4^-] < [PF_6^-] < [TfO^-] < [Tf_2N^-] <$ [methide].[119,123] From this trend it can be seen that the ionic liquids containing the $[Tf_2N^-]$ and [Methide] anions exhibit the highest CO_2 solubility. The sulfonyl moieties present on these anions have been shown using theoretical calculations to undergo weak Lewis acid-Lewis base interactions with CO_2 increasing the CO_2-philicity of the ionic liquids.[128] Fluorination of the anion has also shown to strongly increase the affinity for CO_2, although the mechanism on how this aids CO_2 absorption is not fully understood. Pringle *et al.* conducted a direct investigation into the effect of fluorination of the anion of the ionic liquid on CO_2 solubility using 1-ethyl-3-methylimidazolium bis(triflimide) ionic liquid and its non-fluorinated counterpart bis(methanesulfonyl)imide.[129] It was found that the fluorinated liquid had significantly higher affinity for CO_2.

The nature of the cation was also determined to have an effect on CO_2 solubility in the ionic liquid through variation in the aliphatic chain length on a 1-alkyl-3-methylimidazolium cation combined with the bis(triflimide) anion.[123] It was observed with the three different cations where the alkyl varied from the butyl, hexyl, to the octyl form, that an increase in CO_2 solubility resulted with increased chain length. Moreover,

the effect of fluorination is not limited to the anion with several papers reporting increased CO_2 solubility with increase in the degree of fluorination of the alkyl chains of the cation.[130,131]

1.10.1.2 Chemical absorption of CO_2 in ionic liquids

As mentioned previously there is a second potential mode of CO_2 absorption in ionic liquids. Chemical absorption is dependent on the presence of reactive functional groups in the ionic liquid, particularly primary amine groups. This is the same principle behind the current amine carbon dioxide capture technologies as outlined in Section 1.2.1. When an amine site is exposed to CO_2 it covalently attaches on to the amine adopting a negative charge on the oxygen. To accommodate the newly formed N-C bond, deprotonation of the amine occurs and binds to the amine side on a second molecule of the ionic liquid, thus balancing the negative charge on the carbamate.[42,65] The mechanism is demonstrated in Scheme 1.8 underneath.

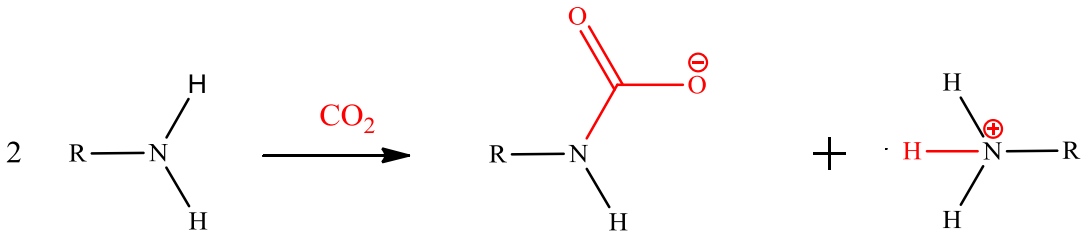

Scheme 1.8: Schematic of the role of amine functionality in the chemical absorption of CO_2.

Amino acid ionic liquids have been synthesised via protonation to form a cation or deprotonation to form an anion.[68,83,86,132-135] These ionic liquids are of particular interest as CO_2 sorbent materials when the amino acid is incorporated due to the presence of the free primary amine and the ease with which these can be incorporated. Some investigations have been carried out using the simple 1,3-dialkylimidazolium and quarternary phosphonium cations (Figure 1.9).[68,136] In work by Zhang *et al.* it was demonstrated that these amino acid anions in conjunction with a tetrabutylphosphonium cation resulted in CO_2 absorption in a 2:1 molar ratio between the ionic liquid and the CO_2 gas.[68] This ratio was further improved to achieve a 1:1 molar ratio between the CO_2 and the ionic liquid which contained the amino acid anions and 3-

aminopropyl(tributyl)phosphonium cation due to the presence of primary amines on both the cation and anion, both of which can be involved in the reaction between the ionic liquid and CO_2.[83]

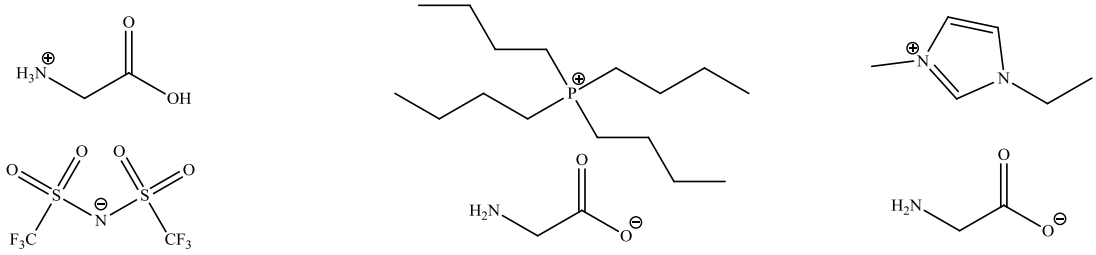

Figure 1.9 Examples of amino acid ionic liquids investigated as CO_2 sorbents.

Although these ionic liquids have the advantage of containing primary amine functionality, which as discussed previously can chemically absorb CO_2, one major disadvantage of these liquids is their high viscosity.[86,89,133] To counteract this problem, work has been conducted using mesoporous materials which have been impregnated with these ionic liquids. These mesoporous materials have high surface areas which the ionic liquids coat and result in an increase in amine sites accessible to the CO_2 gas, increasing absorption of the gas.[68]

1.10.1.3 Optimisation of physical and chemical absorption of CO_2 in ionic liquids

The operation environment can have a huge effect on the CO_2 solubility of the ionic liquids with parameters such as temperature and pressure highly influential on their capabilities. Upon investigations carried out by many research groups, increasing temperatures result in decreasing solubility/absorption of CO_2 in the majority of ionic liquids.[137,138] Research has also shown that increased pressure results in increased absorption of CO_2 in ionic liquids.[69,139,140] Sanchez *et al.* observed that the levels of CO_2 absorbed, were directly proportional to the increase in pressure.[69] This was noted using the ionic liquid 1-(3-aminopropyl)-3-methylimidazolium dicyanamide where the CO_2 molar fraction increased from 0.14 at 0.1 MPa to 0.27 at 1.0 MPa.[69] At increased pressure the CO_2 is forced into the spaces between the ions much more effectively resulting in a higher physical absorption capacity of the ionic liquids.

1.10.2 Separation of CO_2 from flue gases using ionic liquids

1.10.2.1 Impregnated polymer membranes

As discussed in Section 1.3, amines had been impregnated into polymeric membrane with the aim of separating various flue gases from one another. Due to the rising interest in ionic liquids in the gas capture area, they have also been extensively studied in conjunction with membrane technology and have been termed as supported ionic liquid membranes (SILMs). These liquids are impregnated into the pores of polymer membranes such as polyethersulfone (PES), nylon, and poly(vinyldiene fluoride) (PVDF), and play an active role in the separation process with CO_2/N_2 selectivity values reaching up to 57.[66,141] These SILMs have also displayed long lifecycles, attributed to the low vapour pressure of the ionic liquids minimising solvent loss. In general, work on these ionic liquids for separation technology has focused on those containing the BMIM and EMIM cations and anions such as hexafluorophosphates, bis(triflimide) and tetrafluoroborates.[66,142,143]

In addition to the work outlined previously involving simple cations, several liquids, all of which contain different functional groups have been impregnated into polymer membranes in an attempt to enhance selectivity of CO_2 over other gases.[8,9,144,145] A study was carried out on PES membranes which were impregnated with ionic liquids outlined in Figure 1.10.[8] It was observed that using the oligo(ethylene glycol) functionalised ionic liquids (Figure 1.10), increased CO_2/N_2 and CO_2/CH_4 selectivities were achieved in comparison to their alkyl analogues. For example, with CO_2/N_2 and CO_2/CH_4 selectivity values of 23 and 11 respectively, were determined for BMIM Tf_2N in comparison to 1-(2-methoxy)ethyl-3-methylimidazolium bis(triflimide) which achieved values of 30 and 13 respectively.[8]

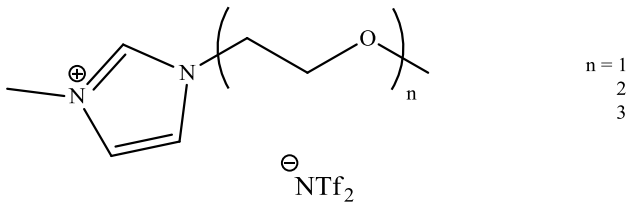

Figure 1.10: Representative structure of oligo(ethylene glycol) ionic liquids used in gas separation technology.

1.10.2.2 Poly(ionic liquid) membranes

An extension of work discussed in Section 1.10.2.1 is the incorporation of polymeric groups into the ionic liquids structure for the purpose of gas sequestration studies.[146,147] Bara *et al.* have synthesised styrene/imidazolium monomers (Figure 1.11(a)) which were polymerised to form polymeric membranes which achieved a CO_2/N_2 and CO_2/CH_4, of 28 and 32 respectively.[148] In a further study by Bara *et al.* they compared these nitrile poly(ionic liquid) membranes to oligo(ethylene glycol) poly(ionic liquids) membranes (monomers of which shown in Figure 1.11(b)).[70] Values for CO_2/N_2 and CO_2/CH_4 values for the two types of polymers were similar with the polymer containing the 3-cyanobutyl group achieving CO_2/N_2 and CO_2/CH_4 selectivity values of 41 and 33 respectively, while that containing the 1-(2-methoxy)ethyl linkage achieved values of 37 and 37 respectively. These selectivity values are approximately 50% higher than values achieved with poly(ionic liquids) containing alkyl chains of the corresponding length indicating that both the nitrile and the ether molecules have a high affinity for CO_2.[146] However, although achieving good selectivity both groups appear to decrease CO_2 permeability through the membrane due to the polarity of the groups.[8]

(a)

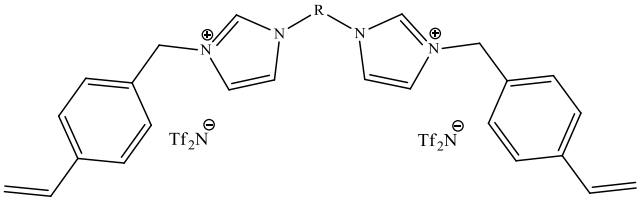

R = -((CH2)6)-
= -((CH2)2O(CH2)2)-
= -((CH2)2O)2(CH2)2)-

(b)

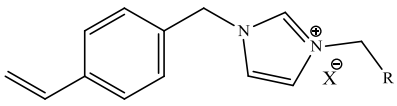

R = C3H6CN
= C5H10CN
= (CH2)OCH3
= ((CH2)2O)2CH3
X = Tf2N

Figure 1.11(a) and (b): Ionic liquids monomer containing styrene polymerisable groups.

1.10.2.3 Ionic Liquid – Poly(ionic liquid) membranes

More recent work has focused on the use of poly(ionic liquid) ionic liquid composites to help improve permeability and selectivity of CO_2 through polymer membranes than other flue gases.[149-152] While ionic liquids polymers can react with the CO_2 gas, the

slow diffusion of the gas through the polymer due to its highly cross linked nature is a major disadvantage.[150] In work presented by Bara *et al.* membranes have been fabricated whereby a styrene based ionic liquid monomer is polymerised in the presence of an ionic liquid such as 1-ethyl-3-methylimidazolium bis(triflimide), which resulted in a material which was 20% free ionic liquid and 80% poly(ionic liquids) in composition preventing a highly cross-linked polymer, increasing the distance between the polymer chains (Figure 1.12).[150] This material achieved a CO_2/N_2 selectivity of 40 which was a 25% increase on the neat poly(ionic liquid). Moreover, an increase of between 300 – 600% in permeability values were recorded for all gases tested due to the larger spaces in the poly(ionic liquid) membranes which were formed due to the ionic liquid inhibiting the degree of cross-linking of the poly(ionic liquid).[150] Therefore these materials potentially represent an interesting new area in gas membrane technology by the incorporation of ionic liquids with differing functionality to optimise the membrane for certain gases.

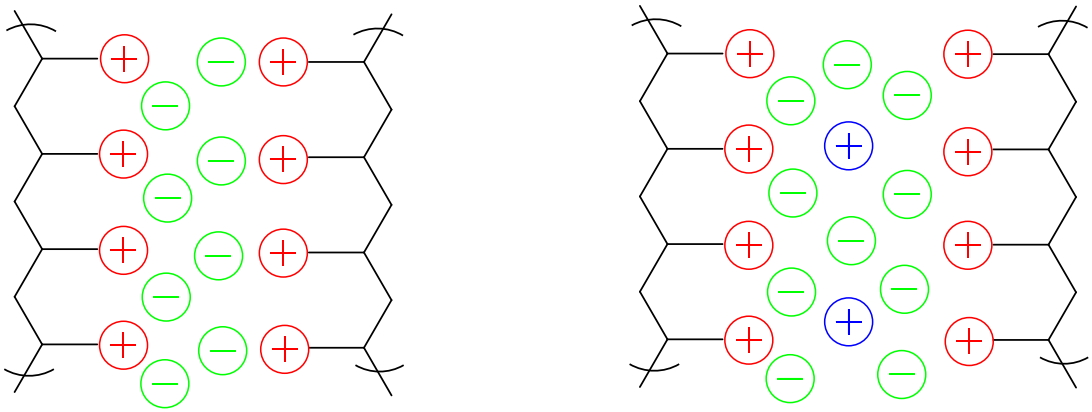

Figure 1.12: Ion arrangement of poly(ionic liquid) – ionic liquid composite membranes: polymer cations (red), free ionic liquid cation (blue), and anion of both the poly(ionic liquid) and free ionic liquid (green).[152]

1.11 Outline of thesis

The work presented in this thesis will address many of the topics discussed during the course of the introduction. The synthesis and characterisation of 49 novel ionic liquids will be presented comprising both imidazolium and phosphonium cations containing conventional and amino acid based anions. Physical properties of a number of the ionic liquids such as refractive index, viscosity and thermal stability have been measured. A

portion of these ionic liquids will be investigated as both CO_2 sorbent materials and also the incorporation of these liquid into polymeric supports to separate CO_2 from N_2.

1.12 References

(1) Rogner, H.-H. Z., Dadi "Climate Change 2007: Mitigation of Climate Change," 2007.

(2) Warrick, R.; Farmer, G. *Transactions of the Institute of British Geographers* **1990**, *15*, 5-20.

(3) Rao, A. B.; Rubin, E. S. *Environmental Science & Technology* **2002**, *36*, 4467-4475.

(4) Buhre, B. J. P.; Elliott, L. K.; Sheng, C. D.; Gupta, R. P.; Wall, T. F. *Progress in Energy and Combustion Science* **2005**, *31*, 283-307.

(5) Figueroa, J. D.; Fout, T.; Plasynski, S.; McIlvried, H.; Srivastava, R. D. *International Journal of Greenhouse Gas Control* **2008**, *2*, 9-20.

(6) White, C. M.; Strazisar, B. R.; Granite, E. J.; Hoffman, J. S.; Pennline, H. W. *Journal of the Air & Waste Management Association* **2003**, *53*, 645-715.

(7) Aaron, D.; Tsouris, C. *Separation Science and Technology* **2005**, *40*, 321-348.

(8) Bara, J. E.; Gabriel, C. J.; Lessmann, S.; Carlisle, T. K.; Finotello, A.; Gin, D. L.; Noble, R. D. *Industrial & Engineering Chemistry Research* **2007**, *46*, 5380-5386.

(9) Bara, J. E.; Gabriel, C. J.; Carlisle, T. K.; Camper, D. E.; Finotello, A.; Gin, D. L.; Noble, R. D. *Chemical Engineering Journal* **2009**, *147*, 43-50.

(10) Chue, K. T.; Kim, J. N.; Yoo, Y. J.; Cho, S. H.; Yang, R. T. *Industrial & Engineering Chemistry Research* **1995**, *34*, 591-598.

(11) Li, G.; Xiao, P.; Webley, P.; Zhang, J.; Singh, R.; Marshall, M. *Adsorption-Journal of the International Adsorption Society* **2008**, *14*, 415-422.

(12) Yong, Z.; Mata, V.; Rodrigues, A. E. *Separation and Purification Technology* **2002**, *26*, 195-205.

(13) Yang, H.; Xu, Z.; Fan, M.; Gupta, R.; Slimane, R. B.; Bland, A. E.; Wright, I. *Journal of Environmental Sciences-China* **2008**, *20*, 14-27.

(14) Rochelle, G. T. *Science* **2009**, *325*, 1652-1654.

(15) Samanta, A.; Zhao, A.; Shimizu, G. K. H.; Sarkar, P.; Gupta, R. *Industrial & Engineering Chemistry Research* **2012**, *51*, 1438-1463.

(16) Sartori, G.; Savage, D. W. *Industrial & Engineering Chemistry Fundamentals* **1983**, *22*, 239-249.

(17) Yeh, A. C.; Bai, H. L. *Science of the Total Environment* **1999**, *228*, 121-133.

(18) Wang, M.; Lawal, A.; Stephenson, P.; Sidders, J.; Ramshaw, C. *Chemical Engineering Research & Design* **2011**, *89*, 1609-1624.

(19) D'Alessandro, D. M.; Smit, B.; Long, J. R. *Angewandte Chemie-International Edition* **2010**, *49*, 6058-6082.

(20) Kittel, J.; Fleury, E.; Vuillemin, B.; Gonzalez, S.; Ropital, F.; Oltra, R. *Materials and Corrosion-Werkstoffe Und Korrosion* **2012**, *63*, 223-230.

(21) Hammond, G. P.; Akwe, S. S. O. *International Journal of Energy Research* **2007**, *31*, 1180-1201.

(22) Feron, P. H. M.; Jansen, A. E. *Energy Conversion and Management* **1995**, *36*, 411-414.

(23) Zhou, S.; Wang, S.; Chen, C. *Industrial & Engineering Chemistry Research* **2012**, *51*, 2539-2547.

(24) Vaidya, P. D.; Kenig, E. Y. *Chemical Engineering & Technology* **2007**, *30*, 1467-1474.

(25) Bai, H. L.; Yeh, A. C. *Industrial & Engineering Chemistry Research* **1997**, *36*, 2490-2493.

(26) Diao, Y. F.; Zheng, X. Y.; He, B. S.; Chen, C. H.; Xu, X. C. *Energy Conversion and Management* **2004**, *45*, 2283-2296.

(27) Kim, Y. J.; You, J. K.; Hong, W. H.; Yi, K. B.; Ko, C. H.; Kim, J.-N. *Separation Science and Technology* **2008**, *43*, 766-777.

(28) Vanderpool, C. D.; Ritsko, J. E.; Chiola, V. 1971; Vol. US 3556725.

(29) Xu, X. C.; Song, C. S.; Andresen, J. M.; Miller, B. G.; Scaroni, A. W. *Energy & Fuels* **2002**, *16*, 1463-1469.

(30) Hiyoshi, N.; Yogo, K.; Yashima, T. *Microporous and Mesoporous Materials* **2005**, *84*, 357-365.

(31) Knowles, G. P.; Graham, J. V.; Delaney, S. W.; Chaffee, A. L. *Fuel Processing Technology* **2005**, *86*, 1435-1448.

(32) Yue, M. B.; Sun, L. B.; Cao, Y.; Wang, Z. J.; Wang, Y.; Yu, Q.; Zhu, J. H. *Microporous and Mesoporous Materials* **2008**, *114*, 74-81.

(33) Serna-Guerrero, R.; Belmabkhout, Y.; Sayari, A. *Adsorption-Journal of the International Adsorption Society* **2010**, *16*, 567-575.

(34) Heydari-Gorji, A.; Belmabkhout, Y.; Sayari, A. *Langmuir* **2011**, *27*, 12411-12416.

(35) Hwang, S. Y.; Yoon, W. J.; Yun, S. H.; Yoo, E. S.; Kim, T. H.; Im, S. S. *Macromolecular Research* **2013**, *21*, 1281-1288.

(36) Teng, I. T.; Chang, Y.-J.; Wang, L.-S.; Lu, H.-Y.; Wu, L.-C.; Yang, C.-M.; Chiu, C.-C.; Yang, C.-H.; Hsu, S.-L.; Ho, J.-a. A. *Biomaterials* **2013**, *34*, 7462-7470.

(37) Selvaraj, M.; Pandurangan, A.; Seshadri, K. S.; Sinha, P. K.; Lal, K. B. *Applied Catalysis a-General* **2003**, *242*, 347-364.

(38) Kresge, C. T.; Leonowicz, M. E.; Roth, W. J.; Vartuli, J. C.; Beck, J. S. *Nature* **1992**, *359*, 710-712.

(39) Zhao, D. Y.; Feng, J. L.; Huo, Q. S.; Melosh, N.; Fredrickson, G. H.; Chmelka, B. F.; Stucky, G. D. *Science* **1998**, *279*, 548-552.

(40) Wei, J.; Liao, L.; Xiao, Y.; Zhang, P.; Shi, Y. *Journal of Environmental Sciences-China* **2010**, *22*, 1558-1563.

(41) Hicks, J. C.; Drese, J. H.; Fauth, D. J.; Gray, M. L.; Qi, G.; Jones, C. W. *Journal of the American Chemical Society* **2008**, *130*, 2902-2903.

(42) Filburn, T.; Helble, J. J.; Weiss, R. A. *Industrial & Engineering Chemistry Research* **2005**, *44*, 1542-1546.

(43) Khatri, R. A.; Chuang, S. S. C.; Soong, Y.; Gray, M. *Energy & Fuels* **2006**, *20*, 1514-1520.

(44) Goeppert, A.; Meth, S.; Prakash, G. K. S.; Olah, G. A. *Energy & Environmental Science* **2010**, *3*, 1949-1960.

(45) Zhang, J.; Singh, R.; Webley, P. A. *Microporous and Mesoporous Materials* **2008**, *111*, 478-487.

(46) Walton, K. S.; Abney, M. B.; LeVan, M. D. *Microporous and Mesoporous Materials* **2006**, *91*, 78-84.

(47) Jacobs, P. A.; Vancauwe.Fh; Vansant, E. F.; Uytterho.Jb *Journal of the Chemical Society-Faraday Transactions I* **1973**, *69*, 1056-1068.

(48) Jacobs, P. A.; Vancauwe.Fh; Vansatn, E. F. *Journal of the Chemical Society-Faraday Transactions I* **1973**, *69*, 2130-2139.

(49) Siriwardane, R. V.; Shen, M. S.; Fisher, E. P. *Energy & Fuels* **2005**, *19*, 1153-1159.

(50) Teramoto, M.; Nakai, K.; Ohnishi, N.; Huang, Q. F.; Watari, T.; Matsuyama, H. *Industrial & Engineering Chemistry Research* **1996**, *35*, 538-545.

(51) Ilconich, J.; Myers, C.; Pennline, H.; Luebke, D. *Journal of Membrane Science* **2007**, *298*, 41-47.

(52) He, X.; Lie, J. A.; Sheridan, E.; Hagg, M.-B. *Industrial & Engineering Chemistry Research* **2011**, *50*, 2080-2087.

(53) Carreon, M. A.; Li, S.; Falconer, J. L.; Noble, R. D. *Journal of the American Chemical Society* **2008**, *130*, 5412-+.

(54) Lu, B.; Lin, Y. S. *Journal of Membrane Science* **2013**, *444*, 402-411.

(55) Fan, S.; Liu, J.; Zhang, F.; Zhou, S.; Sun, F. *Journal of Materials Research* **2013**, *28*, 1870-1876.

(56) Merkel, T. C.; Bondar, V. I.; Nagai, K.; Freeman, B. D.; Pinnau, I. *Journal of Polymer Science Part B-Polymer Physics* **2000**, *38*, 415-434.

(57) Gan, Q.; Rooney, D.; Xue, M.; Thompson, G.; Zou, Y. *Journal of Membrane Science* **2006**, *280*, 948-956.

(58) Chatzidaki, E. K.; Fawas, E. P.; Papageorgiou, S. K.; Kanellopoulos, N. K.; Theophilou, N. V. *European Polymer Journal* **2007**, *43*, 5010-5016.

(59) Scheffknecht, G.; Al-Makhadmeh, L.; Schnell, U.; Maier, J. *International Journal of Greenhouse Gas Control* **2011**, *5*, S16-S35.

(60) Wall, T. F. *Proceedings of the Combustion Institute* **2007**, *31*, 31-47.

(61) Kanniche, M.; Gros-Bonnivard, R.; Jaud, P.; Valle-Marcos, J.; Amann, J.-M.; Bouallou, C. *Applied Thermal Engineering* **2010**, *30*, 53-62.

(62) Anheden, M.; Yan, J. Y.; De Smedt, G. *Oil & Gas Science and Technology-Revue D Ifp Energies Nouvelles* **2005**, *60*, 485-495.

(63) Elaiwi, A.; Hitchcock, P. B.; Seddon, K. R.; Srinivasan, N.; Tan, Y. M.; Welton, T.; Zora, J. A. *Journal of the Chemical Society-Dalton Transactions* **1995**, 3467-3472.

(64) Huddleston, J. G.; Visser, A. E.; Reichert, W. M.; Willauer, H. D.; Broker, G. A.; Rogers, R. D. *Green Chemistry* **2001**, *3*, 156-164.

(65) Bates, E. D.; Mayton, R. D.; Ntai, I.; Davis, J. H. *Journal of the American Chemical Society* **2002**, *124*, 926-927.

(66) Scovazzo, P.; Kieft, J.; Finan, D. A.; Koval, C.; DuBois, D.; Noble, R. *Journal of Membrane Science* **2004**, *238*, 57-63.

(67) Sakellarios, N. I.; Kazarian, S. G. *Ionic Liquids Iiia: Fundamentals, Progress, Challenges, and Opportunities, Properties and Structure* **2005**, *901*, 89-101.

(68) Zhang, J.; Zhang, S.; Dong, K.; Zhang, Y.; Shen, Y.; Lv, X. *Chemistry-a European Journal* **2006**, *12*, 4021-4026.

(69) Sanchez, L. M. G.; Meindersma, G. W.; de Haan, A. B. *Chemical Engineering Research & Design* **2007**, *85*, 31-39.

(70) Bara, J. E.; Gabriel, C. J.; Hatakeyama, E. S.; Carlisle, T. K.; Lessmann, S.; Noble, R. D.; Gin, D. L. *Journal of Membrane Science* **2008**, *321*, 3-7.

(71) Jiang, Y.; Wu, Y.; Wang, W.; Li, L.; Zhou, Z.; Zhang, Z. *Chinese Journal of Chemical Engineering* **2009**, *17*, 594-601.

(72) Bonhote, P.; Dias, A. P.; Papageorgiou, N.; Kalyanasundaram, K.; Gratzel, M. *Inorganic Chemistry* **1996**, *35*, 1168-1178.

(73) Marsh, K. N.; Boxall, J. A.; Lichtenthaler, R. *Fluid Phase Equilibria* **2004**, *219*, 93-98.

(74) Wilkes, J. S.; Levisky, J. A.; Wilson, R. A.; Hussey, C. L. *Inorganic Chemistry* **1982**, *21*, 1263-1264.

(75) Seddon, K. R.; Stark, A.; Torres, M. J. *Pure and Applied Chemistry* **2000**, *72*, 2275-2287.

(76) Gale, R. J.; Osteryoung, R. A. *Journal of the Electrochemical Society* **1980**, *127*, 2167-2172.

(77) Wilkes, J. S.; Zaworotko, M. J. *Journal of the Chemical Society-Chemical Communications* **1992**, 965-967.

(78) Mahmoud, M. E.; Al-Bishri, H. M. *Chemical Engineering Journal* **2011**, *166*, 157-167.

(79) Visser, A. E.; Swatloski, R. P.; Reichert, W. M.; Mayton, R.; Sheff, S.; Wierzbicki, A.; Davis, J. H.; Rogers, R. D. *Chemical Communications* **2001**, 135-136.

(80) Cole, A. C.; Jensen, J. L.; Ntai, I.; Tran, K. L. T.; Weaver, K. J.; Forbes, D. C.; Davis, J. H. *Journal of the American Chemical Society* **2002**, *124*, 5962-5963.

(81) Zhou, F.; Liang, Y.; Liu, W. *Chemical Society Reviews* **2009**, *38*, 2590-2599.

(82) Ferguson, L.; Scovazzo, P. *Industrial & Engineering Chemistry Research* **2007**, *46*, 1369-1374.

(83) Zhang, Y.; Zhang, S.; Lu, X.; Zhou, Q.; Fan, W.; Zhang, X. *Chemistry-a European Journal* **2009**, *15*, 3003-3011.

(84) Ramirez, R. E.; Sanchez, E. M. *Solar Energy Materials and Solar Cells* **2006**, *90*, 2384-2390.

(85) Mahurin, S. M.; Dai, T.; Yeary, J. S.; Luo, H.; Dai, S. *Industrial & Engineering Chemistry Research* **2011**, *50*, 14061-14069.

(86) Tao, G.-h.; He, L.; Liu, W.-s.; Xu, L.; Xiong, W.; Wang, T.; Kou, Y. *Green Chemistry* **2006**, *8*, 639-646.

(87) Bradaric, C. J.; Downard, A.; Kennedy, C.; Robertson, A. J.; Zhou, Y. H. *Green Chemistry* **2003**, *5*, 143-152.

(88) Harjani, J. R.; Singer, R. D.; Garciac, M. T.; Scammells, P. J. *Green Chemistry* **2009**, *11*, 83-90.

(89) Kagimoto, J.; Taguchi, S.; Fukumoto, K.; Ohno, H. *Journal of Molecular Liquids* **2010**, *153*, 133-138.

(90) Fukumoto, K.; Yoshizawa, M.; Ohno, H. *Journal of the American Chemical Society* **2005**, *127*, 2398-2399.

(91) Ennis, E.; Handy, S. T. *Current Organic Synthesis* **2007**, *4*, 381-389.

(92) Matsumi, N.; Miyamoto, M.; Aoi, K. *Journal of Organometallic Chemistry* **2009**, *694*, 1612-1616.

(93) Housecroft, C. E.; Sharpe, A. G. *Inorganic Chemistry*; Pearson Prentice Hall, 2005.

(94) Krossing, I.; Slattery, J. M.; Daguenet, C.; Dyson, P. J.; Oleinikova, A.; Weingaertner, H. *Journal of the American Chemical Society* **2006**, *128*, 13427-13434.

(95) Ngo, H. L.; LeCompte, K.; Hargens, L.; McEwen, A. B. *Thermochimica Acta* **2000**, *357*, 97-102.

(96) Zahn, S.; Bruns, G.; Thar, J.; Kirchner, B. *Physical Chemistry Chemical Physics* **2008**, *10*, 6921-6924.

(97) Campbell, P. S.; Santini, C. C.; Bouchu, D.; Fenet, B.; Rycerz, L.; Chauvin, Y.; Gaune-Escard, M.; Bessada, C.; Rollet, A.-L. *Dalton Transactions* **2010**, *39*, 1379-1388.

(98) Holbrey, J. D.; Seddon, K. R. *Journal of the Chemical Society-Dalton Transactions* **1999**, 2133-2139.

(99) Sun, J.; MacFarlane, D. R.; Forsyth, M. *Ionics* **1997**, *3*, 356-362.

(100) Seddon, K. R. *Journal of Chemical Technology and Biotechnology* **1997**, *68*, 351-356.

(101) Noack, K.; Schulz, P. S.; Paape, N.; Kiefer, J.; Wasserscheid, P.; Leipertz, A. *Physical Chemistry Chemical Physics* **2010**, *12*, 14153-14161.

(102) Izgorodina, E. I.; Maganti, R.; Armel, V.; Dean, P. M.; Pringle, J. M.; Seddon, K. R.; MacFarlane, D. R. *Journal of Physical Chemistry B* **2011**, *115*, 14688-14697.

(103) Hunt, P. A. *Journal of Physical Chemistry B* **2007**, *111*, 4844-4853.

(104) Wasserscheid, P.; Keim, W. *Angewandte Chemie-International Edition* **2000**, *39*, 3772-3789.

(105) Wooster, T. J.; Johanson, K. M.; Fraser, K. J.; MacFarlane, D. R.; Scott, J. L. *Green Chemistry* **2006**, *8*, 691-696.

(106) Hao, Y.; Peng, J.; Hu, S.; Li, J.; Zhai, M. *Thermochimica Acta* **2010**, *501*, 78-83.

(107) Fredlake, C. P.; Crosthwaite, J. M.; Hert, D. G.; Aki, S.; Brennecke, J. F. *Journal of Chemical and Engineering Data* **2004**, *49*, 954-964.

(108) Chan, B.; Chang, N.; Grimmett, M. *Australian Journal of Chemistry* **1977**, *30*, 2005-2013.

(109) Baranyai, K. J.; Deacon, G. B.; MacFarlane, D. R.; Pringle, J. M.; Scott, J. L. *Australian Journal of Chemistry* **2004**, *57*, 145-147.

(110) Oxley, J. D.; Prozorov, T.; Suslick, K. S. *Journal of the American Chemical Society* **2003**, *125*, 11138-11139.

(111) Zanger, M.; Vanderwerf, C. A.; McEwen, W. E. *Journal of the American Chemical Society* **1959**, *81*, 3806-3807.

(112) Tsunashima, K.; Kodama, S.; Sugiya, M.; Kunugi, Y. *Electrochimica Acta* **2010**, *56*, 762-766.

(113) Keating, M. Y.; Gao, F.; Ramsey, J. B. *Journal of Thermal Analysis and Calorimetry* **2011**, *106*, 207-211.

(114) Tokuda, H.; Tsuzuki, S.; Susan, M. A. B. H.; Hayamizu, K.; Watanabe, M. *Journal of Physical Chemistry B* **2006**, *110*, 19593-19600.

(115) Fannin, A. A.; Floreani, D. A.; King, L. A.; Landers, J. S.; Piersma, B. J.; Stech, D. J.; Vaughn, R. L.; Wilkes, J. S.; Williams, J. L. *Journal of Physical Chemistry* **1984**, *88*, 2614-2621.

(116) Fuller, J.; Carlin, R. T.; Osteryoung, R. A. *Journal of the Electrochemical Society* **1997**, *144*, 3881-3886.

(117) Branco, L. C.; Rosa, J. N.; Ramos, J. J. M.; Afonso, C. A. M. *Chemistry-a European Journal* **2002**, *8*, 3671-3677.

(118) Baltus, R. E.; Counce, R. M.; Culbertson, B. H.; Luo, H. M.; DePaoli, D. W.; Dai, S.; Duckworth, D. C. *Separation Science and Technology* **2005**, *40*, 525-541.

(119) Anthony, J. L.; Anderson, J. L.; Maginn, E. J.; Brennecke, J. F. *Journal of Physical Chemistry B* **2005**, *109*, 6366-6374.

(120) Zhang, S. J.; Chen, Y. H.; Li, F. W.; Lu, X. M.; Dai, W. B.; Mori, R. *Catalysis Today* **2006**, *115*, 61-69.

(121) Anthony, J. L.; Maginn, E. J.; Brennecke, J. F. *Journal of Physical Chemistry B* **2002**, *106*, 7315-7320.

(122) Kumelan, J.; Kamps, I. P.-S.; Tuma, D.; Maurer, G. *Journal of Chemical Thermodynamics* **2006**, *38*, 1396-1401.

(123) Aki, S.; Mellein, B. R.; Saurer, E. M.; Brennecke, J. F. *Journal of Physical Chemistry B* **2004**, *108*, 20355-20365.

(124) Blanchard, L. A.; Gu, Z. Y.; Brennecke, J. F. *Journal of Physical Chemistry B* **2001**, *105*, 2437-2444.

(125) Cadena, C.; Anthony, J. L.; Shah, J. K.; Morrow, T. I.; Brennecke, J. F.; Maginn, E. J. *Journal of the American Chemical Society* **2004**, *126*, 5300-5308.

(126) Kazarian, S. G.; Briscoe, B. J.; Welton, T. *Chemical Communications* **2000**, 2047-2048.

(127) Kazarian, S. G.; Vincent, M. F.; Bright, F. V.; Liotta, C. L.; Eckert, C. A. *Journal of the American Chemical Society* **1996**, *118*, 1729-1736.

(128) Raveendran, P.; Wallen, S. L. *Journal of the American Chemical Society* **2002**, *124*, 12590-12599.

(129) Pringle, J. M.; Golding, J.; Baranyai, K.; Forsyth, C. M.; Deacon, G. B.; Scott, J. L.; MacFarlane, D. R. *New Journal of Chemistry* **2003**, *27*, 1504-1510.

(130) Muldoon, M. J.; Aki, S. N. V. K.; Anderson, J. L.; Dixon, J. K.; Brennecke, J. F. *Journal of Physical Chemistry B* **2007**, *111*, 9001-9009.

(131) Almantariotis, D.; Gefflaut, T.; Padua, A. A. H.; Coxam, J. Y.; Gomes, M. F. C. *Journal of Physical Chemistry B* **2010**, *114*, 3608-3617.

(132) Jiang, Y.-Y.; Wang, G.-N.; Zhou, Z.; Wu, Y.-T.; Geng, J.; Zhang, Z.-B. *Chemical Communications* **2008**, 505-507.

(133) He, L.; Tao, G.-H.; Parrish, D. A.; Shreeve, J. n. M. *Journal of Physical Chemistry B* **2009**, *113*, 15162-15169.

(134) Gurkan, B. E.; de la Fuente, J. C.; Mindrup, E. M.; Ficke, L. E.; Goodrich, B. F.; Price, E. A.; Schneider, W. F.; Brennecke, J. F. *Journal of the American Chemical Society* **2010**, *132*, 2116-+.

(135) Ma, J.-w.; Zhou, Z.; Zhang, F.; Fang, C.-g.; Wu, Y.-t.; Zhang, Z.-b.; Li, A.-m. *Environmental Science & Technology* **2011**, *45*, 10627-10633.

(136) He, L.; Tao, G.-H.; Shreeve, J. n. M. *Abstracts of Papers of the American Chemical Society* **2009**, *238*.

(137) Jacquemin, J.; Gomes, M. F. C.; Husson, P.; Majer, V. *Journal of Chemical Thermodynamics* **2006**, *38*, 490-502.

(138) Finotello, A.; Bara, J. E.; Camper, D.; Noble, R. D. *Industrial & Engineering Chemistry Research* **2008**, *47*, 3453-3459.

(139) Shin, E.-K.; Lee, B.-C.; Lim, J. S. *Journal of Supercritical Fluids* **2008**, *45*, 282-292.

(140) Goodrich, B. F.; de la Fuente, J. C.; Gurkan, B. E.; Lopez, Z. K.; Price, E. A.; Huang, Y.; Brennecke, J. F. *Journal of Physical Chemistry B* **2011**, *115*, 9140-9150.

(141) Scovazzo, P.; Havard, D.; McShea, M.; Mixon, S.; Morgan, D. *Journal of Membrane Science* **2009**, *327*, 41-48.

(142) Shiflett, M. B.; Niehaus, A. M. S.; Yokozeki, A. *Journal of Physical Chemistry B* **2011**, *115*, 3478-3487.

(143) Barghi, S. H.; Adibi, M.; Rashtchian, D. *Journal of Membrane Science* **2010**, *362*, 346-352.

(144) Myers, C.; Pennline, H.; Luebke, D.; Ilconich, J.; Dixon, J. K.; Maginn, E. J.; Brennecke, J. F. **2008**, *322*, 28–31.

(145) Bara, J. E.; Carlisle, T. K.; Gabriel, C. J.; Camper, D.; Finotello, A.; Gin, D. L.; Noble, R. D. *Industrial & Engineering Chemistry Research* **2009**, *48*, 2739-2751.

(146) Bara, J. E.; Lessmann, S.; Gabriel, C. J.; Hatakeyama, E. S.; Noble, R. D.; Gin, D. L. *Industrial & Engineering Chemistry Research* **2007**, *46*, 5397-5404.

(147) Carlisle, T. K.; Bara, J. E.; Lafrate, A. L.; Gin, D. L.; Noble, R. D. *Journal of Membrane Science* **2010**, *359*, 37-43.

(148) Bara, J. E.; Hatakeyama, E. S.; Gabriel, C. J.; Zeng, X.; Lessmann, S.; Gin, D. L.; Noble, R. D. *Journal of Membrane Science* **2008**, *316*, 186-191.

(149) Bara, J. E.; Gin, D. L.; Noble, R. D. *Industrial & Engineering Chemistry Research* **2008**, *47*, 9919-9924.

(150) Bara, J. E.; Hatakeyama, E. S.; Gin, D. L.; Noble, R. D. *Polymers for Advanced Technologies* **2008**, *19*, 1415-1420.

(151) Bara, J. E.; Noble, R. D.; Gin, D. L. *Industrial & Engineering Chemistry Research* **2009**, *48*, 4607-4610.

(152) Bara, J. E.; Camper, D. E.; Gin, D. L.; Noble, R. D. *Accounts of Chemical Research* **2010**, *43*, 152-159.

Chapter 2:

Experimental

2.1 Introduction

The work carried out in this chapter is concerned with the development of ionic liquids, and their use in the development of materials for absorption and separation of CO_2 from other atmospheric gases. As mentioned previously ionic liquids are salts which exist as liquids below 100 ^oC, although work here will focus on those which exist as liquids at room temperature. Ionic liquids [1a] – [8c] are synthesised by methods previously outlined in the literature, while the remaining ionic liquids presented in this work are considered novel. All ionic liquids which contain primary amine functionality incorporated by the anion were synthesised using an adaptation of a method first explored by Ohno *et al.*[1] A brief description of the theoretical background of each experimental technique will also be provided.

The absorption of CO_2 by the Ionic Liquid supported by mesoporous silica was carried out via a custom built absorption rig with absorption measured via mass spectrometry. The permeation work was conducted using a custom made rig based in the Chemistry Department built by Dr. Sinead McDermott, postdoctoral researcher on the project. Incorporation of the ionic liquids into the various supports was characterised using infrared spectroscopy (IR), Scanning Electron Microscopy (SEM) and Energy Dispersive Xray (EDX). Thermal Characterisation was carried out using both Differential Scanning Calorimetry (DSC) and Thermogravrimetric Analysis (TGA).

2.2 Instrumentation

Infrared (IR) Spectra were recorded on a Perkin Elmer System 2000 FT spectrometer. Solid samples were finely ground with an excess of dry potassium bromide and pressed into a disk between two die using 9 tonnes of pressure. Liquid samples presented as part of the current work this work were characterised using a a Perkin Elmer Precisely Spectrum 100 FTIR. Liquid samples were analysed on a trough plate 45^o ZnSe crystal and polymer membranes were analysed on a flat-plate 45^o ZnSe crystal, which were positioned on top of a Pike Technologies ATR Max II. All ionic liquids were characterised between 4000 – 650 cm^{-1} at a resolution of 4 cm^{-1}.

All NMR spectra were recorded on a Bruker Avance spectrometer at a probe temperature of 25 ^oC, unless otherwise stated, operating at 300 MHz for the ^1H nucleus , 75.5 MHz for the ^{13}C nucleus, 282 MHz for the ^{19}F nuclei, and 121 MHz for the ^{31}P nuclei. Tetramethylsilane (TMS) was used as internal standard in both ^1H NMR and ^{13}C

NMR where $CDCl_3$ was used and trace acetonitrile (2.09 ppm for ^{1}H NMR, and 1.47 ppm for ^{13}C NMR in D_2O) was used as an internal standard when D_2O was used. The chemical shift for the lock solvent was used as an internal reference for ^{31}P NMR and ^{19}F NMR experiments respectively.[2] Samples were prepared by dissolving 10 – 20 mg in the appropriate deuterated solvent to a height of 4 cm^3. Chemical shifts are given in ppm and coupling constants are given in Hz.

Mass spectrometry was carried out on a LC/TOF-MS model 6210 Time-Of-Flight LC/MS with an electrospray source positive and negative (ESI+/-), capillary 3,500 V, nebuliser spray 30 psig, drying gas 5 L/min and source temperature 325 ^{o}C. The fragmentor was used at 175 V. The LC was a model 1200 Series and injection volumes were typically 10 μL. An Agilent Eclipse XBD-C18 column, 5-micron in diameter was employed. All samples were found to be within 5 ppm of the desired value and presented in units of a.m.u.

Surface analysis of mesoporous silica materials were performed by Dr. Neal Leddy, Centre for Microscopy and Analysis, Trinity College Dublin. Samples were degassed at 80 ^{o}C for 16 hours before undergoing multi-point BET analysis. Results were obtained using Quantachrome Nova 4200e and analysis was performed using Quantachrome NovaWin2.

Scanning Electron Microscopy (SEM) was carried out on a Hitachi S-3200-N with a tungsten filament electron source, maximum magnification of 300,000 and a resolution of 3.5 nm. This microscope was equipped with an Oxford Instrument INCAx-act EDX system with a silicon drift detector. The surface of the SILMs were examined using SEM.

Viscosity of the ionic liquids was determined by Dr. James Kennedy at Athlone Institute of technology using Steady State Rheometry. The method used to study the rheological properties of all of the materials detailed in this study was steady state parallel plate viscometry, utilising an AR1000™ rheometer from TA instruments. The air bearing guard was removed prior to use and the instrument was calibrated for inertia. A geometry was set for the 40 mm steel parallel plate and the instrument was mapped and brought to the test temperature of 25 °C. The gap between the plates was zeroed for a reference point after which the plate was increased to allow the sample loading (0.5

ml). The amount of sample loaded has an effect on the accuracy of the results, and so extreme care was taken during sample loading to ensure the correct fill and gap size (10 microns). The head was brought down onto the sample in incremental steps to avoid wasting material or inducing stress in the sample. Temperature sweep tests under oscillation mode were carried out on all samples. The setup included a temperature sweep from 25 to 80 °C, where a ramp rate of 5 °C/min was applied, at a Frequency of 1 Hz. Each of the results were analysed to identify the change in viscosity as the temperature increased.

Thermal analysis was carried out both in NUI Maynooth (high temperature DSC), and by Dr. James Kennedy and Dr. Alan Murphy, Athlone Institute of Technology (cold temp DSC and thermogravimetric analysis (TGA)). DSC and TGA samples consisted of 2 – 10 mg ionic liquid in either aluminium or alumina pans and scanned at a heating rate of 10 ^{o}C/min. Experiments in NUIM were performed on a Perkin Elmer Pyris 6 while experiments on samples investigated in Athlone Institute of Technology were performed on a Perkin Elmer DSC 7. Analysis of all DSC samples was performed using Pyris software version 7. TGA experiments were carried out on a Perkin Elmer TGA 7 and analysed using TA Universal Analysis.

Refractive index measurements were obtained using a Milton Roy refractometer, model No. 334619, with a precision index scale subdivided into 0.0005nD units.

2.2.1 CO_2 studies instrumentation

2.2.1.1 CO_2 absorption studies

CO_2 absorption values were determined using the rig setup as illustrated in Figure 2.1. Once the support had been impregnated with the ionic liquid, it was placed into a quartz reactor tube and held in place by glass wool either side. This was then connected to the rig and helium was allowed to flow through the sample at a rate of 12 cm^3/min. The sample underwent an initial pre-treatment step whereby the sample was heated up to 100 ^{o}C and held until all water, solvent, and CO_2, which had been absorbed on the bench, were removed. This was performed by tracing each ion mass spectrometry and

when levels had returned to background levels, the sample was cooled to the desired absorption temperature.

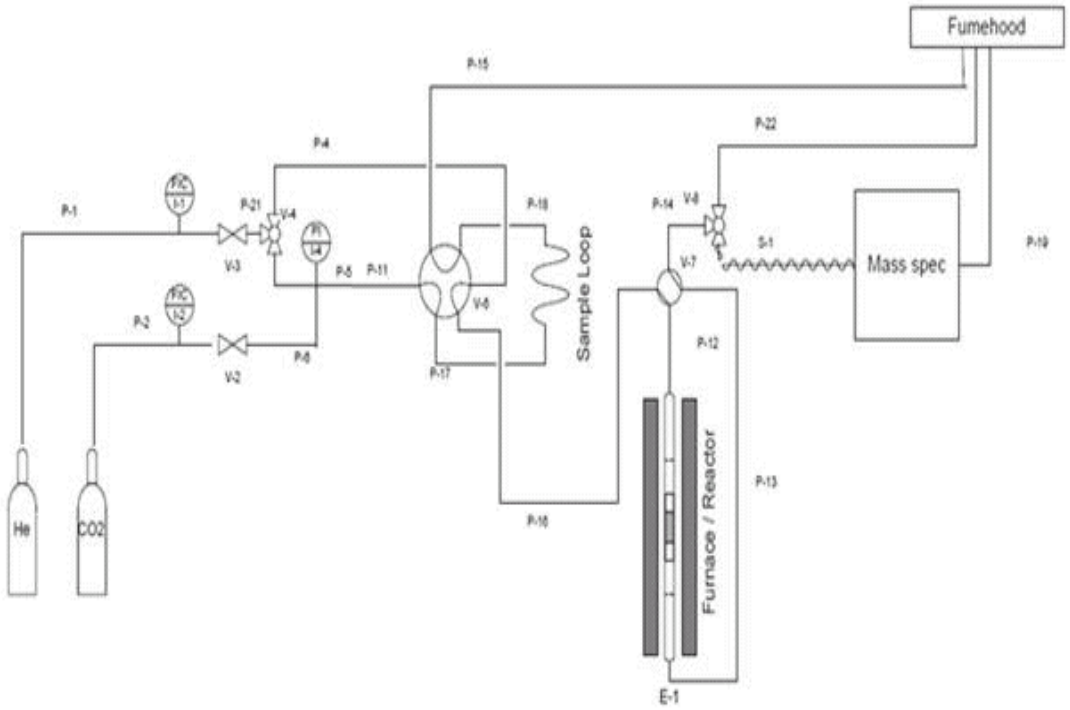

Figure 2.1: Illustration of gas absorption rig

CO_2 (15%) in helium was then allowed to flow through the reactor tube at a rate of 20 cm^3/min to saturate the sample for approximately ten minutes. At this point, CO_2 levels were allowed to return to normal, after which the sample was then heated again to 100 ^oC at a rate of 10 ^oC/ min. The mass spectrometry trace for CO_2 was monitored carefully to see if a peak occurred which related to the absorbed CO_2. Again once the CO_2 trace returned to background levels, a calibration pulse was performed which bypassed the sample. An example of a resulting spectrum is shown in Figure 2.2.

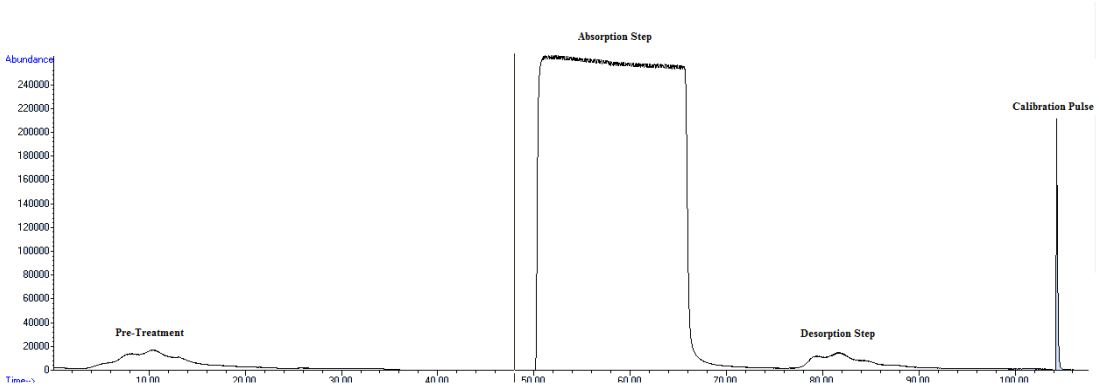

Figure 2.2: Example of absorption Mass Spectrum obtained during CO_2 absorption studies.

The resulting peaks were integrated and the values entered into a calibration plot to determine the amount of CO_2 absorbed per gram of solid tested.

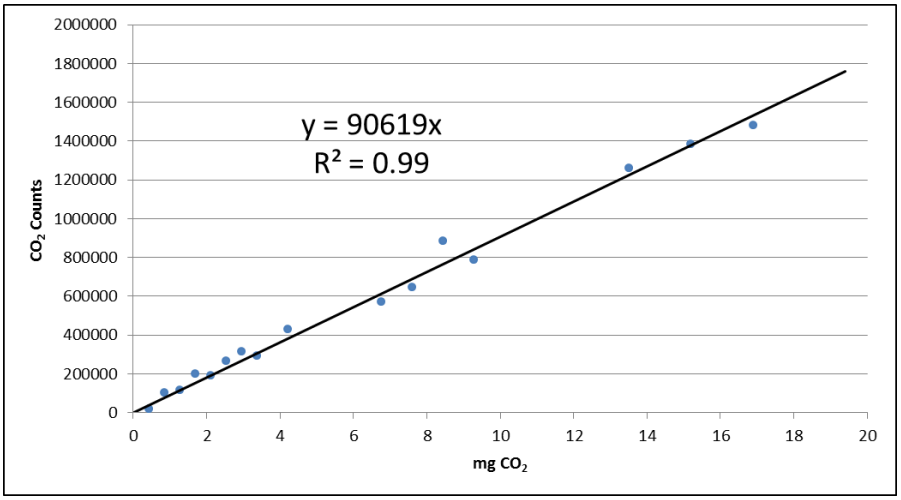

Figure 2.3: Calibration curve relating area under desorbed CO_2 peak to the amount of CO_2 absorbed (mg/g solid).

The quantity of CO_2 absorbed was then determined using Equation 2.1.

$$Quantity\ of\ CO_2\ absorbed\ = \left(\frac{\left(\frac{CO_2\ Counts\ (area)}{Calibrated\ Slope} \right)}{Amount\ of\ Sample\ (g)} \right)$$

(Equation 2.1)

2.2.1.2 Gas permeation studies

Experiments were also conducted to examine the potential use of ionic liquids as separation media for various flue gases. These tests were performed on the permeation rig as described in Figure 2.4 utilising the time lag approach.

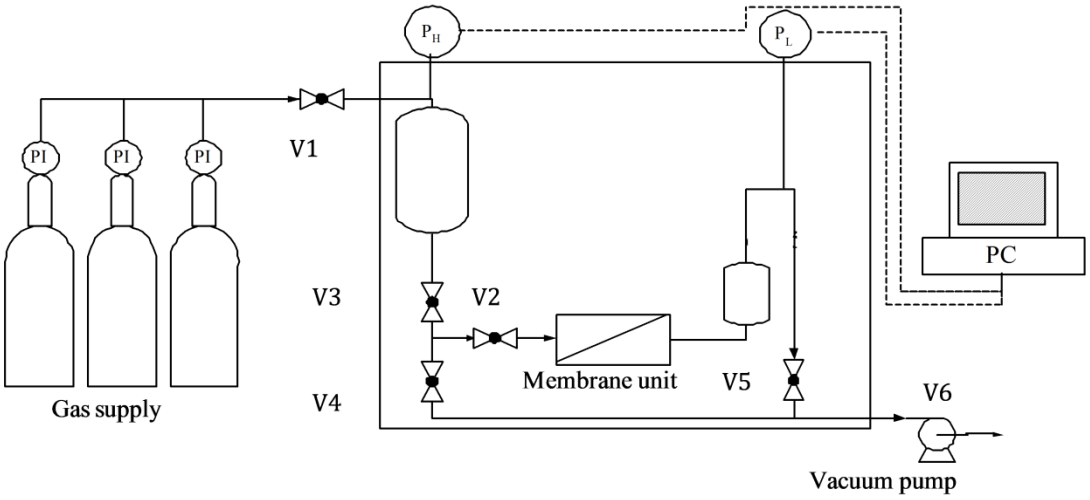

Figure 2.4: Illustration of the gas permeation rig

A membrane impregnated with the ionic liquid of choice was placed in the membrane module. The feed vessel (1000 cm^3) was filled with 1 bar of the gas (CO_2(99%) and N_2(99%)) in question whilst a vacuum was applied to the permeation vessel (73.68 cm^3). The vacuum source was then removed from the permeation side (when a vacuum of $3 – 5 \times 10^{-3}$ mbarr was achieved) and the gas from the feed side released and allowed to pass through the membrane towards the feed side. Different gasses permeated through the membranes at different rates. Variable temperature experiments were performed using a heating jacket which surrounded the module unit. The change in pressure on the feed side was plotted as a function of time. The slope of the linear region of the resulting plot was obtained and the permeability was determined using Equation 2.2,

$$P_i = \frac{(273\ x\ 10^7 Vl(\delta p/\delta t)}{76 \Delta p A T} \qquad \text{(Equation 2.2)}$$

Where V is the permeate vessel volume, l is the thickness of the membrane, (δp/δt) is the rate of change of pressure in the permeate vessel, Δp is the pressure difference over the membrane, A is the area of the membrane, T is the temperature applied to the membrane. Therefore in theory it is possible that if this difference is significant, then a

separation of the respective gases can occur. The selectivity (α), of the ionic liquids towards the gasses were then determined using Equation 2.3.

$$\alpha_{A/B} = \frac{P_A}{P_B} \qquad \text{(Equation 2.3)}$$

2.3 Synthesis of ionic liquids

2.3.1 Chemicals used in the synthesis of ionic liquids

Sodium trifluoromethanesulfonate (98%), sodium trifluoroacetate (98%), sodium dicyanamide (96%), 4-(2-chloroethyl)morpholine hydrochloride (99%), bis(trifluoromethane)sulfonimide lithium salt (≥ 99%), 1-(2-chloroethyl)pyrrolidine hydrochloride (98%), sodium tetrafluoroborate (98%), glycine (98%), d-alanine (99+%), (1R)-(10)-camphorsulfonic acid (98%), 1-(2-chloroethyl)piperidine hydrochloride (98%), 3-bromopropylamine hydrobromide (98%), 1-pyrrolidinebutyronitrile (97%), 1-butylimidazole (98%), 1-methylimidazole, purified by redistillation (≥ 99%), saccharin sodium salt (≥99%), l-lysine (≥ 97%), l-asparagine (≥ 98%), l-leucine (≥ 99%) 1,2 bis(chloroethoxyethane) (97%), imidazole (≥ 99.5%), sodium hydride, (60% dispersion in mineral oil), 2-methoxyethanol (anhydrous 99%), iodomethane (≥ 99%), 2-(2-methoxyethoxy)ethanol (≥ 99%), ethylbromoacetate (98%), and *n*-trioctylphosphine (>97%), 4-bromo-1-butyne (99%) were all purchased from Sigma-Aldrich. d-glutamine (≥ 99.5%), *p*-toluene sulfonyl chloride (≥ 99%), and 1-methylpyrrolidine (≥ 99%) were purchased from Fluka. sodium-1-butanesulfonate was purchased from Alfa Aesar, l-valine (99%) was purchased from Lancaster, and amberlite IRA-400 hydroxide form anion exchange resin was purchased from Supleco.

2.3.2 Synthesis of ionic liquids [1a-8c]

Synthesis of 1-butyl-3-methylimidazolium chloride [1a]

Experimental procedure followed that as described by Ab Rani *et al.*[3] 1-methyl (40 cm^3) was added to 50 cm^3 of anhydrous toluene and the mixture stirred. To this, 90 cm^3 of 1-chlorobutane was added slowly and the mixture was refluxed at 80 ^oC for 24 hours. Once cooled, the two layers were separated. The bottom ionic liquid layer was washed with 3 × 30 cm^3 of ethyl acetate. The ionic liquid layer was recrystallised from ethyl acetate at -20 ^oC and filtered to yield a white solid.

Yield: 75.31 g (86%)

^{1}H NMR: (DMSO) δ= 0.96 (*t*, 3H, *J* = 7.2), 1.36 (*m*, 2H), 1.90 (*m*, 2H), 4.10 (*s*, 3H), 4.36 (*t*, 2H, *J* = 7.2), 7.46 (*pt*, 1H, *J* = 1.7), 7.58 (*pt*, 1H, *J* = 1.7), 10.91 (*s*, 1H).

Synthesis of 1-butyl-3-methylimidazolium tetrafluoroborate [1b]

Synthesis was carried out using an adaptation of Zhang *et al.*[4] [1a] (30 g) was dissolved in 20 cm^3 of acetone. Sodium tetrafluoroborate (18.34 g) was added and this was stirred at room temperature for 24 hours. The solution was then filtered through a plug of celite. The excess solvent was removed under reduced pressure and dried to yield a clear liquid.

Yield: 36.18 g (94%)

^{1}H NMR: (DMSO) δ= 0.89 (*t*, 3H, *J* = 7.3), 1.27 (*m*, 2H), 1.76 (*m*, 2H), 3.84 (*s*, 3H), 4.14 (*t*, 2H, *J* = 7.3), 7.65 (*pt*, 1H, *J* = 1.7), 7.72 (*pt*, 1H, *J* = 1.7), 9.02 (*s*, 1H).

Synthesis of 1-butyl-3-methylimidazolium bis(triflimide) [1c]

Synthesis followed that as outlined by Huddleston *et al.*[5] [1a] (1 g) was dissolved in 10 cm^3 of deionised H_2O and 1.48 g of bis (trifluoromethane) sulfonyl imide lithium salt was added and stirred at room temperature for 24 hours. The resulting layers were separated and the organic layer was dissolved in 20 cm^3 of dichloromethane. This was

washed with 3 × 20 cm^3 of deionised H_2O, and dried over magnesium sulfate before excess solvent was removed under reduced pressure to yield a yellowish liquid.

Yield: 2.23 g (92%)

^{1}H NMR: ($CDCl_3$) δ= 0.95 (*t*, 3H, *J* = 7.3), 1.32 (*m*, 2H), 1.86 (*m*, 2H), 3.93 (*s*, 3H), 4.16 (*t*, 2H, *J* = 7.3), 7.31 (*pt*, 1H, *J* = 1.7), 7.32 (*pt*, 1H, *J* = 1.7), 8.73 (*s*, 1H).

^{13}C NMR: ($CDCl_3$) δ= 13.1, 19.3, 31.8, 36.1, 49.7, 117.6 (*q*, *J* = 320) 122.2, 123.6, 135.6.

Synthesis of 1-butyl-3-methylimidazolium saccharinate [1d]

[1a] (2 g) was dissolved in 30 cm^3 of deionised H_2O and 2.79 g of sodium saccharinate was added and the mixture was stirred at room temperature for 24 hours. Excess water was removed under reduced pressure and 10 cm^3 of dichloromethane was added. The resulting solids were filtered and the filtrate dried over $MgSO_4$ before the excess dichloromethane was removed under reduced pressure to yield a pale yellow liquid.

Yield: 3.38 g (90%)

^{1}H NMR: ($CDCl_3$) δ= 0.86 (*t*, 2H, *J* = 7.3), 1.29 (*m*, 2H), 1.79 (*m*, 2H), 4.04 (*s*, 3H), 4.27 (*m*, 2H), 7.30 (*t*, 1H, *J* = 1.7), 7.38 (*pt*, 1H, *J* = 1.7), 7.57 (*m*, 2H), 7.77 (*m*, 2H), 9.91 (*s*, 1H).

^{13}C NMR: ($CDCl_3$) δ= 13.2, 19.2, 31.9, 36.3, 49.6, 119.5, 122.0, 123.0, 123.6, 131.3, 131.9, 134.6, 137.4, 144.6, 170.1.

Synthesis of 1-butyl-3-methylimidazolium camphorsulfonate [1e]

Synthesis was performed identically to that of [1d], using 2 g of [1a] and 3.2 g of camphorsulfonic acid.

Yield: 4.03 g (95%)

^{1}H NMR: ($CDCl_3$) δ= 0.74 (*s*, 3H), 0.90 (*m*, 3H), 1.06 (*s*, 3H), 1.24-1.32 (*m*, 3H), 1.59-1.97 (*m*, 5H), 2.19-2.25 (*m*, 1H), 2.56-2.71 (*m*, 2H), 3.15-3.20 (*d*, 1H, *J* =1.8), 3.60 (s, 4H), 3.94 (*s*, 3H), 4.19 (*m*, 2H), 7.39 (*pt*, 1H, *J* = 1.7), 7.52 (*pt*, 1H, *J* = 1.7), 9.49 (*s*, 1H).

^{13}C NMR: ($CDCl_3$) δ= 13.3, 19.3, 19.7, 19.8, 24.4, 26.9, 30.0, 32.0, 36.3, 42.5, 42.8, 47.1, 47.8, 49.4, 58.4, 122.0, 123.8, 137.4, 216.8

Synthesis of 1,3-dibutylimidazolium bromide [2a]

The synthesis of [2a] followed that as outlined by Palimkar *et al.*[6] 1-butylimidazole (20 cm^3) was dissolved in 40 cm^3 of anhydrous toluene. To this, 40 cm^3 of 1-bromobutane was added slowly, and the mixture was refluxed at 80 ^oC for 24 hours. The excess solvent was then removed under reduced pressure to yield crude product. The oil was washed with 3 × 20 cm^3 of ethyl acetate before solvent was removed to yield a brown liquid.

Yield: 39.83 g (90%)

^{1}H NMR: ($CDCl_3$) δ= 0.79 (*t*, 6H, *J* = 7.3), 1.21 (*m*, 4H), 1.77 (*m*, 4H), 4.20 (*t*, 4H, *J* = 7.4), 7.52 (*s*, 2H), 10.42 (*s*, 1H).

^{13}C NMR: ($CDCl_3$) δ= 13.3, 19.2, 32.0, 49.5, 122.3, 136.5

Synthesis of 1,3-dibutylimidazolium tetrafluoroborate [2b]

7 cm^3 of [2a] was dissolved in 20 cm^3 of deionised H_2O. 6.8 g of sodium tetrafluoroborate was added and the mixture stirred at room temperature for 24 hours. The product was then extracted with 3 × 30 cm^3 of dichloromethane. The dichloromethane washings were then combined and washed with 10 cm^3 of deionised water and then with 10 cm^3 of brine. The solution was then dried over magnesium sulfate and excess solvent removed under reduced pressure to yield the ionic liquid.

Yield: 8.05 g (97%)

^{1}H NMR: ($CDCl_3$) δ= 0.78 (*t*, 6H, *J* = 7.3), 1.26 (*m*, 4H), 1.77 (*m*, 4H), 4.10 (*t*, 4H, *J* = 7.4), 7.36 (*s*, 2H), 8.74 (*s*, 1H).

^{13}C NMR: ($CDCl_3$) δ= 13.1, 19.1, 31.8, 49.5, 123.0, 135.2.

Synthesis of 1,3-dibutylimidazolium saccharinate. [2c]

This synthesis was performed identically to [2b] using 7.56 g of [2a] and 11 g of sodium saccharinate to yield a viscous liquid.

Yield: 8.92 g (85%)

^{1}H NMR: ($CDCl_3$) δ= 0.86 (*t*, 6H, *J* = 7.3), 1.28 (*m*, 4H), 1.82 (*m*, 4H), 4.28 (*t*, 4H, *J* = 7.4), 7.42 (*s*, 2H), 7.54 (*m* 2H), 7.77 (*m*, 2H) 9.85 (*s*, 1H).

^{13}C NMR: ($CDCl_3$) δ= 13.3, 19.3, 32.1, 49.7, 119.5, 122.1, 123.1, 131.2, 131.8, 134.0, 144.8, 170.2.

Synthesis of 1,3-dibutylimidazolium camphorsulfonate [2d]

The synthesis was performed in similar conditions to that of [2b] using 7.56 g of [2a] and 7.89 g of camphorsulfonic acid to yield a viscous liquid.

Yield: 10.18 g (85%)

^{1}H NMR: ($CDCl_3$) δ = 0.85 (*s*, 3H), 0.95 (*t*, 6H, *J* = 7.3), 1.11 (*s*, 3H), 1.31-1.44 (*m*, 5H), 1.69-2.04 (*m*, 8H), 1.27-2.36 (*dt*, 1H, *J* = 1.8, 3.0) 2.65-2.75 (*m*, 1H), 2.86-3.84 (*dd*, 2H, *J* = 1.8, 2.0), 4.34 (*t*, 4H, *J* = 7.4), 7.31 (*d*, 2H, *J* = 1.8), 10.13 (*s*, 1H)

^{13}C NMR: ($CDCl_3$) δ = 13.4, 19.5, 19.8, 20.0, 24.6, 27.0, 32.1, 42.6, 42.9, 47.4, 47.9, 49.8, 58.5, 121.6, 138.1, 216.8

Synthesis of 1,3-dibutylimidazolium bis(triflimide) [2e]

[2a] (3 g) was dissolved in 20 cm^3 of deionised H_2O. Then 3.95 g of bis (trifluoromethane)sulfonyl imide lithium salt was added and stirred at room temperature for 24 hours. The two phases were separated and the organic layer was dissolved in 10 cm^3 of dichloromethane. This was then washed with 3 × 10 cm^3 of deionised H_2O and dried over magnesium sulfate, before excess solvent was removed to yield a yellow liquid.

Yield: 4.98 (94%)

^{1}H NMR: ($CDCl_3$) δ= 0.95 (*t*, 6H, *J* = 7.3), 1.37 (*m*, 4H), 1.85 (*m*, 4H), 4.18 (*t*, 4H, *J* = 7.4), 7.24 (*d*, 2H, *J* = 1.6), 8.81 (*s*, 1H).

^{13}C NMR: ($CDCl_3$) δ= 13.1, 19.3, 31.9, 49.9, 117.6 (*q*, *J* = 320), 122.3, 135.3.

Synthesis of 1-(3-aminopropyl)-3-methylimidazolium bromide hydrobromide [3a]

Synthesis of [4a] followed that as outlined by Myers *et al.*[7] 3-bromopropylamine hydrobromide [1.1 g] was dissolved in 12 cm^3 of anhydrous ethanol and 0.4 cm^3 of 1-methylimidazole was added. This was refluxed at 75 ^oC for 24 hours. The ethanol was then removed under reduced pressure to yield off white solid. This was recrystalised from ethanol using ethyl acetate and filtered and dried in an oven to yield a white solid.

Yield: 3.32 g (83%)

^{1}H NMR: (D_2O) δ = 2.19 (*m*, 2H), 2.98 (*t*, 2H, *J* = 7.8), 3.82 (*s*, 3H), 4.25 (*t*, 2H, *J* = 7.3), 7.39 (*pt*, 1H, *J* = 1.7), 7.44 (*pt*, 1H. *J* = 1.7), 8.70 (*s*, 1H).

Synthesis of 1-(3-aminopropyl)-3-methylimidazolium bis(triflimide) [3b]

[3a] (2 g) was dissolved in 20 cm^3 deionised H_2O and the pH adjusted to 9 using solid KOH. The excess H_2O was removed under vacuum and a 1:1 ethanol/THF solution was added. The solution was filtered and precipitate removed and filtrate reduced down to yield the bromide only form. The resulting liquid was dissolved in 10 cm^3 of H_2O and

2.3 g of bis(trifluoromethane)sulfonyl imide lithium salt was added and stirred for 24 hours. The resulting layers were separated and the organic layer washed 3 times with 10 cm^3 of H_2O. The liquid was dried over magnesium sulfate and excess solvent removed to yield liquid.

Yield: 2.12 g (76%)

^{1}H NMR: ($CDCl_3$) δ = 2.21 (*m*, 2H), 3.00 (*m*, 2H), 3.84 (*s*, 3H), 4.27 (*t*, 3H, *J* = 7.3), 7.40 (*t*, 1H, *J* = 1.7), 7.47 (*t*, 1H, *J* = 1.7), 8.71 (*s*, 1H).

^{13}C NMR: ($CDCl_3$) δ= 27.5, 35.7, 36.4, 46.4, 117.1 (*q*, *J* = 320), 122.0, 123.9, 134.9

Synthesis of 1-(2-(methoxyethoxy)ethyl)-3-methylimidazolium Iodide [4a]

The tosylate was formed by the reaction of 14.3 g of *p*-toluenesulfonyl chloride with 8.9 cm^3 of 2-(2-methoxyethoxy)ethanol under the same conditions. To alkylate the imidazole, 0.9 g of 60% mineral oil NaH was reacted with 1.2 g of imidazole under the same conditions as mentioned above. The newly formed 1-(2-(methoxyethoxy)ethyl)imidazole (2 cm^3) was reacted with 6.7 cm^3 of iodomethane and the workup again was same as that above to yield a viscous liquid.

Yield: 2.94 g (80%)

^{1}H NMR: ($CDCl_3$) δ = 3.29 (*s*, 3H), 3.49 (*t*, 2H, *J* = 4.5), 3.62 (*t*, 2H, *J* = 4.5), 3.86 (*t*, 2H, *J* = 4.5), 4.04 (*s*, 3H), 4.53 (*t*, 2H, *J* = 4.5), 7.54(*s*, 1H), 7.64(*s*, 1H), 9.63 (*s*, 1H)

^{13}C NMR: ($CDCl_3$) δ = 37.1, 49.8, 59.0, 68.6, 70.3, 71.5, 123.2, 123.4, 136.7.

Synthesis of N-butyl-N-methylpyrrolidinium bromide [5a]

The synthesis of [5a] followed that as outlined by Jagadeeswara Rao *et al.*[8] 1-methylpyrrolidine (6.25 cm^3) was dissolved in 20 cm^3 of anhydrous acetone. 1-bromobutane (6.3 cm^3) was added to the mixture at 0 °C and once added was brought up to room temperature before refluxing at 60 °C for 24 hours. The resulting solid was filtered and dried in an oven at 45 °C. This was then recrystalised by dissolving in

isopropanol and using toluene as antisolvent. The solid was filtered and dried overnight in the oven to yield white precipitate.

Yield: 11.54 g (87%)

^{1}H NMR: ($CDCl_3$) δ = 1.09 (*t*, 3H, *J* = 7.3), 1.47 (*m*, 2H), 1.78 (*m*, 2H), 2.31 (*s*, br, 4H), 3.22 (*s*, 3H), 3.69 (*t*, 2H, *J* = 8.6), 3.85 (*s*, br, 4H)

^{13}C NMR: ($CDCl_3$) δ = 13.7, 19.7, 21.6, 25.9, 48.6, 64.0, 64.4

Synthesis of N-butyl-N-methylpyrrolidinium bis(triflimide) [5b]

[5a] (2 g) was dissolved in 20 cm^3 of deionised H_2O. Bis(trifluoromethane)sulfonyl imide lithium salt (3.45 g) was added and this was stirred at room temperature for 24 hours. The organic layer was removed and dissolved in 15 cm^3 of dichloromethane. This was washed with 3 × 10 cm^3 of deionised H_2O and dried over magnesium sulfate before excess solvent was removed to yield a yellow oil.

Yield: 3.16 g (83%)

^{1}H NMR: 0.95 (*t*, 3H, *J* = 7.0), 1.43 (*m*, 2H), 1.76 (*m*, 2H), 2.21(*m*, 4H), 3.32 (*m*, 4H), 3.46 (*s*, br, 2H), 3.52 (*s*, 3H)

Synthesis of N-(cyanobutyl)-N-methylpyrrolidinium Iodide [6a]

The synthesis of [6a] followed that as described by Nockemann *et al.*[9] 1-pyrrolidinebutanenitrile (5.4 cm^3) was dissolved in 20 cm^3 of anhydrous diethyl ether. This was cooled to 0 ^{o}C and 2.71 cm^3 of iodomethane was added slowly to the mixture. This was allowed to warm to room temperature and was stirred for 24 hours. The excess solvent was then removed under reduced pressure to yield a pale yellow solid.

Yield: 8.13 g (81%)

^{1}H NMR: ($CDCl_3$) δ = 2.17 (*s*, br, 6H), 2.59 (*t*, 2H, *J* = 7.0), 3.02 (*s*, 3H), 3.43 (*m*, 6H)

^{13}C NMR: ($CDCl_3$) δ = 13.9, 19.4, 21.2, 48.1, 62.2, 64.6, 119.8

Synthesis of N-(cyanobutyl)-N-methylpyrrolidinium bis(triflimide) [6b]

[6a] (1 g) was dissolved in 30 cm^3 of deionised H_2O and 1.44 g of bis (trifluoromethane)sulfonyl imide lithium salt was added which was stirred at room temperature for 24 hours. The organic layer was removed, dissolved in dichloromethane and washed with 3 × 20 cm^3 of deionised H_2O. The solution was dried over magnesium sulfate and excess solvent removed to yield a yellow liquid.

Yield: 1.27 g (82%)

^{1}H NMR: ($CDCl_3$) δ = 2.02-2.12 (*m*, 6H), 2.61 (*t*, 2H, *J* = 7.2), 3.00 (*s*, 3H), 3.34-3.60 (*m*, 6H)

^{13}C NMR: ($CDCl_3$) δ = 13.7, 19.4, 20.9, 47.5, 61.4, 63.6, 117.3 (*q*, *J* = 320), 119.5.

Synthesis of triethylene glycol bis(3-methylimidazolium) di(bis(triflimide) [7a]

Synthesis of [7a] followed that as outlined by Holbrey *et al.*[10] 1-methylimidazole (10 cm^3) was dissolved in 30 cm^3 of anhydrous toluene. 1,2-bis(2-chloroethoxy)ethane (14.05 cm^3) was added and this was refluxed at 105 ^oC for 3 days. The solvent was decanted off and the "gum like" product was washed with 10 cm^3 of toluene to yield the chloride form of the salt.

The chloride salt precursor (3.79 g) was dissolved in 15 cm^3 of deionised water, to which 7.1 g of bis(trifluoromethane sulfonyl) lithium salt was added and stirred at room temperature for 24 hours. The organic layer was removed and washed with 3 × 10 cm^3 of deionised water. This was then dissolved in 20 cm^3 of dichloromethane and dried over magnesium sulfate. The excess solvent was removed under vacuum to yield a yellow oil.

Yield: 7.31 g (80%)

^{1}H NMR: ($CDCl_3$) δ= 3.57 (*s*, 4H), 3.75 (*t*, 4H, *J* = 4.8), 3.85 (*s*, 6H), 4.26 (*t*, 4H, *J* = 4.8), 7.29 (*s*, 2H), 7.38 (*s*, 2H), 8.49 (*s*, 2H)

^{13}C NMR: ($CDCl_3$) δ= 35.9, 49.6, 68.3, 70.1, 117.6 (*q*, *J* = 320), 123.0, 123.3 136.0.

Synthesis of 1-ethoxycarbonylmethyl-3-methylimidazolium bromide [8a]

The synthesis of [8a] followed the conditions as outlined by Gathergood *et al.*[11] 1-methylimidazole (5 cm^3) was dissolved in 25 cm^3 of THF and cooled to 0 ^oC, to which 7.2 cm^3 of ethylbromoacetate was added dropwise to the solution and the mixture was slowly brought up to room temperature. This was then allowed to stir for four hours after which the top layer was decanted off. The bottom layer was washed with 3 × 25 cm^3 of ethyl acetate and dried under vacuum to yield a yellow oil.

Yield: 14.02 g (90%)

^{1}H NMR: ($CDCl_3$); δ= 1.23 (*t*, 3H, *J* = 7.3), 4.03 (*s*, 3H), 4.16 (*q*, 2H, *J* = 7.2), 5.43 (*s*, 2H), 7.63 (*t*, 1H, *J* = 1.7), 7.74 (*t*, 1H, *J* = 1.7), 9.99 (*s*, 1H)

^{13}C NMR: ($CDCl_3$) δ= 14.0, 36.8, 50.2, 62.8, 123.2, 123.9, 138.0, 166.0.

Synthesis of 1-ethoxycarbonylmethyl-3-methylimidazolium bis(triflimide) [8b]

[8a] (2 g) was dissolved in 20 cm^3 of deionised water and 2.58 g of lithium bis(triflimide) salt was added and allowed to stir for 3 hours after which two layers had formed. The top layer was decanted off, while the bottom layer was washed with 3 × 10 cm^3 of deionised water. The resulting oil was dissolved in dichloromethane and dried over $MgSO_4$ before the solvent was removed under reduced pressure to yield a colourless oil.

Yield: 3.22 g (89%)

^{1}H NMR: ($CDCl_3$) δ= 1.32 (*t*, 3H, *J* = 7.3), 3.97 (*s*, 3H), 4.28 (*q*, 2H, *J* = 7.2), 5.02 (*s*, 2H), 7.28 (*s*, 1H, *J* = 1.7), 7.35 (*t*, 1H, J = 1.7), 8.88 (*s*, 1H)

^{13}C NMR: ($CDCl_3$) δ= 13.8, 36.6, 50.0, 63.2, 117.6 (q, J = 320), 123.0, 123.7, 137.8, 165.6

Synthesis of 1-ethoxycarbonylmethyl-3-methylimidazolium bromide saccharinate [8c]

[8a] (2 g) was dissolved in 30 cm^3 of acetone and 2.54 g of sodium saccharinate was added and the mixture refluxed for 24 hours. Once cooled the solution was filtered through a bed of celite and the filtrate dried over $MgSO_4$. The excess solvent was removed under reduced pressure to yield a yellow liquid.

Yield: 2.73 g (96%)

^{1}H NMR: ($CDCl_3$); δ= 1.29 (*t*, 3H, *J* = 7.2), 4.07(*s*, 3H), 4.26 (*q*, 2H, *J* = 7.2), 5.45 (*s*, 2H), 7.48(*t*, 1H, *J* = 1.7), 7.61 (*m*, 2H), 7.63(*t*, 1H, *J* = 1.7), 7,93 (*m*, 2H), 10.08(*s*, 1H).

^{13}C NMR ($CDCl_3$); δ= 14.0, 36.7, 50.2, 62.8, 119.7, 122.9, 123.3, 123.8, 131.7, 132.2, 134.0, 138.6, 144.1, 166.1, 169.8.

2.3.3 Synthesis of ionic liquids [9a-11e]

Synthesis of 1-(piperid-1-yl)ethyl-3-methylimidazolium bis (triflimide) [9a]

1-methylimidazole (5 cm^3) was dissolved in 20 cm^3 of anhydrous ethanol to which 11.54 g of 1-(2-chloroethyl)piperidine was added to the vessel and the mixture refluxed at 80 ^oC for 18 hours. A hot filtration was then performed on the mixture to isolate any of the hydrochloride starting material. The filtrate was reduced down under vacuum to yield a yellow crude product which was then washed with 3 × 20 cm^3 of dichloromethane to yield the white 1-(piperid-1-yl)ethyl-3-methyl imidazolium chloride hydrochloride salt.

1-(piperid-1-yl)ethyl-3-methyl imidazolium chloride salt (1 g) was dissolved in 20 cm^3 of deionised H_2O and 0.28 g of NaOH was added and stirred until completely dissolved. Bis (trifluoromethane sulfonyl) imide lithium salt (1.6 g) was added and the solution stirred at room temperature overnight. The resulting two layers were separated. The bottom layer was dissolved in 10 cm^3 of dichloromethane and washed with 3 × 25 cm^3 deionised water. The solution was dried over magnesium sulfate and excess solvent removed to yield a yellowish ionic liquid.

Yield: 1.59 g (89%)

^{1}H NMR: ($CDCl_3$) δ = 1.54 (*m*, 6H), 2.42 (*m*, 4H), 2.67 (*t*, 2H, *J* = 5.7), 4.20 (*t*, 2H, *J* = 5.7), 4.22 (*s*, 3H), 7.27 (*pt*, 1H, *J* = 1.8), 7.46 (*pt*, 1H, *J* = 1.8), 8.69 (*s*, 1H)

^{13}C NMR: ($CDCl_3$) δ = 24.0, 25.9, 36.2, 47.0, 54.2, 57.5, 113.4 (*q* = 321), 123.0, 123.1, 136.1

^{19}F NMR: ($CDCl_3$) δ = -79.0 (*s*)

IR (neat): ṽ = 3156, 3112, 2939, 2856, 2806, 1573, 1457, 1445, 1346, 1327, 1178, 1131, 1050, 963, 924, 848, 788, 758, 739, 702 cm^{-1}

ESI: [M^+] Calculated 194.1652, Observed 194.1658, [M^-] Calculated 279.9178, Observed 279.9184.

Synthesis of 1-(piperid-1-yl)ethyl-3-methyl imidazolium saccharinate [9b]

Initial procedure of synthesis was similar to [9a] to generate the hydrochloride salt. After this, 1 g of IL-Cl was dissolved in deionised H_2O and 0.28 g of NaOH was added and stirred until no solids remained. Sodium saccharinate (0.93 g)was added and the solution was stirred for 24 hours. Excess H_2O was removed under vacuum, and 10 cm^3 of dichloromethane was added and solids were removed via filtration. The solution was dried over magnesium sulfate and excess solvent removed to a yield liquid.

Yield: 1.20 g (92%)

^{1}H NMR: ($CDCl_3$) δ = 1.53 (*m*, 6H), 2.43 (*m*, 4H), 2.75 (*t*, 2H, *J* = 5.7), 4.07 (*s*, 3H), 4.42(*t*, 2H, *J* = 5.7) 7.12 (*pt*, 1H, *J* = 1.8), 7.49 (*pt*, 1H, *J* = 1.8), 7.55 (*m*, 2H), 7.77 (*m*, 2H)

^{13}C NMR: ($CDCl_3$) δ = 24.0, 25.9, 36.5, 46.8, 57.8, 119.7, 122.0, 122.7, 123.1, 131.2, 131.8, 134.8, 144.6, 170.5

IR (neat): ṽ = 3146, 3107, 2934, 2852, 2804, 1627, 1580, 1455, 1384, 1328, 1248, 1138, 1116, 1052, 859, 798, 754, 730, 702, 678, cm^{-1}

ESI: [M^+] Calculated 194.1652, Observed 194.1659, [M^-] Calculated 181.9917, Observed 181.9912.

Synthesis of 1-(piperid-1-yl)ethyl-3-methyl imidazolium dicyanamide [9c]

Synthetic procedure followed that of [9b] with the replacement of the sodium saccharinate with 0.42 g of sodium dicyanamide.

Yield: 0.91 g (93%)

^{1}H NMR: ($CDCl_3$) δ = 1.53 (*m*, 6H), 2.45 (*m*, 4H), 2.74 (*t*, 2H, J = 5.7), 4.04 (*s*, 3H), 4.29 (*t*, 2H, *J* = 5.7), 7.38 (*pt*, 1H, *J* = 1.8), 7.56 (*pt*, 1H, *J* = 1.8), **^{13}C NMR:** ($CDCl_3$) δ = 23.9, 25.8, 36.4, 54.5, 57.8, 119.7, 123.1, 123.2, 136.1

IR (neat): ṽ = 3100, 2935, 2852, 2797, 2227, 2192, 2125, 1666, 1572, 1455, 1352, 1303, 1166, 1121, 1039, 902, 859, 756 cm^{-1}

ESI: [M^+] Calculated 194.1652, Observed 194.1656, [M^-] Calculated 66.0098, Observed 66.0095.

Synthesis of 1-(piperid-1-yl)ethyl-3-methyl imidazolium trifluoroacetate [9d]

Synthetic procedure followed that of [9b] with the replacement of the sodium saccharinate with 0.65 g of sodium trifluoroacetate.

Yield: 1.03 g (90%)

^{1}H NMR: ($CDCl_3$) δ = 1.56 (*m*, 6H), 2.45 (*s*, br, 4H), 2.72 (*t*, 2H, *J* = 5.7), 3.92 (*s*, 3H), 4.32 (*t*, 2H, *J* = 5.7), 7.18 (*pt*, 1H, *J* = 1.7), 7.52 (*pt*, 1H, *J* = 1.5), 9.80 (*s*, 1H)

^{13}C NMR: ($CDCl_3$) δ = 23.9, 25.6, 35.9, 54.1, 57.6, 110.9 (*q*, *J* = 294), 122.7, 122.9, 136.9, 160.8 (*q*, *J* = 34)

^{19}F NMR: ($CDCl_3$) δ = -75.4 (*s*)

IR (neat): ṽ = 3149, 3094, 2938, 2855, 1677, 1573, 1456, 1444, 1354, 1303, 1285, 1258, 1193, 1167, 1117, 1039, 1008, 963, 924, 859, 821, 799, 756, 715, 668 cm^{-1}

ESI: [M^+] Calculated 194.1652, Observed 194.1662, [M^-] Calculated 112.9856, Observed 112.9855.

Synthesis of 1-(piperid-1-yl)ethyl-3-methyl imidazolium trifluoromethane sulfonate [9e]

Synthetic procedure followed that of [9b] with the replacement of the sodium saccharinate with 0.80 g of sodium trifluoromethane sulfonate. This yielded a yellow/brown waxy solid.

Yield: 1.11 g (85%)

^{1}H NMR: ($CDCl_3$) δ = 1.55 (*m*, 6H), 2.42 (*s*, br, 4H), 2.69 (*t*, 2H, *J* = 5.7), 3.97 (*s*, 3H), 4.26 (*t*, 2H, *J* = 5.7), 7.29 (*pt*, 1H, *J* = 1.7), 7.51 (*pt*, 1H, *J* = 1.7), 9.10 (*s*, 1H)

^{13}C NMR: ($CDCl_3$) δ = 23.9, 25.7, 36.1, 46.5, 54.2, 57.6, 114.0 (*q*, *J* = 320), 122.4, 122.7, 138.1,

^{19}F NMR: ($CDCl_3$) δ = -78.5 (*s*)

IR (neat): $\tilde{\nu}$ = 3149, 3098, 2937, 2888, 1574, 1463, 1338, 1252, 1222, 1165, 1157, 1125, 1026, 963, 857, 756 cm^{-1}

ESI: [M^+] Calculated 194.1652, Observed 194.1658, [M^-] Calculated 148.9526, Observed 148.9524.

Synthesis of 1-(morphol-4-yl)ethyl-3-methylimidazolium bis (triflimide) [10a]

1-methylimidazole (5 cm^3) was dissolved in 20 cm^3 of anhydrous ethanol, to which 11.66 g of 4-(2-chloroethyl)morpholine was added and refluxed at 80 ^{o}C for 18 hours. A hot filtration was then performed on the mixture to isolate any of the hydrochloride starting material. The filtrate was reduced down under vacuum to yield a yellow crude product which was then washed with 3 × 20 cm^3 of dichloromethane to yield the white 1-(morphol-4-yl)ethyl-3-methyl imidazolium chloride hydrochloride salt.

1 g of the 1-(morphol-4-yl)ethyl-3-methyl imidazolium salt was dissolved in 20 cm^3 of deionised H_2O. 0.28 g of NaOH was added and stirred until completely dissolved. 1.6 g of bis (trifluoromethane sulfonyl) imide lithium salt was added and the solution stirred at room temperature overnight. The resulting two layers were separated. The bottom layer was dissolved in 10 cm^3 of dichloromethane and washed with 3 × 25 cm^3

deionised water. The solution was dried over magnesium sulfate and excess solvent removed to yield a yellowish ionic liquid.

Yield: 1.58 g (89%)

^{1}H NMR: ($CDCl_3$) δ = 2.49 (*t*, 4H, *J* = 4.3), 2.74 (*t*, 2H, *J* = 5.6), 3.66 (*t*, 4H, *J* = 4.3), 3.93 (*s*, 3H), 4.24 *(t*, 2H, *J* = 5.7), 7.26 (*pt*, 1H, *J* = 1.7), 7.45 (*pt*, 1H, *J* = 1.7), 8.79 (*s*, 1H)

^{19}F NMR: ($CDCl_3$) δ = -79.0 (*s*)

^{13}C NMR: ($CDCl_3$) δ = 36.3, 46.5, 53.2, 57.2, 66.7, 113.4 (*q*, *J* = 320), 123.1, 136.4, 121.9

IR (neat): ṽ = 3157, 3118, 2962, 2855, 2820, 1574, 1456, 1347, 1329, 1132, 1112, 1050, 930, 912, 855, 788, 739 cm^{-1}

ESI: [M^+] Calculated 196.1444, Observed 196.1452, [M^-] Calculated 279.9178, Observed 279.9183

Synthesis of 1-(morphol-4-yl)ethyl-3-methyl imidazolium saccharinate. [10b]

Initial procedure of synthesis was similar to [10a] to generate the hydrochloride salt. After this, 1 g of IL-Cl was dissolved in deionised H_2O and 0.28 g of NaOH was added and stirred until no solids remained. 0.93 g of sodium saccharinate was added and the solution was stirred for 24 hours. Excess H_2O was removed under vacuum, and 10 cm^3 of dichloromethane was added and solids were removed via filtration. The solution was dried over magnesium sulfate and excess solvent removed to yield liquid.

Yield: 1.26 g (89%)

^{1}H NMR: ($CDCl_3$) δ = 2.47 (*t*, 4H, *J* = 4.3), 2.75 (*t*, 2H, *J* = 5.7), 3.61 (*t*, 2H, *J* = 4.3), 4.14 (*s*, 3H), 4.43 (*t*, 2H, *J* = 5.7), 7.28 (*pt*, 1H, *J* = 1.7), 7.47 (*pt*, 1H, *J* = 1.7) 7.57 (*m*, 2H), 7.73 (*m*, 2H)

^{13}C NMR: ($CDCl_3$) δ = 36.5, 46.4, 53.3, 57.6, 66.8, 119.7, 122.5, 123.1, 131.3, 132.0, 134.8, 138.5, 144.6, 170.4

IR (neat): ṽ = 3148, 3105, 2959, 2856, 2816, 1627, 1579, 1455, 1353, 1329, 1249, 1138, 1111, 1069, 10052, 1035, 1017, 946, 854, 798, 756, 679, 702, 654 cm^{-1}

ESI: $[M^+]$ Calculated 196.1444, Observed 196.1452, $[M^-]$ Calculated 181.9917, Observed 181.9913

Synthesis of 1-(morphol-4-yl)ethyl-3-methyl imidazolium dicyanamide. [10c]

Synthetic procedure followed that of [10b] with the replacement of the sodium saccharinate with 0.42 g of sodium dicyanamide.

Yield: 0.85 g (87%)

^{1}H NMR: ($CDCl_3$) δ = 2.40 (*t*, 4H, *J* = 4.3), 2.68 (*t*, 2H, *J* = 5.7), 3.56 (*t*, 4H, *J* = 4.3), 3.89 (*s*, 3H), 4.20 (*t*, 2H, *J* = 5.7), 7.31 (*pt*, 1H, *J* = 1.7), 7.45 (*pt*, 1H, *J* = 1.7), 8.97 (*s*, 1H)

^{13}C NMR: ($CDCl_3$) δ = 36.4, 46.5, 57.2, 66.6, 119.6, 123.1, 123.1, 136.5

IR (neat): ṽ = 3148, 3107, 2959, 2856, 2817, 2227, 2192, 2125, 1571, 1454, 1355, 1299, 1168, 1145, 1111, 1069, 1034, 1017, 929, 911, 853, 767, 666 cm^{-1}

ESI: $[M^+]$ Calculated 196.1444, Observed 196.1452, $[M^-]$ Calculated 66.0098, Observed 66.0096

Synthesis of 1-(morphol-4-yl)ethyl-3-methyl imidazolium trifluoroacetate [10d]

Synthetic procedure followed that of [10b] with the replacement of the sodium saccharinate with 0.65 g of sodium trifluoroacetate.

Yield: 1.04 g (91%)

^{1}H NMR: ($CDCl_3$) δ = 2.50 (*t*, 4H, *J* = 4.4), 2.76 (*t*, 2H, *J* = 5.6), 3.67 (*t*, 4H, *J* = 4.4), 4.00 (*s*, 3H), 4.38 (*t*, 2H, *J* = 5.6), 7.22 *(t*, 1H, *J* = 1.8), 7.45 (*t*, 1H, *J* = 1.8), 10.21 (*s*, 1H)

^{19}F NMR: ($CDCl_3$) δ = -75.3 (*s*)

^{13}C NMR: ($CDCl_3$) δ = 36.2, 46.2, 53.2, 57.5, 66.7, 115.1(*q*, *J* = 320), 122.6, 122.7, 138.4 160.6 (*q*, *J* = 34)

IR (neat): ν̃ = 3151, 3101, 2963, 2858, 2819, 1681, 1573, 1456, 1427, 1358, 1337, 1299, 1277, 1197, 1168, 1110, 1070, 1035, 1018, 930, 913, 854, 821, 799, 768, 716, 653 cm^{-1}

ESI: [M^+] Calculated 196.1444, Observed 196.1452, [M^-] Calculated 112.9856, Observed 112.9854

Synthesis of 1-(morphol-4-yl)ethyl-3-methyl imidazolium trifluoromethane sulfonate [10e]

Synthetic procedure followed that of [11b] with the replacement of the sodium saccharinate with 0.80 g of sodium trifluoromethane sulfonate. This yielded a yellow/brown waxy solid.

Yield: 1.20 g (93%)

^{1}H NMR: ($CDCl_3$) δ = 2.50 (*t*, 4H, *J* = 4.4), 2.76 (*t*, 2H, *J* = 5.6), 3.66 (t, 4H, *J* = 4.4), 3.96 (*s*, 3H), 4.29 (*t*, 2H, *J* = 5.4), 7.36 (*pt*, 1H, *J* = 1.8), 7.52 (*pt*, 1H, *J* = 1.8), 9.04 (*s*, 1H).

^{19}F NMR: ($CDCl_3$) δ = -78.4 (s)

^{13}C NMR: ($CDCl_3$) δ = 36.3, 46.4, 53.2, 57.3, 66.8, 114.0 (*q*, *J* = 320) 123.0, 137.0

IR (neat): ν̃ = 3153, 3115, 2960, 2859, 2816, 1573, 1456, 1357, 1337, 1252, 1223, 1147, 1112, 1070, 1027, 930, 912, 854, 767, 755, 702, 667, 654 cm^{-1}

ESI: [M^+] Calculated 196.1444, Observed 196.1450, [M^-] Calculated 148.9526, Observed 148.9527

Synthesis of 1-(pyrrolid-1-yl)ethyl-3-methylimidazolium bis (triflimide) [11a]

5 cm^3 of 1-methyl imidazole was dissolved in 20 cm^3 of anhydrous ethanol. 10.66 g of 1-(2-chloroethyl) pyrrolidine was added to the vessel and refluxed at 80 ^oC for 18 hours. A hot filtration was then performed on the mixture to isolate any of the hydrochloride starting material. The filtrate was reduced down under vacuum to yield a yellow crude product which was then washed with 3 × 20 cm^3 of dichloromethane to yield the white 1-(pyrrolid-1-yl)ethyl-3-methyl imidazolium chloride hydrochloride salt.

1 g of the 1-(pyrrolid-1-yl)ethyl-3-methyl imidazolium salt was dissolved in 20 cm^3 of deionised H_2O. 0.20 g of NaOH was added and stirred until completely dissolved. 1.3 g of bis (trifluoromethane sulfonyl) imide lithium salt was added and the solution stirred at room temperature overnight. The resulting two layers were separated. The bottom layer was dissolved in 10 cm^3 of dichloromethane and washed with 3 × 25 cm^3 deionised water. The solution was dried over magnesium sulfate and excess solvent removed to yield a yellowish ionic liquid.

Yield: 1.71 g (93%)

^{1}H NMR: ($CDCl_3$) δ = 1.78 (*m*, 4H), 2.55 (*m*, 4H), 2.89 (*t*, 2H, *J* = 5.6), 4.23 (*s*, 3H, 4.23 (*t*, 2H, *J* = 5.6), 7.28 (*pt*, 1H, *J* = 1.7), 7.44 (*pt*, 1H, *J* = 1.7), 8.69 (*s*, 1H)

^{13}C NMR: ($CDCl_3$) δ = 23.5, 36.2, 48.5, 53.7, 54.7, 113.4 (q, = 320), 123.1, 136.1

^{19}F NMR: ($CDCl_3$) δ = -79.1 (s)

IR (neat): $\tilde{\nu}$ = 3157, 3113, 2962, 2859, 2820, 1574, 1456, 1347, 1329, 1222, 1174, 1132, 1112, 1050, 930, 912, 855, 788, 758, 739 cm^{-1}

ESI: [M^+] Calculated 180.1495, Observed 180.1503, [M^-] Calculated 279.9178, Observed 279.9179.

Synthesis of 1-(pyrrolid-1-yl)ethyl-3-methyl imidazolium saccharinate [11b]

Initial procedure of synthesis was similar to [11a] to generate the hydrochloride salt. After this, 1 g of IL-Cl was dissolved in deionised H_2O and 0.20 g of NaOH was added and stirred until no solids remained. 0.93 g of sodium saccharinate was added and the

solution was stirred for 24 hours. Excess H_2O was removed under vacuum, and 10 cm^3 of dichloromethane was added and solids were removed via filtration. The solution was dried over magnesium sulfate and excess solvent removed to yield liquid.

Yield: 1.22 g (84%)

^{1}H NMR: ($CDCl_3$) δ = 1.70 (*m*, 4H), 2.52 (*s*, br, 4H), 2.83 (*t*, 2H, *J* = 5.6), 3.94 (s, 3H), 4.32 (*t*, 2H, *J* = 5.6), 7.21 (*pt*, 1H, *J* = 1.7), 7.40 (*pt*, 1H, *J* = 1.7) 7.53 (*m*, 2H), 7.74 (*m*, 2H), 9.64 (*s*, 1H)

^{13}C NMR: ($CDCl_3$) δ = 23.5, 36.4, 48.3, 53.7, 54.9, 119.7, 122.6, 122.6, 123.8, 131.4, 132.0, 134.6, 137.8, 144.5, 170.4

IR (neat): ṽ = 3149, 3103, 2964, 2802, 2794, 1626, 1579, 1455, 1329, 1248, 1137, 1116, 1052, 945, 854, 755, 731, 703, 679, 654 cm^{-1}

ESI: [M^+] Calculated 180.1495, Observed 180.1500, [M^-] Calculated 181.9917, Observed 181.9922.

Synthesis of 1-(pyrrolid-1-yl)ethyl-3-methyl imidazolium dicyanamide [11c]

Synthetic procedure followed that of [11b] with the replacement of the sodium saccharinate with 0.42 g of sodium dicyanamide.

Yield: 0.91 g (93%)

^{1}H NMR: ($CDCl_3$) δ = 2.48 (*m*, 4H), 2.84 (*t*, 2H, *J* = 5.6), 3.92 (*s*, 3H), 4.21 (*t*, 2H, *J* = 5.6), 7.33 (*pt*, 1H, *J* = 1.7), 7.46 (*pt*, 1H, *J* = 1.7), 9.01 (*s*, 1H)

^{13}C NMR: ($CDCl_3$) δ = 23.6, 36.5, 48.7, 53.8, 54.7, 119.8, 123.1, 123.2, 136.5

IR (neat): ṽ = 3150, 3101, 2961, 2799, 2225, 2190, 2123, 1570, 1458, 1303, 1166, 1055, 935, 902, 849, 750, 703 cm^{-1}

ESI: [M^+] Calculated 180.1495, Observed 180.1505, [M^-] Calculated 66.0098, Observed 66.0099

Synthesis of 1-(pyrrolid-1-yl)ethyl-3-methyl imidazolium trifluoroacetate [11d]

Synthetic procedure followed that of [11b] with the replacement of the sodium saccharinate with 0.65 g of sodium trifluoroacetate.

Yield: 1.08 g (93%)

^{1}H NMR: ($CDCl_3$) δ = 1.77(*m*, 4H), 2.58(*m*, 4H), 2.92(*t*, 2H, *J* = 5.6), 3.97 (*s*, 3H), 4.35 (*t*, 2H, *J* = 5.6), 7.27 (*pt*, 1H, *J* = 1.7), 7.50(*pt*, 2H, *J* = 1.7), 9.93 (*s*, 1H)

^{13}C NMR: ($CDCl_3$) δ = 23.5, 36.2, 48.2, 53.7, 54.9, 113.2 (*q*, *J* = 294), 122.6, 138.2 160.9 (*q*, *J* = 33)

^{19}F NMR: ($CDCl_3$) δ = -78.8 (s)

IR (neat): ṽ = 3151, 3099, 2966, 2806, 1673, 1573, 1459, 1427, 1352, 1294, 1196, 1167, 1116, 822, 799, 758, 715, 657 cm^{-1}

ESI: [M^+] Calculated 180.1495, Observed 180.1501, [M^-] Calculated 112.9856, Observed 112.9855

Synthesis of 1-(pyrrolid-1-yl)ethyl-3-methyl imidazolium trifluoromethane sulfonate [11e]

Synthetic procedure followed that of [11b] with the replacement of the sodium saccharinate with 0.80 g of sodium trifluoromethane sulfonate. This yielded a yellow/brown waxy solid.

Yield: 1.17 g (91%)

^{1}H NMR: ($CDCl_3$) δ = 1.78(*m*, 4H), 2.56(*m*, 4H), 2.90(*t*, 2H, *J* = 5.6), 3.97 (*s*, 3H), 4.35 (*t*, 2H, *J* = 5.6), 7.28 (*pt*, 1H, *J* = 1.7), 7.47(*pt*, 2H, *J* = 1.7), 9.16 (*s*, 1H)

^{19}F NMR: ($CDCl_3$) δ = -78.2 (s)

^{13}C NMR: ($CDCl_3$) δ = 23.5, 36.2, 48.2, 53.7, 54.7, 114.2 (*q*, *J* = 320), 122.9, 123.1, 136.7.

IR (KBr): $\tilde{\nu}$ = 3158, 3117, 2958, 2860, 2809, 2733, 1576, 1476, 1442, 1362, 1326, 1276, 1223, 11923, 1170, 1131, 1046, 1028, 967, 927, 859, 763 cm^{-1}

ESI: $[M^+]$ Calculated 180.1495, Observed 180.1501, $[M^-]$ Calculated 148.9526, Observed 148.9531

2.3.4 Synthesis of ionic liquids [12a-16b]

Synthesis of trioctyl(1-(piperid-1-yl)ethyl)phosphonium bis(triflimide) [12a]

1-(2-chloroethyl)piperidine hydrochloride (3.6 g) was added to 20 cm^3 of ethanol. 8 cm^3 of trioctylphosphine was then added and refluxed at 80 ºC for 24 hours. A hot filtration was performed to remove solid starting material and the excess ethanol was removed under reduced pressure. The oil was dissolved in methanol and washed with 3 × 10 cm^3 of hexane after which the excess hexane was removed to yield the chloride salt.

The chloride precursor (3 g) was dissolved in 10 cm^3 of methanol and 0.26 g of NaOH in 5 cm^3 of water was added. After 10 minutes 1.86 g of lithium bis(triflimide) in 5 cm^3 of water was added and the mixture stirred for 24 hours. The solvent was removed until 5 cm^3 of the liquid remained. Dichloromethane (15 cm^3) was added and the solution was washed with 3 × 10 cm^3 of deionised water. This was dried over $MgSO_4$ and the dichloromethane removed under reduced pressure to yield a clear oil.

Yield: 3.98 g (96%).

^{1}H NMR: ($CDCl_3$) δ = 0.88 (*t*, 9H, *J* = 6.4), 1.28 (*m*, 42H), 2.15 (*m*, 6H), 2.36 (*m*, 6H), 2.63 (*dt*, 2H, *J* = 19.6, 6.0).

^{13}C NMR: ($CDCl_3$) δ = 14.1, 17.0(*d*, *J* = 49), 19.6 (*d*, *J* = 47), 21.5 (d, *J* = 4), 22.5, 23.9, 25.8, 28.7, 28.9, 30.5, 31.6, 51.4 (d, *J* = 5), 54.5, 113.4 (q, *J* = 321).

^{19}F NMR: ($CDCl_3$) δ = -78.7 (*s*).

^{31}P NMR: ($CDCl_3$) δ = 33.6 (*s*).

IR (KBr): ṽ = 2931, 2857, 1467, 1412, 1352, 1332, 1225, 1180, 1137, 1058, 877, 788, 761, 739, 653, 617, 600, 570, 513 cm^{-1}.

ESI: $[M^+]$ Calculated 482.4849, Observed 482.4847, $[M^-]$ Calculated 279.9178, Observed 279.9173.

Synthesis of trioctyl(1-(piperid-1-yl)ethyl)phosphonium dicyanamide [12b]

The synthesis of [12b] followed that as outlined in [12a] with 2 g of the chloride precursor, 0.18 g of NaOH, and 0.4 g of sodium dicyanamide.

Yield: 2.30 g (84%).

^{1}H NMR: ($CDCl_3$) δ = 0.81 (*t*, 9H, *J* = 6.4), 1.21 (*m*, 42H), 2.15 (*m*, 6H), 2.41 (*m*, 6H), 2.57 (*dt*, 2H, *J* = 19.6, 6.0).

^{13}C NMR: ($CDCl_3$) δ = 14.0, 17.0(*d*, *J* = 49.9), 19.1 (*d*, *J* = 47.1), 21.6 (*d*, *J* = 4.7), 22.5, 23.9, 25.8, 28.7, 28.9, 30.6, 31.6, 51.3 (*d*, *J* = 5.7), 54.5, 119.9.

^{31}P NMR: ($CDCl_3$) δ = 33.6 (*s*).

IR (KBr): ṽ = 2928, 2856, 2226, 2189, 2127, 1466, 1411, 1377, 1351, 1309, 1274, 1228, 1196, 1155, 1123, 1033, 878, 747, 664, 524 cm^{-1}.

ESI: $[M^+]$ Calculated 482.4849, Observed 482.4863, $[M^-]$ Calculated 66.0098, Observed 66.0099.

Synthesis of trioctyl(1-(piperid-1-yl)ethyl)phosphonium trifluoroacetate [12c]

The synthesis of [12c] followed that as outlined in [12a] with 0.5 g of the chloride precursor, 0.06 g of NaOH, and 0.3 g of sodium trifluoroacetate.

Yield: 0.62 g (90%).

^{1}H NMR: ($CDCl_3$) δ = 0.81 (t, 9H, J = 6.4), 1.21 (m, 42H), 2.15 (m, 6H), 2.41 (m, 6H), 2.57 (dt, 2H, J = 19.6, 6.0).

^{13}C NMR: ($CDCl_3$) δ = 14.0, 16.7 (*d*, *J* = 49), 18.9 (*d*, *J* = 47), 21.7 (*d*, *J* = 4), 22.5, 23.9, 25.8, 28.7, 28.9, 30.6 (*d*, *J* = 14.0), 31.6, 51.3 (*d*, *J* = 5), 54.5, 113.2 (*q*, *J* = 294), 160.9 (*q*, *J* = 33).

^{31}P NMR: ($CDCl_3$) δ = 33.3 (*s*).

IR (KBr): ṽ = 2929, 2853, 1687, 1459, 1423, 1378, 1352, 1314, 1264, 1176, 1128, 1068, 988, 963, 876, 817, 800, 718 cm^{-1}.

ESI: [M^+] Calculated 482.4849, Observed 482.4866, [M^-] Calculated 112.9856, Observed 112.9851.

Synthesis of trioctyl(1-(piperid-1-yl)ethyl)phosphonium trifluoromethane sulfonate [12d]

The synthesis of [12d] followed that as outlined in [12a] with 0.5 g of the chloride precursor, 0.06 g of NaOH, and 0.25 g of sodium trifluoromethanesulfonate.

Yield: 0.52 g (91%).

^{1}H NMR: ($CDCl_3$) δ = 0.88 (*t*, 9H, *J* = 6.4), 1.27 (*m*, 42H), 2.23 (*m*, 6H), 2.49 (*m*, 6H), 2.62 (*dt*, 2H, *J* = 19.6, 6.0).

^{13}C NMR: ($CDCl_3$) δ = 13.0, 16.0 (*d*, *J* = 49), 18.1 (*d*, *J* = 47), 20.7 (*d*, *J*= 4), 21.5, 22.9, 24.8, 27.9, 29.7, 30.6 (*d*, *J* = 14), 31.6, 50.5 (d, J = 5), 53.5, 114.0 (*q*, *J* = 321).

^{19}F NMR: ($CDCl_3$) δ = -78.3(*s*)

^{31}P NMR: ($CDCl_3$) δ = 33.4 (*s*).

IR (KBr): ṽ = 2925, 2856, 1468, 1460, 1414, 1379, 1350, 1267, 1224, 1151, 1119, 1029, 637 cm^{-1}.

ESI: [M^+] Calculated 482.4849, Observed 482.4875, [M^-] Calculated 148.9526, Observed 148.9522.

Synthesis of trioctyl(1-(piperid-1-yl)ethyl)phosphonium saccharinate [12e]

The synthesis of [12e] followed that as outlined in [12a] with 0.5 g of the chloride precursor, 0.06 g of NaOH, and 0.25 g of sodium sacharinate.

Yield: 0.55 g (92%).

^{1}H NMR: ($CDCl_3$) δ = 0.78 (*t*, 9H, *J* = 6.4), 1.15 (*m*, 42H), 2.30 (*m*, 12H), 2.51 (*dt*, 2H, J = 19.6, 6.0), 7.43 (*m*, 2H), 7.64 (*m*, 2H).

^{13}C NMR: ($CDCl_3$) δ = 14.0, 17.0 (*d*, *J* = 49), 19.1 (*d*, *J* = 47), 21.6 (*d*, *J*= 4), 22.4, 23.9, 25.7, 28.7, 28.8, 30.6 (*d*, *J* = 14), 31.6, 51.5 (*d*, *J* = 5), 54.3, 119.3, 122.9, 130.7, 131.4, 135.0, 145.0, 169.7

^{31}P NMR: ($CDCl_3$) δ = 33.3 (*s*).

IR (KBr): ṽ = 2928, 2856, 1636, 1583, 1466, 1456, 1415, 1378, 1350, 1325, 1272, 1200, 1145, 1117, 1054, 947, 858, 766, 752, 604 cm^{-1}.

ESI: [M^+] Calculated 482.4849, Observed 482.4872, [M^-] Calculated 181.9917, Observed 181.9912.

Synthesis of (1-(morphol-4-yl)ethyl)trioctylphosphonium bis(triflimide) [13a]

1-(2-chloroethyl)piperidine hydrochloride (2.5 g) was added to 20 cm^3 of ethanol. 6 cm^3 of trioctylphosphine was then added and refluxed at 80 ºC for 24 hours. A hot filtration was performed to remove solid starting material and the excess ethanol was removed under reduced pressure. The oil was dissolved in methanol and washed with 3 × 10 cm^3 of hexane after which the excess hexane was removed to yield the chloride salt.

The chloride precursor (0.75 g) was dissolved in 10 cm^3 of methanol and 0.08 g of NaOH in 5 cm^3 of water was added. After 10 minutes 0.5 g of lithium bis(triflimide) in 5 cm^3 of water was added and the mixture stirred for 24 hours. The solvent was removed until 5 cm^3 of the liquid remained. Dichloromethane (15 cm^3) was added and the solution was washed with 3 × 10 cm^3 of deionised water. This was dried over $MgSO_4$ and the dichloromethane removed under reduced pressure to yield a clear oil.

Yield: 0.81 g (78 %).

^{1}H NMR: ($CDCl_3$) δ = 0.89 (*t*, 9H, *J* =7.0), 1.28 (*m*, 36H), 2.26 (*m*, 6H), 2.57 (*m*, 6H), 2.71-2.81 (*dt*, 2H, *J* = 19.6, 6.0), 3.69 (*t*, 4H, *J* = 4.7)

^{13}C NMR: ($CDCl_3$) δ = 14.0, 16.5 (*d*, *J* = 49), 18.9 (*d*, *J* = 47), 21.5 (*d*, *J* = 4), 22.5, 28.7, 28.9, 30.5 (*d*, *J* = 15), 31.6, 51.4 (*d*, *J* = 5), 53.5, 66.4 115.1 (*q*, *J* = 321).

^{19}F NMR: ($CDCl_3$) δ = -78.7 (*s*).

^{31}P NMR: ($CDCl_3$) δ = 33.7 (*s*).

IR (KBr): ṽ = 2930, 2857, 1467, 1413, 1352, 1332, 1266, 1225, 1195, 1137, 1058, 877, 788, 761, 739, 653, 617, 600, 570, 513 cm^{-1}.

ESI: [M^+] Calculated 484.4642, Observed 484.4658, [M^-] Calculated 279.9178, Observed 279.9168.

Synthesis of (1-(morphol-4-yl)ethyl)trioctylphosphonium dicyanamide [13b]

The synthesis of [13b] followed that as outlined in [13a] with 0.75 g of the chloride precursor, 0.08 g of NaOH, and 0.2 g of sodium dicyanamide.

Yield: 0.64 g (89%).

^{1}H NMR: ($CDCl_3$) δ = 0.89 (*t*, 9H, *J* =7.0), 1.21-1.58 (*m*, 36H), 2.29 (*m*, 6H), 2.59 (*s*, br, 6H), 2.86 (*m*, 2H), 3.72 (*s*, br, 4H).

^{13}C NMR: ($CDCl_3$) δ = 14.0, 17.8 (*d*, *J* = 49), 19.1 (*d*, *J* = 47), 21.6 (*d*, J = 4), 22.5, 28.8, 28.9, 30.7 (*d*, *J* = 15), 31.6, 51.2 (*d*, *J* = 5), 53.5, 119.9.

^{31}P NMR: ($CDCl_3$) δ = 33.6 (*s*).

IR (KBr): ṽ = 2955, 2928, 2855, 2226, 2188, 2127, 1459, 1410, 1377, 1357, 1307, 1240, 1142, 1118, 1070, 1034, 878, 747, 664, 524 cm^{-1}.

ESI: [M^+] Calculated 484.4642, Observed 484.4669, [M^-] Calculated 66.0098, Observed 66.0095

Synthesis of 3-aminopropyl(trioctyl)phosphonium bis(triflimide) [14a]

Trioctylphosphine (3 cm^3) was added to 1.83 g of 3-bromopropylamine hydrobromide in 20 cm^3 of ethanol and refluxed at 78 ^oC for 48 hours. Excess ethanol was removed under reduced pressure. The product was dissolved in 10 cm^3 of methanol and washed with 3 × 10 cm^3 of hexane. The product was dissolved in 10 cm^3 of hexane and washed with 3 × 10 cm^3 of deionised water. The organic layer was dried over $MgSO_4$ and excess solvent removed to yield viscous liquid.

0.5 g of the bromo precursor was dissolved in 10 cm^3 of methanol. KOH was added until a pH of 10 was achieved. Lithium bis(triflimide) (0.35 g) was added and the solution stirred overnight .Excess solvent was removed under reduced pressure. Dichloromethane (10 cm^3) was added and washed with 3 × 10 cm^3 of deionised water. The organic layer was dried over $MgSO_4$ and excess solvent removed to yield colourless oil.

Yield: 0.64 g (89%).

^{1}H NMR: ($CDCl_3$) δ = 0.88(*t*, 9H, *J* = 7.0), 1.27 - 1.78 (*m*, 38H), 2.07 – 2.31(*m*, 10H) 2.85 (*t*, 2H, *J* = 5.6)

^{19}F NMR: ($CDCl_3$) δ = -78.9 (*s*)

^{13}C NMR: ($CDCl_3$) δ = 14.0, 16.0 (*d*, *J* = 49), 18.4 (*d*, *J* = 47), 21.5(*d*, *J* = 5), 22.5, 24.6 (*d*, *J* = 5), 28.7, 28.9, 30.5 (*d*, *J* = 15), 31.6, 41.5 (d, *J* = 19), 112.8 (*q*, *J* = 320)

^{31}P NMR: ($CDCl_3$) δ = 33.6 (*s*)

IR (KBr): ṽ =3410, 3367, 2930, 2858, 2736, 1580, 1466, 1351, 1225, 1194, 1137, 1058, 788, 739, 618, 570, 514 cm^{-1}.

ESI: [M^+] Calculated 428.4380, Observed 428.4386, [M^-] Calculated 279.9178, Observed 279.9168

Synthesis of 3-aminopropyl(trioctyl)phosphonium dicyanamide [14b]

The procedure followed that as outlined for ionic liquid [14a], using 0.50 g of the bromide precursor, and 0.20 g of sodium dicyanamide.

Yield: 0.39 g (93%).

^{1}H NMR: ($CDCl_3$) δ = 0.88 (*t*, 9H, *J* = 7.0), 1.28 – 1.71 (*m*, 40H), 2.19 (*m*, 6H), 2.37 (*m*, 2H), 2.89 (*t*, 2H, *J* = 5.6)

^{13}C NMR: ($CDCl_3$) δ = 14.0, 16.0 (*d*, *J* = 49), 18.7 (*d*, *J* = 47), 21.6 (*d*, *J* = 5), 22.5, 24.8 (*d*, *J* = 5), 28.8, 28.9, 30.6 (*d*, *J* = 15), 31.8, 41.7 (*d*, *J* = 19), 119.2

^{31}P NMR: ($CDCl_3$) δ = 33.4 (*s*)

IR (KBr): $\tilde{\nu}$ = cm^{-1} 3406, 3383, 1955, 2929, 2857, 2230, 2191, 2131, 1624, 1157, 1466, 1351, 1332, 1225, 1191, 1137, 1058, 894, 789, 652, 617, 600, 570, 514 cm^{-1}

ESI: [M^+] Calculated 428.4380, Observed 428.4386, [M^-] Calculated 66.0098, Observed 66.0097

Synthesis of but-3-yn-1-yl(trioctyl)phosphonium bromide [15a]

Trioctylphosphine (2.40 cm^3) was added to 4-bromo-1-butyne (0.5 cm^3) in ethanol (10cm^3) and refluxed at 78 ^{o}C for 48 hours. Excess solvent was removed from the vessel, afterwhich the product was dissolved in warm hexane (5 cm^3) and extracted and extracted with 3 x 10 cm^3 of acetonitrile. The excess solvent was removed to yieldwaxy white solid.

Yield: 2.53 g (93%)

^{1}H NMR: ($CDCl_3$) δ = 0.88 (*t*, 9H, *J* = 7.0), 1.27 – 1.68 (*m*, 36H), 2.14 (*t*, 1H, *J* = 2.6), 2.47 – 2.56 (*m*, 6H), 2.72 – 2.82 (*m*, 2H), 2.89 – 2.91 (*m*, 2H).

^{13}C NMR: ($CDCl_3$) δ = 12.1 (*d*, *J* = 5), 13.3, 18.0 (*d*, *J* = 48), 19.2 (*d*, *J* = 46), 21.6 (*d*, *J* = 4), 22.3, 28.7, 28.8, 30.5 (*d*, *J* = 15), 31.4, 71.7, 80.8 (*d*, *J* = 6)

^{31}P NMR: ($CDCl_3$) δ = 33.8 (*s*).

IR (KBr): ṽ = 3417, 3314, 3296, 3192, 2956, 2912, 1854, 2115, 1617, 1466, 1427, 1378, , 1341, 1263, 1243, 1205, 1170, 1101, 1059, 1033, 1012, 949, 854, 824, 721, 710, 639, 627, 538, 516, 470 cm^{-1}.

ESI: $[M^+]$ Calculated 423.4114, Observed 423.4135, $[M^-]$ Calculated 78.9183, Observed 78.9185

Synthesis of but-3-yn-1-yl(trioctyl)phosphonium bis(triflimide) [15b]

[15a] (1.0 g) was dissolved in methanol and 0.56 g of lithium bis(triflimide) was added and stirred over night at room temperature. Excess methanol was removed under reduced pressure after which 10 cm^3 of dichloromethane was added to the sample. This was washed with 3 × 5 cm^3 of water, dried over $MgSO_4$ and excess solvent removed under vacuum to yield colourless oil.

Yield: 1.30 g (94%)

^{1}H NMR: ($CDCl_3$) δ = 0.88 (*t*, 9H, *J* = 7.0), 1.21 – 1.68 (*m*, 36H), 2.18 (*m*, 7H), 2.46 (*m*, 2H), 2.64 (*m*, 2H)

^{13}C NMR: ($CDCl_3$) δ = 12.1 (*d*, *J* = 5), 13.9, 17.1(*d*, *J* = 48), 19.3 (*d*, *J* = 46), 21.4 (*d*, *J* = 4), 22.5, 28.6, 28.8, 30.3 (*d*, *J* = 15), 31.6, 72.0, 80.2 (*d*, *J* = 6), 113.4 (*q*, *J* = 321)

^{19}F NMR: (CDCl3) δ = -78.8(*s*)

^{31}P NMR: ($CDCl_3$) δ = 34.2(*s*)

IR (KBr): ṽ = 3469, 3313, 3297, 2957, 2930, 2859, 2118, 1466, 1410, 1351, 1321, 1225, 1193, 1137, 1058, 950, 788, 762, 739, 724, 653, 617 cm^{-1}.

ESI: $[M^+]$ Calculated 423.4114, Observed 423.4133, $[M^-]$ Calculated 279.9178, Observed 279.9178

Synthesis of trioctyl(1-(pyrrol-1-yl)ethyl)phosphonium chloride [16a]

Trioctylphosphine (1.95 cm^3) was added to a solution of 1-(2-chloroethyl)pyrrole (0.5 cm^3) in 30 cm^3 of anhydrous DMF and refluxed for 48 hours at 90 ^oC. The excess DMF was removed under reduced pressure and the product was dissolved in 5 cm^3 of warm hexane. The product was then extracted using acetonitrile (10 cm^3) until no trace of the pyrrole precursor remained.

Yield: 0.72 g (79%).

^{1}H NMR: ($CDCl_3$) δ = 0.88 (*t*, 9H, *J* = 7.0), 1.26 - 1.49 (*m*, 36H), 2.17 (*m*, 6H), 3.32 (*m*, 2H), 4.41 - 4.51 (*dt*, 2H, *J* = 6.5, 18.4), 6.79 (*t*, 2H, *J* = 2.0), 6.16 (*t*, 2H, *J* = 2.0)

^{13}C NMR: ($CDCl_3$) δ = 12.1, 17.3 (*d*, *J* = 46), 19.9 (*d*, *J* = 47), 20.1 (*d*, *J* = 4), 20.6, 26.9, 27.0, 28.7 (*d*, *J* = 15), 29.7, 40.7 (*d*, *J* = 6), 107.8, 118.5.

^{31}P NMR: ($CDCl_3$) δ = 31.5 (*s*).

IR (KBr): ṽ = 2955, 2871, 2856, 1622, 1501, 1460, 1410, 1383, 1284, 1243, 1225, 1172, 1115, 1094, 1068, 1058, 1032, 1013, 858, 732, 713, 597cm^{-1}.

ESI: [M^+] Calculated 464.4380, Observed 464.4390

Synthesis of trioctyl(1-(pyrrol-1-yl)ethyl)phosphonium bis(triflimide) [16b]

Yield: 0.64 g (89%).

^{1}H NMR: ($CDCl_3$) δ = 0.88 (*t*, 9H, *J* = 6.9), 1.22-1.39 (*m*, 36H), 1.88 (*m*, 6H), 2.77 (*m*, 2H), 4.26-4.37 (*dt*, 2H, *J* = 6.5, 18.4), 6.18 (*t*, 2H, *J* = 2.0), 6.69 (*t*, 2H, *J* = 2.0)

^{19}F NMR: ($CDCl_3$) δ = -78.6 (*s*)

^{13}C NMR: ($CDCl_3$) δ = 13.0, 17.1 (*d*, *J* = 46), 20.1 (*d*, *J* = 4), 20.5 (*d*, *J* = 47), 21.5, 27.6, 27.8, 29.3 (*d*, *J* = 15), 30.6, 41.1 (*d*, *J* = 6), 109.1, 112.4 (*q*, *J* = 321), 120.97

^{31}P NMR: ($CDCl_3$) δ = 31.7 (*s*)

IR (KBr): ṽ = 2956, 2929, 2858, 1499, 1460, 1351, 1331, 1291, 1261, 1225, 1196, 1137, 1091, 1058, 801, 737, 654, 618, 570, 514 cm^{-1}.

ESI: [M^+] Calculated 464.4380, Observed 464.4396, [M^-] Calculated 279.9178, Observed 279.9174

2.3.5 Synthesis of ionic liquids [AAIL1-AAIL21]

Synthesis of 1-(piperid-1-yl) ethyl-3-methylimidazolium d-alaninate [AAIL1]

1 g of 1-(piperid-1-yl) ethyl-3-methyl imidazolium chloride hydrochloride salt was dissolved in 50 cm^3 of deionised H_2O. This was then passed through an amberlite IRA-400 OH form anion exchange resin column, approximately 150 mm in length, to remove the hydrochloride moiety.

The IL-Cl was then diluted down to a 2% w/v solution with deionised H_2O and chilled to 0^oC. This was then passed again through a column of amberlight anion exchange resin hydroxide form. The solution was then added drop wise to 0.55 g of d-alanine and the resulting mixture allowed stir for 24 hours. After this time the excess H_2O was removed under vacuum at temperature no higher than 50 ^oC. 20 cm^3 of 9:1 acetonitrile/methanol solution was added and stirred vigorously for 1 hour to precipitate excess free amino acid. This was then filtered before excess solvent was removed under vacuum to yield the ionic liquid.

Yield: 0.88 g (83%)

^{1}H NMR: (D_2O) δ = 1.13 (*d*, 3H, *J* = 7.0), 1.48 (*m*, 6H), 2.41 (m, 4H), 2.76 (*t*, 2H, *J* = 6.9), 3.23 (*q*, 1H, *J* = 7.0), 3.80 (*s*, 3H), 4.27 (*t*, 2H, *J* = 6.9), 7.35 (*d*, 1H, *J* = 1.9), 7.42 (*d*, 1H, *J* = 1.9)

^{13}C NMR: (D_2O) δ = 20.0, 23.1, 24.5, 35.6, 45.8, 51.3, 53.6, 57.0, 122.2, 123.6, 183.9

IR (KBr): ṽ = 3182, 3151, 3091, 2999, 2936, 2853, 2809, 1598, 1505, 1456, 1408, 1390, 1356, 1302, 1259, 1168, 1152, 1122, 1038, 1016, 963, 923, 857, 758, 748, 703, 6533, 620, 581, 570 cm^{-1}.

ESI: [M^+] Calculated 194.1652, Observed 194.1658, [M^-] Calculated 88.0404, Observed 88.0408

Synthesis of 1-(piperid-1-yl) ethyl-3-methyl imidazolium l-leucinate [AAIL2]

The initial preparation was similar to that mention previously [AAIL1], to prepare the chloride IL, however 1 g of 1-(piperid-1-yl)-3-methyl imidazolium chloride hydrochloride salt was reacted with 0.8 g of l-leucine. The work up was as that described above.

Yield: 1.05 g (82%)

^{1}H NMR: (D_2O) δ = 0.80 (*d*, 3H, *J* = 5.0), 0.82 (*d*, 3H, *J* = 5.0), 1.51 (*m*, 9H), 2.41 (*t*, 4H, *J* = 5.1), 2.75 (*t*, 2H, *J* = 6.9), 3.24 (*t*, 1H, *J* = 5.7), 3.80 (*s*, 3H), 4.26 (*t*, 2H, *J* = 6.9), 7.34 (*d*, 1H, J = 1.9), 7.42 (*d*, 1H, *J* = 1.9)

^{13}C NMR: (D_2O) δ = 20.3, 21.5, 22.3, 23.5, 23.7, 34.8, 42.5, 45.052.8, 56.2, 121.3, 122.8, 170.0

IR (neat): ṽ = 3371, 3282, 3144, 3090, 2934, 2855, 2801, 1571, 1467, 1455, 1442, 1382, 1351, 1302, 1282, 1256, 1170, 1106, 1098, 1076, 964, 921, 856, 756 cm^{-1}.

ESI: [M^+] Calculated 194.1652, Observed 194.1659, [M^-] Calculated 130.0874, Observed 130.0869

Synthesis of 1-(piperid-1-yl)ethyl-3-methyl imidazolium l-lysinate [AAIL3]

The initial preparation was similar to that mention previously [AAIL1], to prepare the chloride IL, however 1 g of 1-(piperid-1-yl)-3-methyl imidazolium chloride hydrochloride salt was reacted with 0.75 g of l-lysine. The work up of AAIL3 was as that described above.

Yield: 1.02 g (80%)

^{1}H NMR: (D_2O) δ = 1.42 (*m*, 12H), 2.41 (*t*, 4H, *J* = 5.1), 2.66 (*t*, 2H, *J* = 5.1), 2.78 (*t*, 2H, *J* = 7.0), 3.80 (*s*, 3H), 4.27 (*t*, 2H, *J* = 7.0), 7.35 (*d*, 1H, *J* = 1.9), 7.41 (*d*, 1H, *J* = 1.9)

^{13}C NMR: (D_2O) δ = 22.1, 23.1, 24.5, 29.7, 34.1, 35.6, 39.9, 45.8, 53.6, 55.8, 57.0, 122.2, 123.6, 183.0.

IR (neat): ṽ = 3350, 3265, 3140, 3140, 3068, 2930, 2851, 2801, 1563, 1445, 1433, 1386, 1352, 1302, 1170, 1120, 1083, 1039, 962, 921, 859, 814, 757, 702, 657 cm^{-1}.

ESI: [M^+] Calculated 194.1652, Observed 194.1658, [M^-] Calculated 145.0983, Observed 145.0979

Synthesis of 1-(piperid-1-yl)ethyl-3-methyl imidazolium d-glutaminate [AAIL4]

The initial preparation was similar to that mention previously [AAIL1], to prepare the chloride IL, however 1 g of 1-(piperid-1-yl)-3-methyl imidazolium chloride hydrochloride salt was reacted with 0.66 g of d-glutamine. The work up was as that described earlier.

Yield: 1 g (80%)

^{1}H NMR: (D_2O) δ = 1.23 -1.46 (*m*, 6H), 1.77 (*m*, 2H), 2.19 (*t*, 2H, *J* = 8.3), 2.38 (*s*, br, 4H), 2.72 (*t*, 2H, *J* = 7.0) , 3.15 (*t*, 1H, *J* = 6.5), 3.76 (*s*, 3H) 4.24 (*t*, 2H, *J* = 7.0), 7.31 (*d*, 1H, *J* = 1.7), 7.38 (*d*, 1H, *J* = 1.7)

^{13}C NMR: (D_2O) δ = 23.1, 24.5, 30.6, 31.6, 45.8, 53.6, 55.4, 122.1, 123.5, 179.1, 182.0

IR (KBr): ṽ = 3408, 2938, 2850, 1635, 1580, 1485, 1470, 1454, 1422, 1359, 1336, 1316, 1283, 1190, 1169, 1126, 1086, 1056, 1040, 1008, 926, 895, 860, 849, 810, 776, 757, 743, 706 cm^{-1}

ESI: [M^+] Calculated 194.1652, Observed 194.1661, [M^-] Calculated 145.0619, Observed 145.0617

Synthesis of 1-(piperid-1-yl)ethyl-3-methyl imidazolium d-asparaginate [AAIL5]

The initial preparation was similar to that mention previously [AAIL1], to prepare the chloride IL, however 1 g of 1-(piperid-1-yl)-3-methyl imidazolium chloride hydrochloride salt was reacted with 0.70 g of d-asparagine. The work up was as that described earlier.

Yield: 1.08 g (88%)

^{1}H NMR: (D_2O) δ = 1.23- 1.43 (*m*, 6H), 2.26-2.58 (*m*, 6H), 2.72 (*t*, 2H, *J* = 7.0), 3.27 (*t*, 1H, *J* = 4.7), 3.76 (*s*, 3H), 4.23 (*t*, 2H, *J* = 7.0), 7.31 (*d*, 1H, *J* = 1.7), 7.38 (*d*, 1H, *J* = 1.7)

^{13}C NMR: (D_2O) δ = 22.3, 23.7, 34.7, 39.3, 45.0, 52.8, 56.2, 121.3, 122.7, 175.7, 180.1

IR (neat): ṽ = 3345, 3291, 3146, 3088, 2932, 2852, 2805, 1664, 1563, 1464, 1382, 1351, 1300, 1282, 1253, 1168, 1121, 1038, 1008, 962, 920, 859, 756, 657 cm^{-1}.

ESI: [M^+] Calculated 194.1652, Observed 194.1654, [M^-] Calculated 131.0462, Observed 131.0463.

Synthesis of 1-(piperid-1-yl)ethyl-3-methyl imidazolium d-glycinate [AAIL6]

The initial preparation was similar to that mention previously [AAIL1], to prepare the chloride IL, however 1 g of 1-(piperid-1-yl)-3-methyl imidazolium chloride hydrochloride salt was reacted with 0.35 g of d-glycine. The work up was as that described earlier.

Yield: 0.82 g (81%)

^{1}H NMR: (D_2O) δ = 1.47 (*m*, 6H), 2.41 (*t*, 4H, *J* = 7.0), 2.76 (*t*, 2H, *J* = 4.7), 3.11 (*s*, 2H), 3.80 (*s*, 3H), 4.27 (*t*, 2H, *J* = 7.0), 7.34 (*d*, 1H, *J* = 1.9), 7.42 (*d*, 1H, *J* = 1.9)

^{13}C NMR: (D_2O) δ = 22.3, 23.7, 34.8, 43.4, 45.0, 52.8, 56.2, 121.3, 122.8, 179.8

IR (KBr): ṽ = 3348, 3265, 3144, 3077, 2932, 2852, 1568, 1455, 1440, 1387, 1353, 1302, 1170, 1118, 1084, 1038, 958, 922, 861, 820, 757 cm^{-1}.

ESI: [M^+] Calculated 194.1652, Observed 194.1657, [M^-] Calculated 74.0248, Observed 74.0245

Synthesis of 1-(piperid-1-yl)ethyl-3-methyl imidazolium l-valinate [AAIL7]

The initial preparation was similar to that mention previously [AAIL1], to prepare the chloride IL, however 1 g of 1-(piperid-1-yl)-3-methyl imidazolium chloride

hydrochloride salt was reacted with 0.52 g of l-valine. The work up was as that described earlier.

Yield: 1.00 g (86%)

^{1}H NMR: (D_2O) δ = 0.79 (*d*, 3H, *J* = 6.8), 0.84 (*d*, 3H, *J* = 6.8), 1.47 (*m*, 6H), 1.88 (*m*, 1H), 2.41 (*m*, 4H), 2.75 (*t*, 2H, *J* = 7.0), 3.04 (*d*, 1H, *J* = 4.9), 3.78 (*s*, 3H), 4.26 (*t*, 2H, *J* = 7.0), 7.35 (*d*, 1H, *J* = 1.7), 7.41 (*d*, 1H, *J* = 1.7)

^{13}C NMR: (D_2O) δ = 16.5, 18.7, 24.5, 30.9, 35.6, 45.8, 53.6, 57.0, 61.3, 122.2, 123.6, 180.7

IR (KBr): ṽ = 3089, 2935, 2852, 2796, 1590, 1457, 1218, 1387, 1364, 1168, 1119, 1060, 1021, 905, 828, 760, 648, 619, 543 cm^{-1}.

ESI: [M^+] Calculated 194.1652, Observed 194.1655, [M^-] Calculated 116.0717, Observed 116.0711

Synthesis of 1-(morphol-4-yl)ethyl-3-methylimidazolium d-alaninate[AAIL8]

1 g of 1-(morphol-4-yl)ethyl-3-methyl imidazolium chloride hydrochloride salt was dissolved in 10 cm^3 of deionised H_2O. This was then passed through an amberlite IRA-400 OH form anion exchange resin column, approximately 150 mm in length, to remove the hydrochloride moiety.

The IL-Cl was then diluted down to a 2% w/v solution with deionised H_2O and chilled to 0 ^oC. This was then passed again through a column of amberlight anion exchange resin hydroxide form. The solution was then added dropwise to 0.55 g of d-alanine and the resulting mixture allowed stir for 24 hours. After this time the excess H_2O was removed under vacuum at temperature no higher than 50 ^oC. 20 cm^3 of 9:1 acetonitrile/methanol solution was added and stirred vigorously for 1 hour to precipitate excess free amino acid. This was then filtered before excess solvent was removed under vacuum to yield the ionic liquid.

Yield: 0.82 g (77%)

^{1}H NMR: (D_2O) δ = 1.15 (*d*, 3H, *J* = 7.0), 2.52 (*t*, 4H, *J* = 4.8), 2.81 (*t*, 2H, *J* = 6.6), 3.21 (*q*, 1H, *J* = 7.0), 3.66 (*t*, 4H, *J* = 4.8), 3.81 (*s*, 3H) 4.29 (*t*, 2H, *J* = 6.6), 7.35 (*d*, 1H, *J* = 1.9), 7.44 (*d*, 1H, *J* = 1.9)

^{13}C NMR: (D_2O) δ = 19.3, 34.8, 44.7, 50.5, 51.6, 55.8, 121.4, 122.7, 183.3

IR (KBr): ṽ = 3421, 3158, 3109, 2937, 2859, 2846, 1594, 1456, 1412, 1385, 1356, 1304, 1257, 1245, 1167, 1122, 1039, 963, 923, 860, 775, 758, 758, 656 cm^{-1}

ESI: [M^+] Calculated 196.1444, Observed 196.1449, [M^-] Calculated 88.0404, Observed 88.0400

Synthesis of 1-(morphol-4-yl)ethyl-3-methyl imidazolium l-leucinate [AAIL9]

The initial preparation was similar to that mention previously [AAIL1], to prepare the chloride IL, however 1 g of 1-(morphol-4-yl)-3-methyl imidazolium chloride hydrochloride salt was reacted with 0.8 g of l-leucine. The work up was as that described above.

Yield: 1.01 g (79%)

^{1}H NMR: (D_2O) δ = 0.80 (*d*, 3H, *J* = 4.7), 0.82 (*d*, 3H, *J* = 4.7), 1.32 (*m*, 2H), 1.42 (*m*, 1H), 2.52 (*t*, 2H, *J* = 4.8), 2.66 (*t*, 2H, *J* = 4.8), 2.81 (*t*, 2H, *J* = 6.6), 3.19 (*t*, 1H, *J* = 4.9), 3.81 (*s*, 3H), 4.29 (*t*, 2H, *J* = 6.6), 7.36 (*d*, 1H, *J* = 1.9), 7.44 (*d*, 1H, *J* = 1.9)

^{13}C NMR: (D_2O) δ = 21.3, 22.3, 24.3, 35.6, 43.7, 45.5, 52.4, 54.4, 56.7, 66.0, 122.3, 123.6, 183.5

IR (KBr): ṽ = 3365, 3250, 3092, 2956, 2871, 2863, 1578, 1515, 1455, 1407, 1385, 1364, 1341, 1298, 1224, 1210, 1172, 1146, 1114, 1070, 1035, 1018, 930, 913, 854, 769 cm^{-1}.

ESI: [M^+] Calculated 196.1444, Observed 196.1452, [M^-] Calculated 130.0874, Observed 130.0869.

Synthesis of 1-(morphol-4-yl)ethyl-3-methyl imidazolium l-lysinate [AAIL10]

The initial preparation was similar to that mention previously [AAIL1], to prepare the chloride IL, however 1 g of 1-(morphol-4-yl)-3-methyl imidazolium chloride hydrochloride salt was reacted with 0.75 g ofl-lysinate. The work up of [AAIL3] was as that described above.

Yield: 0.91 g (72%)

^{1}H NMR: (D_2O) δ = 1.33-1.49 (*m*, 6H), 2.50 (*m*, 6H), 2.78 (*t*, 2H, *J* = 6.6), 3.10 (*t*, 1H, *J* = 6.5), 3.62 (*t*, 4H, *J* = 4.7), 3.77 (*s*, 3H), 4.25 (*t*, 2H, *J* = 6.6), 7.33 (*d*, 1H, *J* = 1.7), 7.41 (*d*, 1H, *J* = 1.7)

^{13}C NMR: (D_2O) δ = 22.2, 31.0, 34.3, 35.6, 40.1, 45.5, 52.4, 55.8, 56.7, 65.9, 122.2, 123.5, 183.5

IR (neat): ṽ = 3345, 3278, 3140, 3060, 2929, 2853, 2810, 1560, 1454, 1384, 1356, 1331, 1297, 1172, 1146, 1146, 1172, 1146, 1112, 1069, 1036, 1017, 929, 912, 853, 816, 767 cm^{-1}.

ESI: [M^+] Calculated 196.1444, Observed 196.1442, [M^-] Calculated 145.0983, Observed 145.0984.

Synthesis of 1-(morphol-4-yl)ethyl-3-methyl imidazolium d-glutaminate [AAIL11]

The initial preparation was similar to that mention previously [AAIL1], to prepare the chloride IL, however 1 g of 1-(morphol-4-yl)-3-methyl imidazolium chloride hydrochloride salt was reacted with 0.66 g of d-glutamine. The work up was as that described earlier.

Yield: 0.90 g (70%)

^{1}H NMR: (D_2O) δ = 1.78 (*m*, 2H), 2.19 (*t*, 2H, *J* = 6.5), 2.48 (*t*, 4H, *J* = 4.8), 2.78 (*t*, 2H, *J* = 6.6), 3.15 (*t*, 1H, *J* = 8.3), 3.63 (*t*, 4H, *J* = 4.8), 3.77 (*s*, 3H), 4.25 (*t*, 2H, *J* = 6.6), 7.32 (*d*, 1H, *J* = 1.9), 7.40 (*d*, 1H, *J* = 1.9)

^{13}C NMR: (D_2O) δ = 30.6, 31.6, 34.8, 44.7, 51.6, 52.4, 55.9, 65.1, 121.4, 122.7, 175.8, 180.3

IR (neat): ṽ = 3410, 3160, 3103, 2964, 2872, 1666, 1576, 1455, 1405, 1360, 1333, 1300, 1171, 1146, 1114, 1069, 1035, 1018, 929, 923, 854, 769, 654, 621 cm^{-1}

ESI: [M^+] Calculated 196.1444, Observed 196.1448, [M^-] Calculated 145.0619, Observed 145.0613.

Synthesis of 1-(morphol-4-yl)ethyl-3-methyl imidazolium d-asparaginate [AAIL12]

The initial preparation was similar to that mention previously [AAIL1], to prepare the chloride IL, however 1 g of 1-(morphol-4-yl)-3-methyl imidazolium chloride hydrochloride salt was reacted with 0.70 g of d-asparagine. The work up was as that described earlier.

Yield: 1.02 g (86%)

^{1}H NMR: (D_2O) δ = 1.98-2.84 (*m*, 2H, *J* = 4.6), 2.61 (*m*, 4H), 2.81 (*t*, 2H, *J* = 6.6), 3.41 (*t*, 1H, *J* = 4.7), 3.82 (*s*, 3H), 4.29 (*t*, 2H, *J* = 6.6), 7.36 (*d*, 1H, *J* = 1.9), 7.44 (*d*, 1H, *J* = 1.9)

^{13}C NMR: (D_2O) δ = 34.8, 39.5, 44.7, 51.6, 52.4, 55.9, 65.1, 121.4, 122.7, 175.8, 180.3

IR (neat): ṽ = 3345, 3296, 3144, 3084, 2957, 2854, 2796, 1666, 1563, 1454, 1378, 1359, 1296, 1273, 1170, 1145, 1111, 1069, 1035, 1018, 929, 912, 853, 766, 701cm^{-1}.

ESI: [M^+] Calculated 196.1444, Observed 196.1448, [M^-] Calculated 131.0462, Observed 131.0459.

Synthesis of 1-(morphol-4-yl)ethyl-3-methyl imidazolium glycinate [AAIL13]

The initial preparation was similar to that mention previously [AAIL1], to prepare the chloride IL, however 1 g of 1-(morphol-4-yl)-3-methyl imidazolium chloride hydrochloride salt was reacted with 0.35 g of d-glycine. The work up was as that described earlier.

Yield: 0.73 g (72%)

^{1}H NMR: (D_2O) δ = 2.48 (*t*, 4H, *J* = 4.7), 2.78 (*t*, 2H, *J* = 6.7), 3.09 (*s*, 2H), 3.63 (*t*, 4H, *J* = 4.7), 3.77 (*s*, 3H), 4.25 (*t*, 2H, *J* = 6.9), 7.33 (*d*, 1H, *J* = 2.0), 7.40 (*d*, 1H, *J* = 2.0)

^{13}C NMR: (D_2O) δ = 35.6, 44.2, 45.5, 52.4, 65.9, 122.2, 123.5, 180.4.

IR (neat): ν̃ = 3380, 3269, 3149, 3082, 2856, 2853, 2810, 1563, 1453, 1378, 1295, 1271, 1170, 1146, 1100, 1069, 1035, 1017, 929, 912, 854, 816, 767 cm^{-1}.

ESI: [M^+] Calculated 196.1444, Observed 196.1441, [M^-] Calculated 74.0248, Observed 72.0245.

Synthesis of 1-(morphol-4-yl)ethyl-3-methyl imidazolium l-valinate [AAIL14]

The initial preparation was similar to that mention previously [AAIL8], to prepare the chloride IL, however 1 g of 1-(morphol-4-yl)-3-methyl imidazolium chloride hydrochloride salt was reacted with 0.52 g of l-valine. The work up was as that described earlier.

Yield: 0.97 g (85%)

^{1}H NMR: (D_2O) δ = 0.81 (*d*, 6H, *J* = 6.9), 0.84 (*d*, 6H, *J* = 6.9), 1.88 (*m*, 1H), 2.48 (*t*, 4H, *J* = 4.4), 2.77 (*t*, 2H, *J* = 6.8), 3.04 (*d*, 1H, *J* = 5.5), 3.62 (t, 4H, *J* = 4.7), 3.77 (*s*, 3H), 4.25 (*t*, 2H, *J* = 6.7), 7.32 (*d*, 1H, *J* = 1.8), 7.40 (*d*, 1H, *J* = 1.8)

^{13}C NMR: (D_2O) δ = 15.6, 17.9, 30.2, 34.8, 44.7, 51.6, 55.9, 60.6, 65.1, 121.4, 122.7, 180.4

IR (neat): ν̃ = 3356, 3256, 3089, 2958, 28572815, 1573, 1455, 1400, 1359, 1297, 1274, 1173, 1109, 1065, 1017, 970, 929, 912, 854, 767 cm^{-1}.

ESI: [M^+] Calculated 196.1444, Observed 196.1451, [M^-] Calculated 116.0717, Observed 116.0716.

Synthesis of 1-(pyrrolid-1-yl)ethyl-3-methylimidazolium d-alaninate [AAIL15]

1-(pyrrolid-1-yl)ethyl-3-methyl imidazolium chloride hydrochloride salt (1 g) was dissolved in 10 cm^3 of deionised H_2O. This was then passed through an amberlite IRA-400 OH form anion exchange resin column, approximately 150 mm in length, to remove the hydrochloride moiety.

The IL-Cl was then diluted down to a 2% w/v solution with deionised H_2O and chilled to 0 ^oC. This was then passed again through a column of amberlight anion exchange resin hydroxide form. The solution was then added dropwise to 0.55 g of d-alanine and the resulting mixture allowed stir for 24 hours. After this time the excess H_2O was removed under vacuum at temperature no higher than 50 ^oC. 20 cm^3 of 9:1 acetonitrile/methanol solution was added and stirred vigorously for 1 hour to precipitate excess free amino acid. This was then filtered before excess solvent was removed under vacuum to yield the ionic liquid.

Yield: 0.93 g (88%)

^{1}H NMR: (D_2O) δ = 1.18 (*d*, 3H, *J* = 7.0), 1.69 (*s*, br, 4H), 2.91 (*t*, 2H, *J* = 6.6), 3.30 (*q*, 1H, *J* = 7.0), 3.81 (*s*, 3H), 4.26 (*t*, 2H, *J* = 6.6), 7.36 (*d*, 1H, *J* = 1.7), 7.43 (*d*, 1H, *J* = 1.7)

^{13}C NMR: (D_2O) δ = 19.6, 22.6, 35.6, 47.9, 51.2, 53.3, 54.5, 122.1, 123.1, 183.2.

IR (neat): $\tilde{\nu}$ = 3371, 3273, 3140, 3064, 2902, 2877, 2793, 1562, 1455, 1384, 1350, 1293, 1236, 1170, 1057, 956, 931, 903, 837, 773 cm^{-1}

ESI: [M^+] Calculated 180.1495, Observed 180.1490, [M^-] Calculated 88.0404, Observed 88.0407

Synthesis of 1-(pyrrolid-1-yl)ethyl-3-methyl imidazolium l-leucinate [AAIL16]

The initial preparation was similar to that mention previously [AAIL15], to prepare the chloride IL, however 1 g of 1-(pyrrolid-1-yl)-3-methyl imidazolium chloride hydrochloride salt was reacted with 0.8 g of l-leucine. The work up was as that described above.

Yield: 1.04 g (84%)

^{1}H NMR: (D_2O) δ = 0.81 (*d*, 3H, *J* = 5.0), 0.84 (*d*, 3H, *J* = 5.0),1.34 (*m*, 4H), 1.65 (*m*, 5H), 2.51 (*m*, 4H), 2.91 (*t*, 2H, *J* = 7.0), 3.18 (*t*, 1H, *J* = 5.7), 3.80 (*s*, 3H), 4.26 (*t*, 2H, *J* = 7.0), 7.36 (*d*, 1H, *J* = 1.7), 7.43 (*d*, 1H, *J* = 1.7)

^{13}C NMR: (D_2O) δ = 21.3, 22.3, 22.6, 24.3, 43.8, 47.9, 48.8, 53.3, 54.5, 122.1, 136.4, 182.3

IR (neat): ṽ = 3380, 3265, 3149, 3091, 2952, 2868, 2797, 1562, 1459, 1431, 1381, 1360, 1336, 1291, 1271, 1170, 1056, 951, 847, 763, 745 cm^{-1}.

ESI: [M^+] Calculated 180.1495, Observed 180.1494, [M^-] Calculated 130.0874, Observed 130.0868

Synthesis of 1-(pyrrolid-1-yl)ethyl-3-methyl imidazolium l-lysinate [AAIL17]

The initial preparation was similar to that mention previously [AAIL15], to prepare the chloride IL, however 1 g of 1-(pyrrolid-1-yl)-3-methyl imidazolium chloride hydrochloride salt was reacted with 0.75 g of l-lysine. The work up was as that described above.

Yield: 1.10 g (85%)

^{1}H NMR: (D_2O) δ = 1.44 (*m*, 6H), 1.65 (*m*, 4H), 2.48 (*m*, 6H), 2.88 (*t*, 2H, *J* = 6.6), 3.11 (*t*, 1H, *J* = 6.4), 3.77 (*s*, 3H), 4.23 (*t*, 2H, *J* = 6.6), 7.32 (*d*, 1H, *J* = 2.0), 7.40 (*d*, 1H, *J* = 2.0)

^{13}C NMR: (D_2O) δ = 22.1, 22.6, 30.5, 34.2, 35.6, 40.0, 47.8, 53.3, 54.4, 55.8, 122.1, 123.6, 183.5

IR (neat): ṽ = 3363, 3273, 3144, 3060, 2932, 2868, 2850, 2792, 1562, 1458, 1383, 1349, 1325, 1170, 1134, 1091, 1056, 956, 854, 817, 764, 745 cm^{-1}.

ESI: [M^+] Calculated 180.1495, Observed 180.1493, [M^-] Calculated 145.0983, Observed 145.0979

1-(pyrrolid-1-yl)ethyl-3-methyl imidazolium d-glutaminate [AAIL18]

The initial preparation was similar to that mention previously [AAIL15], to prepare the chloride IL, however 1 g of 1-(pyrrolid-1-yl)-3-methyl imidazolium chloride hydrochloride salt was reacted with 0.66 g of d-glutamine. The work up was as that described earlier.

Yield: 0.98 g (77%)

^{1}H NMR: (D_2O) δ = 1.68 (*m*, 6H), 2.22 (*t*, 2H, *J* = 8.3), 2.50 (*m*, 4H), 2.91 (*t*, 2H, *J* = 6.7), 3.20 (*t*, 1H, *J* = 6.5), 3.80 (*s*, 3H), 4.26 (*t*, 2H, *J* = 6.7), 7.36 (*d*, 1H, *J* = 2.0), 7.44 (*d*, 1H, *J* = 2.0)

^{13}C NMR: (D_2O) δ = 21.8, 29.8, 30.8, 34.8, 47.0, 52.5, 53.7, 54.6, 121.3, 122.8, 128.3, 181.2

IR (neat): ṽ = 3363, 3229, 3130, 3076, 2872, 2796, 1670, 1562, 1458, 1385, 1284, 1169, 1102, 1054, 954, 901, 876, 854, 765 cm^{-1}.

ESI: [M^+] Calculated 180.1495, Observed 180.1494, [M^-] Calculated 145.0619, Observed 145.0619

Synthesis of 1-(pyrrolid-1-yl)ethyl-3-methyl imidazolium d-asparaginate [AAIL19]

The initial preparation was similar to that mention previously [AAIL15], to prepare the chloride IL, however 1 g of 1-(pyrrolid-1-yl)-3-methyl imidazolium chloride hydrochloride salt was reacted with 0.70 g of d-asparagine. The work up was as that described earlier.

Yield: 1.07 g (87%)

^{1}H NMR: (D_2O) δ = 1.68 (*m*, 4H), 2.29-2.61 (*m*, 6H), 2.91 (*t*, 2H, *J* = 6.6), 3.48 (*t*, 1H, *J* = 4.7), 3.81 (*s*, 3H), 4.27 (*t*, 2H, *J* = 6.7), 7.36 (*d*, 1H, *J* = 2.0), 7.44 (*d*, 1H, *J* = 2.0)

^{13}C NMR: (D_2O) δ = 21.8, 34.8, 39.5, 47.0, 52.5, 52.7, 53.6, 121.3, 122.8, 175.8, 180.2

IR (neat): ṽ = 3340, 3287, 3140, 3077, 2963, 2877, 2796, 1667, 1564, 1449, 1380, 1351, 1338, 1169, 1056, 1029, 954, 905, 855, 764, 701 cm^{-1}.

ESI: [M^+] Calculated 180.1495, Observed 180.1494, [M^-] Calculated 131.0462, Observed 131.0464

Synthesis of 1-(pyrrolid-1-yl)ethyl-3-methyl imidazolium glycinate [AAIL20]

The initial preparation was similar to that mention previously [AAIL15], to prepare the chloride IL, however 1 g of 1-(pyrrolid-1-yl)-3-methyl imidazolium chloride hydrochloride salt was reacted with 0.35 g of d-glycine. The work up was as that described earlier.

Yield: 0.78 g (77%)

^{1}H NMR: (D_2O) δ = 1.65 (*m*, 4H), 2.50 (*m*, 4H), 2.86 (*t*, 2H, *J* = 6.6), 3.05 (*s*, 2H), 3.76 (*s*, 3H), 4.22 (*t*, 2H, *J* = 6.6), 7.31 (*d*, 1H, *J* = 2.0), 7.39 (*d*, 1H, *J* = 2.0)

^{13}C NMR: (D_2O) δ = 22.6, 35.6, 44.4, 47.9, 53.3, 54.5, 122.1, 123.7, 180.9

IR (neat): ṽ = 3367, 3265, 3140, 3069, 2962, 2873, 2792, 1562, 1457, 1379, 1353, 1288, 1253, 1168, 1056, 958, 934, 875, 816, 763 cm^{-1}.

ESI: [M^+] Calculated 180.1495, Observed 180.1494, [M^-] Calculated 74.0248, Observed 74.0245

Synthesis of 1-(pyrrolid-1-yl)ethyl-3-methyl imidazolium l-valinate [AAIL21]

The initial preparation was similar to that mention previously [AAIL15], to prepare the chloride IL, however 1 g of 1-(pyrrolid-1-yl)-3-methyl imidazolium chloride hydrochloride salt was reacted with 0.52 g of l-valine. The work up was as that described earlier.

Yield: 0.96 g (82%)

^{1}H NMR: (D_2O) δ = 0.78 (*d*, 3H, *J* = 7.0), 0.83(*d*, 3H, *J* = 7.0), 1.68 (*m*, 4H), 1.84 (*m*, 2H), 2.49 (*m*, 4H), 2.93 (*m*, 3H), 3.80 (*s*, 3H), 4.26 (*t*, 2H, *J* = 6.6), 7.35 (*d*, 1H, *J* = 2.0), 7.43 (*d*, 1H, *J* = 2.0)

^{13}C NMR: (D_2O) δ = 16.6, 18.9, 22.6, 35.6, 47.9, 53.3, 54.5, 61.7, 122.1, 123.7, 182.4

IR (neat): ṽ =3371, 3265, 3144, 3086, 2958, 2788, 1562, 1458, 1382, 1364, 1296, 1273, 1240, 1169, 1054, 954, 931, 853, 852, 816, 754 cm^{-1}

ESI: [M^+] Calculated 180.1495, Observed 180.1496, [M^-] Calculated 116.0717, Observed 116.0716

2.4 Impregnation of supports using ionic liquids

2.4.1 Materials used in the impregnation of ionic liquids onto solid supports

Silica (mesostructured) MCM-41(hexagonal), surface area 1000 cm^3/g, pore size 3.5-3.9 nm was purchased from Sigma-Aldrich.

2.4.2 Preparation of supported ionic liquid membranes for permeability studies

A polymeric membrane was held under vacuum oven for at 40 ^oC for 20 hours. Using a syringe (1cm^3), 0.6 cm^3 of the ionic liquid was placed onto the membrane and remained under vacuum for a further 5 hours. After this time excess ionic liquid was removed via blotting with filter paper to yield the SILM.

2.4.3 Preparation of ionic liquid impregnated silica for absorption studies

Ionic liquids were impregnated into the solid support by dissolving the ionic liquid in methanol and added it slowly to the silica. The suspension was stirred for 2 hours and the excess solvent removed under vacuum to yield silica impregnated with the ionic liquid. Loadings were done using a weight loading percentage and were formed using the equation below.

$$\%\, Weight\ Loading = \frac{Mass\ ionic\ liquid}{Mass\ \ of\ ionic\ liquid + Mass\ of\ support} \times \frac{100}{1}$$

(Equation 2.4)

2.5 References

(1) Fukumoto, K.; Yoshizawa, M.; Ohno, H. *Journal of the American Chemical Society* **2005**, *127*, 2398.

(2) Vandervelde, D.; www.mangia.caltech.edu/NMR_doc.html: 2013; Vol. 2013.

(3) Ab Rani, M. A.; Brant, A.; Crowhurst, L.; Dolan, A.; Lui, M.; Hassan, N. H.; Hallett, J. P.; Hunt, P. A.; Niedermeyer, H.; Perez-Arlandis, J. M.; Schrems, M.; Welton, T.; Wilding, R. *Physical Chemistry Chemical Physics* **2011**, *13*, 16831.

(4) Zhang, S.; Chen, Z.; Qi, X.; Deng, Y.; Zhang, S.; Chen, Z.; Qi, X.; Deng, Y. *New Journal of Chemistry* **2012**, *36*, 1043.

(5) Huddleston, J. G.; Visser, A. E.; Reichert, W. M.; Willauer, H. D.; Broker, G. A.; Rogers, R. D. *Green Chemistry* **2001**, *3*, 156.

(6) Palimkar, S. S.; Siddiqui, S. A.; Daniel, T.; Lahoti, R. J.; Srinivasan, K. V. *ChemInform* **2004**, *35*.

(7) Myers, C.; Pennline, H.; Luebke, D.; Ilconich, J.; Dixon, J. K.; Maginn, E. J.; Brennecke, J. F. *Journal of Membrane Science* **2008**, *322*, 28.

(8) Rao, C. J.; Venkatesan, K. A.; Nagarajan, K.; Srinivasan, T. G.; Rao, P. R. V. *Electrochimica Acta* **2009**, *54*, 4718.

(9) Nockemann, P.; Pellens, M.; Van Hecke, K.; Van Meervelt, L.; Thijs, B.; Vanecht, E.; Parac-Vogt, T. N.; Mehdi, H.; Schaltin, S.; Fransaer, J.; Zahn, S.; Kirchner, B.; Binnemans, K. *Chemistry - A European Journal* **2010**, *16*, 1849.

(10) Holbrey, J. D.; Visser, A. E.; Spear, S. K.; Reichert, W. M.; Swatloski, R. P.; Broker, G. A.; Rogers, R. D. *Green Chem.* **2003**, *5*, 129.

(11) Nicholas Gathergood, M. T. G., Peter J. Scammells *Green Chem.* **2004**, *6*, 166.

Chapter 3:

Synthesis and Characterisation of Imidazolium Ionic Liquids

3.1 Introduction

In this chapter work will be presented on the full synthesis and characterisation of ionic liquids [1a]-[8c] which have already been reported in the literature and novel ionic liquids [9a]-[11e] and [AAIL1]-[AAIL21]. This involves the assignment of both carbon and proton signals of each spectra, as outlined in Chapter 2, with the corresponding chemical structure of the ionic liquid, utilising DEPT 45 and 135, HSQC, and COSY experiments. In conjunction, major IR bands as well as accurate mass will be presented where relevant to further confirm the structure of the ionic liquids. Accurate mass values are quite important, particularly when examining the amino acid, to illustrate the formation of an anion from an acid. Thermal properties will also be presented such as melting points and decomposition values, and how the experimental procedure may alter these results.

3.2 Synthesis and characterisation of ionic liquids from literature [1a-8c]

Several ionic liquids from the literature were synthesised with the aim of being incorporated into the gas absorption/separation studies. The ionic liquids chosen were ones whose viscosities were low and thermal stability were high, or those which contained functional groups which were known to increase the gas absorption separation capabilities of the liquids. Presented in Scheme 3.1, are the 8 different classes of ionic liquids which were synthesised throughout the course of this study. In general as the ionic liquids formed in this section were known so characterisation was only carried out using ^{1}H NMR spectroscopy. Characterisation data of these ionic liquids were consistent with that found in the literature. However some deviations from the synthetic procedures set out in the literature were made.

During the synthesis of [1c], the anion exchange reaction was performed in water instead of acetone. This was performed to avoid the use of a celite plug, which was used to remove the metal salt in [1b], which was deemed unnecessary due to the solubility of the lithium salts (starting material and byproduct) in water and the insoluble nature of the resulting ionic liquid allowing for easy removal of impurities without compromising yield. However the use of a celite plug was unavoidable during the synthesis of [1b] due to the tendency for HF to form when the tetrafluroborates are exposed to water.[1]

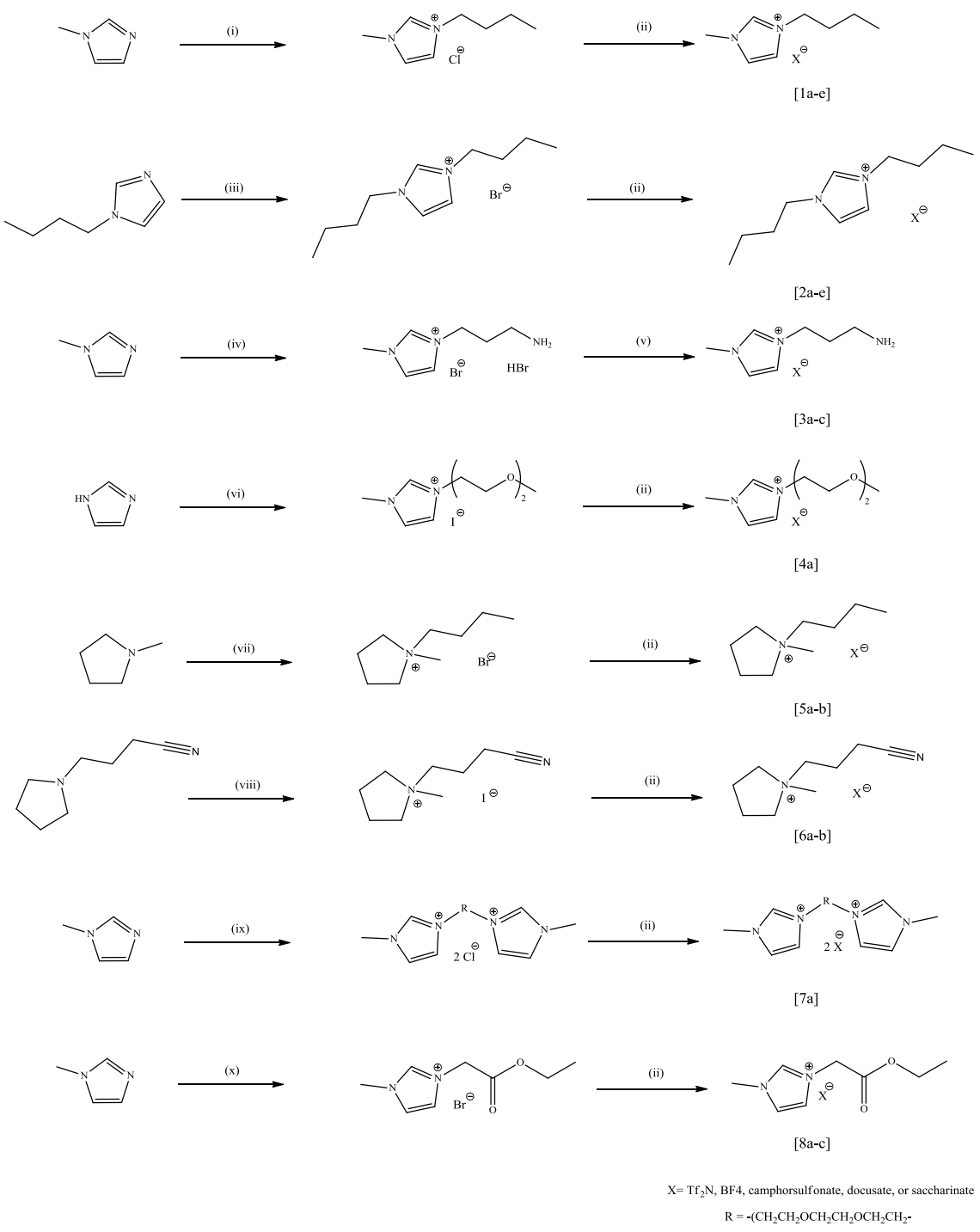

Scheme 3.1: Synthesis of previously known ionic liquids, (i) 1-chlorobutane, toluene 80 ºC, 24 h, (ii) Li/NaX, water, rt, 24 h, (iii) 1-bromobutane, toluene, 80 ºC, 24 h, (iv) 3-bromopropylamine, EtOH, 78 ºC, 24 h, (v) KOH, Li/NaX, water, rt, 24 h, (vi) NaH, 1-(2-methoxy(ethoxy))tosylate, THF, 60 ºC, 24 h, (vii) 1-bromobutane, acetone, 60 ºC, 24 h, (viii) MeI, diethylether, rt, 24 h, (ix) 1,2-bis(2-chloroethoxy)ethane, toluene, 90 ºC, 72 h, (x) bromoethylacetate, THF, rt, 24 h.

The pyrrolidinum salts [5a-6b] were formed as stated in the literature, however it was noted that quick transport of the salts to an inert atmosphere was essential due to their highly hygroscopic nature. Overlapping of the Pyrrolidinium proton signals with those of the alkyl chains often made the interpretation of the ^{1}H NMR spectrum difficult.

Ionic liquid [7a] was the most difficult to synthesise due to the need for quaternisation reactions to occur at either end of the alkyl chains to form the di-cationic species. As a result it was essential to use the 2:1 mole equivalence of 1-methylimidazole and 1,2-bis(2-chloroethoxyethane) in the first step of the reaction. As reported the chloride salt has a "gum like" appearance and made removal of the neat product to start purification impossible. As reported in the literature it was dissolved in the water and the metathesis reaction was performed to generate the bis(triflimide) species which were always much less viscous than their halide counterparts, making purification possible. The reaction was also worked up after 2 days of refluxing, however from the ^{1}H NMR spectrum recorded it was clear that two species of imidazole were present due to two C2 imidazolium proton signals. However this reflux time was successfully reduced by using smaller scale reactions as well as reducing amount of solvent present.

Ionic liquids [8a-c] were also successfully synthesised however the carbonyl group present on the cation structure had a negative effect on viscosity (determined by observation only) with higher viscosity liquids being produced. As such these were deemed an unattractive material for gas permeability studies.

While the ionic liquids synthesised had many attractive CO_2 capture features such as carbonyl, esters, and sulfonyl groups, it was decided that these would not proceed to the gas testing phase. The camphorsulfonate and docusate salts were significantly more viscous than others formed and also some of these ionic liquids were already being used in gas testing experiments in the literature. Therefore a further range of novel ionic liquids (Section 3.3) were synthesised with increased nitrogen content and it was hoped that these would be more successful in terms of gas capture/separation.

3.3 Synthesis and characterisation of ionic liquids containing conventional anions [9a-11e]

3.3.1 Synthesis and purification of ionic liquids [9a-9e]

As mentioned in Chapter 1, the typical synthesis of the 1,3-dialkylimidazolium salts are through an S_N2 reaction, whereby the 1-alkylimidazole acts as a nucleophile attacking the carbon adjacent to the leaving group or halide due to its electron deficiency. This is the approach used in the synthesis of the majority of ionic liquids presented in this work (Scheme 3.2). The synthesis of the ionic liquids involved the quaternisation of 1-methylimidazole with 3 different halide species respectively; 1-(2-chloroethyl)piperidine hydrochloride, 1-(2-chloroethyl)pyrrolidine hydrochloride, and 4-(2-chloroethyl)morpholine hydrochloride. These cations have been found in literature however none of these have been found to be used in conjunction with the anions employed as part of this study. The ionic liquid halide salt precursor from all 3 reactions (Scheme 3.2) produced white solids and therefore proved much easier than those which yielded liquid halide precursors, for example [2a] and [8a]. A common contaminant of ionic liquids is 1-methylimidazole, and due to its high boiling point (216 ^oC) and the inability to distil ionic liquids due to their negligible vapour pressure, can prove difficult to remove. However it was found that washing the ionic liquid precursors with cool dichloromethane was sufficient to effectively remove it from the salts. However, the formation of solids as precursors to the ionic liquid introduced an additional purity issue. Unlike ionic liquids [1a-8c] where the alkylating agents such as 1-bromobutane were liquids, for the 3 cations mentioned above, the alkylating agents which were hydrochloride salts, are solids and so proved to be contaminants which were detected using ^1H NMR spectroscopy.

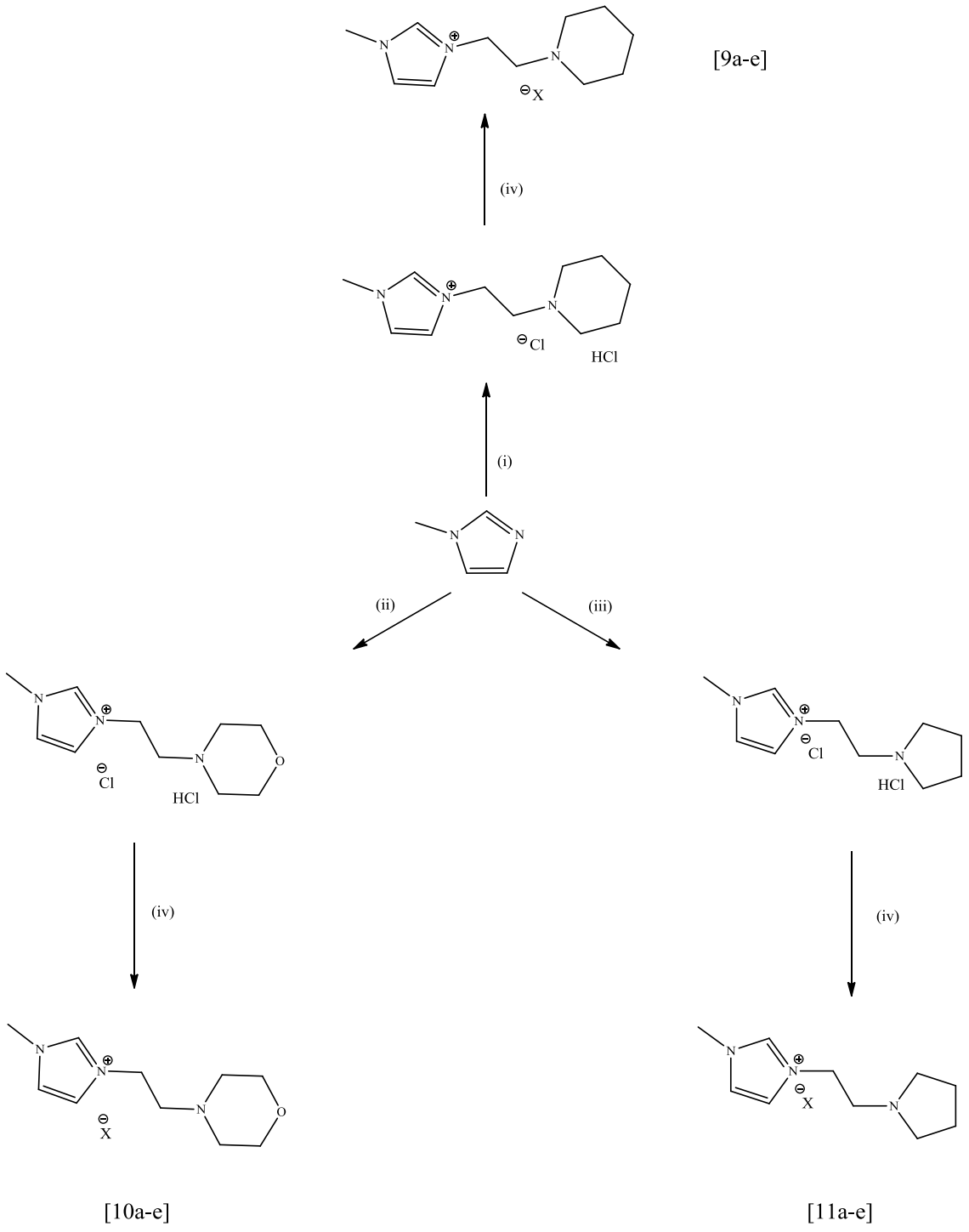

Scheme 3.2: Strategy for the synthesis of ionic liquids with conventional anions (i) 1-(2-chloroethyl)piperidine hydrochloride, ethanol, 75 ºC, 16 h, (ii) 4-(2-chloroethyl)morpholine hydrochloride, 4:1 ethanol/toluene, 74 ºC, 16 h, (iii) 1-(2-chloroethyl)pyrrolidine hydrochloride, 75 ºC, 16 h, (iv) 1.2 mole equivalent. NaOH, 1.2 mole equivalent NaX/LiX, rt, 24 h, where x = bis(triflimide), saccharinate, dicyanamide, trifluoroacetate, or trifluoromethanesulfonate.

In general, alkylating agents are added in excess (typically 1.4 mole equivalent) in relation to the 1-methylimidazole, to ensure complete quaternisation of the imidazole unit occurs. However with the alkylating agent now the main source of contamination, it was decided to reduce the reaction to 1 mole equivalent of the alkylating agents. Unfortunately its presence was still evident in the NMR spectra of the product (Figure 3.1). During the experiments, a suspension formed in the reaction vessel, after the 16 hour period. Hot filtration was performed on the suspension and both the precipitate and resulting solid extracted from the filtrate were analysed. The precipitate was determined to be unreacted alkylating agent, as demonstrated in Figure 3.1 with the signals arising from the H atoms on the ethyl chain signals of the starting material clearly evident at 3.50 ppm (black trace) and the filtrate yielded a pure white compound, that of the quaternised hydrochloride salt (blue trace).

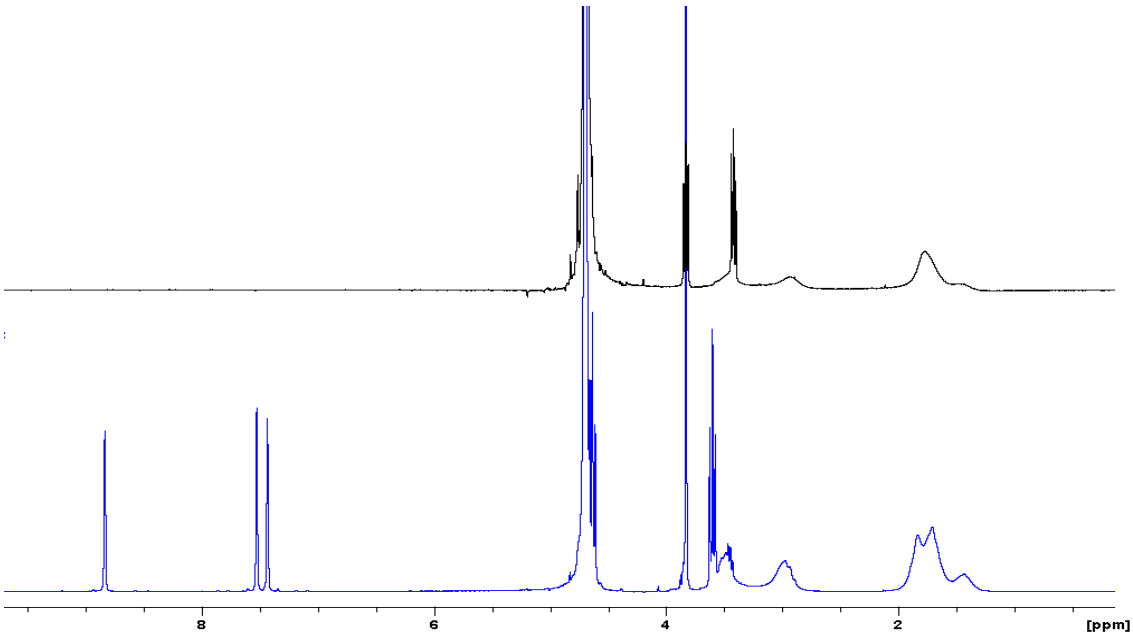

Figure 3.1: ^{1}H NMR spectra of 1-(2-chloroethyl)piperidine hydrochloride (-), and 1-methyl-3-(piperid-1-yl)ethylimidazolium chloride hydrochloride and unreacted 1-(2-chloroethyl)piperidine hydrochloride (-).

In the case of the reaction with the 1-methyl-3-(morphol-4-yl)ethylimidazolium hydrochloride salts, the yields were significantly lower, with values approximately 25% less than when the reaction was carried out to generate the other two cations. It had also been observed that the reaction to generate this cation also yielded a much higher amount of unreacted alkylating agent during hot filtration, indicating an issue with

solubility of the starting hydrochloride salt in ethanol. A binary solvent system was employed utilising a 4:1 ethanol/toluene mixture, which resulted in an increased yield of approximately 15% (from 62% to 77%) in comparison to previous experiments.

The extraction of the ionic liquid hydrochloride salts differed slightly depending on the cation employed. The 1-methyl-3-(piperid-1-yl)ethylimidazolium chloride hydrochloride salt was extracted via the removal of solvent under reduced pressure to yield a yellowish solid that was then washed with cold dichloromethane to yield the white salt. Removal of the solvent from both the 1-methyl-3-(morphol-4-yl)ethylimidazolium chloride hydrochloride and 1-methyl-3-(pyrrolid-1-yl)ethylimidazolium chloride hydrochloride salts proved problematic due to their affinity for the reaction solvent resulting in products with an oil-like appearance. To overcome this, ice cold dichloromethane was added and the mixture was stirred, which resulted in the precipitation of the white salts.

To obtain the desired ionic liquids, the hydrochloride salts were reacted with 1.2 mole equivalent of NaOH to remove the HCl moiety of the ionic liquid precursor, followed by a metathesis reaction with 1.2 mole equivalent of the sodium/lithium salt with that anion. A wide variety of solvents can be used to carry out these reactions in order to minimise contact with water, however this was not possible with the systems employed here due to poor solubility of the hydroxide salts in organic solvent, therefore the reaction was carried out in water. Incorporation of the new anion as the counter ion to the cation was monitored using ^{1}H NMR spectroscopy. The signal for the C2 hydrogen of the imidazole ring in the ^{1}H NMR spectra recorded of the ionic liquids was also used as an indication of purity of the sample due to the strong relationship between anion type and chemical shift the C2 hydrogen. It was this that enabled chemical purity to be checked. If two signals were observed for the C2 hydrogen atoms in the ^{1}H NMR, this indicated that two different anions were present. In the majority of cases, sodium chloride which was formed as a byproduct and unreacted sodium salt reactants remained in solution. Due to the limited solubility of these salts in dichloromethane, removal via precipitation at cold temperatures was achieved. When a product proved insoluble in dichloromethane, a celite plug was employed to remove the sodium salts. This involved the dissolution of the liquid in a suitable organic solvent and passing the sample through a bed of celite. The celite plug is constructed from a slurry of celite with a solvent which

the metal salt contaminant is insoluble, resulting in the removal of the salt and allowing the filtrate with the ionic liquid to pass through under vacuum. The solvent was then removed to yield the pure ionic liquid. Washing was continued until a negative result was obtained for the silver nitrate test for the presence of chlorides.

Typically ^{1}H NMR spectroscopy would be used in conjunction with the silver nitrate test to indicate the level of purity of the sample. Both ^{1}H NMR and ^{13}C NMR were employed to check for the presence of these unreacted sodium/lithium salts. The latter proved particularly useful due to the absence of protons in a numner of these anions and so the presence of the anion could be determined from the signals of the carbon atoms of the lithium/sodium salts. These compounds were generally considered pure when no chloride was detected using the silver nitrate test and peaks for the Na/Li salt of the anion were not detected using NMR spectroscopy.

3.3.2 Characterisation of ionic liquids [9a]-[11e]

All NMR spectroscopy data presented in this section were obtained using $CDCl_3$ as the deuterated solvent with the #, ~, and * symbols indicating overlapping signals. In the case where overlapping signals occur the combined integral is given. All chemical shifts were given in ppm and coupling constants are in Hz.

3.3.2.1 ^{1}H NMR, ^{13}C NMR, and IR assignment of ionic liquids [9a-9e]

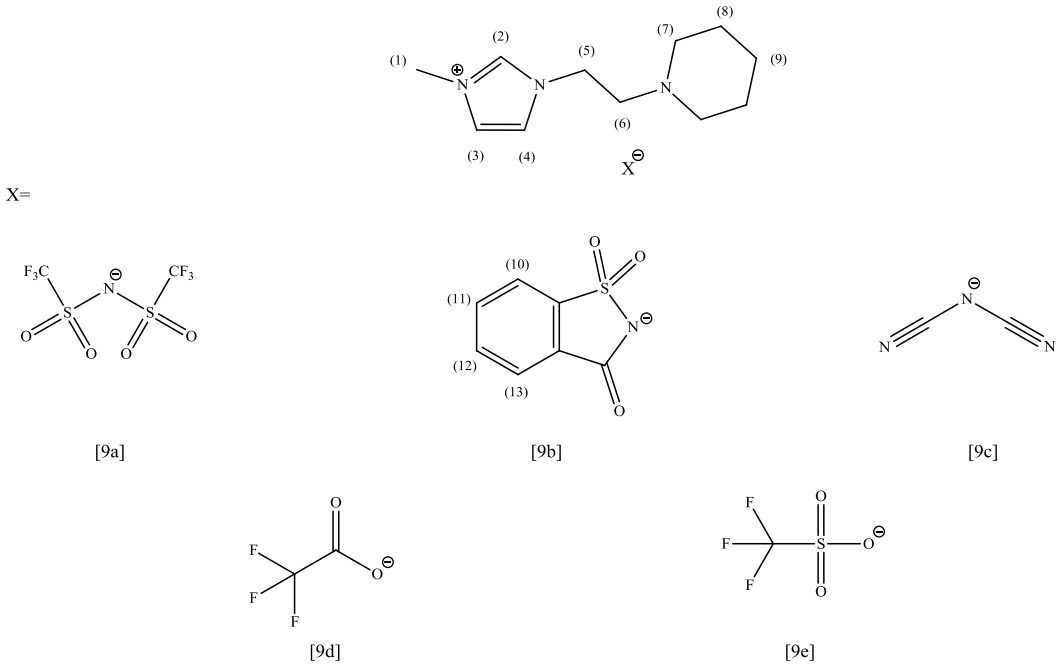

Figure 3.2: Structure of the 1-methyl-3-(piperid-1-yl)ethyl-3-methylimidazolium cation and its respective anions [9a-e].

Table 3.1: ^{1}H NMR assignment of salts [9a-e].

	[9a]	[9b]	[9c]
H1	4.22 (*s*, 3H)	4.07 (*s*, 3H)	4.04 (*s*, 3H)
H2	8.69 (*s*, 1H)	10.16 (*s*, 1H)	9.10 (*s*, 1H)
H3	7.27 (*pt*, 1H, *J* = 1.8)	7.12 (*pt*, 1H, *J* = 1.8)	7.38 (*pt*, 1H, *J* = 1.8)
H4	7.46 (*pt*, 1H, *J* = 1.8)	7.49 (*pt*, 1H, *J* = 1.8)	7.56 (*pt*, 1H, *J* = 1.8)
H5	4.20 (*t*, 2H, *J* = 5.7)	4.42 (*t*, 2H, *J* = 5.7)	4.29 (*t*, 2H, *J* = 5.7)
H6	2.67 (*t*, 2H, *J* = 5.7)	2.75 (*t*, 2H, *J* = 5.7)	2.74 (*t*, 2H, *J* = 5.7)
H7	2.42 (*m*, 4H)	2.43 (*m*, 4H)	2.45 (*m*, 4H)
H8	1.54 (*m*, 6H)*	1.53 (*m*, 6H)˜	1.59 (*m*, 6H)*
H9	1.54 (*m*, 6H)*	1.53 (*m*, 6H)˜	1.59 (*m*, 6H)*
H10	-	7.77 (*m*, 2H)*	-
H11	-	7.55 (*m*, 2H) #	-
H12	-	7.55 (*m*, 2H) #	-
H13	-	7.77 (*m*, 2H)*	-

	[9d]	[9e]
H1	3.92 (*s*, 3H)	3.97 (*s*, 3H)
H2	9.80 (*s*, 1H)	9.10 (*s*, 1H)
H3	7.18 (*pt*, 1H, *J* = 1.7)	7.29 (*pt*, 1H, *J* = 1.7)
H4	7.52 (*pt*, 1H, *J* = 1.7)	7.51 (*pt*, 1H, *J* = 1.7)
H5	4.32 (*t*, 2H, *J* = 5.7)	4.26 (*t*, 2H, *J* = 5.7)
H6	2.72 (*t*, 2H, *J* = 5.7)	2.69 (*t*, 2H, *J* = 5.7)
H7	2.45 (*s*, br, 4H)	2.42(*s*, br, 4H)
H8	1.56 (*m*, 6H)*	1.55 (*m*, 6H)*
H9	1.56 (*m*, 6H)*	1.55 (*m*, 6H)*

Table 3.2: ^{13}C NMR assignment of salts [9a-e].

	[9a]	[9b]	[9c]	[9d]	[9e]
Primary Carbon	36.2	36.5	36.4	36.0	36.1
Secondary Carbon	24.1 25.9 47.0 54.3 57.5	24.1 25.9 46.9 54.3 57.9	23.9 25.8 47.1 54.5 57.8	23.9 25.6 46.6 54.1 57.6	23.9 25.7 46.5 54.2 57.6
Tertiary Carbon	123.0 123.1 136.1	119.7 122.0 122.7 123.1 131.2 131.8 138.7	123.1 123.2 136.1	122.7 122.9 136.9	122.4 122.7 138.1
Quaternary Carbon	113.4 (*q*, *J* = 321)	134.8 144.6 170.5	119.7	110.9 (*q*, *J* = 294) 160.8 (*q*, *J* = 34)	114.0 (*q*, *J* = 320)

Table 3.3: Infrared Characterisation of salts [9a-e].

	C=O (cm^{-1})	SO_2^- (cm^{-1})	C≡N (cm^{-1})
[9a]	-	1327 1131	-
[9b]	1627	1328 1138	-
[9c]	-	-	2125 2192 2227
[9d]	1677	-	-
[9e]	-	1338 1125	-

3.3.2.2 ^{1}H NMR, ^{13}C NMR and IR assignment of ionic liquids [10a-10e]

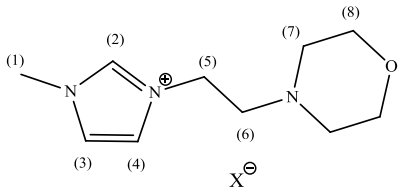

X =

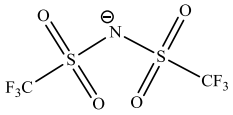

[10a]

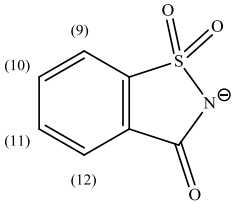

[10b]

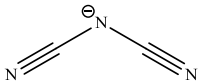

[10c]

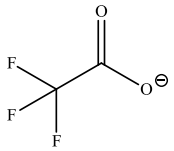

[10d]

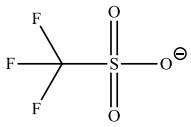

[10e]

Figure 3.3: Illustration of 1-methyl-3-(morphol-4-yl)ethyl-3-methylimidazolium cation and its respective anions [10a-e].

Table 3.4: ^{1}H NMR assignment of salts [10a-e].

	[10a]	[10b]	[10c]
H1	3.93 (*s*, 3H)	4.14 (*s*, 3H)	3.89 (*s*, 3H)
H2	8.79 (*s*, 1H)	9.85 (*s*, 1H)	8.97 (*s*, 1H)
H3	7.26 (*pt*, 1H, *J* = 1.7)	7.28 (*pt*, 1H, *J* = 1.7)	7.31 (*pt*, 1H, *J* = 1.7)
H4	7.45 (*pt*, 1H, *J* = 1.7)	7.47 (*pt*, 1H, *J* = 1.7)	7.42 (*pt*, 1H, *J* = 1.7)
H5	4.24 (*t*, 2H, *J* = 5.6)	4.43 (*t*, 2H, *J* = 5.7)	4.43 (*t*, 2H, *J* = 5.7)
H6	2.74 (*t*, 2H, *J* = 5.6)	2.75 (*t*, 2H, *J* = 5.7)	2.68 (*t*, 2H, *J* = 5.7)
H7	2.49 (*t*, 4H, *J* = 4.3)	2.47 (*t*, 4H, *J* = 4.3)	2.40 (*t*, 4H, *J* = 4.3)
H8	3.66 (*t*, 4H, *J* = 4.3)	3.61 (*t*, 4H, *J* = 4.3)	3.56 (*t*, 4H, *J* = 4.3)
H9	-	7.73(*m*, 2H) *	-
H10	-	7.57(*m*, 2H) #	-
H11	-	7.57(*m*, 2H) #	-
H12	-	7.73 (*m*, 2H) *	-

	[10d]	[10e]
H1	4.00 (*s*, 3H)	3.96 (*s*, 3H)
H2	10.21 (*s*, 1H)	9.04 (*s*, 1H)
H3	7.22 (*pt*, 1H, *J* = 1.8)	7.36 (*pt*, 1H, *J* = 1.8)
H4	7.45 (*pt*, 1H, *J* = 1.8)	7.52 (*pt*, 1H, *J* = 1.8)
H5	4.38 (*t*, 2H, *J* = 5.6)	4.29 (*t*, 2H, *J* = 5.6)
H6	2.76 (*t*, 2H, *J* = 5.6)	2.76 (*t*, 2H, *J* = 5.6)
H7	2.50 (*t*, 4H, *J* = 4.4)	2.50 (*t*, 4H, *J* = 4.4)
H8	3.67 (*t*, 4H, *J* = 4.4)	3.66 (*t*, 4H, *J* = 4.4)

Table 3.5: ^{13}C NMR assignment of salts [10a-e].

	[10a]	[10b]	[10c]	[10d]	[10e]
Primary Carbon	36.3	36.5	36.4	36.2	36.3
Secondary Carbon	46.5 53.2 57.2 66.7	46.4 53.3 57.6 66.8	46.5 53.2 57.2 66.6	46.2 53.2 57.5 66.7	46.4 53.2 57.3 66.8
Tertiary Carbon	123.1* 136.4	119.7 122.5* 123.1 131.3 132.0 138.5	123.1 123.1 136.5	122.6 122.7 138.4	123.0 123.0 137.0
Quaternary Carbon	113.6 (*q*, *J* = 320)	134.8 144.6 170.4	119.6	115.1(*q*, *J* = 320), 160.6(*q*, *J* = 34.2)	114.3(*q*, *J* = 320.0)

* Denotes overlapping peaks

Table 3.6: Infrared Characterisation of salts [10a-e].

	C=O (cm^{-1})	SO_2^- (cm^{-1})	C≡N (cm^{-1})
[9a]	-	1329 1132	-
[9b]	1627	1329 1138	-
[9c]	-	-	2125 2192 2227
[9d]	1681	-	-
[9e]	-	1337 1147	-

3.3.2.3 ^{1}H NMR, ^{13}C NMR, and IR assignment of ionic liquids [11a-11e]

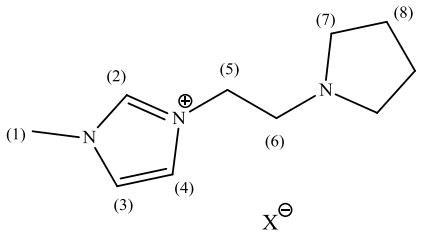

X =

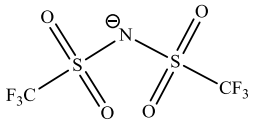

[11a]

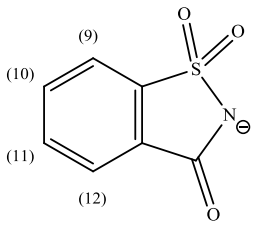

[11b]

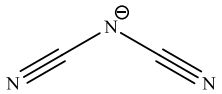

[11c]

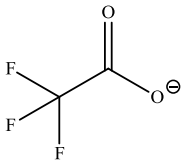

[11d]

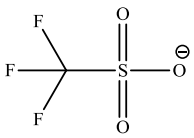

[11e]

Figure 3.4: Structure of 1-methyl-3-(pyrrolid-1-yl)ethyl-3-methylimidazolium cation and its respective anions [11a-e].

Table 3.4: ^{1}H NMR assignment of salts [11a-e].

	[11a]	[11b]	[11c]
H1	4.23 (*s*, 3H)	3.94 (*s*, 3H)	3.92 (*s*, 3H)
H2	8.69 (*s*, 1H)	9.64 (*s*, 1H)	9.01 (*s*, 1H)
H3	7.28 (*pt*, 1H, *J* = 1.7)	7.21 (*pt*, 1H, *J* = 1.7)	7.33 (*pt*, 1H, *J* = 1.7)
H4	7.44 (*pt*, 1H, *J* = 1.7)	7.40 (*pt*, 1H, *J* = 1.7)	7.46 (*pt*, 1H, *J* = 1.7)
H5	4.23 (*t*, 2H, *J* = 5.6)	4.32 (*t*, 2H, *J* = 5.6)	4.21 (*t*, 2H, *J* = 5.6)
H6	2.89 (*t*, 2H, *J* = 5.6)	2.83 (*t*, 2H, *J* = 5.6)	2.84 (*t*, 2H, *J* = 5.6)
H7	2.55 (*m*, 4H)	2.52 (*s*, 4H, br)	2.48 (*m*, 4H)
H8	1.78 (*m*, 4H)	1.70 (*m*, 4H)	1.69 (*m*, 4H)
H9	-	7.74 (*m*, 2H)*	-
H10	-	7.53 (*m*, 2H) #	-
H11	-	7.53 (*m*, 2H) #	-
H12	-	7.74 (*m*, 2H)*	-

	[11d]	[11e]
H1	3.97 (*s*,3H)	3.97 (*s*, 3H)
H2	9.93 (*s*, 1H)	9.16 (*s*, 1H)
H3	7.27 (*pt*, 1H, *J* = 1.7)	7.28 (*pt*, 1H, *J* = 1.7)
H4	7.50 (*pt*, 1H, *J* = 1.7)	7.47 (*pt*, 1H, *J* = 1.7)
H5	4.35 (*t*, 2H, *J* = 5.6)	4.29 (*t*, 2H, *J* = 5.6)
H6	2.92 (*t*, 2H, *J* = 5.6)	2.90 (*t*, 2H, *J* = 5.6)
H7	2.58 (*m*, 4H)	2.56 (*m*, 4H)
H8	1.77 (*m*, 4H)	1.78 (*m*, 4H)

Table 3.8: ^{13}C NMR assignment of salts [11a-e].

	[11a]	[11b]	[11c]	[11d]	[11e]
Primary Carbon	36.2	36.4	36.5	36.2	36.2
Secondary Carbon	23.5 48.5 53.7 54.7	23.5 48.3 53.7 54.9	23.6 48.7 53.8 54.7	23.5 48.2 53.7 54.9	23.5 48.2 53.7 54.7
Tertiary Carbon	123.1* 136.1	119.7 122.6 122.6 123.8 131.4 132.0 137.8	123.1 123.2 136.5	122.6* 138.2	122.9 123.1 136.7
Quaternary Carbon	113.4 (*q*, *J* = 320)	134.6 144.5 170.4	119.8	113.2 (*q*, *J* = 294.8), 160.9 (*q*, *J* = 33.5)	114.2 (*q*, *J* = 320)

* Denotes overlapping peaks

Table 3.9: Infrared Characterisation of salts [11a-e].

	C=O (cm^{-1})	SO_2^- (cm^{-1})	C≡N (cm^{-1})
[11a]	-	1347 1132	-
[11b]	1627	1329 1138	-
[11c]	-	-	2123 2190 2225
[11d]	1673	-	-
[11e]	-	1326 1137	-

3.3.2.4 ^{1}H NMR characterisation of ionic liquids [9a]-[11e]

From Section 3.3.2, the data observed for all liquids (chemical shifts, integration, and coupling constants) were as expected. Some differences arose in respect to the anion within each cation set. The hydrogen at the C2 position of the imidazole ring is strongly involved in the hydrogen bonding between the cation and the anion, and therefore

sensitive to anion exchange. Examination of Figure 3.5 which shows the ^{1}H NMR spectra for the 1-methyl-3-(piperid-1-yl)ethylimidazolium cation with a series of anions [9a-e] highlights this trend. The chemical shift of the signal corresponding to the C2 hydrogen atom varies with the position varying from 8.60 ppm when the bis(triflimide) anion is present to 10.16 ppm when the saccharinate anion is present. These trends were also observed for the 1-methyl-3-(pyrrolid-1-yl)ethylimidazolium cation and the 1-methyl-3-(morphol-4-yl)ethylimidazolium cations, illustrating that the position of imidazolium signals of ionic liquids on a ^{1}H NMR spectra were anion dependant.

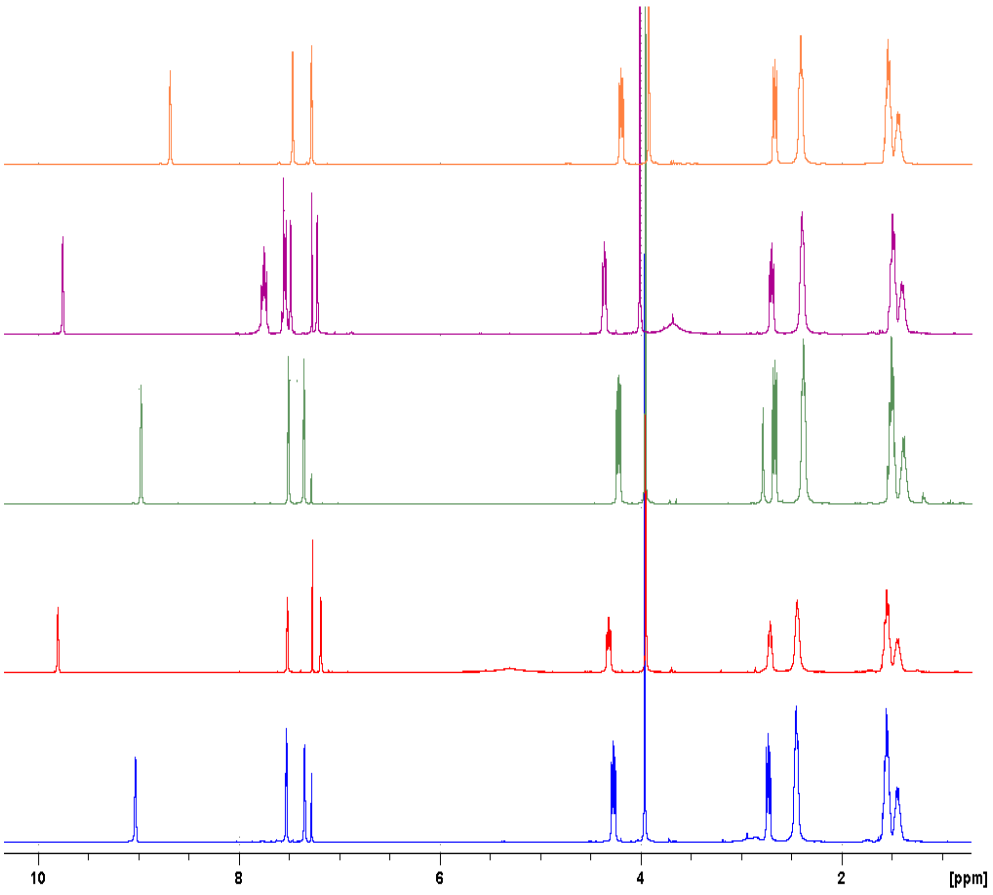

Figure 3.5: ^{1}H NMR spectra of salts with the 1-methyl-3-(piperid-1yl)ethylimidazolium cation with bis(triflimide) [9a] (-), saccharinate [9b] (-), dicyanamide [9c] (-), trifluoroacetate [9d] (-), and trifluoromethanesulfonate anion [9e] (-).

While it is clear from Figure 3.5, the effect the anion has on the chemical shift of the proton signals relating to the imidazolium ring, what is also demonstrated is the effect, or lack thereof that it has on signals further away from the charged centre. In the case of the [9a-e] salts, the signals relating to the hydrogen atom at the C4 position of the piperidine ring at approximately 1.55 ppm (denoted as (9) in Figure 3.2), show little to no variation in chemical shift, with a difference of only 0.05 ppm observed. The trend

of decreasing chemical shift variation as the distance from the positively charged centre of the cation is consistent across all three cations.

Another trend observed in the ^{1}H NMR spectra of these imidazolium ionic liquids is the appearance of triplets or pseudo triplets for the C4 and C5 hydrogen signals of the imdiazolium ring (denoted (3) and (4) in Figure 3.2). These two hydrogen atoms are inequivalent due to the asymmetry of the cation and as such will couple to each other resulting in a doublet. However it is possible for long range coupling due to the conjugation of the imidazolium ring to the C2 hydrogen atoms which should produce a doublet of doublets. The present of triplet indicates similar coupling constant resulting in the formation of these *pseudo* triplets as the doublet of doublet signals overlap with the central peak crest displaying much larger intensity than its two auxillary counterparts. This coupling is further confirmed by work presented in Section 3.3.3.4 in which the exchange of hydrogen atoms with deuterium atoms at the C2 position of the imidazolium ring results in the observation of doublets for both the C4 and C5 hydrogen atom signals.

3.3.2.5 ^{13}C NMR characterisation of ionic liquids [9a]-[11e]

From Section 3.3.2, the data observed for all liquids were as expected, with the total number of carbon signals as well as the correct division of these into primary, secondary, tertiary and quaternary carbon signals as determined from the DEPT NMR spectroscopy experiments.

A prominent feature of the ^{13}C NMR spectra recorded of a number of ionic liquids was the splitting of carbon signals due to the presence of fluorine as such is the case with the TFA^{-}, Tf_2N^{-}, and $TFMS^{-}$ anions. All three have one carbon atom directly bound to three fluorine atoms. Due to ^{19}F isotope being 100% naturally abundant it produces strong NMR signals comparable to ^{1}H NMR spectrum.[2] Due to ^{19}F isotope possessing a spin of ½, the same splitting rule applies as that of protons (n+1). Therefore the presence of three fluorine atoms beside one carbon atom would result in a quartet of carbon signals. Likewise, the ^{13}C isotope also has the ability to split the fluorine signals in the NMR spectrum, however due to the ^{13}C isotope being only 1% naturally abundant this is often difficult to see. The effect of coupling to the fluorine nuclei does seem to cause some discrepancies in the literature, with respect to the ^{13}C NMR spectra of certain ionic liquids with some erroneously reporting two individual signals, while there is a small

number of papers which recognise the signals as a quartet as in the case of BMIM-Tf_2N.[3-5] Coupling between ^{19}F and ^{13}C nuclei is also evident across three bond lengths. This longer range coupling is particularly evident when dealing with the TFA^- anions whereby not only is the adjacent carbon signal split by the three fluorine atoms, but also the carbonyl signal, although the splitting constants are significantly reduced. This is evident in the ^{13}C NMR spectra of salt [9d] presented in Figure 3.3 where the quartet relating to the splitting of the signal for the carbon of the carbonyl group by the 3 equivalent fluorine at a distance of 2 bond lengths is clearly visible at 160.8 ppm. The carbon atom directly adjacent to the three fluorine atoms also undergoes splitting resulting in a quartet, however this can be difficult to observe due to the proximity of the signals of the C4 and C5 atoms signals of the imidazolium ring at 122.7 ppm and 122.9 ppm, and the potential of overlapping with some of the signals.

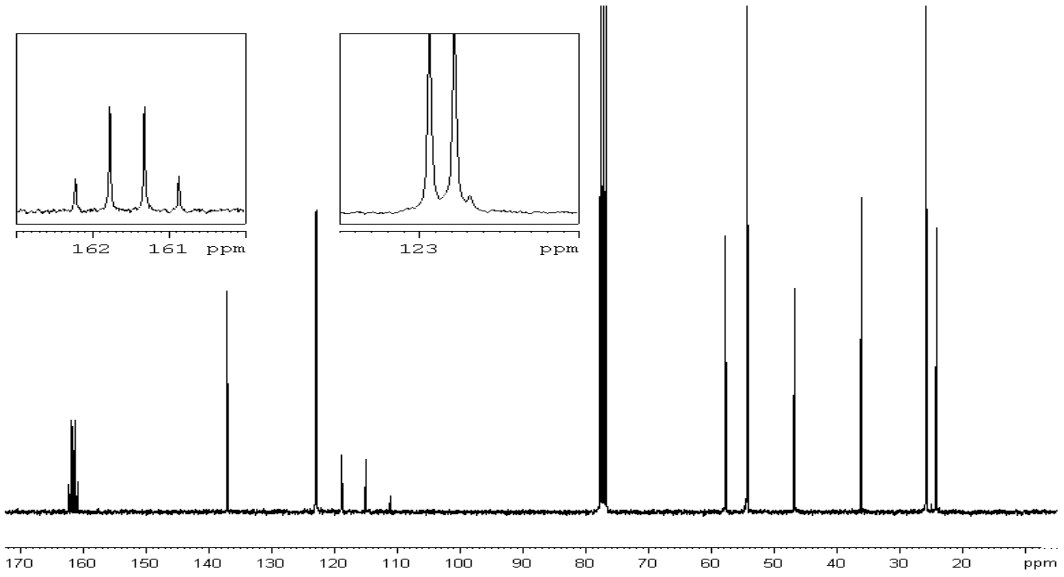

Figure 3.6: ^{13}C NMR spectrum of ionic liquid [9d].

3.3.2.6 IR characterisation of ionic liquids [9a-11e].

Infrared spectroscopy proved to be an extremely useful tool due to its sensitivity to various functional groups, indicating their presence in conjunction with the C2 hydrogen signal shift in the ^1H NMR spectra when no proton signals for the anion were present. The sulfonyl moieties present in the Tf_2N^-, $TFMS^-$, TFA^-, and saccharinate anions were easily identifiable due to the stretches at approximately 1350 cm^{-1} (asymmetric) and as 1175 cm^{-1} (symmetric). The ionic liquids which contain carbonyl

groups (saccharinate and TFA^-) also displayed a strong band between 1600 -1700 cm^{-1} due to the large dipole of the bond. The dicyanamide salts have 3 characteristic bands from approximately 2100 – 2200 cm^{-1}, which arise from the C≡N asymmetric and symmetric stretches of medium strength with the stronger intensity band due to the overlap of the C-N asymmetric and symmetric stretches.[6]

3.4 Synthesis and characterisation of amino acid functionalised ionic liquids [AAIL1-21]

3.4.1 Synthesis and purification of [AAIL1-21]

The synthesis of the ionic liquid chloride hydrochloride salts followed that as outlined in Section 3.3.1. In order to synthesise the amino acid ionic liquids an adaptation of the procedure was employed due to the unavailability or expense of amino acid sodium salts. To avoid this issue, the use of hydroxide functionalised ionic liquids was incorporated into the synthetic procedure. Hydroxide functionalised resins have been employed by groups such as Ohno *et al* [7] whereby the metathesis reaction occurs when an aqueous solution of the ionic liquid is passed through the resin to generate the hydroxide form of the ionic liquid, with NaCl as a byproduct. The hydroxide form is quite unstable and in the presence of an acid, de-protonation of the acid occurs, resulting in the formation of water and the incorporation of the conjugate base as the anion.

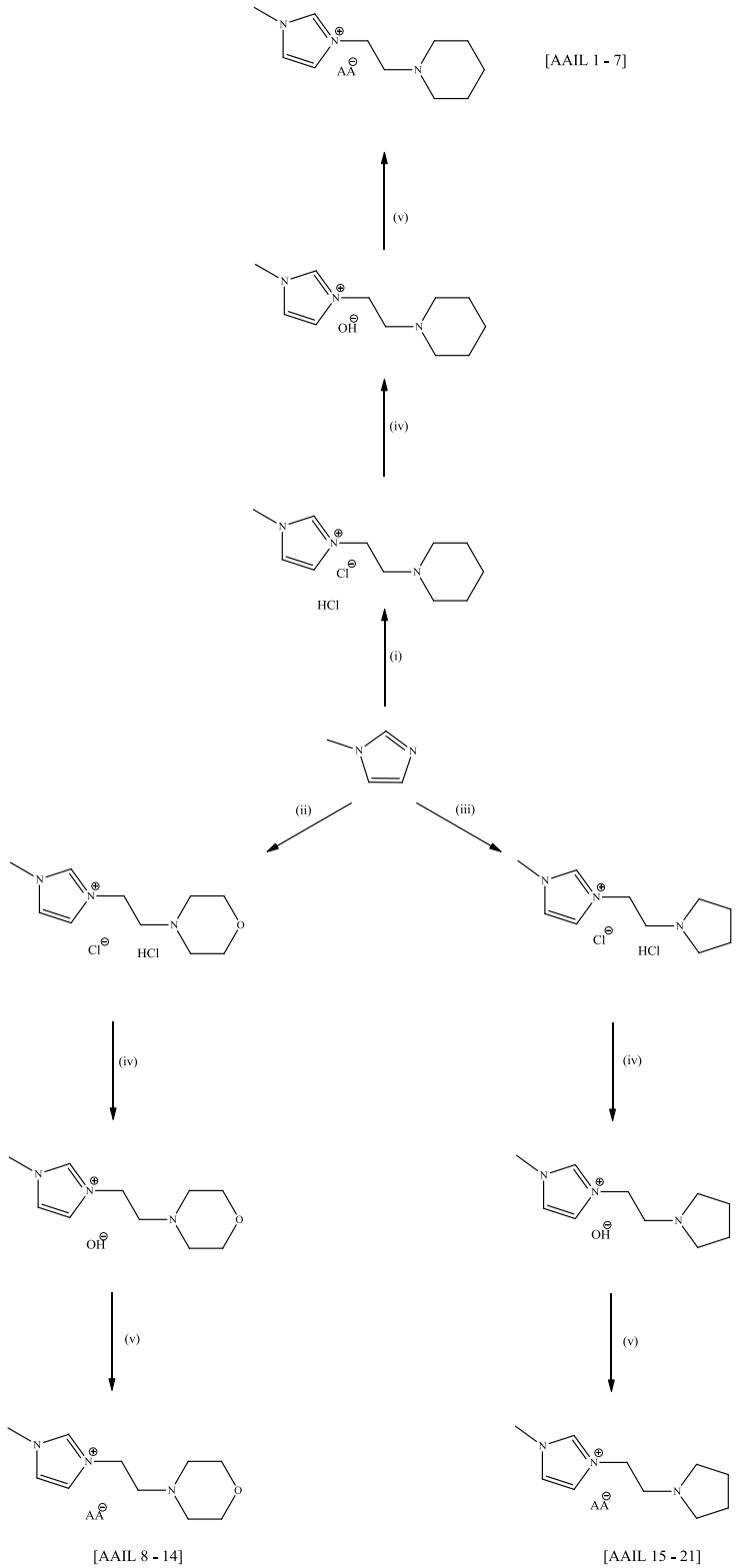

Scheme 3.3: Strategy for the synthesis of ionic liquids with simple anions (i) 1-(2-chloroethyl)piperidine hydrochloride, ethanol, 75 ºC, 16 h, (ii) 4-(2-chloroethyl)morpholine hydrochloride, 4:1 ethanol/toluene, 75 ºC, 16 h, (iii) 1-(2-chloroethyl)pyrrolidine hydrochloride, 75 ºC, 16 h (iv) 2 × IRA 400 OH^- anion exchange resin, 4 ºC, H_2O, (v) 1.2 mole equivalent amino acid, H_2O, rt, 24 h.

In order to obtain the desired ionic liquids, it is imperative that the hydrochloride moiety be removed, either before, or after the quaternisation reaction with 1-alkylimidazole. It was decided that this would be performed after, due to the ionic liquid hydrochloride salt being insoluble in dichloromethane, resulting in higher purity of the ionic liquid precursor via filtration, and subsequent washing of the hydrochloride salt with cold dichloromethane. However problems arose during the synthesis of the amino acid functionalised ionic liquids in comparison to simple anion based ionic liquids which are outlined below. To minimise the risk of fouling of the resin, 1.2 moles equivalent of base was added to the salt. The NaCl byproduct, which had the potential to interfere with the resin, was removed from solution by the addition of dichloromethane and the chloride ionic liquid isolated. This then underwent anion exchange via the use of anion exchange resin to generate the hydroxide form and was then added to an amino acid solution to yield the amino acid functionalised ionic liquid. An example of a resulting ^{1}H NMR spectrum for a typical recorded amino acid ionic liquid 1-methyl-2-(morphol-4-yl)ethylimidazolium l-lysinate, is given in Figure 3.7. The spectrum exhibits the presence of impurities with multiple signals of low intensity, in particular at around the 8.0 – 9.0 ppm with quite a noisy baseline as well as broadening of the signals corresponding to the morpholine ring at approximately 3.50 ppm. To investigate the origin of the impurities, all ^{1}H NMR spectra of starting materials, including the neutral amino acids were obtained, and it was determined that these were not the origin of the contamination. The ion exchange resin is an insoluble polymer matrix consisting of a polystyrene - quaternary ammonium derivative, and so attention focused in this area to determine if the contaminants evident in the aromatic region of the ^{1}H NMR spectrum were due to the resin, however this was also proved to be negative. Finally, the neutralisation step (removal of the HCl moiety) was investigated. The ^{1}H NMR spectra of the ionic liquid was obtained directly after the addition of base and isolation through the removal of the water under reduced pressure. The product of this had never been examined as the chloride liquids are not well known for the gas solubility properties step and the absence of problems during the synthesis of the simple anion based liquids. These spectra clearly indicated that contamination of the liquids was occurring during this step of the process, most likely due to degradation of the ionic liquid unit illustrated in Figure 3.8. Reduction of the NaOH from 1.2 to 1.0 moles equivalent still resulted in degradation of the liquids.

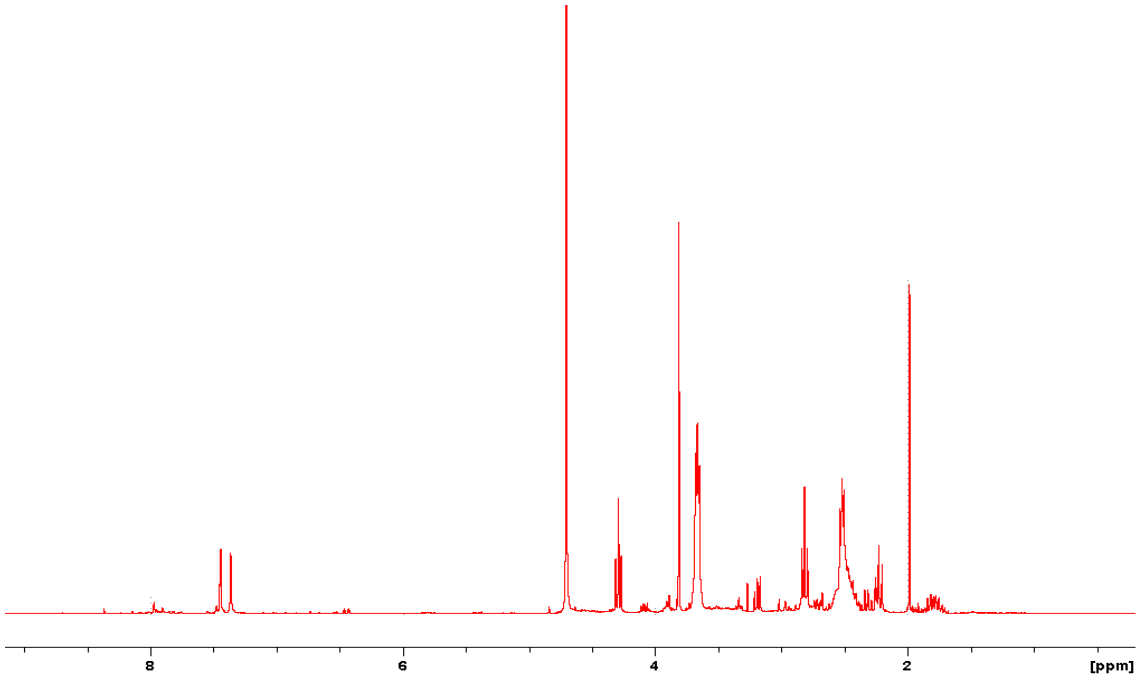

Figure 3.7: ^{1}H NMR spectrum of 1-methyl-3-(morphol-4-yl)ethylimidazolium l-lysinate.

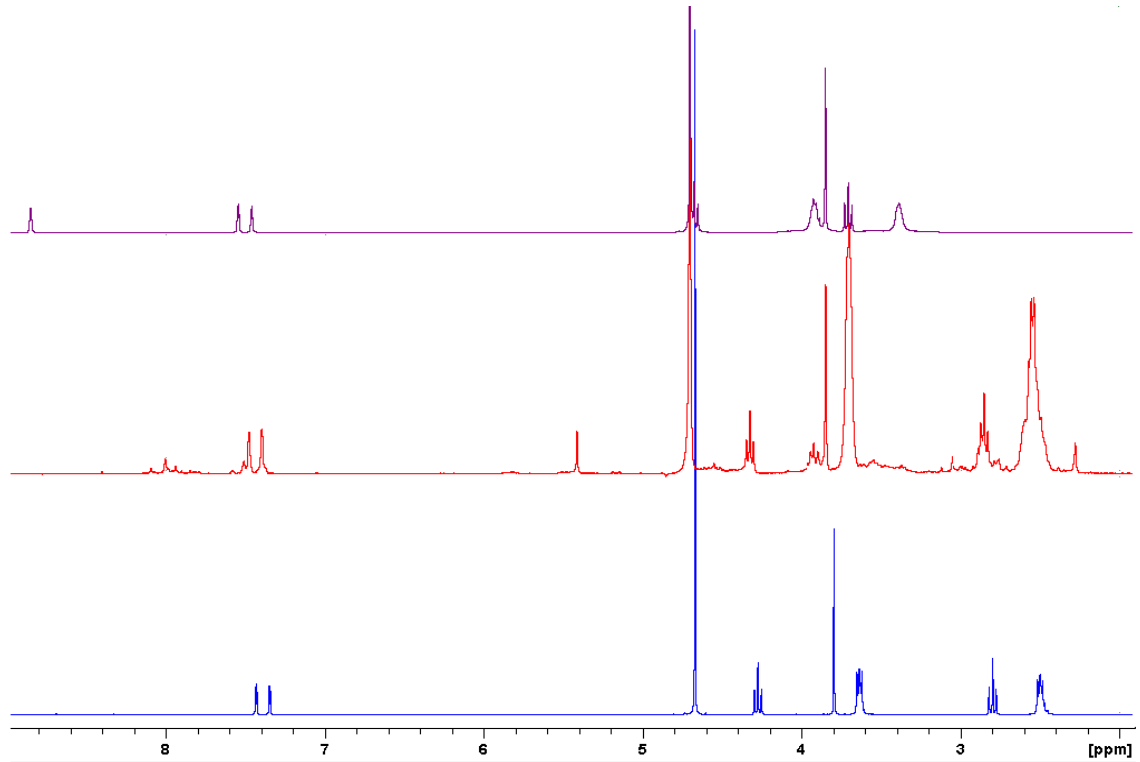

Figure 3.8: ^{1}H NMR spectra of 1-methyl-3-(morphol-4-yl)ethylimidazolium chloride hydrochloride (-), 1-methyl-3-(morphol-4-yl)ethylimidazolium chloride after treatment with 1.2 mole equivalent NaOH (-), 1-methyl-3-(morphol-4-yl)ethylimidazolium chloride after 1st passage through anion exchange resin column(-). All the above spectra were recorded in D_2O.

Upon examination of the literature, there appeared to be little to no information on the degradation of imidazolium based ionic liquids. However, degradation of imidazole

derivatives, such as 7-methylguanosine purines was published in 1966.[8,9] Chetsanga *et al*. investigated the kinetics of a ring opening reaction by incubating 7-methylguanosine with 0.2 M NaOH at 37 ºC and performed HPLC on samples at various times. They were then able to determine the mechanism of degradation by observing the changing chromatographic peaks and retention times exhibited by the sample over time. This demonstrated a decrease in the levels of 7-methylguanosine as it is degraded into various species. From these studies they determined that under alkaline conditions, there is a nucleophillic attack at the C2 position of the imidazole unit by the hydroxyl ion. This results in the formation of a carbinolamine species and a loss of aromaticity of the imidazole ring due to the newly formed σ bond with the hydroxyl ion at the C2 position of the imidaozle. It is well documented that the C2 position of imidazoles are acidic in nature hence nucleophillic attack would occur at this site.[10] This results in a ring opening reaction to relieve the strain imposed by the presence of the hydroxyl bond. This mechanism is presented in Scheme 3.4 and is in agreement with that also proposed by Hecht *et al*. in 1976.[11]

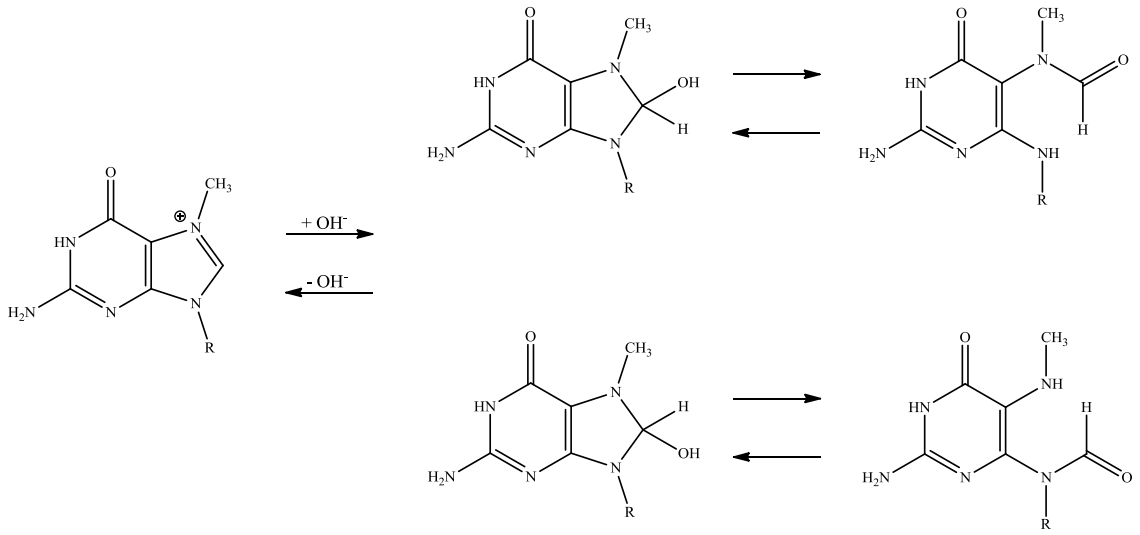

Scheme 3.4: Proposed mechanism of the degradation of 7-methylguanosine under alkaline conditions.[8]

Degradation of the imidazolium unit can also occur without the presence of an "external" base. Work reported in the literature on the poly(ionic liquid), poly(1-[(2-methylaryloyloxy)ethyl]-3-butylimidazolium hydroxide) also demonstrated that degradation can occur when hydroxides are employed as the counter ion.[11] Investigations into the polymers chemical stability in an alkaline environment were

conducted in the presence of aqueous KOH at 80 ºC up to 186 hours. It was observed that the imidazolium cation became less stable with increasing pH. The presence of water was also deemed to have a beneficial effect on the chemical stability of the cation. At 90% and 50% relative humidity, no degradation of the polymer was observed. However, when the relative humidity was decreased to 10%, degradation of the polymer was detected by ^{1}H NMR spectroscopy at approximately 9.9% of the total amount of polymer present.[11] From ^{1}H NMR data it was observed that several peaks around 8.55 ppm arose due to the formation of formyl groups due to the ring opening reaction as outlined in Scheme 3.5.

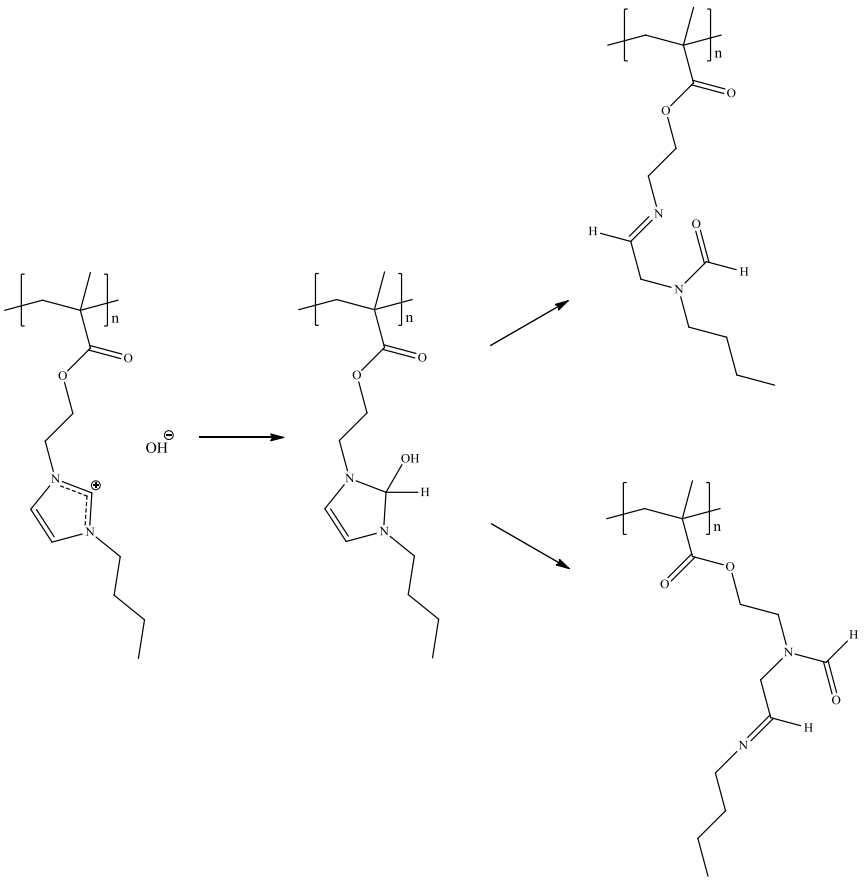

Scheme 3.5: Proposed mechanism of degradation of poly(1-[(2-methacryloyloxy)ethyl]-3-butylimidazolium hydroxide under alkaline conditions.

Upon examining both Schemes 3.4 and 3.5 it would appear that the imidazole degradation proceeds by identical pathways regardless of its substituents. Upon examination of the ^{1}H NMR spectra presented in Figure 3.8 (red trace), several signals can be observed at around 8.0 - 8.2 ppm which could arise from the formation of formyl groups. Also the broadening and increased integration of the peaks corresponding to

the morpholine ring may be as a direct result of the ring opening reaction and the signals for the protons which were formerly at the C4 and C5 position of the aromatic ring, which would shift upfield due to a loss of aromaticity of the imidazole ring.

In order to circumvent the decomposition of the ionic liquids in the neutralisation step, an alternative route to the use of the NaOH as explained below, was employed. Due to the strong acidic nature of HCl, it was believed that it could be removed via the anion exchange resin, due to its dissociation into anions, in an acid/base neutralisation reaction. From ^{1}H NMR data presented in Figure 3.8 (blue trace) and 3.9, it is evident that removal of the HCl moiety occurred. However it was clear that only the chloride form of the salt was present and that the resin had failed to convert the ionic liquid from its chloride to hydroxide form. The resulting solution was passed through a new anion exchange resin column and that incorporation of the amino acid (l-leucinate) as the anion had occurred was indicated by the presence of the signal for the α hydrogen which was a triplet at 3.19 ppm and the signal for the methyl groups at 0.82 ppm which had an integral of 6H.

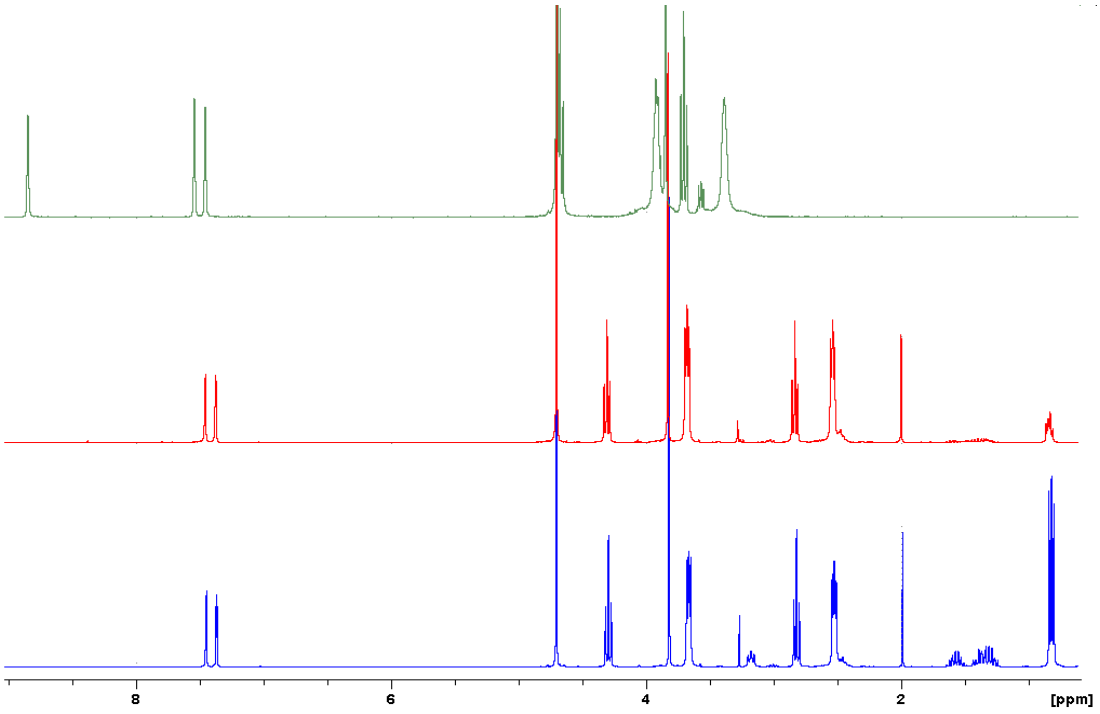

Figure 3.9: ^{1}H NMR spectra of 1-methyl-3-(morphol-4-yl)ethylimidazolium chloride hydrochloride (-), 1-methyl-3-(morphol-4-yl)ethylimidazolium chloride after 1st passage through OH^{-} functionalised ion exchange resin (-), 1-methyl-3-(morphol-4-yl)ethylimidazolium l-leucinate (-), recorded in D_2O.

From various experiments, it was found that the height of the anion exchange resin was quite important, too short and incomplete exchange of the anions occurred and lengthening of the column lead to degradation of the ionic liquid due prolonged exposure of the ionic liquids to basic conditions thus limiting the scale by which the ionic liquids could be synthesised. Pre-treatment of the anion exchange resin also proved vital in achieving a pure ionic liquid. It was not possible to use the resin as received due to high levels of residual base present in the resin during its production which resulted in degradation of the ionic liquid. Pre-washing with substantial amounts of water (200 cm^3) for a column of height 10 cm was performed and eliminated the degradation of the ionic liquid.

3.4.2 Characterisation of ionic liquids [AAIL1-21]

All NMR data presented in this section were obtained using D_2O as the deuterated solvent with the #, ~, and * symbols indicating overlapping signals. In the case where overlapping signals occurs the combined integral is given. All chemical shifts were given in ppm and coupling constants are in Hz.

3.4.2.1 ^{1}H NMR, ^{13}C NMR, and IR assignment of ionic liquids [AAIL1-7]

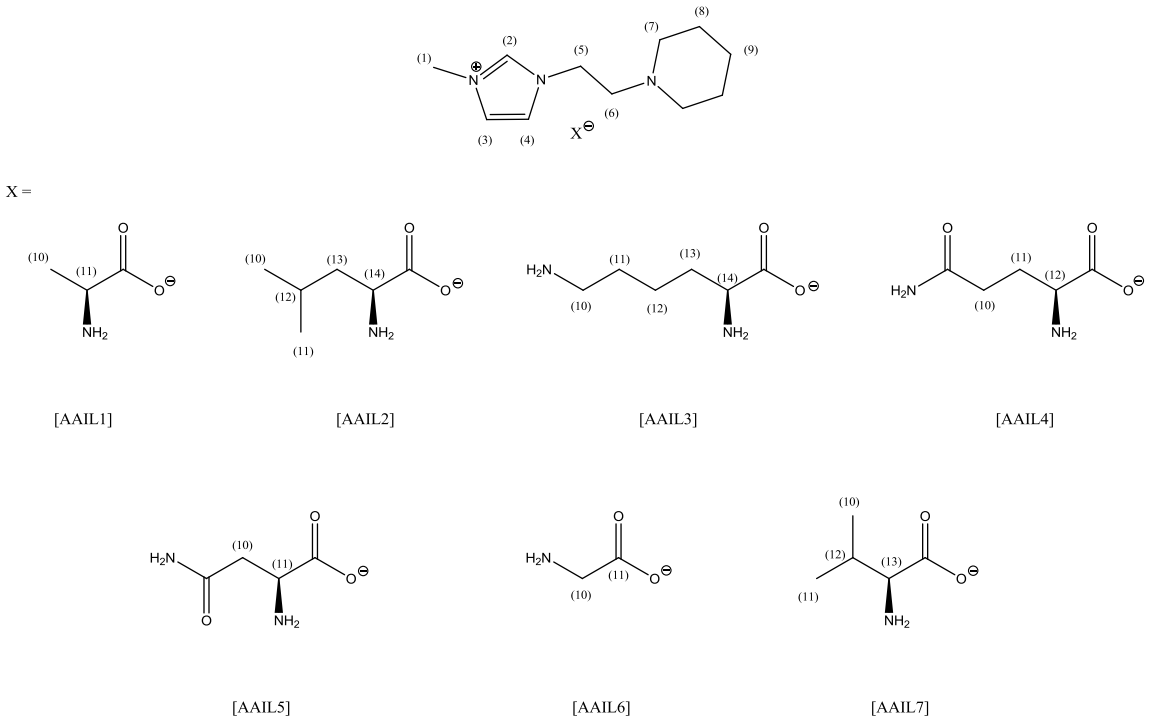

Figure 3.10: Structure of 1-methyl-3-(piperid-1-yl)ethylimidazolium cation and its respective amino acid based anions [AAIL1-7].

Table 3.10: ^{1}H NMR Assignment of ionic liquids [AAIL1-7].

	[AAIL1]	[AAIL2]	[AAIL3]
H1	3.80 (*s*, 3H)	3.80 (*s*, 3H)	3.80 (*s*, 3H)
H2	D_2O exchange	D_2O exchange	D_2O exchange
H3	7.35 (*d*, 1H, *J* = 1.9)	7.34 (*d*, 1H, *J* = 1.9)	7.35 (*d*, 1H, *J* = 1.9)
H4	7.42 (*d*, 1H, *J* = 1.9)	7.42 (*d*, 1H, *J* = 1.9)	7.42 (*d*, 1H, *J* = 1.9)
H5	4.27 (*t*, 2H, *J* = 6.9)	4.26 (*t*, 2H, *J* = 6.9)	4.27 (*t*, 2H, *J* = 7.0)
H6	2.76 (*t*, 2H, *J* = 6.9)	2.75 (*t*, 2H, *J* = 6.9)	2.78 (*t*, 2H, *J* = 7.0)
H7	2.41 (*m*, 4H)	2.41 (*t*, 4H, *J* = 5.1)	2.41 (*t*, 4H, *J* = 5.1)
H8	1.20 -1.48 (*m*, 6H)*	1.23 -1.51 (*m*, 9H)*	1.21 -1.42 (*m*, 12H)*
H9	1.20 -1.48 (*m*, 6H)*	1.23 -1.51 (*m*, 9H)*	1.21 -1.42 (*m*, 12H)*
H10	1.13 (*d*, 3H, *J* = 7.0)	0.80 (*d*, 3H, *J* = 5.0)	2.66 (*t*, 2H, *J* = 5.1)
H11	3.23 (*q*, 1H, *J* = 7.0)	0.82 (*d*, 3H, *J* = 5.0)	1.21 -1.42 (*m*, 12H)*
H12	-	1.51 (*m*, 9H)*	1.21 -1.42 (*m*, 12H)*
H13	-	1.51 (*m*, 9H)*	1.21 -1.42 (*m*, 12H)*
H14	-	3.24 (*t*, 1H, *J* = 5.7)	3.15 (*t*, 1H, *J* = 6.6)

	[AAIL4]	[AAIL5]
H1	3.76 (*s*, 3H)	3.76 (*s*, 3H)
H2	D_2O exchange	D_2O exchange
H3	7.31 (*d*, 1H, *J* = 1.7)	7.31 (*d*, 1H, *J* = 1.7)
H4	7.38 (*d*, 1H, *J* = 1.7)	7.38 (*d*, 1H, *J* = 1.7)
H5	4.24 (*t*, 2H, *J* = 7.0)	4.23 (*t*, 2H, *J* = 7.0)
H6	2.72 (*t*, 2H, *J* = 7.0)	2.72 (*t*, 2H, *J* = 7.0)
H7	2.38 (*s*, br, 4H)	2.26-2.58 (*m*, 6H)*
H8	1.23 -1.46 (*m*, 6H)$^{\#}$	1.23 -1.43 (*m*, 6H)$^{\#}$
H9	1.23 -1.46 (*m*, 6H)$^{\#}$	1.23 -1.43 (*m*, 6H)$^{\#}$
H10	2.19 (*t*, 2H, *J* = 8.3)	2.26-2.58 (*m*, 6H)*
H11	1.77 (m, 2H)	3.27 (*q*, 1H, *J* = 4.7)
H12	3.15 (t, 1H, J = 6.5)	-

	[AAIL6]	[AAIL7]
H1	3.80 (*s*, 3H)	3.78 (*s*, 3H)
H2	D_2O exchange	D_2O exchange
H3	7.34 (*d*, 1H, *J* = 1.7)	7.35 (*d*, 1H, *J* = 1.7)
H4	7.42 (*d*, 1H, *J* = 1.7)	7.41 (d, 1H, *J* = 1.7)
H5	4.27 (*t*, 2H, *J* = 7.0)	4.26 (*t*, 2H, *J* = 7.0)
H6	2.76 (*t*, 2H, *J* = 7.0)	2.75 (*t*, 2H, *J* = 7.0)
H7	2.41 (*m*, 4H)	2.41 (*m*, 4H)
H8	1.22 -1.47 (*m*, 6H)*	1.22 -1.47 (*m*, 6H)*
H9	1.22 -1.47 (*m*, 6H)*	1.22 -1.47 (*m*, 6H)*
H10	3.11 (*s*, 2H)	0.79 (*d*, 3H, *J* = 6.8)
H11	-	0.84 (*d*, 3H, *J* = 6.8)
H12	-	1.88 (*m*, 1H)
H13	-	3.04 (*d*, 1H, *J* = 5.0)

Table 3.11: ^{13}C NMR assignment of ionic liquids [AAIL1-7].

	AAIL1	AAIL2	AAIL3	AAIL4	AAIL5	AAIL6	AAIL7
Primary Carbons	20.0 35.6	34.8 20.3 21.5	35.6	35.5	34.7	34.8	16.5 18.7 35.6
Secondary Carbons	23.1 24.5 45.8 53.6 57.0	22.3 23.5 42.5 45.0 52.8 56.2	22.1 23.1 24.5 29.7 34.1 39.9 45.8 53.6 57.0	23.1 24.5 20.6 31.6 45.8 53.6 57.0	22.3 23.7 39.3 45.0 52.8 56.2	22.3 23.7 43.4 45.0 52.8 56.2	23.1 24.5 45.8 53.6 57.0
Tertiary Carbons	51.3 122.2 123.6	23.7 53.4 121.3 122.8	55.8 122.2 123.6	55.4 122.1 123.5	51.6 121.3 122.7	121.3 122.8	30.9 61.3 122.2 123.6
Quaternary Carbons	183.9	183.5	183.0	179.1 182.0	175.7 180.1	179.8	180.7

Table 3.12: IR assignment of ionic liquids [AAIL1-7].

	AAIL1	AAIL2	AAIL3	AAIL4	AAIL5	AAIL6	AAIL7
NH_2 (cm^{-1})	Not observed due to H_2O band	3371 3282	3350 3265	Not observed due to H_2O band	3345 3291	3348 3265	Not observed due to H_2O band
C=O (cm^{-1})	1594	1571	1563	1635 1580	1664 1563	1567	1575

3.4.2.2 ^{1}H NMR, ^{13}C NMR, and IR, assignment of ionic liquids [AAIL8-14]

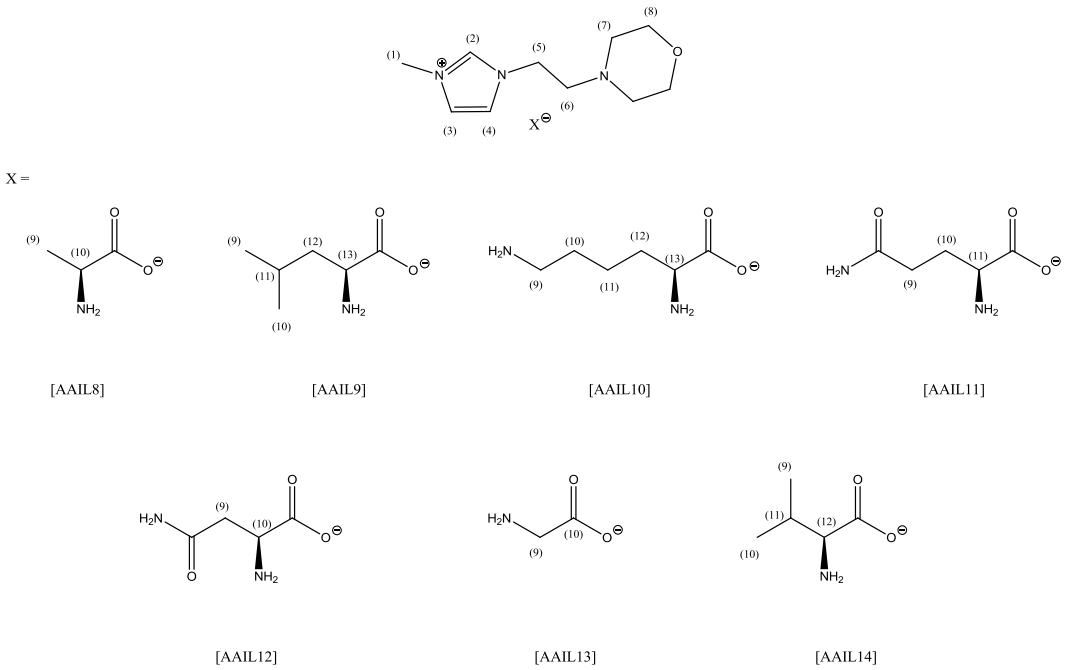

Figure 3.11: Structure of the 1-methyl-3-(morphol-4-yl)ethylimidazolium cation and its respective amino acid based anions [AAIL8-14].

Table 3.13: ^{1}H NMR Assignment of ionic liquids [AAIL1-7].

	[AAIL8]	[AAIL9]	[AAIL10]
H1	3.81 (*s*, 3H)	3.81 (*s*, 3H)	3.77 (*s*, *3*H)
H2	D_2O exchange	D_2O exchange	D_2O exchange
H3	7.35 (*d*, 1H, *J* = 1.9)	7.36 (*d*, 1H, *J* = 1.9)	7.33 (*d*, 1H, *J* = 1.9)
H4	7.44 (*d*, 1H, *J* = 1.9)	7.44 (*d*, 1H, *J* = 1.9)	7.41 (*d*, 1H, *J* = 1.9)
H5	4.29 (*t*, 2H, *J* = 6.6)	4.29 (*t*, 2H, *J* = 6.6)	4.25 (*t*, 2H, *J* = 6.6)
H6	2.81 (*t*, 2H, *J* = 6.6)	2.81 (*t*, 2H, *J* = 6.6)	2.78 (*t*, 2H, *J* = 6.6)
H7	2.52 (*t*, 4H, *J* = 4.8)	2.52 (*t*, 4H, *J* = 4.8)	2.50 (*m*, 6H)*
H8	3.66 (*t*, 4H, *J* = 4.8)	3.66 (*t*, 4H, *J* = 4.8)	3.62 (*t*, 4H, *J* = 4.7)
H9	1.15 (*d*, 3H, *J* = 7.0)	0.80 (*d*, 3H, *J* = 4.7)	2.50 (*m*, 6H)*
H10	3.21 (*q*, 1H, *J* = 7.0)	0.82 (*d*, 3H, *J* = 4.7)	1.33-1.49 (*m*, 6H)$^{\#}$
H11	-	1.42 (*m*, 1H)	1.33-1.49 (*m*, 6H)$^{\#}$
H12	-	1.32 (*m*, 2H)	1.33-1.49 (*m*, 6H)$^{\#}$
H13	-	3.19 (*t*, 1H, *J* = 5.7)	3.10 (*t*, 1H, *J* = 6.5)

	[AAIL11]	[AAIL12]
H1	3.77 (*s*, 3H)	3.81 (*s*, 3H)
H2	D_2O exchange	D_2O exchange
H3	7.32 (*d*, 1H, *J* = 1.9)	7.36 (*d*, 1H, *J* = 1.9)
H4	7.40 (*d*, 1H, *J* = 1.9)	7.44 (*d*, 1H, *J* = 1.9)
H5	4.25 (*t*, 2H, *J* = 6.6)	4.29 (*t*, 2H, *J* = 6.6)
H6	2.78 (*t*, 2H, *J* = 6.6)	2.81 (*t*, 2H, *J* = 6.6)
H7	2.48(*t*, 4H, *J* = 4.8)	2.61 (*m*, 6H)*
H8	3.63 (*t*, 4H, *J* = 4.8)	3.66 (*t*, 4H, *J* = 4.8)
H9	2.19 (*t*, 2H, *J* = 6.5)	1.98-2.84 (*m*, 6H, *J* = 4.6)*
H10	1.78 (*m*, 2H)	3.49 (*q*, 1H, *J* = 4.7)
H11	3.15 (*t*, 1H, *J* = 8.3)	-

	[AAIL13]	[AAIL14]
H1	3.77 (*s*, 3H)	3.77 (*s*, 3H)
H2	D_2O exchange	D_2O exchange
H3	7.33 (*d*, 1H, *J* = 2.0)	7.32 (*d*, 1H, *J* = 1.8)
H4	7.40 (*d*, 1H, *J* = 2.0)	7.40 (*d*, 1H, *J* = 1.8)
H5	4.25 (*t*, 2H, *J* = 6.7)	4.25 (*t*, 2H, *J* = 6.7)
H6	2.78 (*t*, 2H, *J* = 6.7)	2.77 (*t*, 2H, *J* = 6.7)
H7	2.48 (*t*, 4H, *J* = 4.7)	2.48 (*t*, 4H, *J* = 4.7)
H8	3.63 (*t*, 4H, *J* = 4.7)	3.62 (*t*, 4H, *J* = 4.7)
H9	3.09 (*s*, 2H)	0.81 (*d*, 3H, *J* = 6.9)
H10	-	0.84 (*d*, 3H, *J* = 6.9)
H11	-	1.88 (*m*, 1H)
H12	-	3.04 (*d*, 1H, *J* = 5.5)

Table 3.14: ^{13}C NMR assignment of ionic liquids [AAIL8-14].

	AAIL8	AAIL9	AAIL10	AAIL11	AAIL12	AAIL13	AAIL14
Primary Carbons	19.3 34.8	21.3 22.3 35.6	35.6	34.8	34.8	35.61	15.6 17.9 34.8
Secondary Carbons	44.7 51.6 55.8 65.1	43.7 45.5 52.4 56.7 66.0	22.2 31.0 34.3 40.1 45.5 52.4 56.7 65.9	30.6 31.6 45.5 52.4 56.7 65.9	39.5 44.7 51.6 55.9 65.1	44.2 45.5 52.4 56.7 65.9	44.7 51.6 55.9 65.1
Tertiary Carbons	50.5 121.4 122.7	24.3 54.4 122.3 123.6	55.8 122.2 123.5	55.4 122.2 123.5	52.4 121.4 122.7	122.2 123.5	30.2 60.6 121.4 122.7
Quaternary Carbons	183.3	183.5	183.5	178.2 181.2	175.8 180.3	180.4	180.4

Table 3.15: IR assignment of ionic liquids [AAIL8-14].

	AAIL8	AAIL9	AAIL10	AAIL11	AAIL12	AAIL13	AAIL14
NH_2 (cm^{-1})	Not observed due to H_2O band	3349 3268	3345 3278	Not observed due to H_2O band	3345 3296	3380 3269	3356 3256
C=O (cm^{-1})	1586	1562	1560	1666 1576	1666 1563	1563	1573

3.4.2.3 ^{1}H NMR, ^{13}C NMR, and IR, assignment of ionic liquids [AAIL15-21]

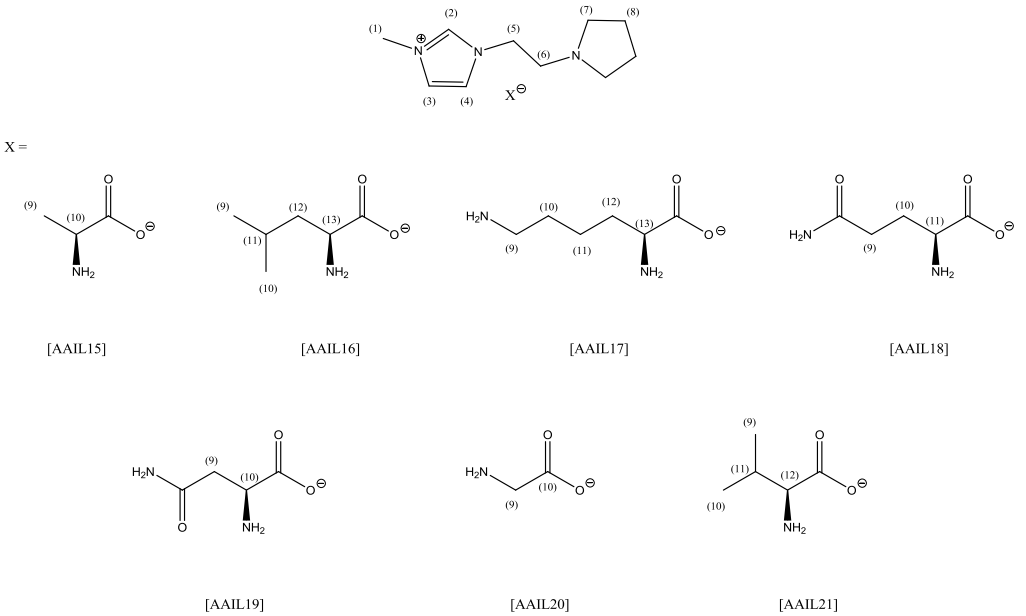

Figure 3.12: Structure of the 1-methyl-3-(pyrrolid-1-yl)ethylimidazolium cation and its respective amino acid based anions [AAIL15-21].

Table 3.16: ^{1}H NMR assignment of ionic liquids [AAIL15-21]

	[AAIL15]	[AAIL16]	[AAIL17]
H1	3.81 (*s*, 3H)	3.80 (*s*, 3H)	3.77 (*s*, 3H)
H2	D_2O Exchange	D_2O Exchange	D_2O Exchange
H3	7.36 (*d*, 1H, *J* = 1.7)	7.36 (*d*, 1H, *J* = 1.7)	7.32 (*d*, 1H, *J* =1.7)
H4	7.43 (*d*, 1H, *J* = 1.7)	7.43 (*s*, 1H, *J* = 1.7)	7.40 (*d*, 1H, *J* = 1.7)
H5	4.26 (*t*, 2H, *J* = 6.6)	4.26 (*t*, 2H, *J* = 6.7)	4.23 (*t*, 2H, *J* = 6.6)
H6	2.91 (*t*, 2H, *J* = 6.6)	2.91 (*t*, 2H, *J* = 6.7)	2.88 (*t*, 2H, *J* = 6.6)
H7	2.50 (*s*, br, 4H)	2.51 (*m*, 4H)	2.48 (*m*, 6H)*
H8	1.69 (*s*, br, 4H)	1.65 (*m*, 5H)*	1.65 (*m*, 4H)
H9	1.18 (*d*, 3H, *J* = 7.0)	0.81 (*d*, 3H, *J* = 5.0)	2.48(*m*, 6H)*
H10	3.30 (*q*, 1H, *J* = 7.0)	0.84 (*d*, 3H, *J* = 5.0)	1.44 (*m*, 6H)#
H11	-	1.65 (*m*, 5H)*	1.44 (*m*, 6H)#
H12	-	1.34 (*m*, 4H)	1.44 (*m*, 6H)#
H13	-	3.18 (*t*, 1H, *J* = 5.7)	3.11 (*t*, 1H, *J* = 6.4)

	[AAIL18]	[AAIL19]
H1	3.80 (*s*, 3H)	3.81 (*s*, 3H)
H2	D_2O exchange	D_2O exchange
H3	7.36 (*d*, 1H, *J* = 1.7)	7.36 (*d*, 1H, *J* = 1.7)
H4	7.44 (*d*, 1H, *J* = 1.7)	7.44 (*d*, 1H, *J* =1.7)
H5	4.26 (*t*, 2H, *J* = 6.7)	4.27 (*t*, 2H, *J* = 6.7)
H6	2.91 (*t*, 2H, *J* = 6.7)	2.91 (*t*, 2H, *J* = 6.7)
H7	2.50 (*m*, 4H)	2.29-2.61 (*m*, 6H)*
H8	1.68 (*m*, 6H)*	1.68 (*m*, 4H)
H9	2.22 (*t*, 2H, *J* = 8.3)	2.29-2.61 (*m*, 6H)*
H10	1.68 (*m*, 6H)*	3.48 (*q*, 1H, *J* = 4.7)
H11	3.20 (*t*, 1H, *J* = 6.5)	-

	[AAIL20]	[AAIL21]
H1	3.76 (*s*, 3H)	3.80 (*s*, 3H)
H2	D_2O exchange	D_2O exchange
H3	7.31 (*d*, 1H, *J* = 1.7)	7.35 (*d*, 1H, *J* = 1.7)
H4	7.39 (*d*, 1H, *J* = 1.7)	7.43 (*d*, 1H, *J* = 1.7)
H5	4.22 (*t*, 2H, *J* = 6.6)	4.26 (*t*, 2H, *J* = 6.6)
H6	2.86 (*t*, 2H, *J* = 6.6)	2.93 (*m*, 3H)*
H7	4.63 (*m*, 4H)	2.49 (*m*, 4H)
H8	1.65 (*m*, 4H)	1.68 (*m*, 4H)
H9	3.05 (*s*, 2H)	0.78 (*d*, 3H, *J* = 7.0)
H10	-	0.83 (*d*, 3H, *J* = 7.0)
H11	-	1.84 (*m*, 2H)
H12	-	2.93 (*m*, 3H)*

Table 3.17: ^{13}C NMR assignment of ionic liquids [AAIL15-21]

	AAIL15	AAIL16	AAIL17	AAIL18	AAIL19	AAIL20	AAIL21
Primary Carbons	19.6 35.6	21.3 22.3 35.6	34.8	34.8	34.8	35.6	16.6 18.9 35.6
Secondary Carbons	22.6 47.9 53.3 54.5	22.6 43.8 47.9 53.3 54.5	21.8 29.8 30.8 47.0 52.5 53.7	21.8 29.8 30.8 47.0 52.5 53.7	21.8 39.5 47.0 52.7 53.6	22.6 44.4 47.9 53.3 54.5	22.6 47.9 53.3 54.5
Tertiary Carbons	51.2 122.1 123.1	24.3 48.8 122.1 136.4	54.6 121.3 122.8	54.6 121.3 122.8	52.5 121.3 122.8	122.1 123.7	31.5 61.7 122.1 123.7
Quaternary Carbons	183.2	182.3	178.3 181.2	178.3 181.2	175.8 180.2	180.9	182.4

Table 3.18: IR assignment of ionic liquids [AAIL15-21]

	AAIL15	AAIL16	AAIL17	AAIL18	AAIL19	AAIL20	AAIL21
NH_2 (cm^{-1})	3356 3278	3372 3265	3354 3275	3363 3229	3358 3291	3352 3276	3363 3279
C=O (cm^{-1})	1587	1562	1569	1670 1562	1663 1564	1571	1564

3.4.2.4 ^{1}H NMR characterisation of ionic liquids [AAIL1-21]

Hydrogen/deuterium exchange is well-documented and well understood with an abundance of literature in relation to its occurrence at functional groups such as amines and hydroxides. The process involves rapid interchange of hydrogen and deuterium at the site, rendering the signal undetectable or barely visible in the resulting NMR spectra. Various solvents will have different effects which range from small broad peaks for amines in deuterated methanol to the absence of peaks in solvents such as D_2O. This effect can be readily seen in systems reported in this thesis and in particular with the amino acid based ionic liquids with the disappearance of primary amine signals in the anions of the liquids. However, a more peculiar effect was the disappearance of the signals corresponding to both the proton (H(2)) and carbon (C(2)) signals of the imidazole ring in their respective NMR data for all amino acid ionic liquids [AAIL1-21]. There are two possible explanations which explain this phenomena, opening of the imidazole ring due to the basic nature of the anion exchange resin that it was passed through, or that hydrogen/deuterium exchange was also according at the C(2) position of the imidazole ring. A ring opening reaction appears unlikely, due to the position of the signals relating to H(4) and H(5). The results of a ring opening reaction would be the loss of conjugation, which would result in a substantial shift of the signals upfield. However as can be seen in Figure 3.13, there is only a negligible shift in the spectra in comparison to its chloride counterpart and as such indicate the presence of the conjugated system.

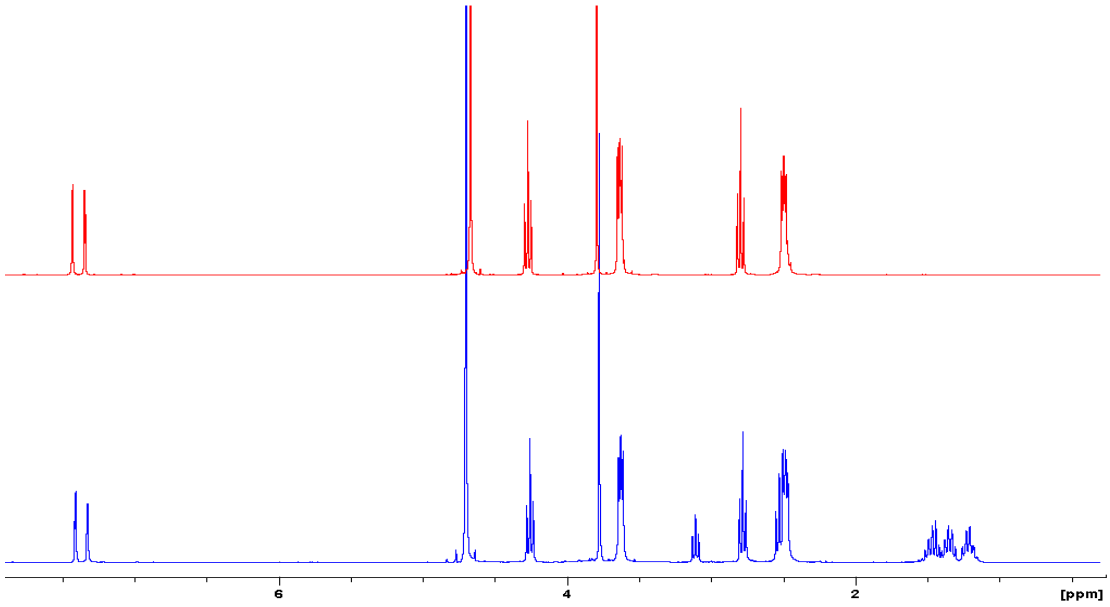

Figure 3.13: ^{1}H NMR sprectrum of 1-(methyl)-3-(morphol-4-yl)ethylimidazolium chloride (-), and 1-methyl-3-(morphol-4-yl)ethylimidazolium lysinate (-).

To investigate potential deuterium exchange at the H(2) position of the imidazole ring, salt [9e] an ionic liquid which is miscible in both D_2O and $CDCl_3$ was examined. From Figure 3.14, the effect that the D_2O has on the NMR spectra of the ionic liquids can be seen with the presence of the H(2) signal in the $CDCl_3$ spectra, but the absence of this signal in the D_2O ran spectra, thus indicating a solvent effect and the presence of deuterium exchange. It was later found that this effect was also witnessed by Lozano *et al,*[12] where they also performed NMR spectral analysis of BMIM Cl in D_2O and also had the absence of the H(2) signal. Mass spectrum results obtained for the respective liquids indicate the structure of the cation has remained intact, thus further proving deuterium-hydrogen exchange is occurring. The emergence of the anion protons are also evident with the multiplet at 1.33-1.49 ppm due to the *β*, *γ*, and *ε*, proton signals for the lysinate structure and the α proton signal at 3.10 ppm, with the proton signal overlapping with the θ proton signal overlapping with the morpholine ring signal.

The first evidence of deuterium exchange at the H(2) position of an imidazole ring was first proposed by Olofson *et al.* in 1964, where deuterium was exchanged under mild conditions.[10] Since then extensive work has been carried out on deuterium exchange in imidazole based compounds and in particular ionic liquids. Due to the acidic nature of the H(2) hydrogen, and its role in hydrogen bonding with the anions, the tendency for hydrogen-deuterium exchange to occur tends to be anion dependent, with increased anion basicity resulting in increased deuterium exchange.[13] This results in some ionic

liquids requiring no external base to undergo hydrogen/deuterium exchange while those liquids with a non-basic or weakly coordinating anion are less likely to undergo deuterium exchange, unless an external base is present.

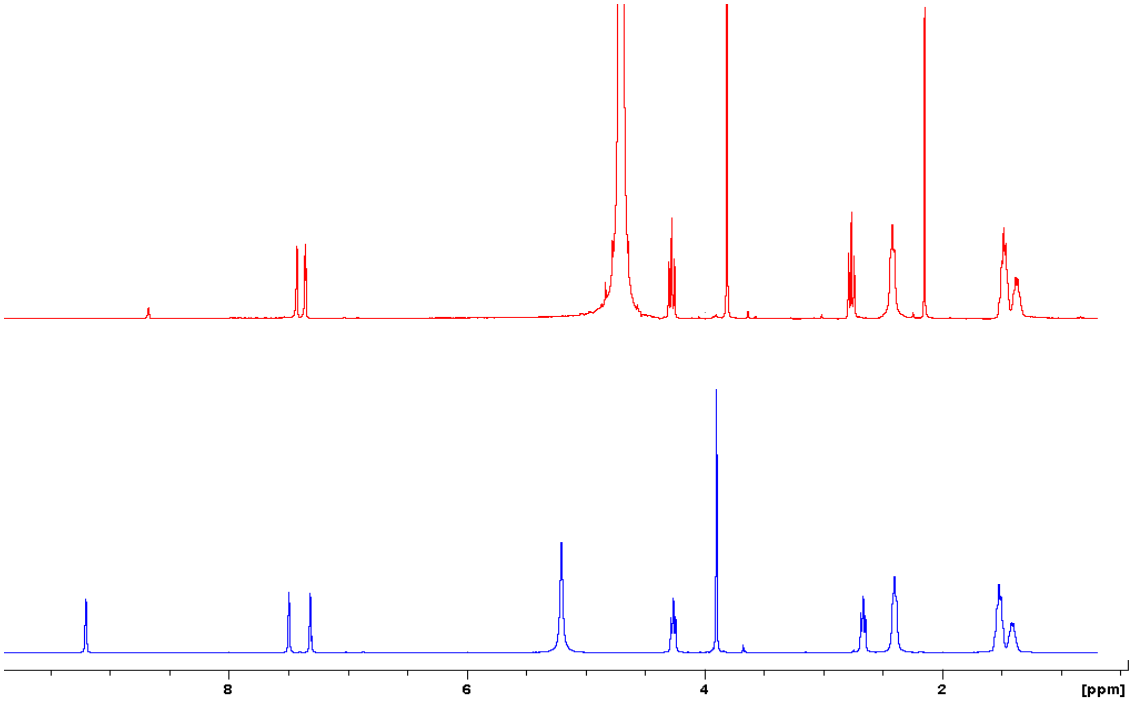

Figure 3.14: ^{1}H NMR spectra of 1-methyl-3-(piperid-1-yl)ethyl imidazolium trifluoroacetate in D_2O (-), and 1-methyl-3-(piperid-1-yl)ethyl imidazolium trifluoroacetate in $CDCl_3$ (-).

This hydrogen deuterium exchange not only affects the C2 hydrogen signal of the imidazole ring but also the hydrogen signals in the C4 and C5 position. As previously mentioned in Section 3.3.2.4, the C4 and C5 proton signals produced pseudo triplets due to coupling with each other and also long range coupling with the C2 proton signal producing a doublet of doublets whose coupling constants were small enough to appear as a triplet. As already established in this section deuterium exchange occurs between the acidic C2 proton and deuterium from the NMR solvent resulting in the loss of that signal in the ^{1}H NMR when polar solvents were used. It is due to this that the C4 and C5 proton signals of all the amino acid ionic liquids appear as doublets in the ^{1}H NMR spectra when D_2O is used, as a proton is no longer present at the C2 position of the imidazole ring and as such there is no further splitting of the C4 and C5 proton signals.

Another feature of the ^{1}H NMR data of the amino acid ionic liquids is perhaps most evident when examining the ionic liquids containing the leucinate and valinate anion. These contain protons which appear to be chemically equivalent but give rise to

different signals due to the presence of the chiral centre which generates this diastereotopic effect resulting in this inequivalency. For [AAIL16] and [AAIL21], this lack of symmetry is most noticeable when examining the methyl substituents (Figure 3.12), where if the two methyl groups were equivalent, then one signal, a doublet would be produced due to splitting with the adjacent tertiary proton signal. However, two doublets were observed in both the leucinate and valinate species for the methyl groups. All protons in the anionic structure are diastereotopic however the inequivalency is only large enough to be observed when this dimethyl branching is present.

3.4.2.5 ^{13}C NMR characterisation of ionic liquids [AAIL1-21]

Hydrogen-deuterium exchange as for the ^{1}H NMR spectra (Section 3.4.3.4), also appears to have an effect on the ^{13}C NMR spectra of the ionic liquids (Figure 3.15). Similar to the loss of the C2 hydrogen signal in the ^{1}H NMR spectra, it has also been observed that the signal corresponding to the C2 carbon also disappears in the presence of D_2O. Although undocumented in the literature, we would propose that this is also due to the deuterium exchange resulting in lengthening relaxation times and broadening of the signal and disappearance into the base line. This theory is furthered enhanced when examining the ^{13}C NMR spectra of salt [9d] which demonstrates the effect deuterium exchange has on the ^{13}C NMR spectra with the C2 signal present when dissolved in $CDCl_3$, and its disappearance when dissolved in D_2O.

As also mentioned in Section 3.4.3.4, a lack of equivalency in the methyl signals for the two methyl groups in the valinate and leucinate anions can also be observed in the ^{13}C NMR spectra, with the emergence of two signals instead of one at 16.6 and 18.9 ppm which were verified as methyl signals by DEPT 135 and HSQC spectroscopy experiments. This further proves the inequivalent nature of the two methyl groups but as is observed from the ^{1}H NMR spectra, no further signs of inequivalency across the anionic structure was observed due to the small changes in the chemical shifts involved.

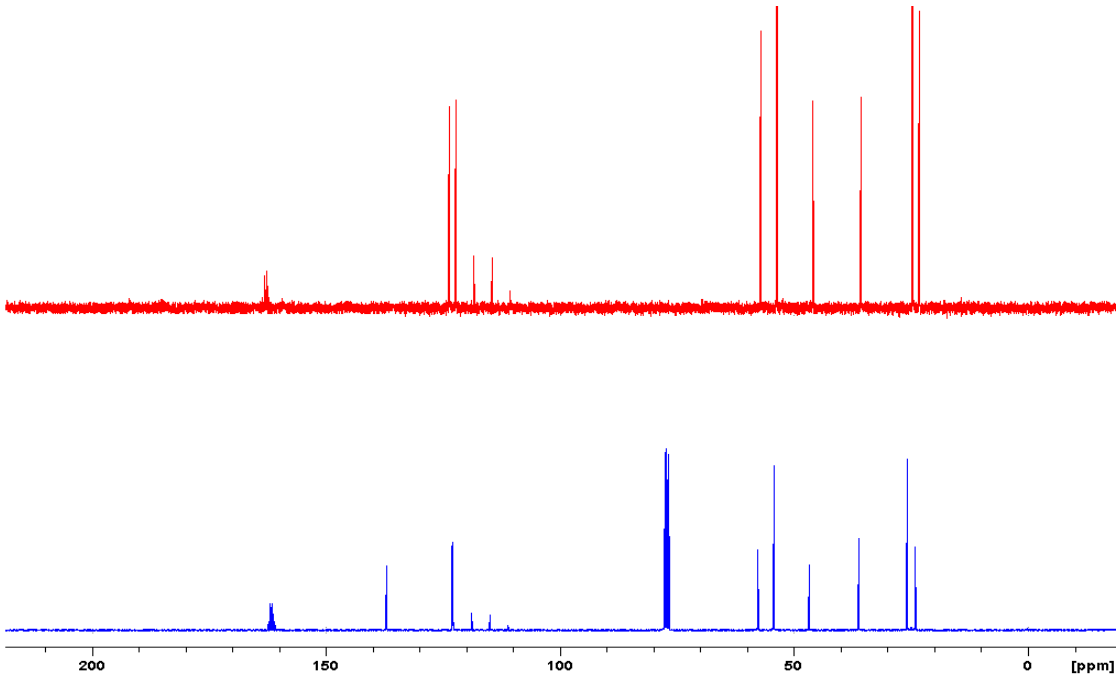

Figure 3.15: ^{13}C NMR spectra of 1-methyl-3-(piperid-1-yl)ethyl imidazolium trifluoroacetate in D_2O (-), and 1-methyl-3-(piperid-1-yl)ethyl imidazolium trifluoroacetate in $CDCl_3$ (-).

3.4.2.6 IR characterisation of ionic liquids [AAIL1-21]

The predominate features of interest in the IR spectra of the amino acid ionic liquids are the carbonyl stretching bands (typically 1560 cm^{-1}) and amine bands (around 3200 – 3300 cm^{-1}) and these values are consistent with other amino acid ionic liquid analogues found in the literature.[14,15] From the IR data of the ionic liquids, the emergence of two peaks corresponding to the N-H stretch indicates the presence of a primary amine which is in contrast to the free amino acid where a broad singlet was observed in this region due to the zwitterion effect. This indicates the lack of zwitterion activity and that the formation of the carboxylate species has been successful. This is further confounded by the shifts in wavenumber for the C=O stretch for example, with the [AAIL6] carbonyl stretching band for [AAIL6] observed at 1568 cm^{-1}, a shift of approximately 40 cm^{-1} from that observed in its zwitterionic state. This indicates the presence of the carboxylate species and further confirms the incorporation of the amino acid as the anionic species of the liquid. These features were typical in all amino acid ionic liquid infrared spectra which were analysed.

3.4.2.7 Mass spectrum data of ionic liquids [AAIL 1- 21]

Due to the hygroscopic nature, and high viscosity of ionic liquids, difficulties arose in the complete removal of solvent and water from some of the ionic liquids. Elemental

analysis was performed on some liquids. However it was found that a reproducible value could not be obtained upon repeated analysis of the same sample, with variation in the results as a direct result of the presence of residual solvents. Rigorous drying in combination with storage under an inert environment did not help alleviate the problem resulting in no reliable data from elemental analysis. This appears to be a common problem due to the abundance of papers on ionic liquids which solely give accurate mass spectrometry as a means of confirming the identity of the salts.[16-19] Mass Spectrometry was used as an alternative technique in confirming the structure of the ionic liquids utilising both positive and negative ionisation modes. In particular, this technique was most crucial when characterising the amino acid ionic liquids, due to the higher viscosity demonstrated with all amino acid based ionic liquids, and in confirming the conversion of the neutral amino acid to its anionic state and thus incorporation into the ionic liquid (Table 3.19). Positive ionisation mode was also performed to determine the accurate mass of the cation, the results of which can be found in Chapter 2.

Table 3.19: Accurate mass of anion obtained from ESI mass spectrometry recorded in the negative ionisation mode.

Ionic Liquid	Negative Ionisation		Ionic Liquid	Negative Ionisation	
	Calculated (a.m.u)	Observed (a.m.u)		Calculated (a.m.u)	Calculated (a.m.u)
[AAIL1]	88.0404	88.0408	**[AAIL12]**	131.0462	131.0459
[AAIL2]	130.0874	130.0869	**[AAIL13]**	74.0248	74.0245
[AAIL3]	145.0983	145.0979	**[AAIL14]**	116.0717	116.0716
[AAIL4]	145.0619	145.0617	**[AAIL15]**	88.0404	88.0407
[AAIL5]	131.0462	131.0463	**[AAIL16]**	130.0874	130.0868
[AAIL6]	74.0248	74.0245	**[AAIL17]**	145.0983	145.0979
[AAIL7]	116.0717	116.0711	**[AAIL18]**	145.0619	145.0619
[AAIL8]	88.0404	88.0400	**[AAIL19]**	131.0462	131.0464
[AAIL9]	130.0874	130.0869	**[AAIL20]**	74.0248	74.0245
[AAIL10]	145.0983	145.0984	**[AAIL21]**	116.0717	116.0716
[AAIL11]	145.0619	145.0613			

3.5 Physical characterisation of a number of ionic liquids synthesised

The following section pertains to the physical characterisation of ionic liquids which were deemed to be of interest from the CO_2 permeability and absorption data presented in the subsequent Chapter 4. Presented in this section is the thermal analysis, such as decomposition and melting points, as well as viscosity measurements, and refractive indexes. The data will mainly be presented in a manner such as to ascertain the effect that both the cation and the anion have on each of the physical properties.

3.5.1 Thermal analysis of ionic liquids

3.5.1.1 Thermal stability studies of ionic liquids

Determination of the thermal stability of the ionic liquids (9a-11e, and AAIL 17 and 20) was also a key area of investigation due to the potential application of these materials as CO_2 sorbents, which would expose them to elevated temperatures. Thermogravrimetic analysis and low temperature DSC analysis were carried out with the help of Dr. James Kennedy and Alan Murphy at Athlone Institute of Technology. Room temperature to high temperature DSC analysis was carried out at NUIM. Figure 3.16 shows the TGA profiles and illustrates the effect that both the anion and cation have on the thermal stability. Each ionic liquid was exposed to the temperature range 25 – 600 ^oC at an increase rate of 10 ^oC per minute under N_2.

From Figure 3.16, it is clear that the anion has a significant effect on thermal stability of the liquids. The salt [9d] is seen to have the lowest T_{onset} (decomposition onset) value with decomposition occurring at 190 ^oC, whereas [9e] demonstrated the highest thermal stability with a T_{onset} value of 287 ^oC. These trends fall into line with those discovered by Bonhote *et al.* using the 1-ethyl-3-methylimidazolium cation and TFA^-, Tf_2N^-, and $TFMS^-$ anion.[20] During their study they observed that the ionic liquid containing the TFA^- anion had the T_{onset} with a value of 150 ^oC, while the other two anions had similar values of T_{onset} of 440 ^oC observed for both. While increased hydrophobicity has been linked to increase T_{onset} values, Pringle *et al.* have demonstrated that lower nucleophilicity of the anion can also result in increased thermal stability.[21]

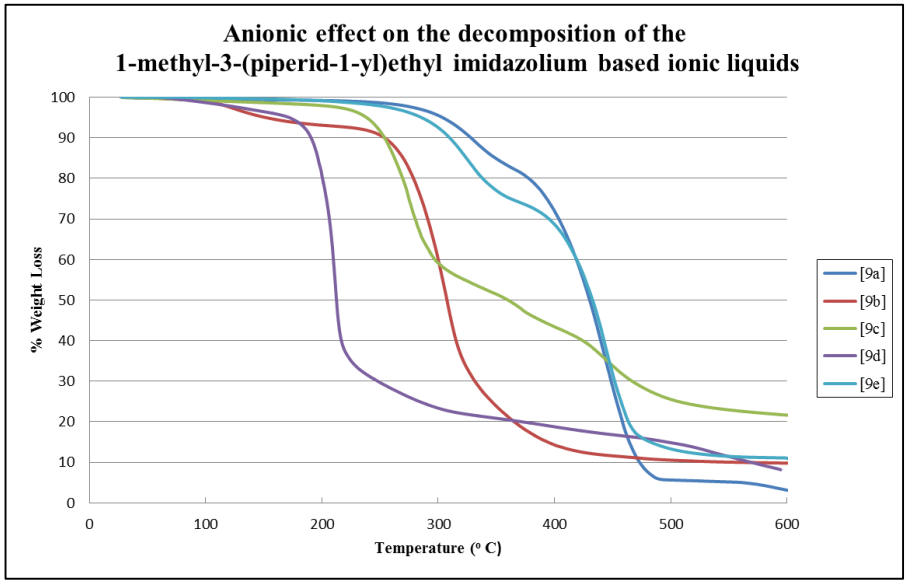

Figure 3.16: TGA profile demonstrating the effect of the anion on the thermal stability using the 1methyl-3-(piperid-1-yl)ethyl imidazolium cation.

The cation appears to have much less of an effect on the thermal stability than the anion. From Figure 3.17, using the TFMS anion with the three cations, the T_{onset} values obtained for the liquids are 287, 280, and 337 ^{o}C, for salts [9e], [10e], and [11e], which is unsurprising giving the similarity of the structures.

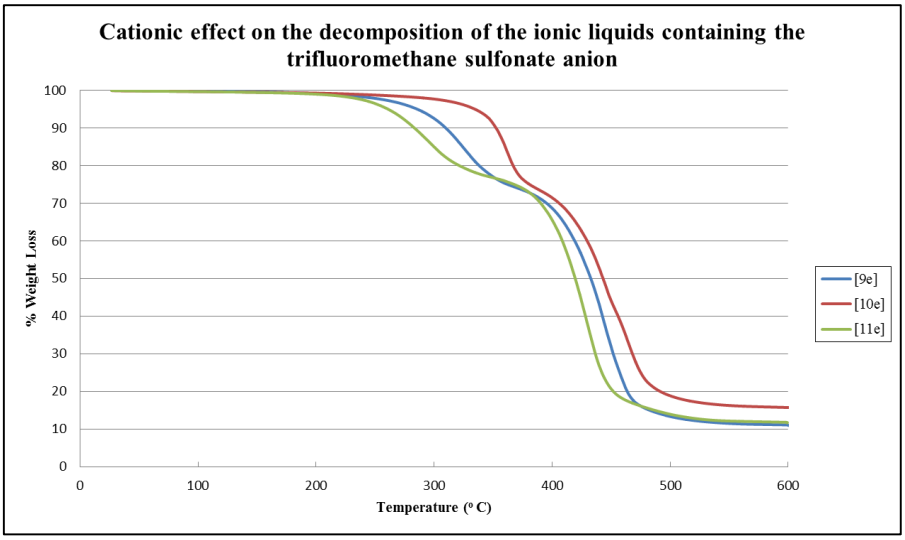

Figure 3.17: TGA profile demonstrating the effect of the cation on the thermal stability using the trifluoromethanesulfonate anion.

During investigations performed by Chan *et al.* it was observed that decomposition of the imidazolium ionic liquids followed a reverse S_N2 pathway whereby the anion attacked the alkyl groups, dealkylating the imidazolium (Scheme 3.6). This results in destabilisation of the imidazole structure and the formation of simple imidazole

derivatives, alkanes and alkenes.[22] The ionic liquids investigated as part of this project could behave in a similar manner and as such it would be expected the thermal stability of the ionic liquids would be anion dependent.

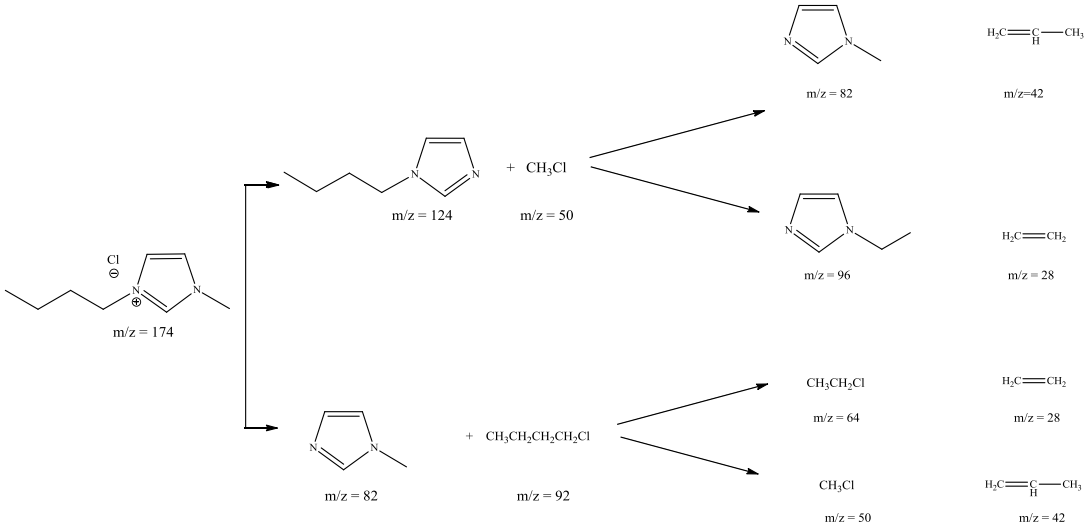

Scheme 3.6: Proposed decomposition pathway of 1-butyl-3-methylimidazolium chloride.

Table 3.20: Decomposition values of ionic liquids.

Ionic Liquid	T_{onset} (°C)	Heat Flow	Ionic Liquid	T_{onset} (°C)	Heat Flow
[9a]	300	Exo	[10e]*	280	Exo
[9b]	280	Exo	[11a]	300	Exo
[9c]	260	Exo	[11b]	286	Exo
[9d]*	190	Exo	[11c]	263	Exo
[9e]*	287	Exo	[11d]*	185	Exo
[10a]	295	Exo	[11e]*	337	Exo
[10b]	283	Exo	[AAIL17]	325	Exo
[10c]	250	Exo	[AAIL19]	230	Exo
[10d]*	185	Exo			

*** indicates the use of alumina pans instead of platinum pans which were used when investigating the other samples**

Pan composition used in the thermal analysis of ionic liquids can have an effect on the thermal characterisation of ionic liquids.[23] Sample pan has shown to have a large influence on T_{onset} values with a difference of over 100 °C observed by Ngo *et al.* with the 1-ethyl-3-methylimidazolium hexafluorophosphate liquid using the aluminium and

alumina pans (375 and 481 ºC).[23,24] A shift in heat flow for exothermic to endothermic was also observed. It has been shown that due to the halides present in ionic liquids can react with the aluminium present in the pans resulting in a lower T_{onset} value and the formation of the jagged pattern as seen in Figure 3.16(a). It was decided to also investigate using Differential Scanning Calorimetry (DSC) the effect of that alumina and aluminium pans had on the thermal profiles of the liquids under N_2, the result of which can be seen in Figure 3.18(a) and (b).

(a)

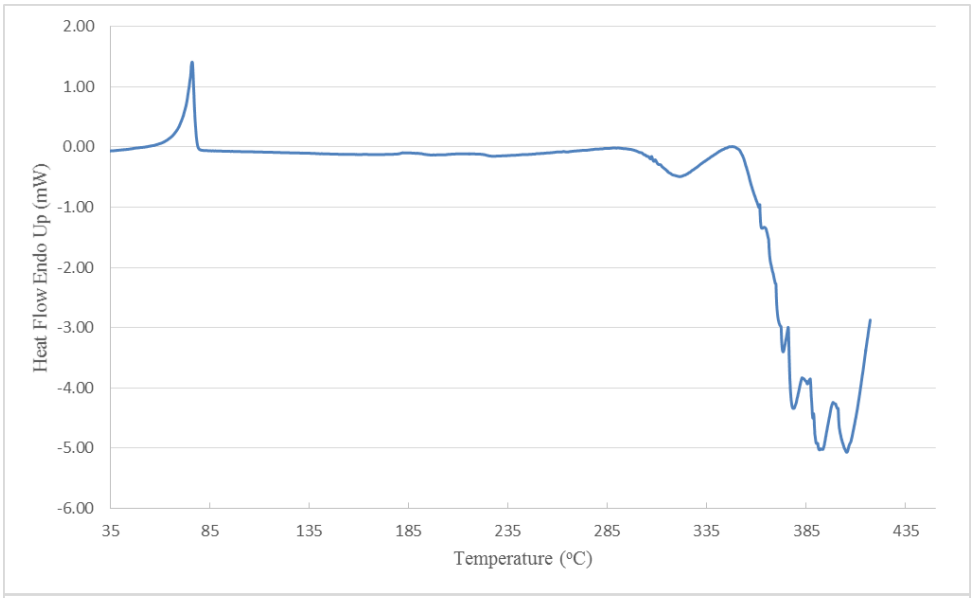

(b)

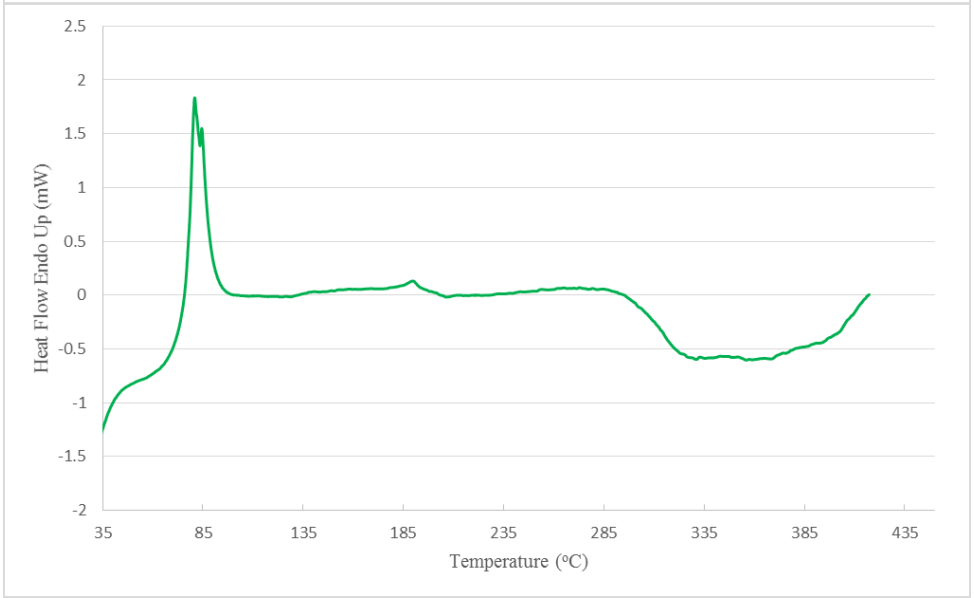

Figure 3.18: DSC profiles of [11e] using (a) aluminium (-), and (b) alumina pans (-) (heat flow as a function of temperature).

The DSC profiles of [11e] in the different pans are very similar up to 300 ºC, after which an exothermic process, which from the TGA results can be concluded as

decomposition is observed. The jagged nature of the exothermic process has now disappeared, a characteristic trait that was observed in all ionic liquids tested. This was due to the absence of the aluminium pans due to their higher reactivity of the aluminium with ionic liquids at elevated temperatures, promoting their early decomposition when compared to the alumina and platinum pans.[23,25] The exothermicity of decomposition is most likely due to the presence of the sulfonyl groups in the anion which can lead to the formation of sulfur dioxide as decomposition occurs.[23] In all cases where DSC was performed, the ionic liquids exhibited exothermic decomposition with both the alumina and aluminium pans, due to the functional groups present on the anion. To examine whether decomposition could switch from an exothermic to an endothermic process, the chloride precursor to the [9a-e] salts were investigated. As shown in Figure 3.19 (a) and (b), decomposition switched from an exothermic process to an endothermic process, upon changing from aluminium to alumina pans. This can be explained by the absence of oxygen atoms or sulfonates in the ionic liquid structure preventing the formation of SO_2 and CO_2 allowing for the endothermic process of decomposition to dominate.

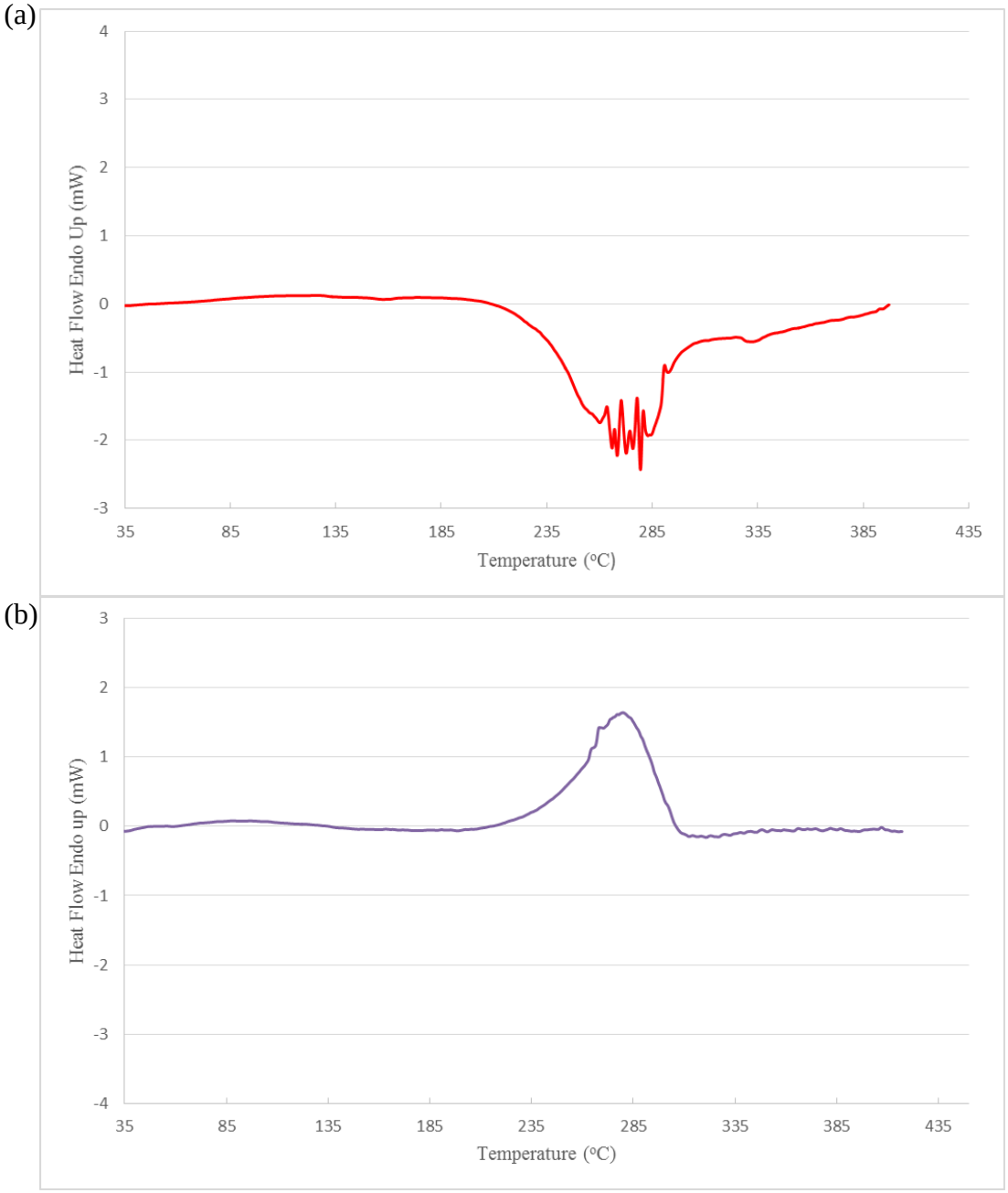

Figure 3.19: DSC profile of the chloride precursor for the [9a-e] salts using (a) aluminium (-), and (b) alumina (-) DSC pans (heatflow as a function of temperature).

3.5.1.2 Melting points of ionic liquids

The melting points of the ionic liquids were also examined using DSC under a N_2 atmosphere. In the case of the ionic liquids formed using the $TFMS^-$ anion ([9e], [10e], and [11e]), where they existed as solids at room temperature, DSC was performed from 25 – 400 °C to determine their melting points. These were obtained using aluminium pans with a T_m of 80 - 85 °C recorded for [11e] (Figure 3.18(a)) with T_m values of the other ionic liquids presented in Table 3.21. Low temperature DSC was also performed

to try and ascertain the melting points of the ionic liquids. This involved cooling the samples down to -50 ^{o}C in the DSC and heating at a rate of 10 degrees per minute. Unfortunately these results proved inconclusive with no clear melting points. An example of one of these low temperature DSC profiles is shown in Figure 3.20.

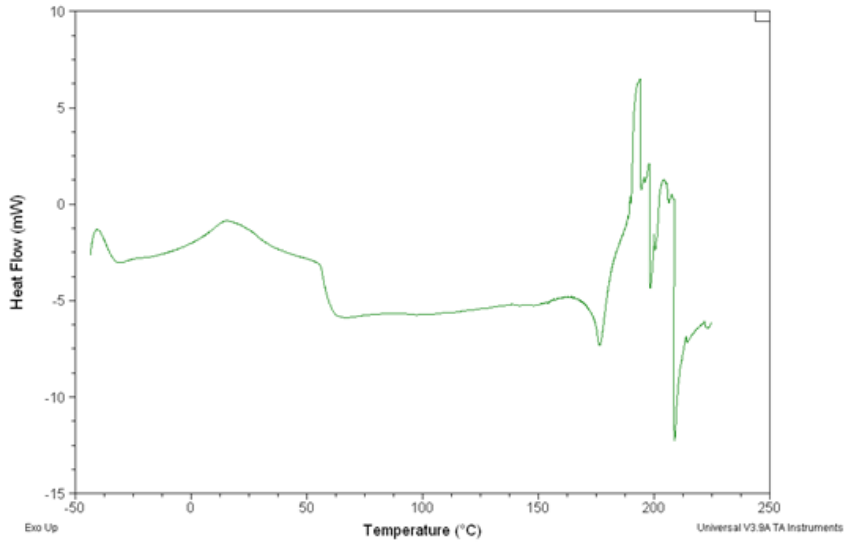

Figure 3.20: Low temperature DSC curve of ionic liquid [10d].

From the low temperature DSC profile shown above it is clear that there is no significant endothermic event which could correspond to a distinguishable melting point. Literature precedent shows that there is significant difficulty in obtaining melting points of ionic liquids due to the low temperatures at which they occur with the Tf_2N and TFMS anions in conjunction with the di-substituted imidazoles.[23] Moreover, although purified as much as possible, the ionic liquid may still contain traces of solvent, and this coupled with the tendency for the ionic liquids to form glasses only adds to the problem and this is what we believe to be occurring with these traces.[20] This could be affected by the rapid rate of cooling (10 degrees/ minute) which prevent the ions from packing uniformly resulting in the glass formation. Full details of all thermal analysis performed on the ionic liquids can be found in Table 3.21.

Table 3.21: Determination of melting points of ionic liquids as determined via DSC analysis.

Ionic Liquid	Pan Composition	T_m (°C)
[9e]	Alumina	71 – 79
[10e]	Alumina	48 - 58
[11e]	Alumina	80 - 85

3.5.2 Viscosity of the Ionic Liquids

As explained in Chapter 1, the aim of this project was to determine the gas sequestration possibilities of the ionic liquids. As evident in the subsequent Chapter 5, viscosity plays a key role in the potential of these liquids and as such it was vital that it be determined. The viscosity of ionic liquids that were used in the permeability studies, were prioritised for viscosity measurements and were analysed from 298 – 352 K using a rheometer which were carried out by Dr. James Kennedy at Athlone Institute of Technology. These values were then referenced to a known standard [1c], and the results of which are displayed in Table 3.22 and Figure 3.21.[26]

Table 3.22: Viscosity of ionic liquids over the 298 – 353 K temperature range.

	Viscosity (mPa.s)					
Temperature (K)	**[1c]**	**[9a]**	**[9c]**	**[9d]**	**[10a]**	**[11a]**
298	50.0	115.0	91.3	3654.3	285.0	105.8
303	41.7	94.2	76.8	2543.1	240.4	89.8
308	35.3	74.1	60.2	1551.6	178.9	70.0
313	30.6	59.7	48.7	987.9	135.9	57.3
318	26.5	48.9	40.4	654.9	105.8	47.1
323	23.5	41.0	34.0	449.9	85.1	40.4
328	20.9	34.9	29.3	316.8	70.0	35.1
333	18.9	30.6	25.5	235.4	58.3	31.0
338	17.5	26.5	22.5	178.5	49.8	28.9
343	16.4	23.0	20.5	139.4	42.9	26.4
348	15.1	21.0	18.4	110.5	37.6	26.0
353	14.4	19.5	16.6	89.3	33.2	24.8

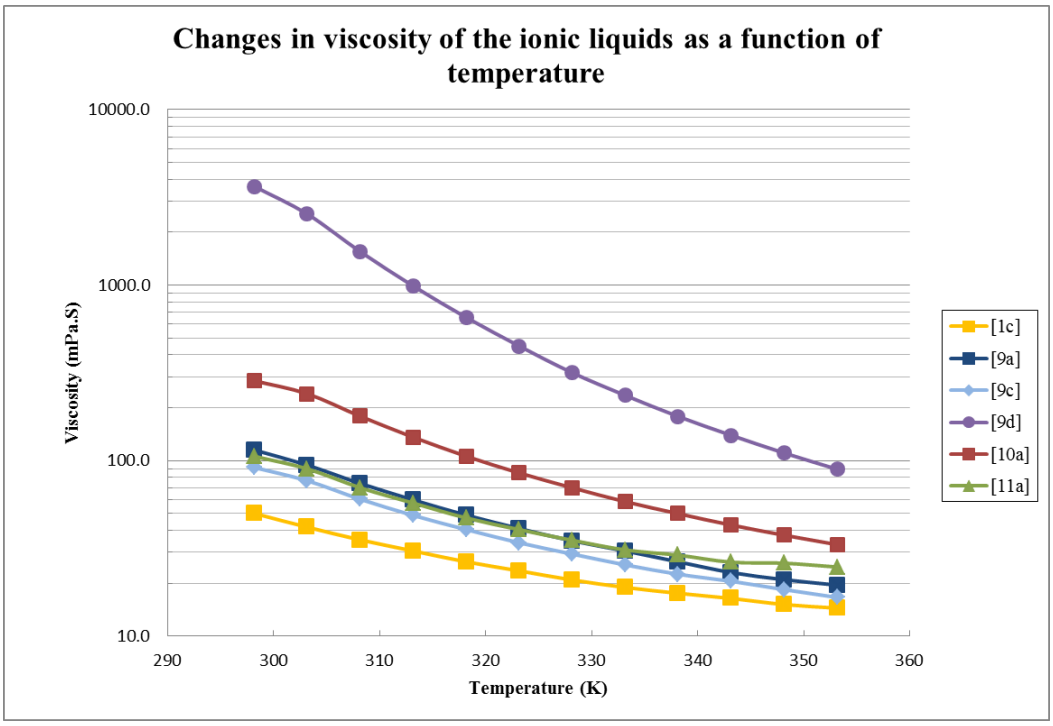

Figure 3.21: Viscosity of ionic liquids over the 298 – 353 K temperature range.

Previous studies have shown that increases in hydrogen bonding result in liquids which are more viscous in nature.[20] In work conducted by Bonhote *et al.*[20] using 1-methyl-3-alkylimidazolium bis(triflimide) it was observed that increasing the alkyl substituent from an ethyl to a butyl group resulted in a viscosity change of 52 - 83 mPa.s which was attributed to changes in Van Der Waals interactions. From Figure 3.21 and Table 3.21 it is evident that choice of anion appears to be the dominant factor governing the viscosity of the liquids with the cation having a much more reduced effect.

Ionic liquids [9a] and [11a], which contain the bis(triflimide) anion exhibit similar values with [11a] viscosity slightly less than that of [9a] at 298 K. From this study it can be seen that ionic liquid [10a], which contains the bis(triflimide) anion, has a viscosity of approximately 385 mPa.s at 298 K, indicating that the cation can influence viscosity of liquids. The viscosity of [10a] which differs from [9a] only by the presence of a morpholine ring rather than a piperidine ring, is three times as viscous. From this it is clear that it is the oxygen that is affecting the viscosity. In a study by Zhou *et al.* where the *N*-butyl-*N*-methyl substituted morpholinium and piperidinium cations were investigated, a five times increase in the viscosity was observed by the incorporation of the oxygen atom in the six membered ring system.[27] This has been attributed to an increase in polarity of the ionic liquids resulting in an increase in dipole – dipole

interactions and thus an increase in viscosity. From this literature precedent, it is proposed that the ionic liquids used in this study act in a similar manner albeit with the *N*-heterocycles attached to the alkyl appendages and not the charged centre.

The anion was also shown to have an effect on the viscosity of the ionic liquids. The dicyanamide anion was found to produce low viscosity liquids with values similar to those observed with the bis(triflimide) anion. This can be attributed to the small anion size while others denote that the delocalisation of charge on the anion will like the bis(triflimide) result in weaker cationic – anionic interactions.[20,21] Typically, the TFA salts tend to exhibit higher viscosity values than the DCA^- and TF_2N^- based ionic liquids.[20,21] This may be due to an increase in hydrogen bonding between the C2 hydrogen of the cation, which has been shown to interact strongly with the anion, and the carbonyl present on the anion.[28] This is in line with those trends observed in Figure 3.5 in which the C2 signal for [9a] occurs at 8.79 ppm as opposed to 10.21 ppm for [9d]. As discussed in Section 3.3.2.4, the more downfield the signal occurs the greater the hydrogen bonding between the cation and the anion.

From Figure 3.22 it is seen that the viscosity of all liquids decrease with increasing temperature, with [9d] demonstrating the most significant change from 3654.3 mPa.s, to 89.3 mPa.s over the temperature range. From the data, it is clear that the viscosity is inversely proportional to temperature as shown in Figure 3.22.

In Chapter 1, Section 1.9, it was highlighted that small amounts of chloride impurities may result in significant changes to the viscosity of the ionic liquids.[29] In work presented in the review by Seddon *et al.* on the ionic liquids EMIM BF_4 and BMIM NO_3, it was shown that similar traces of chloride impurity can have varying results depending on the anion employed.[29] An increase in viscosity of 50% was recorded for the EMIM BF_4 ionic liquid compared to nearly a 200% increase in that observed for BMIM NO_3. This may be due to the influence of the chloride impurity on the packing structure of the ionic liquid. Therefore it is likely that small amounts of impurities in the ionic liquids here are also having an effect on viscosity.

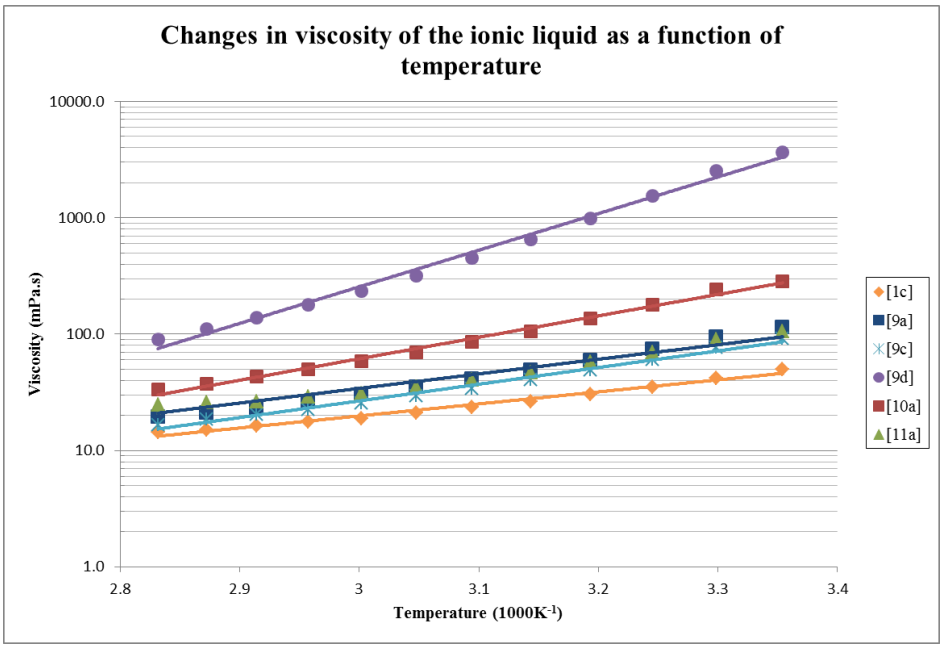

Figure 3.22: Chart demonstrating the relationship between viscosity and temperature.

3.5.3 Refractive index of ionic liquids

The refractive indices of the Tf_2N^-, TFA^-, and DCA^- salts were determined at 298 K and are presented in Table 3.22. From these, it is quite clear that the anion is the dominant factor. From this study the following trend is observed with the refractive indices DCA^- > TFA^- > Tf_2N^- which is also the trend that is followed in the literature when the 1-ethyl-3-methylimidazolium cation was investigated at 293 K (1.5151 > 1.4405 > 1.4231).[20,30]

Table 3.22: Refractive index values of some ionic liquids at 298 K.

Ionic liquid	Temperature (K)	Refractive Index
[9a]	298	1.4465
[9c]	298	1.5235
[9d]	298	1.4575
[10a]	298	1.4485
[10c]	298	1.5250
[10d]	298	1.4635
[11a]	298	1.4465
[11c]	298	1.5215
[11d]	298	1.4570

Decreases in refractive index values are well established to be as a result of the reduced molar volume of the liquid or unoccupied part of the ionic liquids molar volume.[31,32] Ion size does contribute to refractive indices, dicyanamides are known to have larger refractive index values which are attributed to their small anion size. This reduces the amount of free space within the molar volume resulting in higher refractive index values.

3.6 Conclusions

From this chapter, almost 57 ionic liquids, 36 of which were novel were successfully synthesised combining new cations with both conventional and amino acid based anions. These two categories of ionic liquids had unique sets of challenges in synthesis and purification. These were fully characterised by a variety of spectroscopic techniques. Conventional anions tended to produce less viscous ionic liquids, and seemed to be less susceptible to degradation during the synthesis under basic conditions. These ionic liquids should be synthesised in a one pot reaction whereas in the case of the amino acid ionic liquids several different steps including the use of anion exchange resins were employed. Alternatively during synthesis of AAILs, degradation occurred upon isolation of the chloride precursor after removal of the hydrochloride precursor with base. From work conducted on purines it was seen that the hydrogen at the C2 position of the imidazolium unit was attacked by the hydoxyl ion resulting in the opening of the ring. It is proposed that the liquids studied in this thesis suffered from a similar degradation mechanism.

The position of the C2 proton signal also appears to be anion dependent and is a solid indication of the occurrence of the metathesis reaction in anions where no hydrogen atoms are present in the anion. This is not unique to the liquids studied here and is widely reported. The anion is known to interact quite strongly with the acidic C2 hydrogen. The position of the C2 signal is based on the nucleophilicity of the anion, with higher nucleophilic anions resulting in a more downfield shift of the C2 signal in the ^{1}H NMR spectra.

It was also observed that the choice of solvent had a significant effect on the NMR spectra of the liquids. Due to the low solubility of the AAIL in $CDCl_3$, D_2O was used as the solvent and for both the ^{1}H and ^{13}C NMR spectra, the signals at the C2 position on the imidazolium ring disappeared. It is known these protons are quite acidic and

readily exchange with deuterium in polar solvents, resulting in the disappearance of the proton signal. However, the carbon signal was also observed to disappear, most likely due to fast relaxation of the nuclei due to the rapid proton-deuterium exchange, and not ring opening reactions.

A number of the ionic liquids were studied with respect to their thermal and physical properties. All physical properties of the ionic liquids are strongly dependent on the anion, with viscosity, melting point, thermal stability, and refractive index all demonstrating trends based on the incorporated anions. Much of these are related to the strength of interactions between the cations and the anions, and as such changes in the anion will affect this greatly. In terms of viscosity the ionic liquids with the Tf_2N^- and DCA^- anions, were less viscous materials than their TFA counterparts, and although the viscosities of the AAILs were not obtained, they were significantly more viscous by appearance with a more "gum like" appearance. The $TFMS^-$ and TF_2N^- produced the most thermally stable ionic liquids with the TFA^- producing the least stable of the conventional anion based ionic liquids with the some amino acid ionic liquids also demonstrating good thermal stability.

3.7 References

(1) Plechkova, N. V.; Seddon, K. R. *Chemical Society Reviews* **2008**, *37*, 123.

(2) Kalinowski, H. O.; Berger, S.; Braun, S. *Carbon-13 NMR Spectroscopy*; John Wiley & Sons Ltd.: Stuttgart, 1988.

(3) Huddleston, J. G.; Visser, A. E.; Reichert, W. M.; Willauer, H. D.; Broker, G. A.; Rogers, R. D. *Green Chemistry* **2001**, *3*, 156.

(4) Chu, Y.; Deng, H.; Cheng, J.-P. *The Journal of Organic Chemistry* **2007**, *72*, 7790.

(5) Creary, X.; Willis, E. D.; Gagnon, M. *Journal of the American Chemical Society* **2005**, *127*.

(6) Dahl, K.; Sando, G. M.; Fox, D. M.; Sutto, T. E.; Owrutsky, J. C. *Journal of Chemical Physics* **2005**, *123*.

(7) Fukumoto, K.; Yoshizawa, M.; Ohno, H. *Journal of the American Chemical Society* **2005**, *127*, 2398.

(8) Chetsanga, C. J.; Makaroff, C. *Chemico-Biological Interactions* **1982**, *41*, 235.

(9) Jones, A. S.; Mian, A. M.; Walker, R. T. *Journal of the Chemical Society C-Organic* **1966**, 692.

(10) Olofson, R. A.; Thompson, W. R.; Michelman, J. S. *J. Am. Chem. Soc.* **1964**, *86*, 1865.

(11) Ye, Y.; Elabd, Y. A. *Macromolecules* **2011**, *44*, 8494.

(12) Lozano, P.; Bernal, B.; Recio, I.; Belleville, M.-P. *Green Chemistry* **2012**, *14*, 2631.

(13) Handy, S. T.; Okello, M. *J Org Chem* **2005**, *70*, 1915.

(14) Zhang, J.; Zhang, S.; Dong, K.; Zhang, Y.; Shen, Y.; Lv, X. *Chemistry-a European Journal* **2006**, *12*, 4021.

(15) Zhang, Y.; Zhang, S.; Lu, X.; Zhou, Q.; Fan, W.; Zhang, X. *Chemistry-a European Journal* **2009**, *15*, 3003.

(16) Tao, G.-h.; He, L.; Liu, W.-s.; Xu, L.; Xiong, W.; Wang, T.; Kou, Y. *Green Chemistry* **2006**, *8*, 639.

(17) Ni, B.; Zhang, Q.; Headley, A. D. *Green Chemistry* **2007**, *9*, 737.

(18) Harjani, J. R.; Singer, R. D.; Garciac, M. T.; Scammells, P. J. *Green Chemistry* **2009**, *11*, 83.

(19) Myles, L.; Gore, R.; Spulak, M.; Gathergood, N.; Connon, S. J. *Green Chemistry* **2010**, *12*, 1157.

(20) Bonhote, P.; Dias, A. P.; Papageorgiou, N.; Kalyanasundaram, K.; Gratzel, M. *Inorganic Chemistry* **1996**, *35*, 1168.

(21) Pringle, J. M.; Golding, J.; Baranyai, K.; Forsyth, C. M.; Deacon, G. B.; Scott, J. L.; MacFarlane, D. R. *New Journal of Chemistry* **2003**, *27*, 1504.

(22) Chan, B.; Chang, N.; Grimmett, M. *Australian Journal of Chemistry* **1977**, *30*, 2005.

(23) Ngo, H. L.; LeCompte, K.; Hargens, L.; McEwen, A. B. *Thermochimica Acta* **2000**, *357*, 97.

(24) McEwen, A. B.; Ngo, H. L.; LeCompte, K.; Goldman, J. L. *Journal of the Electrochemical Society* **1999**, *146*, 1687.

(25) Kosmulski, M.; Gustafsson, J.; Rosenholm, J. B. *Thermochimica Acta* **2004**, *412*, 47.

(26) Vranes, M.; Dozic, S.; Djeric, V.; Gadzuric, S. *Journal of Chemical and Engineering Data* **2012**, *57*, 1072.

(27) Zhou, Z. B.; Matsumoto, H.; Tatsumi, K. *Chemistry-a European Journal* **2006**, *12*, 2196.

(28) Hunt, P. A. *Journal of Physical Chemistry B* **2007**, *111*, 4844.

(29) Seddon, K. R.; Stark, A.; Torres, M. J. *Pure and Applied Chemistry* **2000**, *72*, 2275.

(30) Soriano, A. N.; Doma, B. T., Jr.; Li, M.-H. *Journal of the Taiwan Institute of Chemical Engineers* **2010**, *41*, 115.

(31) Deetlefs, M.; Seddon, K. R.; Shara, M. *Physical Chemistry Chemical Physics* **2005**, *8*, 642.

(32) Hasse, B.; Lehmann, J.; Assenbaum, D.; Wasserscheid, P.; Leipertz, A.; Froeba, A. P. *Journal of Chemical and Engineering Data* **2009**, *54*, 2576.

Chapter 4:

Synthesis and Characterisation of Phosphonium Ionic Liquids

4.1 Introduction

In this chapter work will be presented on the challenges experienced in the synthesis of ionic liquids using the quaternary phosphonium salts and the full characterisation of these ionic liquids [12a] – [16b]. As outlined in Chapter 3, this involves the assignment of both carbon and proton signals for each of the respective spectra, as outlined in Chapter 2, with the corresponding chemical structure of the ionic liquid, utilising DEPT 45 and 135, HSQC, and COSY experiments. In conjunction major IR bands as well as accurate mass values will be presented where relevant to further confirm the structure of the ionic liquids.

Phosphonium salts have attracted much attention in recent years due to their many favourable properties such as lower solubility in water, and antimicrobial properties, and can be applied in the research of solar cells, and media for CO_2 capture and sequestration.[1-7] They have many significant advantages over their imidazolium counterparts such as increased thermal stability, and increased hydrophobicity which is useful from a purification standpoint.[8,9] Also presented in this chapter is some preliminary work on the development of ionic liquids monomers and attempted polymerisation of these to grow poly(ionic liquids). This is potentially an exciting route of investigation as these can potentially be used as polymeric supports which can be impregnated with ionic liquids to produce a high functioning ionic liquid hybrid flue gas separating system as has been performed before. Work in this chapter will focus on the use of the trioctylphosphine as the ionic liquid precursor in all cases. Examples of some of the quaternary phosphonium cations which have been reported in the literature are given in Figure 4.1 below.[4,6,10]

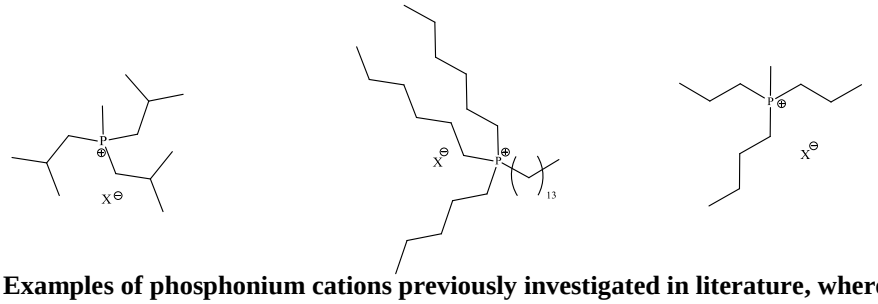

Figure 4.1: Examples of phosphonium cations previously investigated in literature, where x = Tf_2N.

4.2 Synthesis and purification of ionic liquids [12a-14b]

In Chapter 3 it was explained that the synthesis of the imidazolium cations followed an S_N2 pathway whereby the imidazole acting as a nucleophile attacking the carbon adjacent to the halide species. The synthesis of the phosphonium salts follow the same

pathway with the phosphine precursor (trioctylphosphine) acting as the nucleophile (Scheme 4.1).

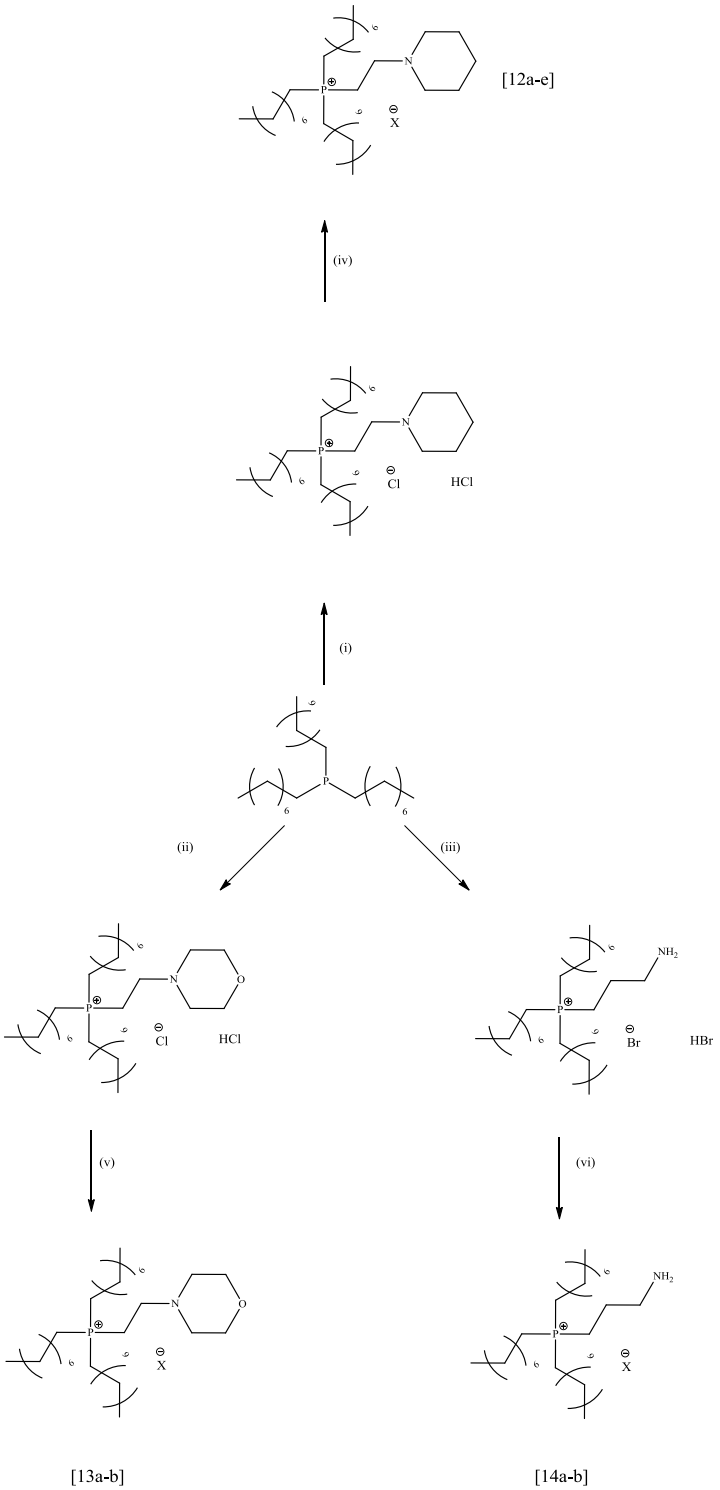

Scheme 4.1: Synthesis of ionic liquids [12a]-[14b] (i) 1-(2-chloroethyl)piperidine hydrochloride, ethanol, 75 ºC, 48 h, (ii) 4-(2-chloroethyl)morpholine hydrochloride, 4:1 ethanol/toluene, 75 ºC, 48 h (iii) 3-bromopropylamine hydrobromide, 75 ºC, 48 h, (iv-vi) 1.2 mole equivalent. NaOH /KOH, NaX/LiX, rt, 1:1 H_2O/methanol, 24 h, where X = bis(triflimide), saccharinate, dicyanamide, trifluoroacetate, and trifluoromethanesulfonate.

The synthesis of the ionic liquids involved the quaternisation of trioctylphosphine derivative with 3 different halide species respectively; 1-(2-chloroethyl)piperidine hydrochloride, 4-(2-chloroethyl)morpholine hydrochloride, and 3-bromopropylamine hydrobromide. The reaction conditions were kept similar to that employed with the imidazoles although due to the bulkiness of the precursor, the reactions took place over 48 instead of 24 hours.

4.2.1 Synthesis, purification, and characterisation of ionic liquids [12a-14b]

4.2.1.1 Synthesis and purification of ionic liquids [12a-e]

As was previously used for the imidazole salts, it was decided to use the alkylating agent in excess due to the ease of removal of the alkylating agents upon completion of the reaction. The quaternisation reaction between the trioctylphosphine and the 1-(2-chloroethyl)piperidine resulted in a suspension. The solid was removed by filtration and upon inspection using ^{1}H NMR spectroscopy was confirmed to be starting alkylating agent as was found to be the case in the imidazole based salts. The excess solvent was removed under reduced pressure and dichloromethane was added to precipitate out the hydrochloride ionic liquid salts. However, no precipitate formed most likely due to the cations being less polar than that of the imidazolium analogues, allowing for the solubility of the salts in the dichloromethane. This solvent was removed and ^{1}H NMR spectrum was obtained of the crude product. As can be seen in Figure 4.2(a) and (b), both the ^{1}H and ^{31}P NMR spectra show the presence of impurities.

From Figure 4.2(a) it is clear that although some alkylating reagent had precipitated out, not all of the excess has been removed as evident by the triplet which can be seen at 4.04 ppm corresponding to the proton signals of the H atoms of the ethyl chain. Due to the large size of the cation and the level of overlapping of its signals, it is difficult to confirm if there is any unreacted starting trioctylphosphine material. This was monitored through the use of ^{31}P NMR spectroscopy. In Figure 4.2(b), the presence of the trioctylphosphine is confirmed by the singlet observed at -30.8 ppm, and the presence of the quaternised phosphine is confirmed by the singlet at 32.7 ppm.[11]

(a)

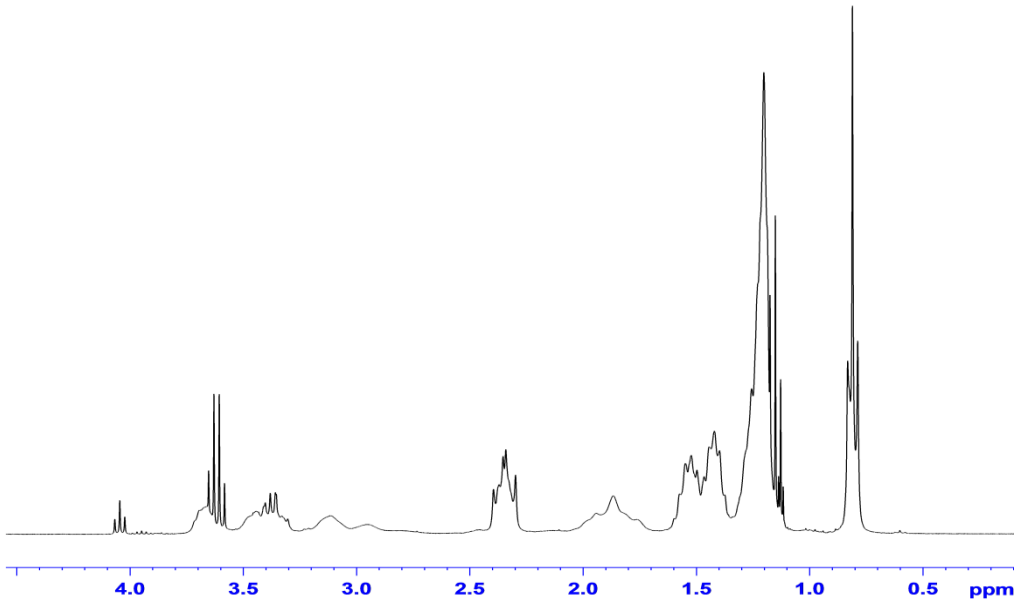

(b)

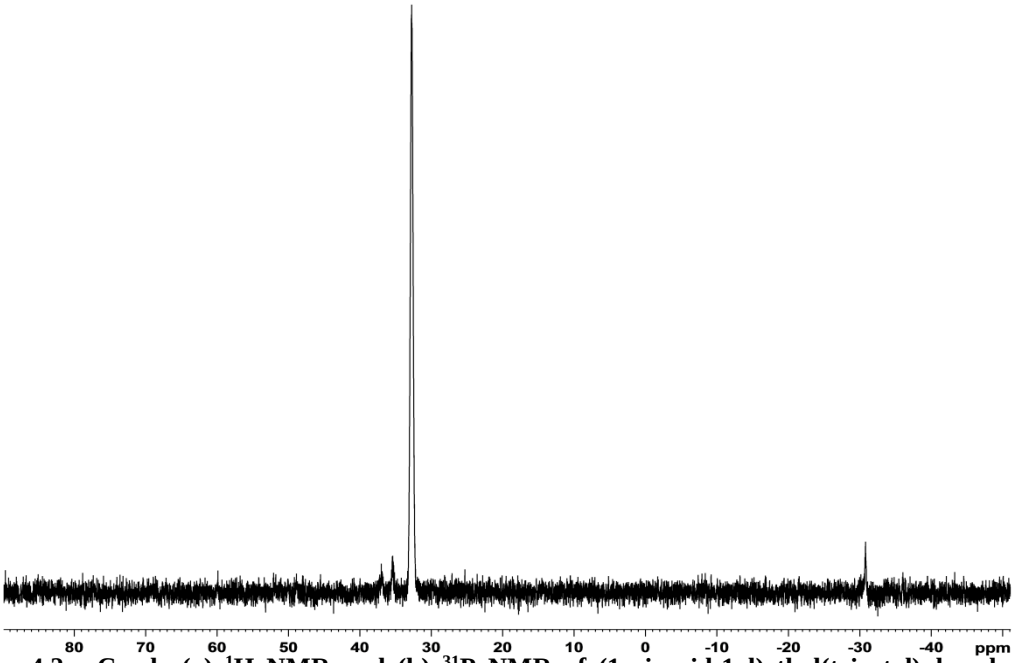

Figure 4.2: Crude (a) ^{1}H NMR and (b) ^{31}P NMR of (1-piperid-1yl)ethyl(trioctyl)phosphonium chloride hydrochloride.

The product was washed with the n-hexane which successfully removed the trioctylphosphine as confirmed by the ^{31}P NMR spectrum shown in Figure 4.3. It had been observed during the synthesis of the imidazolium salts that the alkylating agents were all water soluble. It would be expected due to the long alkyl chains of the cations that the phosphonium ionic liquid salts would be water insoluble. Therefore purification was attempted by washing the product with water to remove the 1-(2-chloroethyl)piperidine hydrochloride and extraction of the phosphonium salt with dichloromethane. However, a milky white suspension resulted with no distinguishable

layers which are required to facilitate separation. It was decided to proceed with the metathesis without removal of the alkylating agent. It was believed that the removal could be achieved at a later stage and that the presence of the alkylating agent would not interfere in the reaction. Moreover the halide ionic liquids were of limited interest in gas capture technologies due to high viscosity values of the halide species.

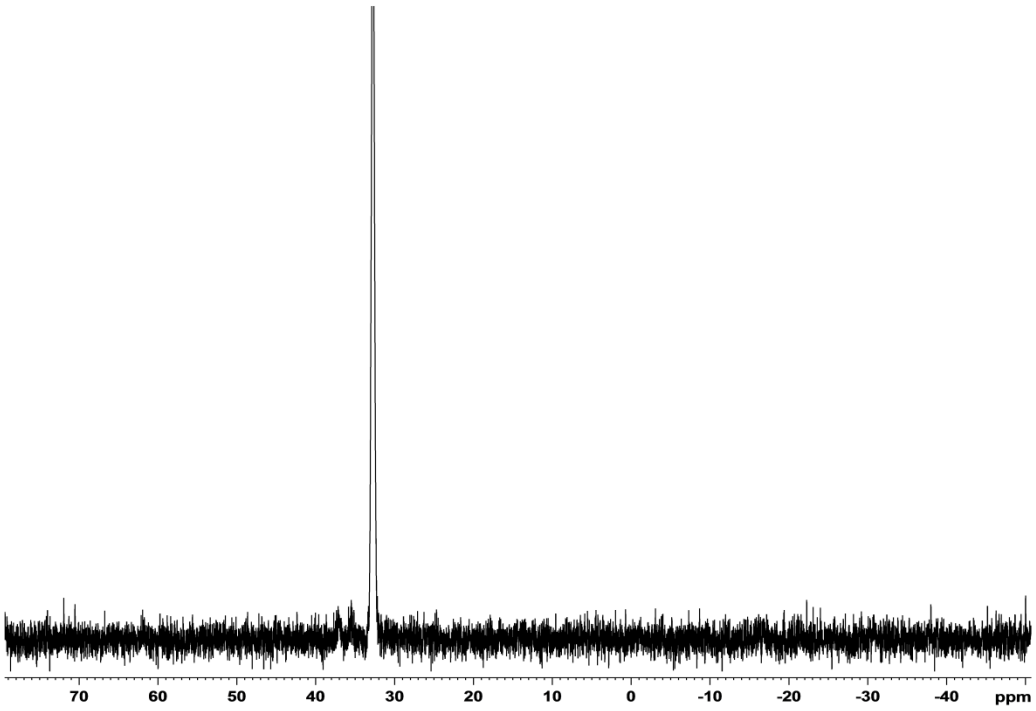

Figure 4.3: ^{31}P NMR of (1-piperid-1yl)ethyl(trioctyl)phosphonium chloride hydrochloride after hexane wash.

As mentioned earlier, these ionic liquids had displayed hydrophobic characteristics. In Chapter 3, it was explained that the metathesis reaction was carried out in deionised H_2O due to the imidazolium halides all being water soluble. A mixed solvent approach was adopted for the anion exchange of the phosphonium ionic liquids consisting of water and methanol at room temperature overnight. This binary system would allow for the addition of the NaOH due to its limited solubility in organic solvents, the dissolution of the sodium salts with the desired anion, and it was hoped that due to the hydrophobicity of the liquid, that all water soluble byproducts and impurities from the quaternerisation reaction would remain in the water, while the ionic liquid could be separated without any of these being present in the liquid. Upon separation the ionic liquid was dissolved in dichloromethane and washed with water and dried. From Figure 4.4 which shows ionic liquid [12a], it is clear that this approach was successful in the

removing the alkylating agent which was present in the spectrum of the chloride analogue.

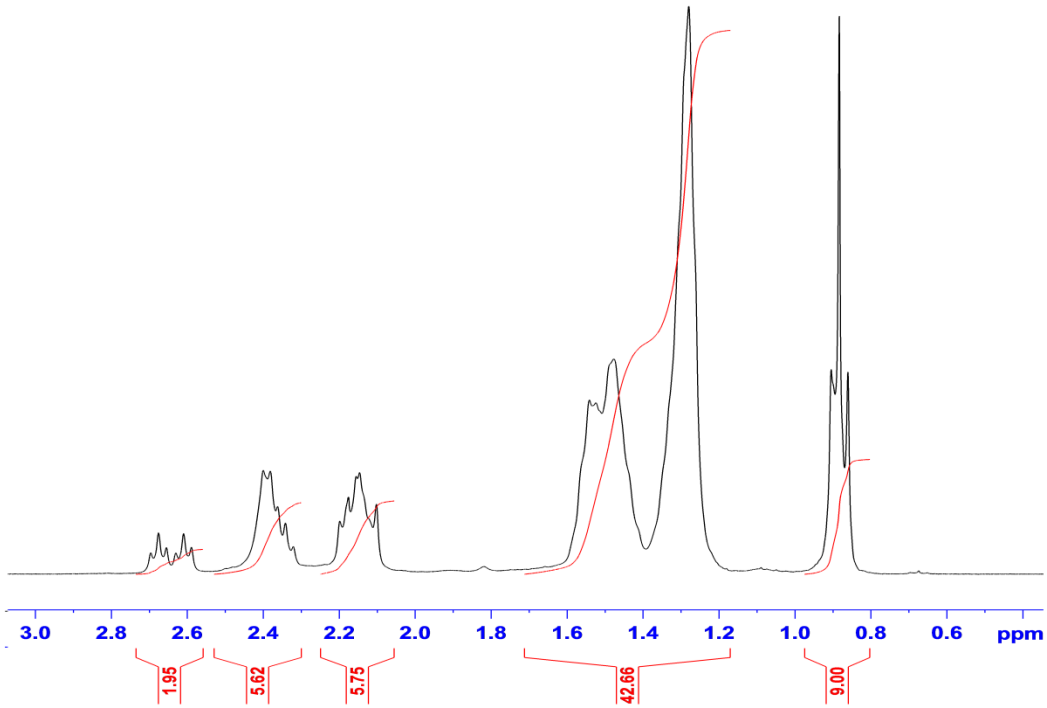

Figure 4.4: ^{1}H NMR Spectrum of ionic liquid [12a] after metathesis reaction formed using a dual solvent approach.

4.2.1.2 Synthesis and purification of ionic liquids [13a-b]

The synthesis of ionic liquids [13a-b] followed a similar route to that of the [12a-e] salts. The alkylating agent was 4-(2-chloroethyl)morpholine hydrochloride and the reaction was conducted in a 5:1 ethanol/toluene system due to the lower solubility of the alkylating agent in ethanol which was observed during the synthesis of the imidazolium analogues. After the quaternisation reaction, the excess solvent was removed and the product dissolved in methanol and washed with hexane to remove any unreacted trioctylphosphine. Upon examination of the ^{31}P NMR spectrum of the reaction products there a signal at 32.9 ppm which corresponds to the 1-(morphol-4-yl)ethyl(trioctyl) phosphonium chloride hydrochloride salt (Figure 4.5(a)). There was no presence of the trioctylphosphine signal which was seen in the case of the 1-(piperid-1-yl)ethyl(trioctyl)phosphonium based ionic liquids (Section 4.2.1.1). However there was a signal at approximately 48.7 ppm which corresponded to the trioctylphosphine in its oxidised form. The trioctylphosphine oxide was generated as a result of air entering the flask during the reaction or due to the trioctylphosphine converting to the oxide form as a result of exposure during the hexane washing stage. Many papers discuss the risk of

contamination of the oxide form in the liquid but none seem to discuss a method for its removal.[12] The ^{1}H NMR spectrum (Figure 4.5(b)) also indicates the presence of unreacted alkylating material as evident from the triplet at 4.05 ppm which corresponds to the hydrogen atoms directly adjacent to the oxygen in the morpholine ring.

(a)

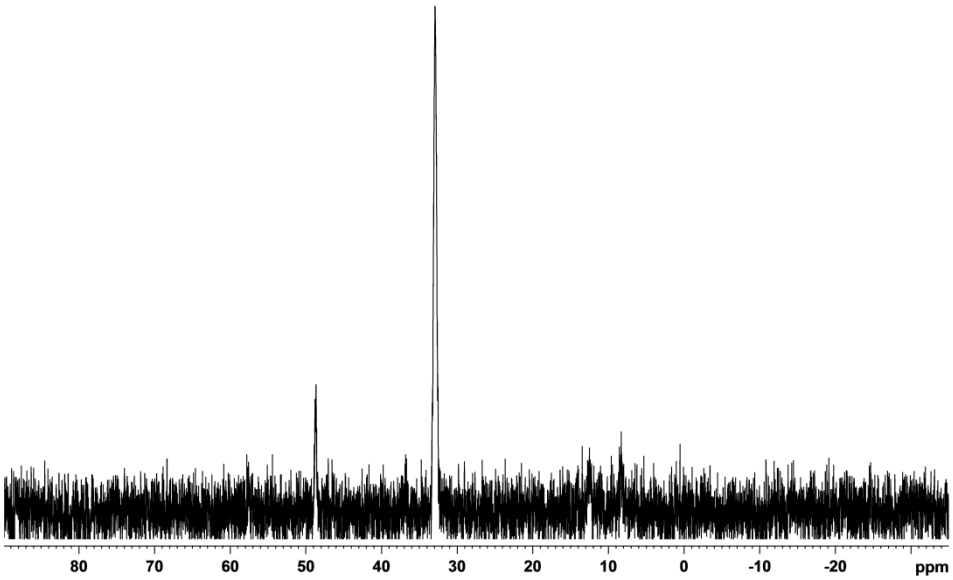

(b)

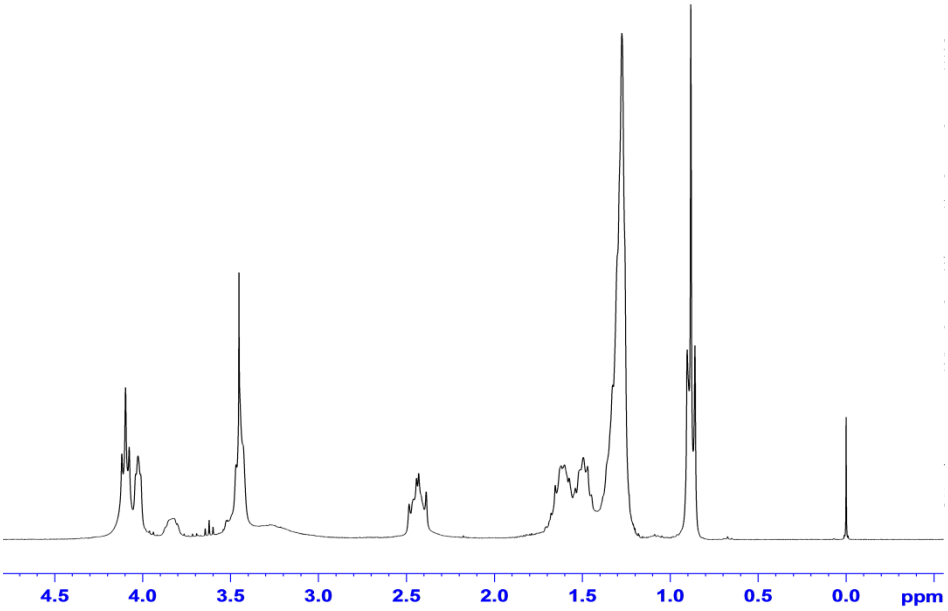

Figure 4.5: ^{31}P NMR (a), and ^{1}H NMR (b) spectra, of crude 4-(morphol-4-yl)ethyl(trioctyl)phosphonium chloride hydrochloride salt

Purification of the hydrochloride salt was attempted via the conditions used in Section 4.2.1.1. Due to the solubility of trioctylphosphine in hexane the product was redissolved in methanol and again washed with hexane but from the subsequent ^{31}P

NMR spectrum it was clear that little of the oxide had been removed. After the failure of this approach it was decided to investigate the potential of washing the material with water to remove the trioctylphosphine oxide due to the presence of the phosphorus – oxygen dipole. However like the [12a-e] salts, alkylating starting material was still present and this produced a milky appearance to the liquid, making separation of the layers impossible. Finally, from the first purification attempt mentioned above it was evident that the oxide form was soluble in methanol. Therefore, it was decided to conduct hexane washing in the absence of methanol. Due to the limited solubility observed for the quaternised phosphonium salts in hexane at room temperatures, the oxide could be easily removed without minimal loss of product. This method proved successful as can be seen from the resulting ^{31}P NMR of the hydrochloride precursor salt (Figure 4.6) by the removal of the oxide peak at 48.5 ppm.

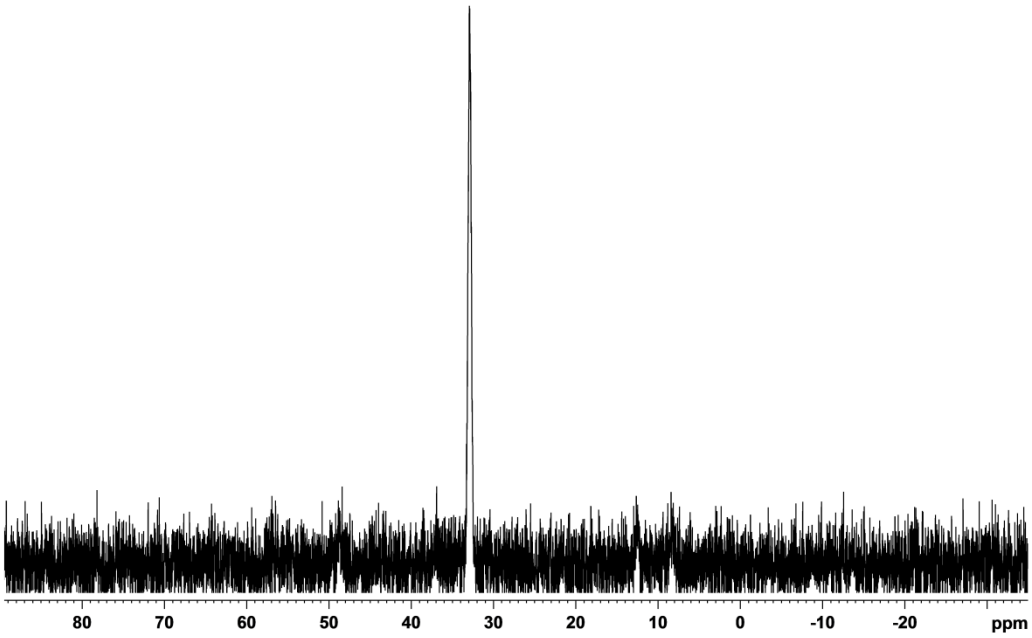

Figure 4.6: ^{31}P NMR spectrum of 4-(morphol-4-yl)ethyl(trioctyl)phosphonium chloride hydrochloride salt after hexane only wash.

Due to previous experience of the removal of the alkylating starting material during the metathesis step using a methanol/water solvent mix (Section 4.2.1.1), the metathesis reaction proceeded despite small traces of 4-(2-chloroethyl)morpholine hydrochloride present in the sample. The removal of the alkylating agent during this step was successful as was the excess sodium salts, both of which were monitored using ^{1}H NMR and ^{13}C NMR spectroscopy where appropriate.

4.2.1.3 Synthesis and purification of ionic liquids [14a-b]

The synthesis of these salts followed a similar method to those out lined in Section 4.2.1.1 and 4.2.1.2 with reaction conditions and solvents remaining constant. Amine functionalised phosphonium ionic liquids have been synthesised previously.[3,13] These consisted of an aminopropyl(tributyl)phosphonium cation whereby tributylphosphine was quaternised with 3-bromopropylamine hydrobromide before subsequent metathesis reactions were performed. This approach of amine functionalization has also been seen in conjunction with imidazolium cations and was adopted for this study. From the ^{31}P NMR spectrum recorded, no traces of trioctylphosphine or its oxide form were observed. The dual solvent approach was adopted to remove the excess alkylating agent which was present. NaOH (1.2 mole equivalents) was added along with the sodium/lithium salts to remove the hydrobromide moiety during the metathesis and allow anion exchange to occur. However, from the resulting ^{1}H NMR spectrum it appears that a mixture of hydrobromide and bromide ionic liquid existed.

In previous work groups have employed a range of techniques to remove the hydrobromide moiety via the use of anion exchange, sodium methoxide, and pH adjustment.[5,14,15] It was decided due to ease, to pursue the adjustment of pH route. In imidazolium based solutions described in the literature, the pH was adjusted to a value of 8 to remove the hydrobromide when generating a bis(triflimide) ionic liquid. In earlier work performed as part of the current research study using an imidazolium analogue of the desired phosphonium salt, it was observed that altering the ionic liquid aqueous solution to pH 8 was not completely effective in removing the HBr moiety. A moderately basic solution was most likely used for the imidazolium liquids due to the vulnerability to degradation in basic conditions. The phosphoniums do not display such an effect therefore the pH was increased to a pH 10 to ensure deprotonation of the amine from NH_3^+ to NH_2. The binary solvent approach (ethanol/water) was adopted during the metathesis reaction and prepared by those conditions outlined in Section 4.2.1.1. The ^{1}H NMR spectrum of one of these ionic liquids with primary amine functionalised cation [14a] is presented in Figure 4.7.

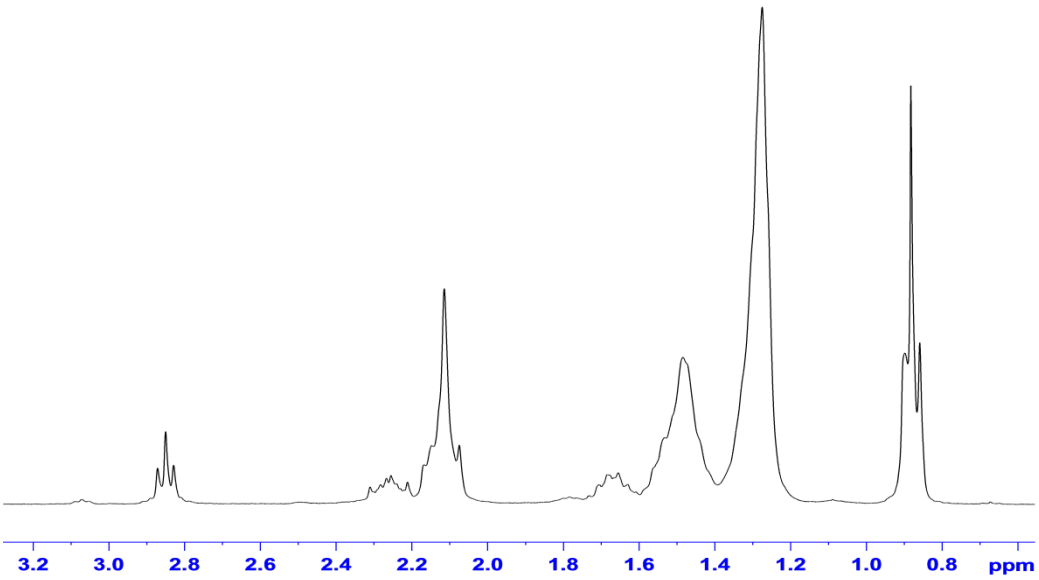

Figure 4.7: ^{1}H NMR Spectrum of ionic liquid [14a].

4.2.2 ^{1}H NMR, ^{13}C NMR, and IR characterisation of ionic liquids [12a-14b]

All NMR spectroscopy data presented in this section were recorded using $CDCl_3$ as the deuterated solvent with the symbols #, *, and ~ indicating overlapping signals. In the case where overlapping signals occur, the combined integral is given. This is true for all NMR spectroscopy data presented throughout Chapter 4.

4.2.2.1 ^{1}H NMR, ^{13}C NMR, and IR characterisation of ionic liquids [12a-12e]

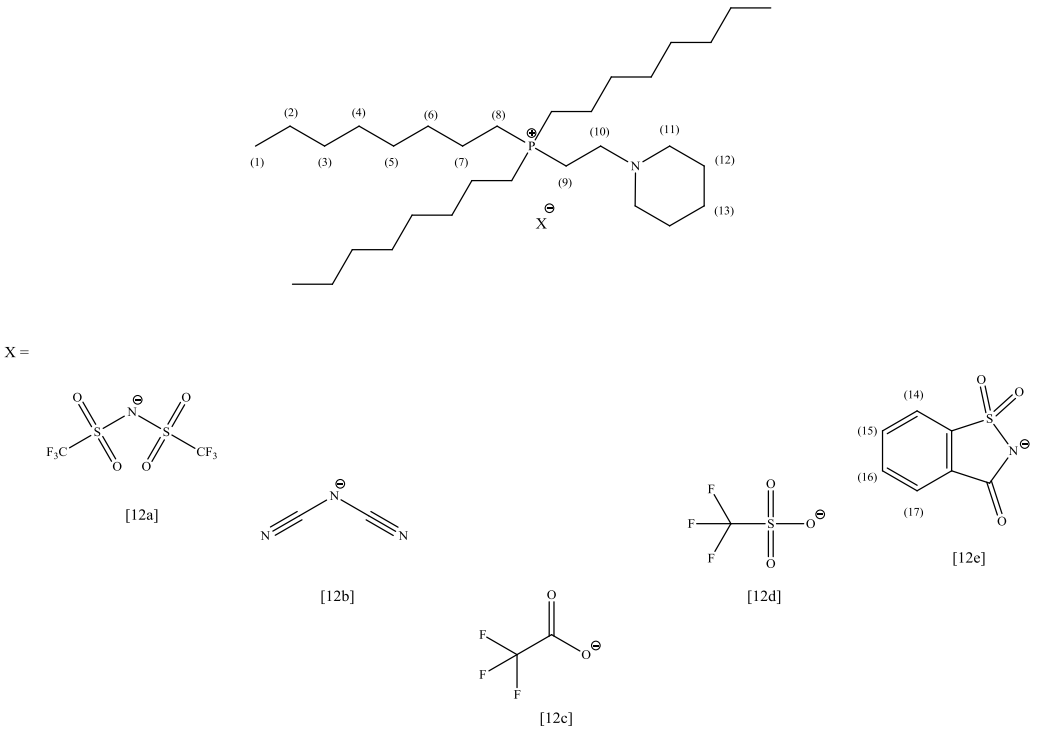

Figure 4.8: Illustration of (1-piperid-1yl)ethyl(trioctyl)phosphonium cation and its respective anions [12a-e].

Table 4.1: ^{1}H NMR assignment of ionic liquids [12a-e].

	[12a]	[12b]	[12c]
H1	0.88 (*t*, 9H, *J* = 6.4)	0.81 (*t*, 9H, *J* = 6.4)	0.81 (*t*, 9H, *J* = 6.4)
H2	1.28 (*m*, 42H)*	1.21 (*m*, 42H)*	1.21 (*m*, 42H)*
H3	1.28 (*m*, 42H)*	1.21 (*m*, 42H)*	1.21 (*m*, 42H)*
H4	1.28 (*m*, 42H)*	1.21 (*m*, 42H)*	1.21 (*m*, 42H)*
H5	1.28 (*m*, 42H)*	1.21 (*m*, 42H)*	1.21 (*m*, 42H)*
H6	1.28 (*m*, 42H)*	1.21 (*m*, 42H)*	1.21 (*m*, 42H)*
H7	1.28 (*m*, 42H)*	1.21 (*m*, 42H)*	1.21 (*m*, 42H)*
H8	2.15 (*m*, 6H)	2.15 (*m*, 6H)	2.15 (*m*, 6H)
H9	2.36 (*m*, 6H)$^{\#}$	2.41 (*m*, 6H)$^{\#}$	2.41 (*m*, 6H)$^{\#}$
H10	2.63 (*dt*, 2H, *J* = 19.0, 6.0)	2.57 (*dt*, 2H, *J* = 19.6, 6.0)	2.57 (*dt*, 2H, *J* = 19.6, 6.0)
H11	2.36 (*m*, 6H)$^{\#}$	2.41 (*m*, 6H)$^{\#}$	2.41 (*m*, 6H)$^{\#}$
H12	1.28 (*m*, 42H)*	1.21 (*m*, 42H)*	1.21 (*m*, 42H)*
H13	1.28 (*m*, 42H)*	1.21 (*m*, 42H)*	1.21 (*m*, 42H)*

	[12d]	[12e]
H1	0.88 (*t*, 9H, *J* = 6.4)	0.78 (*t*, 9H, *J* = 6.4)
H2	1.27 (*m*, 42H)*	1.15 (*m*, 42H)*
H3	1.27 (*m*, 42H)*	1.15 (*m*, 42H)*
H4	1.27 (*m*, 42H)*	1.15 (*m*, 42H)*
H5	1.27 (*m*, 42H)*	1.15 (*m*, 42H)*
H6	1.27 (*m*, 42H)*	1.15 (*m*, 42H)*
H7	1.27 (*m*, 42H)*	1.15 (*m*, 42H)*
H8	2.23 (*m*, 6H)	2.30 (*m*, 12H)$^{\#}$
H9	2.49 (*m*, 6H)$^{\#}$	2.30 (*m*, 12H)$^{\#}$
H10	2.62 (*dt*, 2H, *J* = 19.6, 6.0)	2.51 (*dt*, 2H, *J* = 19.6, 6.0)
H11	2.49 (*m*, 6H)$^{\#}$	2.30 (*m*, 12H)$^{\#}$
H12	1.27 (*m*, 42H)*	1.15 (*m*, 42H)*
H13	1.27 (*m*, 42H)*	1.15 (*m*, 42H)*

H14	-	7.64 (*m*, 2H)~
H15	-	7.43 (*m*, 2H)^
H16	-	7.43 (*m*, 2H)^
H17	-	7.64 (*m*, 2H)~

Table 4.2: ^{13}C NMR assignment of ionic liquids [12a-e].

	[12a]	**[12b]**	**[12c]**
Primary Carbons	14.1	14.0	14.0
Secondary Carbons	17.0 (*d*, *J* = 49) 19.6 (*d*, *J* = 47) 21.5 (*d*, *J* = 4) 22.5 23.9 25.8 28.7 28.9 30.5 (*d*, *J* =14) 31.6 51.4 (*d*, *J* = 5) 54.5	17.0 (*d*, *J* = 49) 19.1 (*d*, *J* = 47) 21.6 (*d*, *J* = 4) 22.5 23.9 25.8 28.7 28.9 30.6 (*d*, *J* =14) 31.6 51.3 (*d*, *J* = 5) 54.5	16.7 (*d*, *J* = 49) 18.9 (*d*, *J* = 47) 21.7 (*d*, *J* = 4) 22.5 23.9 25.8 28.7 28.9 30.6 (*d*, *J* = 14) 31.6 51.3 (*d*, *J* = 5) 54.5
Tertiary Carbons	-	-	-
Quaternary Carbons	113.4 (*q*, *J* = 321)	119.9	113.2 (*q*, *J* = 294) 160.9 (*q*, *J* = 33)

	[12d]	**[12e]**
Primary Carbons	13.0	14.0
Secondary Carbons	16.0 (*d*, *J* = 49) 18.1 (*d*, *J* = 47) 20.7 (*d*, *J* = 4) 21.5 22.9 24.8 27.9 29.7 30.6 (*d*, *J* = 14.0) 31.6 50.5 (*d*, *J* = 5) 53.5	17.0 (*d*, *J* = 49) 19.1 (*d*, *J* = 47) 21.6 (*d*, *J*= 4) 22.4 23.9 25.7 28.7 28.8 30.6 (*d*, *J* = 14) 31.6 51.5 (*d*, *J* = 5) 54.3
Tertiary Carbons	-	119.3 122.9 130.7 131.4
Quaternary Carbons	114.0 (*q*, *J* = 321)	135.0 145.0 169.7

Table 4.3: Infrared assignment of salts [12a-e].

	C=O	SO_2^-	C≡N
[12a]	-	1137 1352	-
[12b]	-	-	2127 2189 2226
[12c]	1687	-	-
[12d]	-	1151 1350	-
[12e]	1636	1117 1350	-

4.2.2.2 ^{1}H NMR, ^{13}C NMR, and IR characterisation of ionic liquids [13a-13b]

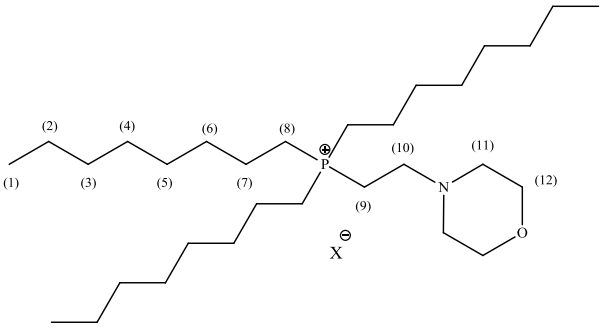

X =

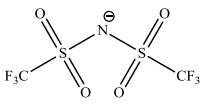

[13a]

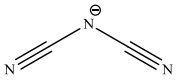

[13b]

Figure 4.9: Illustration of (1-morphol-4-yl)ethyl(trioctyl)phosphonium cation and its respective anions [13a-b].

Table 4.4: ^{1}H NMR assignment of ionic liquids [13a-b].

	[13a]	**[13b]**
H1	0.89 (*t*, 9H, *J* = 7.0)	0.89 (*t*, 9H, *J* = 7.0)
H2	1.28 (*m*, 36H)*	1.21-1.58 (*m*, 36H)*
H3	1.28 (*m*, 36H)*	1.21-1.58 (*m*, 36H)*
H4	1.28 (*m*, 36H)*	1.21-1.58 (*m*, 36H)*
H5	1.28 (*m*, 36H)*	1.21-1.58 (*m*, 36H)*
H6	1.28 (*m*, 36H)*	1.21-1.58 (*m*, 36H)*
H7	1.28 (*m*, 36H)*	1.21-1.58 (*m*, 36H)*
H8	2.26 (*m*, 6H)	2.29 (*m*, 6H)
H9	2.57 (*m*, 6H)$^{\#}$	2.59 (*s*, br, 6H)$^{\#}$
H10	2.71-2.81(*dt*, 2H, *J* = 19.6, 6.0)	2.86 (*m*, 2H)
H11	2.57 (*m*, 6H)$^{\#}$	2.59 (*s*, br, 6H)$^{\#}$
H12	3.69 (*t*, 4H, *J* = 4.7)	3.72 (*s*, br, 4H)

Table 4.5: ^{13}C NMR assignment of ionic liquids [13a-b].

	[13a]	**[13b]**
Primary Carbon	14.0	14.0
Secondary Carbon	16.5 (*d*, *J* = 49) 18.9 (*d*, *J* = 47) 21.5 (*d*, *J*= 4) 22.5 28.7 28.9 30.5 (*d*, *J* = 15) 31.6 51.4 (*d*, *J*= 5) 53.5 66.4	17.8 (*d*, *J* = 49) 19.1 (*d*, *J* = 47) 21.6 (*d*, *J* = 4) 22.5 28.8 28.9 30.7 (*d*, *J* = 15) 31.6 51.2 (*d*, *J* = 5) 53.5 66.6
Tertiary Carbon	-	-
Quaternary Carbon	115.1 (*q*, *J* = 321)	119.9

Table 4.6: Infrared assignment of salts [13a-b].

	SO_2^-	C≡N
[13a]	1137 1352	-
[13b]	-	2127 2188 2226

4.2.2.3 ^{1}H NMR, ^{13}C NMR, and IR characterisation of ionic liquids [14a-14b]

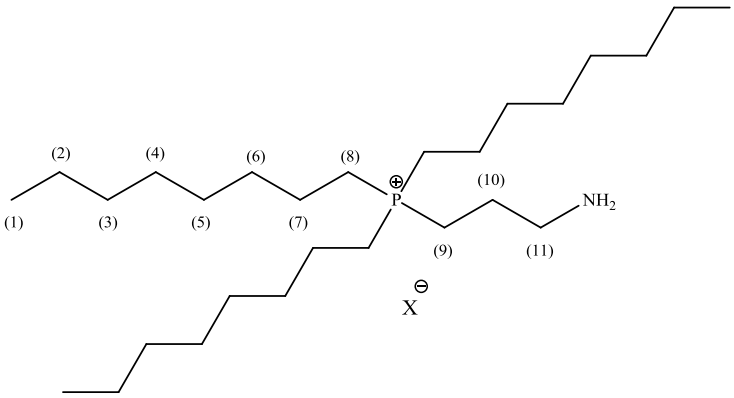

X =

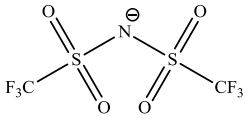

[14a]

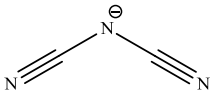

[14b]

Figure 4.10: Illustration of 3-aminopropyl(trioctyl)phosphonium cation and its respective anions [14a-b].

Table 4.7: ^{1}H NMR assignment of ionic liquids [14a-b].

	[14a]	[14b]
H1	0.88 (*t*, 9H, *J* = 7.0)	0.88 (*t*, 9H, *J* = 7.0)
H2	1.27-1.78 (*m*, 38H)*	1.28 – 1.71 (*m*, 40H)*
H3	1.27-1.78 (*m*, 38H)*	1.28 – 1.71 (*m*, 40H)*
H4	1.27-1.78 (*m*, 38H)*	1.28 – 1.71 (*m*, 40H)*
H5	1.27-1.78 (*m*, 38H)*	1.28 – 1.71 (*m*, 40H)*
H6	1.27-1.78 (*m*, 38H)*	1.28 – 1.71 (*m*, 40H)*
H7	1.27-1.78 (*m*, 38H)*	1.28 – 1.71 (*m*, 40H)*
H8	2.07 – 2.31 (*m*, 10H)$^{\#}$	2.19 (*m*, 6H)
H9	1.27-1.78 (*m*, 38H)*	1.28 – 1.71 (*m*, 40H)*
H10	2.07 – 2.31 (*m*, 10H)$^{\#}$	2.37 (*m*, 2H)
H11	2.85 (*t*, 2H, *J* = 5.6)	2.89 (*t*, 2H, *J* = 5.6)
NH_2	2.07 – 2.31 (*m*, 10H)$^{\#}$	1.28 (*m*, 40H)*

Table 4.8: ^{13}C NMR assignment of ionic liquids [14a-b].

	[14a]	[14b]
Primary Carbons	14.0	14.0
Secondary Carbons	16.0 (*d*, *J* = 49) 18.4 (*d*, *J* = 47) 21.5 (*d*, *J* = 5) 22.5 24.6 (*d*, *J* = 5) 28.7 28.9 30.5 (*d*, *J* = 15) 31.6 41.5 (*d*, *J* = 19)	16.0 (*d*, *J* = 49) 18.7 (*d*, *J* = 47) 21.6 (*d*, *J* = 5) 22.5 24.8 (*d*, *J* = 5) 28.8 28.9 30.6 (*d*, *J* = 15) 31.8 41.7 (*d*, *J* = 19)
Tertiary Carbons	-	-
Quaternary Carbons	112.8 (*q*, *J* = 320)	119.2

Table 4.9: IR assignment of ionic liquids [14a-b]

	[14a]	[14b]
NH_2 (cm^{-1})	3410 3367	3406 3383
SO_2 (cm^{-1})	1351 1137	-
C≡N (cm^{-1})	-	2230 2191 2131

4.2.3 ^{1}H NMR characterisation of ionic liquids [12a-14b]

From the ^{1}H NMR (Figure 4.4), the quaternisation of the phosphorus atom using the alkylating agents can be confirmed. Due to the NMR activity of the phosphorus, coupling between the phosphorus and the hydrogen atoms occurs. From Figure 4.8, it can be seen that the cation contains an ethyl chain in between a phosphorus and nitrogen atom. From Figure 4.4 in which the ^{1}H NMR spectrum of a typical phosphonium ionic liquid [12a] is presented, a doublet of triplets is observed between 2.58 – 2.69 ppm which is the signal corresponding to protons directly adjacent in the nitrogen in the ethyl chain with the piperidine ring terminal. This was determined from the integration of 2H, its chemical shift, and also due to the coupling constants by the phosphorus atom which are much smaller than the signal denoted as (9) in Figure 4.10 which is further away from the phosphorus cationic centre. From the imidazole ionic liquids [9a-e], the approximate chemical shifts of the piperidine signal denoted (11) - (13) were known, and it is clear that these overlap with the signals for trioctyl groups (typically 1.28 – 1.54 ppm) of the cationic backbone with the signals corresponding to the signal for the H atoms denoted (12) and (13). Overlapping was further confirmed by the change in integration when compared to the trioctylphosphine precursor. The signals for H atoms (11) were seen to overlap with those for the H atoms denoted (9) at 2.31 – 2.40 ppm in [12a] which was confirmed from the COSY NMR spectra.

The choice of anion can be seen to have an effect on the chemical shift of the signals arising from the protons directly adjacent to the cationic phosphorus centre (signals denoted (8), (9), and (10)) due to its influence on the electron density around these

hydrogen atoms. The chemical shift dependence of these H atoms signals as a result of the anion employed is highlighted in Figure 4.11 where the ^{1}H NMR spectra of [12a], [12b], and [12d], are presented. From these spectra, it can be observed that weakly coordinating anions resulting in signals remaining more downfield in the ^{1}H NMR spectra as seen in the case of the imidazolium ionic liquids with the hydrogen at the C2 position of the imidazole ring.[16] This property is a convenient way to monitor the reaction and to ensure that the metathesis reaction has occurred in the cases where protons are absent from the anion. It is clearly evident that the choice of anion affects the chemical shift of both the (9) and (10) protons. Shifting of the signal corresponding to the H atom denoted as (9) signal is observed, with the overlapping of the signal with (11) in both [12a] and [12b] (approximately 2.40 ppm), however this also appears to be shifted downfield in [12d] with the emergence of the multiplet corresponding to signals of the protons (9) emerging from the signal of the H atoms denoted as (11).

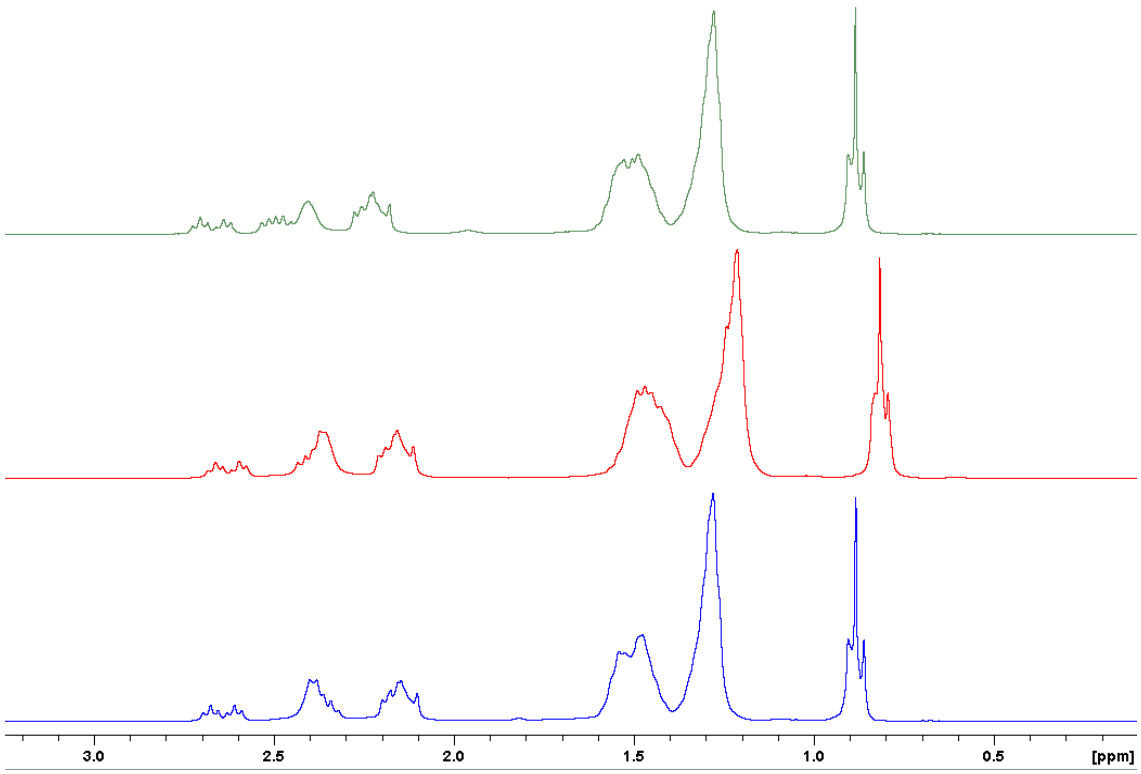

Figure 4.11: ^{1}H NMR spectra of ionic liquids [12a] (-), [12b] (-), and [12d] (-).

An example of the ^{1}H NMR spectrum recorded of 4-(morphol-4-yl)ethyl(trioctyl)phosphonium cation with the bis(triflimide) anion [13a], can be seen in Figure 4.12. The inclusion of an oxygen atom has a significant effect on the chemical shift of signal denoted (12) in Figure 4.9 when compared to its 1-(piperid-1-

yl)ethyl(trioctyl)phosphonium analogue. A difference in chemical shift of approximately 2 ppm was observed, 1.28 ppm for [12a] and 3.69 ppm for [13a] due to the deshielding effect of the oxygen. A smaller effect on the chemical shifts of signals (9), (10), and (11), were also observed of approximately 0.1 ppm.

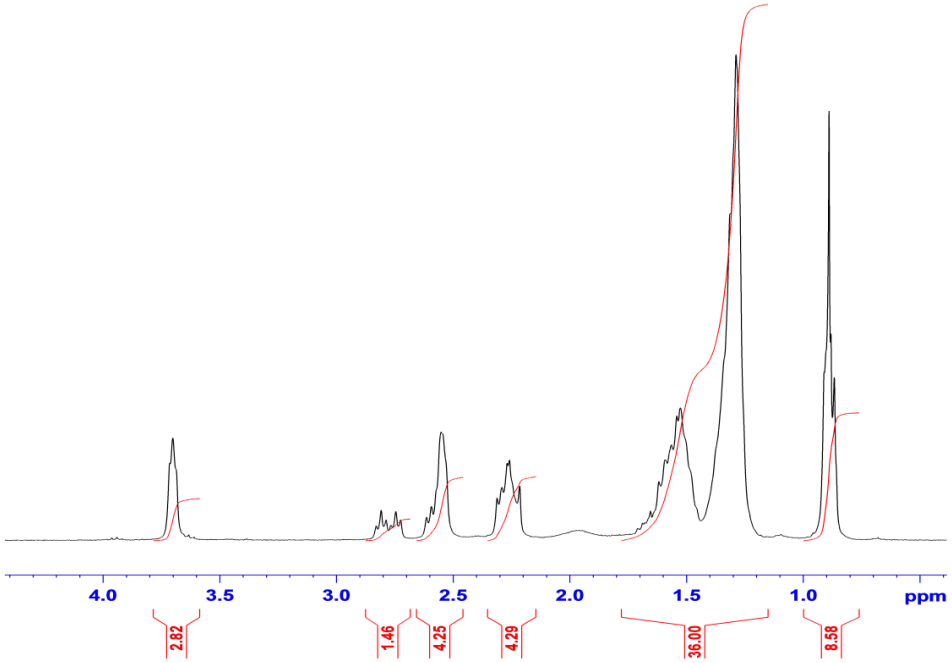

Figure 4.12: ^{1}H NMR of 4-(morphol-4-yl)ethyl(trioctyl)phosphonium bis(triflimide)

In the [14a-b] ionic liquids, the propyl chain adjacent to the primary amine is evident in both ^{1}H NMR and ^{13}C NMR spectra. In the case of [14a], the quaterisation can be confirmed due to the presence of a triplet at 2.85 ppm which are the signals corresponding to the protons denoted as (11), and multiplet signal at 1.67 ppm which arose from the protons denoted as (9), whereby the multiplet relates to the signals of the protons denoted as (10) in Figure 4.10 can be determined by COSY NMR spectroscopy to occur at 2.24 ppm. The broad singlet at 2.44 ppm with an integral of 2 confirms the presence of the primary amine moiety. An accurate mass of 428.4386 a.m.u (M+) was observed also indicating the presence of the free primary amine.

4.2.4 ^{13}C NMR characterisation of ionic liquids [12a-14b]

As observed in the ^{1}H NMR spectra, the charged phosphorus also contributes towards splitting of the signals of the carbon atoms in the ^{13}C NMR. Due to ^{31}P possessing a spin of ½, the same splitting rules apply to that of protons (n+1).[12] Therefore doublets

were observed in the signals for the carbon atoms no greater than 3 bond lengths away from the phosphorus centre. This was a trend seen in all ionic liquids composed of the phosphorus cation backbone. In the case of the [12a-e] ionic liquids, a doublet can be seen at approximately 16.0 ppm which corresponds to the carbon adjacent to the phosphorus atom on the ethylpiperidine linkage with the adjacent carbon typically appearing at 51.0 ppm. On the cation, carbon phosphorus coupling occurs at the α, β, and γ carbon producing doublets at 19.0, 21.0, and 30.0 ppm. The peak trends of the ^{13}C NMR seem to oppose those of the ^{1}H NMR whereby those signals closer to the positive phosphorus centre appear at higher chemical shifts than those at the end of the octyl chains in the ^{1}H NMR whereby the opposite is true in the ^{13}C NMR. This was found to be true for all the phosphonium ionic liquids presented in this chapter. From the Wittig reaction it is well known that the α hydrogen atoms on the quaternary phosphonium salts are quite acidic and can be removed by base to form ylide.[17] We propose that this can explain the opposing trends in the ^{1}H NMR and ^{13}C NMR as the bonding in these phosphonium salts can be represented by the two resonance structures shown in Figure 4.13. These assignments were confirmed using HSQC analysis (Figure 4.14). The assignments were further confirmed by the magnitude of the J_{PC} coupling constants with the larger constants indicating the carbons atoms relating to that signals proximity to the phosphorus atom.

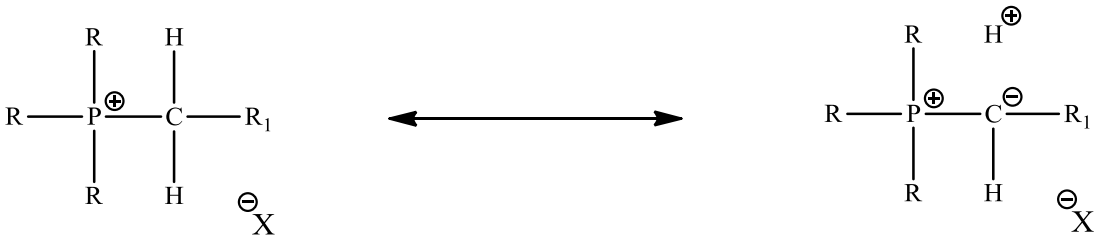

Figure 4.13: Resonance stuctures of a typical phosphonium cation synthesised as part of this study where X = anion, R = octyl chains and R_1 represent different functional groups .

An example of this splitting can be seen in Figure 4.14(a) which shows the ionic liquid [12a] ^{13}C NMR spectrum (0 – 130 ppm), and Figure 4.14(b) which shows the ionic liquid [12a] spectrum from 0 – 40 ppm to aid in the observation of the splitting. Like the imidazolium ionic liquids containing the Tf_2N^-. TFA^-, and $TFMS^-$ anions, ^{13}C - ^{19}F coupling is also observed with quartets observed typically from 113.0 – 126.0 ppm due to the ½ spin state of ^{19}F isotope. This produces quartets for the CF_3 signals in the case

of each anion and also produces a quartet signal for the carbonyl carbon present in the TFA^- anion.

(a)

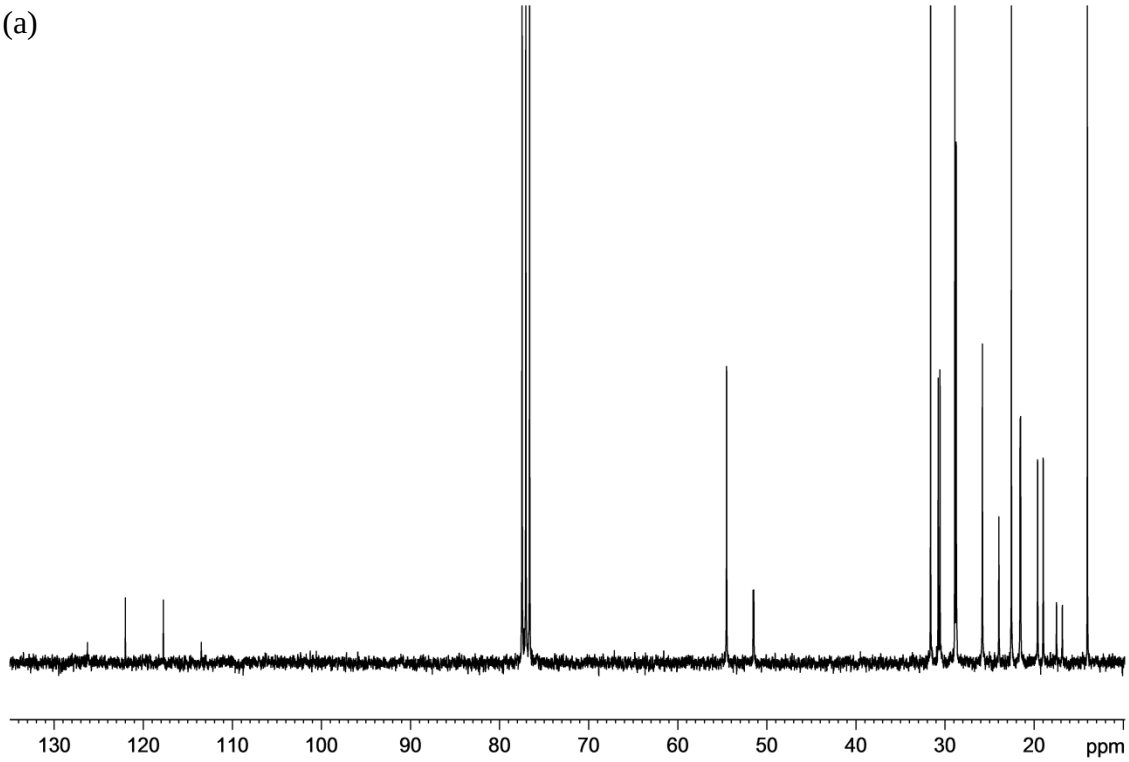

(b)

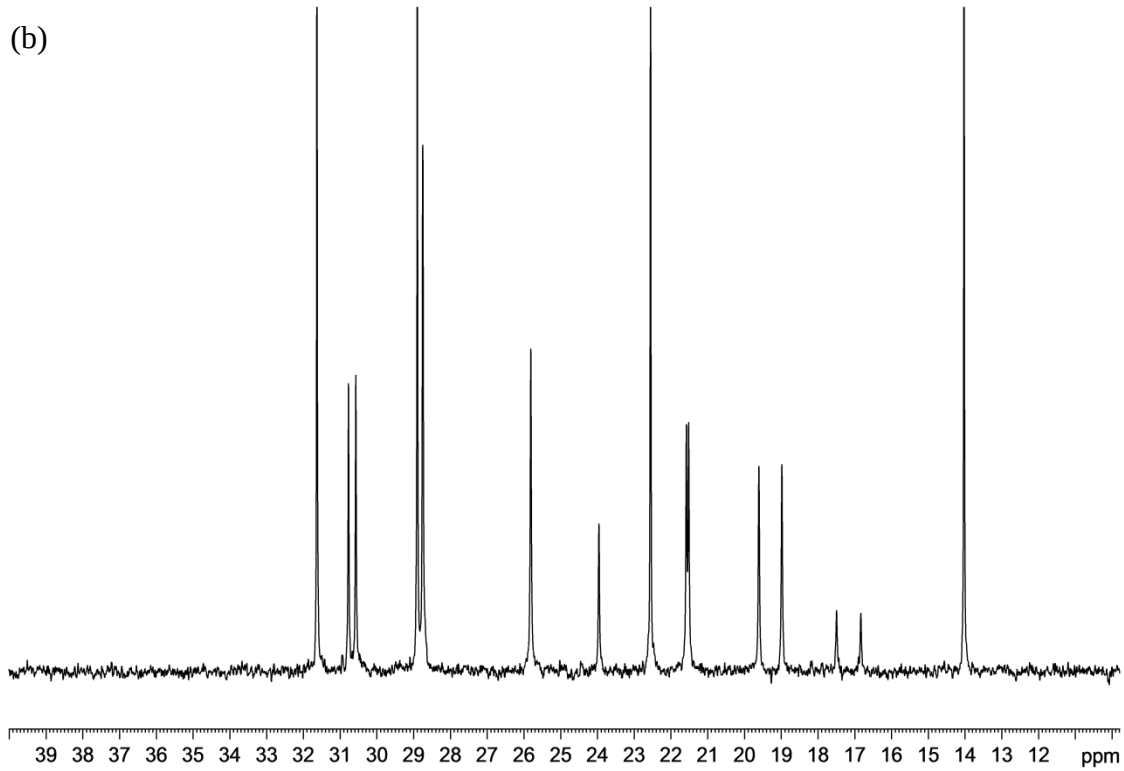

(c)

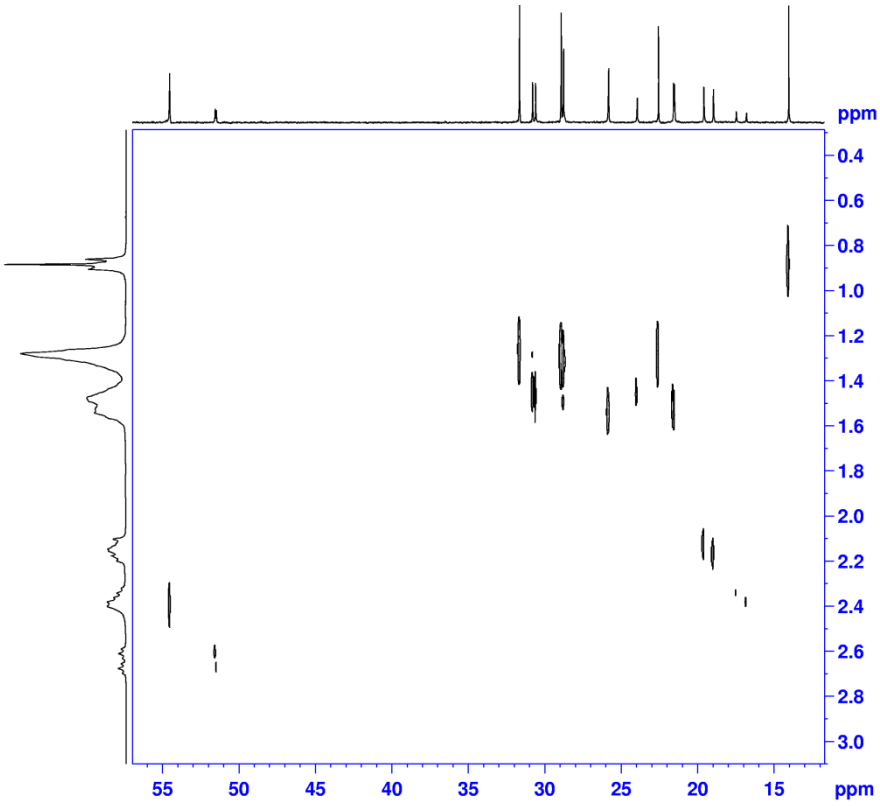

Figure 4.14: (a) Full ^{13}C NMR spectrum of [12a], (b) 0 – 40 ppm ^{13}C NMR spectrum of [12a], and (c) HSQC spectrum of [12a].

The morpholine ring also has an effect on the ^{13}C NMR spectrum when compared to its piperidine analogue. The ^{13}C NMR spectra of [13a] in Figure 4.15(a) and (b), also exhibits characteristic chemical shifts for the signals of the carbon atoms adjacent to the oxygen atom resulting in a difference in chemical shift of 25.8 ppm for [12a] to 66.6 ppm for [13a]. The phosphorus also couples to the carbon atoms identically to that observed for the [12a-e] with carbon atoms no greater than 3 bond lengths away from the phosphorus atom producing doublets. A similar trend was observed with [14a] and [14b].

(a)

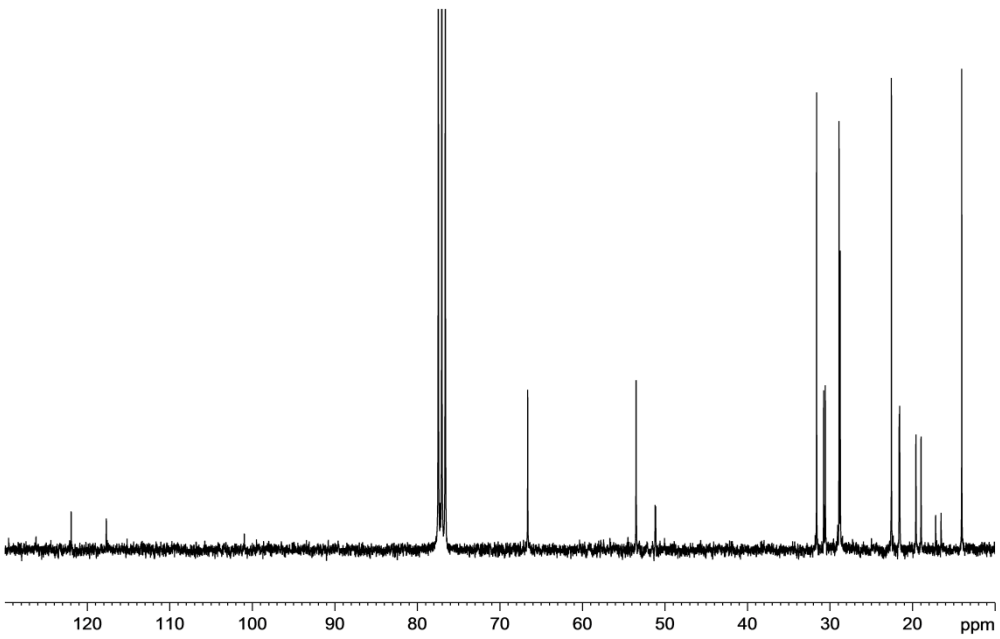

(b)

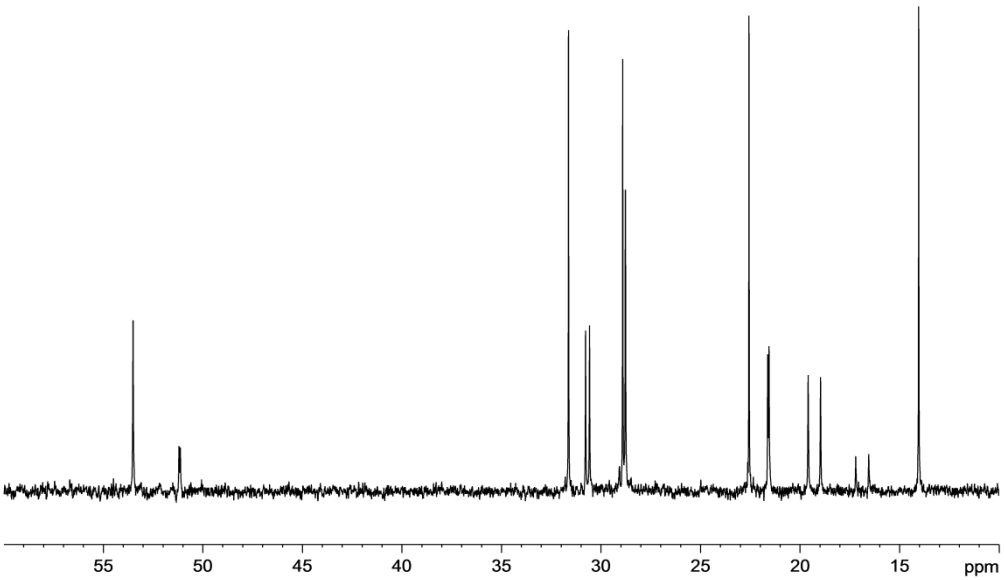

Figure 4.15: (a) ^{13}C NMR (full), and (b) ^{13}C NMR (0 – 55 ppm) of 4-(morphol-4-yl)ethyl(trioctyl) phosphonium bis(triflimide).

4.2.5 IR characterisation of ionic liquids [12a-14b]

IR spectra of these salts generally showed the same features as those outlined in Section 3.3.2.6, upon incorporation of the simple anions. The IR spectra of [14a-14b] was used to determine the presence of the N-H stretches at 3300 – 3200 cm^{-1} of the primary amine moiety present on the cation. Two stretches were found 3383 cm^{-1} and 3406 cm^{-1} indicating the free primary amine in the [14b] ionic liquid with similar stretches observed in [14a].

4.3 Attempted synthesis of ionic liquids containing azide functionality for potential use in click chemistry and characterisation of salts [15a - 15b].

4.3.1 Attempted synthesis of azide functionalised ionic liquid

As highlighted in Chapter 1, ionic liquids can be targeted to a specific task by the addition of certain functionalities into the structure of the ionic liquid.[13,18-20] As previously discussed for the imidazolium cations combined with the amino acid anions, the amine functionality is of great interest due to its ability to form covalent bonds with free CO_2. One major drawback to the use of the amino acid anions was the visible increase in the viscosity which was observed. Therefore, modification of the cation to incorporate amine functionality into the liquid which can be seen in Section 4.2.3 is of interest and a number of reseachers have previously reported this in the literature.[3,13] One drawback of the method used in the synthesis of the liquids [14a-b] is the use of the hydrochloride/hydrobromide salts which protect the amine during the quaternisation of the phosphine. This requires additional treatment of the liquid to convert to a primary amine and make it a free site for CO_2 capture. The approach in this section is to generate a quaternary phosphonium salts with an alkyl halide chain which can be converted into azide form and reacted with an alkynyl amine which would result in the introduction of the amine into the cationic backbone of the liquid without the need for protecting groups. A schematic of this is shown in Scheme 4.2.

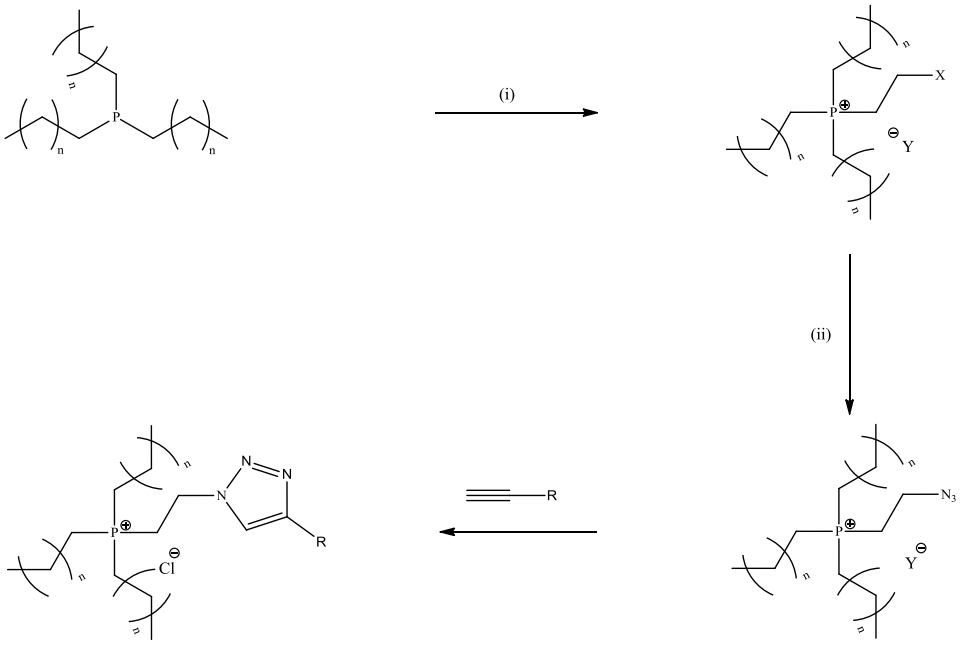

Scheme 4.2: Attempted synthetic route of azide ionic liquids and subsequent click reaction, (i) 1,2 dihalide ethane, EtOH, rt, 48 h, (ii)NaN_3, EtOH, 78 ºC, 24 h, alkyne functionalised species.

To generate the terminal halide chain onto the phosphorus cation, the trioctylphosphine was added dropwise to the solution of 1,2-dibromoethane in ethanol (20 cm^3) at 50 ^oC and allowed to stir for 24 hours. The sample was found to contain traces of the trioctylphosphine oxide species and was removed by washing with hexane. From the ^1H NMR spectrum recorded of the crude product mixture (Figure 4.16), it is clear that the disubstitued form has been generated whereby a second phosphine unit was quaternised at the terminal halide site yielding the double charged phosphonium salt. The lack of the doublet of triplets and multiplets which arise from the newly alkylated (ethyl chain) phosphonium salt which suggest inequivalency of the two proton signals (i.e monosubstituted phosphonium salt) were seen for the previous phosphonium ionic liquids. The phosphorus hydrogen coupling would seem to confirm the presence of the disubstituted form and the absence of the monosubstituted form. The presence of the newly formed doublet at 3.29 ppm, indicate the presence of the symmetrical species due to the ethyl hydrogen atoms now being equivalent and being split by the single phosphorus atom to form a doublet. An accurate mass of 847.7017 a.m.u (M^{2+}) in the positive ionisation mode confirmed the presence of the di-substituted species.

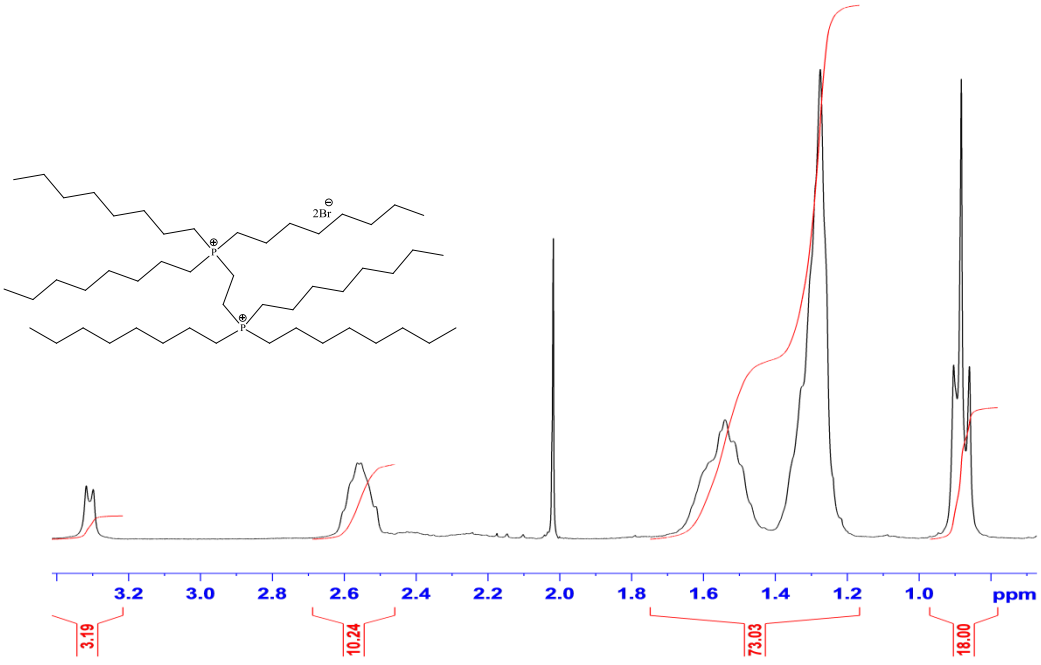

Figure 4.16: Crude ^1H NMR spectrum of reaction of trioctylphosphine with 1,2-dibromoethane at 50 ^oC indicating the presence of the doubly charged phosphonium cation.

In order to prevent the formation of the disubstituted phosphonium salt forming, it was thought that the lowering of temperature to 0 ^oC, as well as increased amounts of solvent could aid in the formation of the monosubstituted phosphonium salt.

Unfortunately, these efforts proved unsuccessful and the disubstituted forms were generated even under these conditions. In order to combat this problem 1-bromo-2-chloroethane was employed as the alkylating agent to generate the phosphonium salt with an alkyl halide terminal chain. Previous work conducted with imidazoles and the use of bromo-chloro alkyls had been shown to selectivity generate salts with halide terminal chains. The reaction was repeated using the conditions initially employed when alkylating with the dibromo species. As shown in Figure 4.17(a), this resulted in the generation of the disubstituted species once again as the doublet relating to the ethyl linkage of this species was observed at 3.29 ppm.

The reaction was repeated with the temperature decrease to 0 ^{o}C, and all other conditions kept constant. From the ^{1}H NMR recorded of the crude mixture which is presented in Figure 4.16(b), the presence of the disubstituted species was observed due to the doublet relating to the ethyl chain signals of the disubstituted species present once again. Signals corresponding to the monosubstituted species were also present with a doublet of triplets at 4.00 – 4.19 ppm and multiplet at 3.40 ppm. The phosphorus and hydrogen coupling, indicating the presence of inequivalent hydrogens in the chain which can only be due to the presence of the chloroethyl chain. Accurate masses of 847.6988 a.m.u (M^{2+}) and 477.3225 a.m.u (M^{+}) confirmed the presence of the both species. From this, it is clear that the reaction may not be controllable under these conditions and as such an alternative approach was required to prevent the formation of the disubstituted product.

(a)

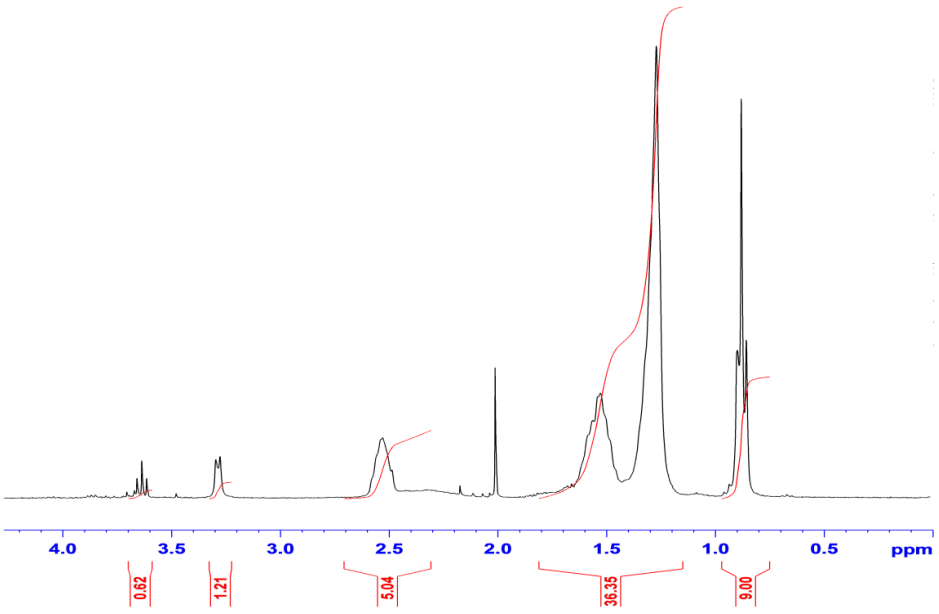

(b)

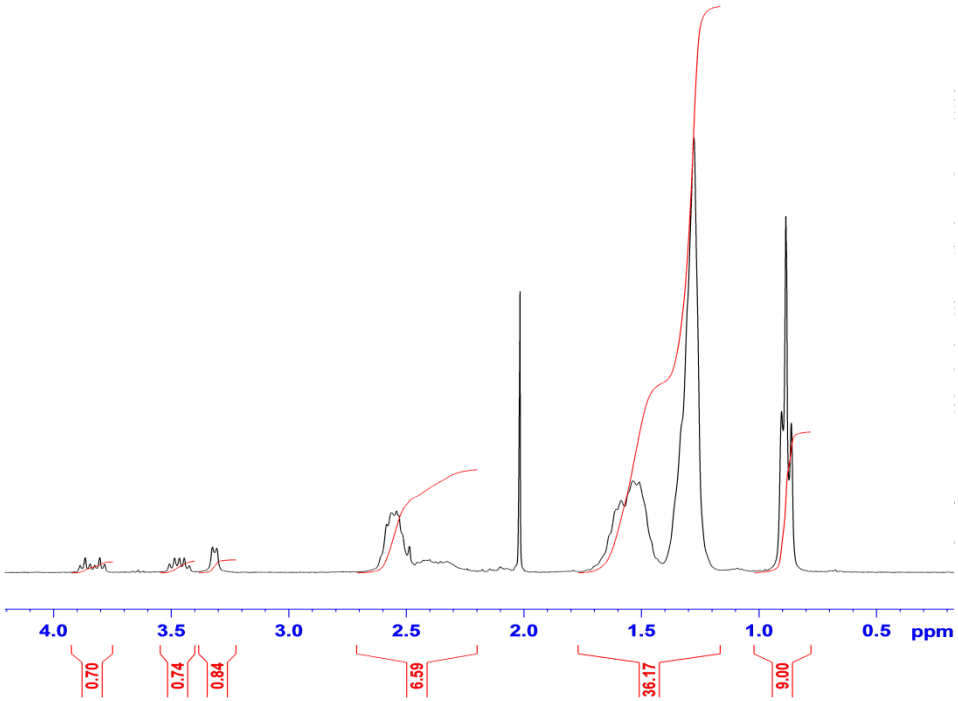

Figure 4.17: ^{1}H NMR spectra of the reaction mixture of trioctylphosphine and 1-bromo-2-chloroethane in ethanol at (a) 50 ºC, and (b) 0 ºC.

4.3.2 Synthesis and purification of alkyne functionalised ionic liquid [15a-b]

A different strategy was developed to form the desired triazole product. In this synthetic route the phosphonium salt would contain the alkyne moiety (Scheme 4.3). The route also allowed for the possibility of generating ionic liquid polymers via an azide-alkyne Huisgen cycloaddition reaction involving azide functionalised pyrrole monomers. Our research group in unpublished work has successfully attached alkyne functionalised ferrocene onto these azide functionalised polypyrrole films. Consequently, it is believed that a similar approach could be adopted using alkyne functionalised ionic liquids due to identical functional groups being involved in both reactions.[21]

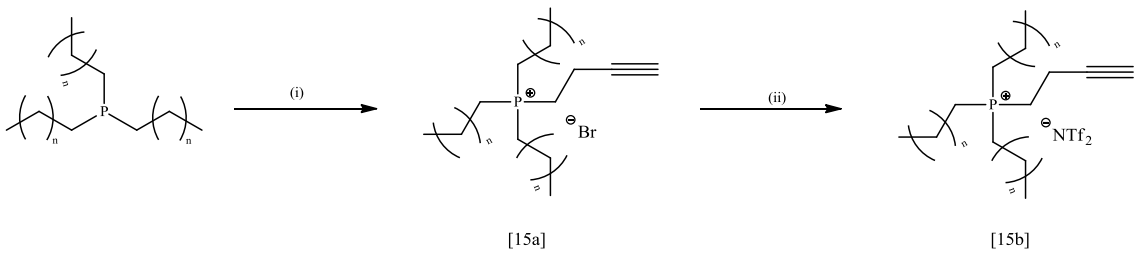

Scheme 4.3: Proposed synthetic route of alkyne ionic liquids containing the Tf_2N anion, (i) 4-bromo-1-butyne, EtOH, 80 ºC, 48 h, (ii) $LiTf_2N$, MeOH, rt, 24 h.

Synthesis of the alkyne ionic liquids followed that outlined in Scheme 4.3. Like in earlier cases, the crude product (waxy yellow appearance) contained both

trioctylphosphine and the trioctylphosphine oxide as determined using ^{31}P NMR spectroscopy. Although the peaks for the desired product were difficult to identify due to the high levels of ethanol still present in the sample, the ^{31}P NMR indicated that the quaternisation reaction had been successful due to the presence of the singlet at 33.8 ppm, which is the characteristic chemical shift of the signal arising from the quaternised phosphonium salts. The product was washed with hexane to remove impurities before being dissolved in acetonitrile to aid in the transference of the solid into a vessel. Upon drying of the material under reduced pressure, a white waxy solid was produced. From the resulting ^{1}H NMR spectrum (Figure 4.18 (red)), the alkyne units of the liquid are clearly visible by the signals which are a triplet (2.14 ppm), and the multiplets (2.72 – 2.78 ppm and 2.80 – 2.91 ppm). The complicated splitting of the signals imposed due to the proximity of the related hydrogen atoms to the phosphorus atom, and is also indicative that quaternisation is successful. Anion exchange was performed to then subsequently generate the bis(triflimide) form (Figure 4.18 (blue)).

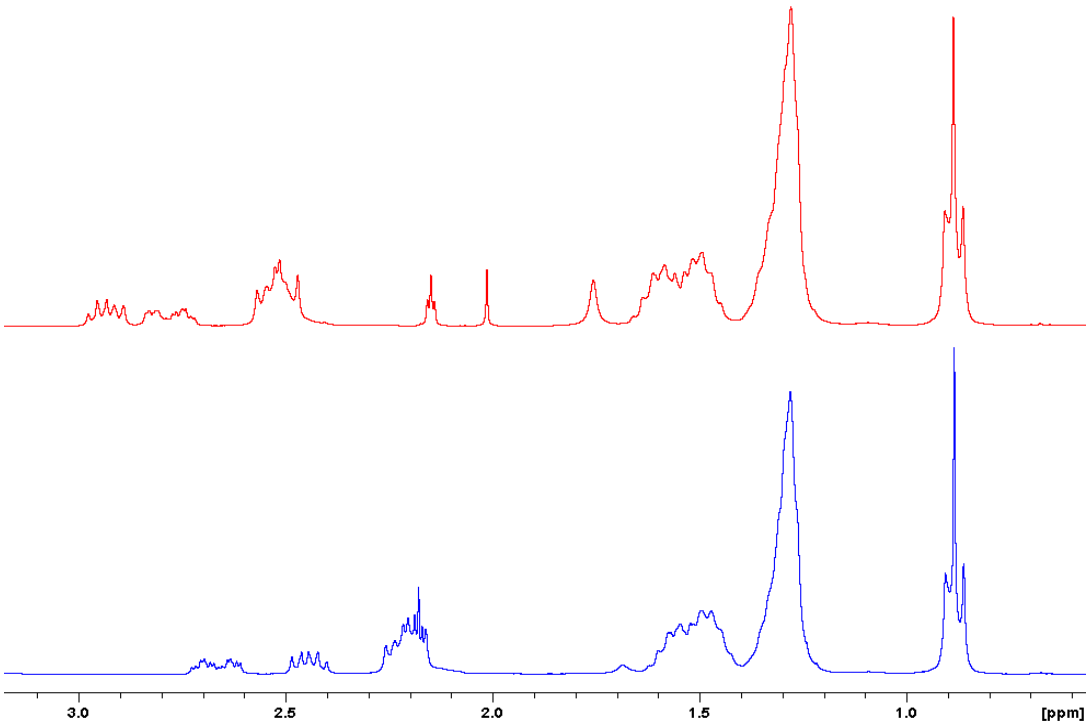

Figure 4.18: ^{1}H NMR spectra of ionic liquids [15a] (-), and [15b] (-) in $CDCl_3$.

4.3.2.1 ^{1}H NMR, ^{13}C NMR, and IR characterisation of ionic liquids [15a-b]

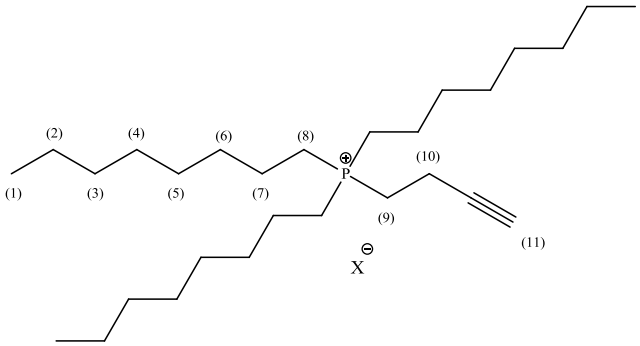

X =

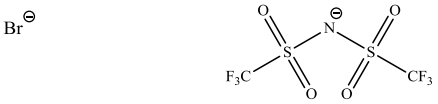

[14a] [14b]

Figure 4.19: Structure of the (but-3-yn-1-yl)trioctylphosphonium cation and its respective anions [15a-b].

Table 4.10: ^{1}H NMR assignment of ionic liquids [15a-b].

	[15a]	[15b]
H1	0.88 (*t*, 9H, *J* = 7.0)	0.88 (*t*, 9H, *J* = 7.0)
H2	1.27 – 1.68 (*m*, 36H)*	1.21 – 1.68 (*m*, 36H)*
H3	1.27 – 1.68 (*m*, 36H)*	1.21 – 1.68 (*m*, 36H)*
H4	1.27 – 1.68 (*m*, 36H)*	1.21 – 1.68 (*m*, 36H)*
H5	1.27 – 1.68 (*m*, 36H)*	1.21 – 1.68 (*m*, 36H)*
H6	1.27 – 1.68 (*m*, 36H)*	1.21 – 1.68 (*m*, 36H)*
H7	1.27 – 1.68 (*m*, 36H)*	1.21 – 1.68 (*m*, 36H)*
H8	2.47 – 2.56 (*m*, 6H)	2.18 (*m*, 7H)#
H9	2.89 (*m*, 2H)	2.46 (*m*, 2H)
H10	2.72 (*m*, 2H)	2.64 (*m*, 2H)
H11	2.14 (*t*, 1H, *J* = 2.6)	2.18 (*m*, 7H)#

Table 4.11: ^{13}C NMR assignment of ionic liquids [15a-b].

	[15a]	[15b]
Primary Carbons	13.3	13.9
Secondary Carbons	12.1(*d*, *J* = 5) 18.0 (*d*, *J* = 48) 19.2 (*d*, *J* = 46) 21.6 (*d*, *J* = 4) 22.3 28.7 28.8 30.5 (*d*, *J* = 15) 31.4	12.1(*d*, *J* = 5) 17.1 (*d*, *J* = 48) 19.3 (*d*, *J* = 46) 21.4 (*d*, *J* = 4) 22.5 28.6 28.8 30.3 (*d*, *J* = 15) 31.6
Tertiary Carbons	71.7	72.0
Quaternary Carbons	80.8 (*d*, *J* = 6)	80.2 (*d*, *J* = 6) 113.4 (*q*, *J* = 321)

Table 4.12: IR assignment of ionic liquids [15a-b]

	[15a]	[15b]
SO_2 (cm^{-1})	-	1351 1137
C≡C-H (cm^{-1})	3314	3313
C≡C (cm^{-1})	2115	2118

4.3.2.2 ^{1}H NMR characterisation of ionic liquids [15a-b]

^{1}H NMR spectra of the bromide [15a] (red trace) and bis(triflimide) [15b] (blue trace) are presented in Figure 4.18. The examination of the ^{1}H NMR spectrum of [15a] from 0.00 – 2.00 ppm is consistent with the formation of trioctylphosphonium ionic liquids with the signals denoted in Figure 4.19 as (1) - (7) present with traces of acetonitrile present at 2.01 ppm. A triplet is observed at 2.14 ppm which integrates as 1H was

determined to be the signal relating to the hydrogen atom (11) in Figure 4.18. Although this was expected to be a singlet, it is most likely that due to the short bond length of the alkyne unit that long range coupling occurs with the (10) hydrogen atoms. This assignment was confirmed from COSY experiment which showed that the H(10) signal at 2.72 ppm. This type of splitting is also consistent with the precursor 4-bromo-1-butyne.[22] This leaves the multiplet at 2.89 ppm to be the signal relating to the hydrogen atoms denoted as (9) due to the multiplet from 2.47 – 2.56 ppm having previously been assigned as the signal relating to hydrogen atoms denoted as (8) in Figure 4.19.

The ^{1}H NMR spectrum of [15b] is also presented in Figure 4.18 and clear differences can be observed between it and that of its halide precursor. The signals of the hydrogen atoms directly adjacent to the charged phosphorus centre exhibit small shifts with different anions. It can be observed that the signal arising from the hydrogen atoms denoted as (8) in Figure 4.19 has an upfield shift from 2.47 ppm to 2.18 ppm and overlaps with the (11) signal whereas the signal denoted as (9) also shifts upfield from 2.89 ppm for the chloride to 2.46 ppm for the Tf_2N^- anion. From Table 4.10 it can be observed that the magnitude of this upfield shift of the proton signals decreases as the distance of the associated atoms from the phosphorus cationic centre increases.

4.3.2.3: ^{13}C NMR characterisation of ionic liquids [15a-15b]

Presented below in Figure 4.20 (green trace), is the ^{13}C NMR spectrum of ionic liquid [15a]. Carbon phosphorus coupling once again features largely in the spectrum for the signals which arise from carbon atoms which are three bonds or less away from the phosphorus centre. These can be seen as doublets at 12.1 ppm, 18.0 ppm, and the signal for the quaternary alkynyl carbon at 80.8 ppm. Unusually it appears that the quaternary carbon also presents itself in both the DEPT 45 (Figure 4.20 (orange trace)) and DEPT 135 experiments. This is due to the polarisation transfer from the terminal alkyne proton due to the magnitude of the $^{2}J_{CH}$.[23] It is also the large $^{1}J_{CH}$ value typically over 200 Hz that accounts for the poor signal intensity of the alkynyl carbon signals. To fully confirm that this signal was infact that of the quaternary carbon HSQC spectrum analysis was conducted and thus proved the signal to be quaternary by the absence of coupling of this signal to any of the atoms in the spectrum.

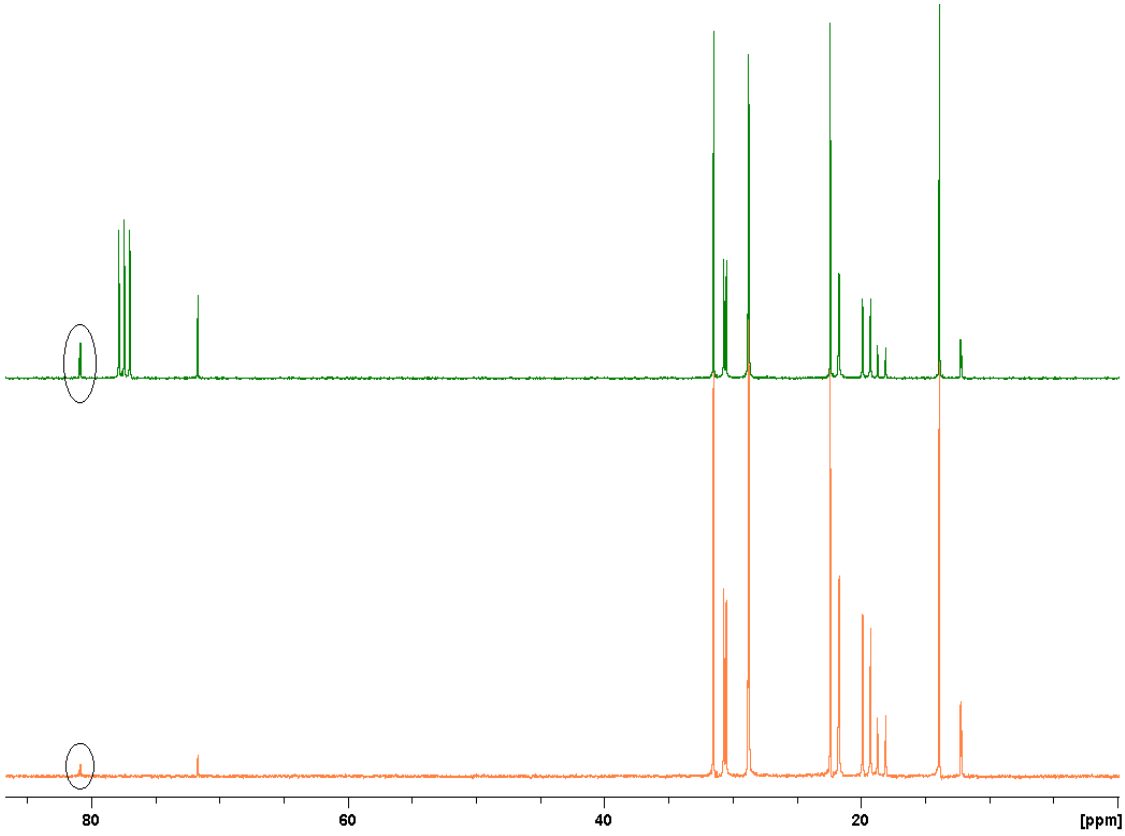

Figure 4.20: ^{13}C NMR (-), and DEPT 45 (-) spectra of ionic liquids [15a] in $CDCl_3$.

4.3.2.4: IR characterisation of ionic liquids [15a-15b]

As shown in Table 4.12 the incorporation of the alkyne moiety for the chloride salt [15a] was confirmed by the presence of the IR bands which were assigned to the C≡C stretch at 2115 cm^{-1} and the C≡C-H stretch at 3314 cm^{-1}. The corresponding stretches were also found in the bis(triflimide) salt. The IR of [15b] also confirmed the presence of the bis(triflimide) anion due to the 1350 cm^{-1} sulfonyl asymmetric stretching band and the 1137 cm^{-1} sulfonyl asymmetric stretching band.

4.4 Development of ionic liquid functionalised pyrroles and polymerisation

As will be mentioned in Chapter 5, poly(ionic liquids) have become an area of great interest for several applications in gas capture, separation, and as antimicrobial agents.[2-4,7,24,25] Therefore it was decided that inclusion of a polymerisable group (other than alkynyl) onto the ionic liquid cation would be the best approach due to the abundance of halide functionalised monomer groups, thus allowing for inclusion via quaternisation of the trioctylphosphine. Due to the experience in the research group in the use, growth and functionalization of pyrrole, it was a logical choice to develop a pyrrole derivative which could then be subsequently polymerised on an electrode.[26-29]

4.4.1 Synthesis and purification of ionic liquid functionalised pyrrole monomers [16a-b]

The pyrrole derivative 1-(2-chloroethyl)pyrrole was reacted under identical conditions (apart from the solvent employed) to those used for all phosphonium salts in this chapter (Scheme 4.4). The reaction mixture was refluxed in DMF at 90 ºC for 48 hours.

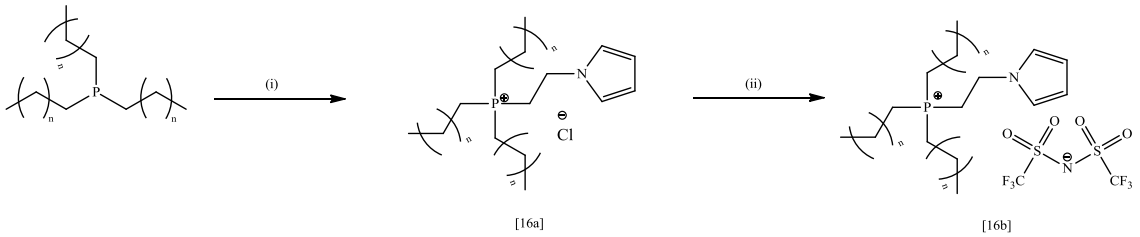

Scheme 4.4: Synthesis of trioctyl(1-(pyrrol-1-yl)ethyl)phosphonium bis(triflimide. (i) DMF, 78 ºC, 48 h, (ii) $LiTf_2N$, MeOH, rt, 24 h, (n=6).

The crude product was isolated from the solvent and it was then dissolved in methanol and washed with hexane to remove any unreacted trioctylphosphine. However from the ^{1}H NMR and ^{31}P NMR spectra recorded, it was evident that traces of the trioctylphosphine oxide has been generated during the course of the reaction (Figure 4.21(a) and (b)). This can be seen due to the proton signals corresponding to the long alkyl chains which appear as a small multiplet at 1.65 ppm, which are shifted downfield in comparison to the analogous signals for the quaternary phosphonium salt. The presence of the of the trioctylphosphine oxide is more clearly observed due to the signal at 48.7 ppm in the ^{31}P NMR spectrum corresponding to the phosphorus(5) species. The signal for the quaternary phosphonium salt can also be seen in the NMR with a signal at 31.5 ppm, however there is no signal at approximately -33.0 ppm indicating that no trioctylphosphine remained. From Figure 4.21(a), it is also evident that traces of the 1-(2-chloroethyl)pyrrole remained in the product mixture by the triplets at 3.73 ppm and 4.24 ppm (ethyl chain) and signals at 6.16 and 6.69 ppm (pyrrole ring). From the relative size of these signals to those of the product it would appear that a large quantity of the 1-(2-chloroethyl)pyrrole remained most likely due to the formation of the oxide species preventing the quaternisation to occur. Evidence of the DMF (reaction solvent) remaining in the product mixture is also evident by the signals at 2.88 and 2.95 ppm.

(a)

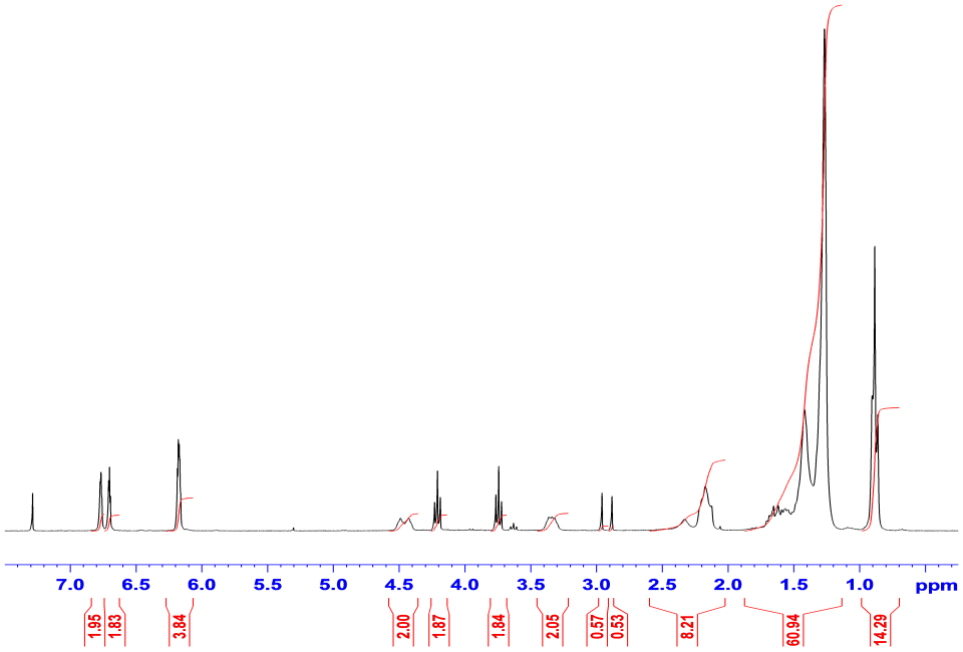

(b)

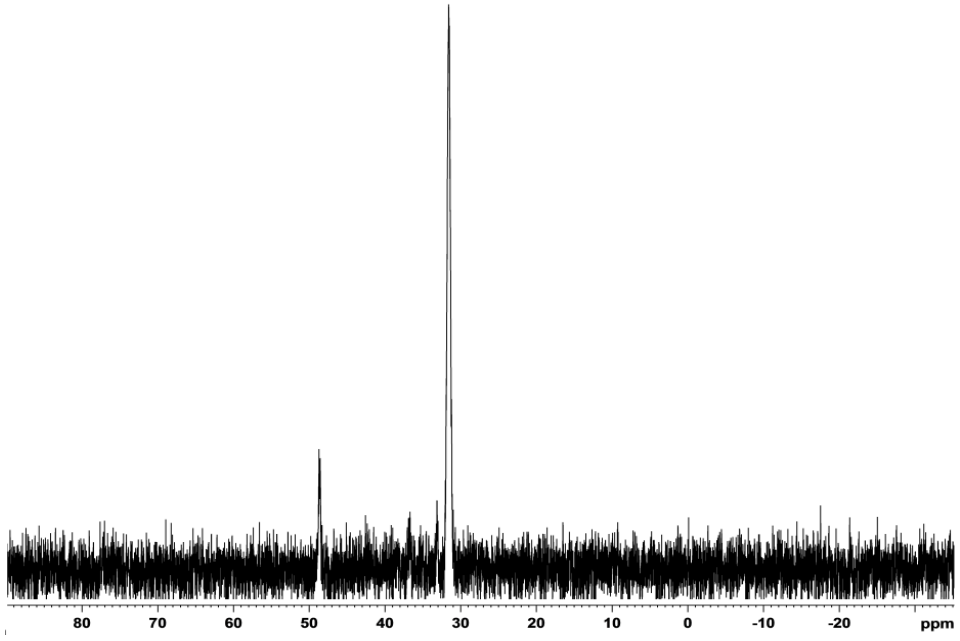

Figure 4.21: (a) ^{1}H NMR (crude), (b) ^{31}P NMR (crude) spectra of ionic liquid [16a].

As discussed in Section 4.2.1 washing the product with hexane had been successful in extracting the trioctylphosphine oxide. However, this had resulted in a decrease in percentage yield due to the quaternary phosphonium salts also displaying some solubility in hexane. To minimise this loss alternative routes of purification were investigated. One such system employed was the use of hexane and acetonitrile. The product was dissolved in acetonitrile and washed with the hexane with little success. It was noted that upon heating of the sample that dissolution of the complete reaction mixture into hexane occurred. The hexane solution was then cooled to room

temperature and the phosphonium salt was extracted into acetonitrile. The trioctylphosphine oxide remained in the non-polar layer. This work up proved to be successful, with the product separated from the oxide form and with minimal loss of sample and the loss of the 48.7 ppm phosphorus oxide signal (Figure 4.22).

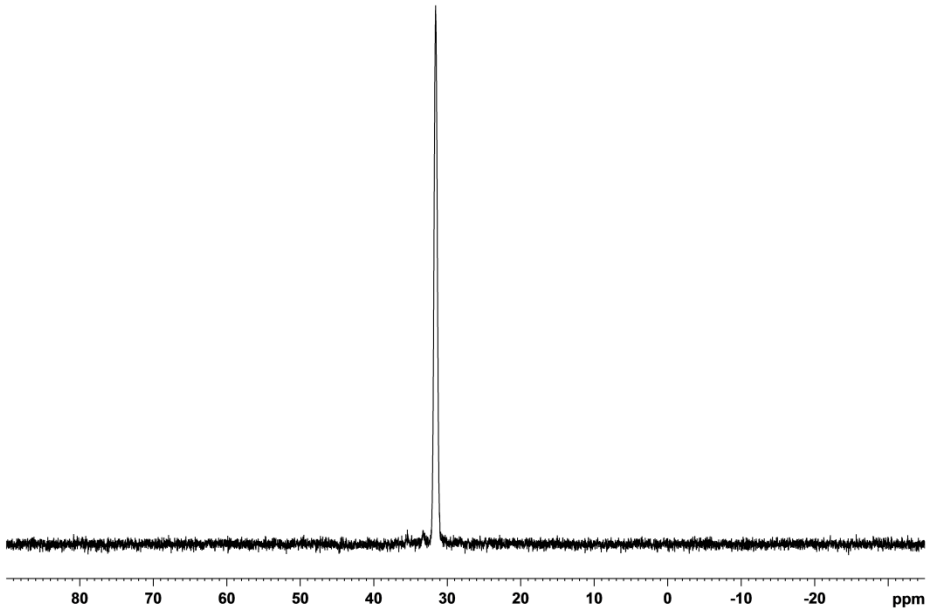

Figure 4.22: ^{1}H NMR spectrum of [16a] after extraction from hexane with acetonitrile.

While the work-up was effective at removal of the trioctylposphine oxide, an addition benefit was also noted with the use of this extraction system. Upon examination of ^{1}H NMR spectrum, a decrease in the integrals of the 1-(2-chloroethyl)pyrrole in comparison to the quaternised salt was observed. This indicated that this work up was not solely effective in removal of the oxide but also removed the pyrrole impurity. Several extractions were required to complete the removal of the pyrrole derivative. In total 10 extractions were required for complete removal (Figure 4.23). The extractions clearly show the gradual decrease in the signals corresponding to the ethyl chain and pyrrole ring assigned of the 1-(2-chloroethyl)pyrrole earlier in this section.

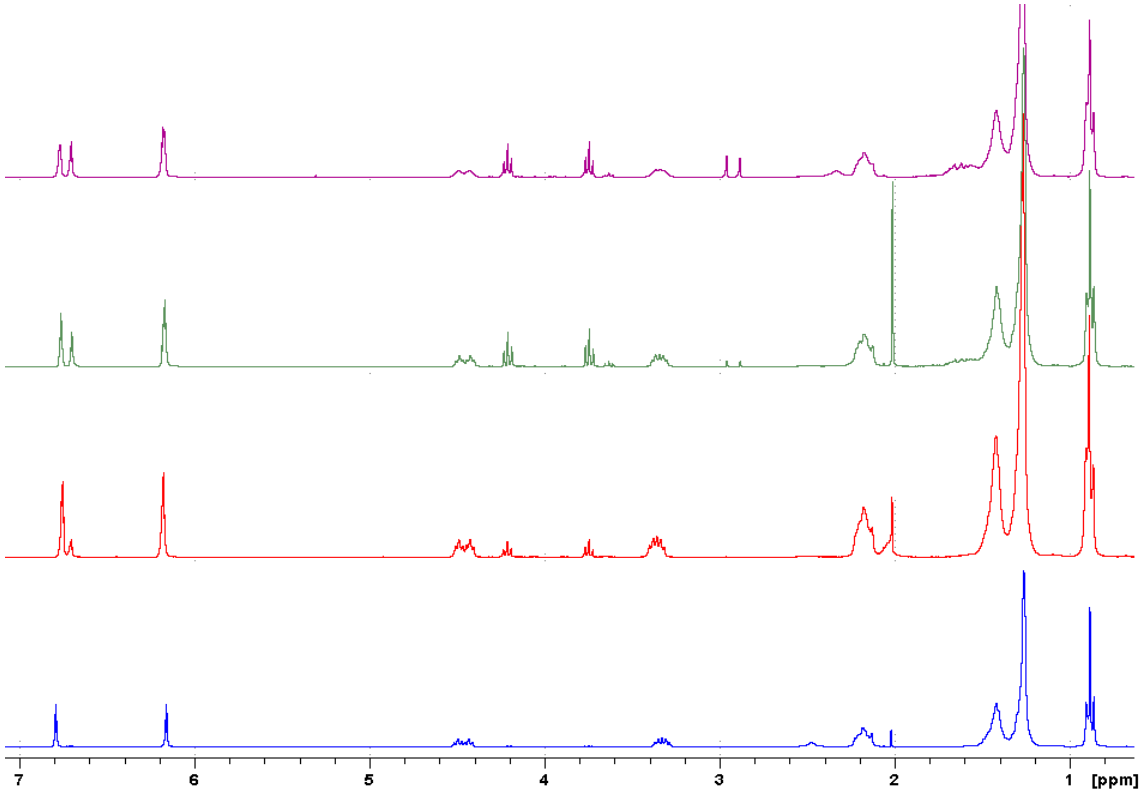

Figure 4.23: ^{1}H NMR spectra of the purification process of [16a] crude (-), after 3 extractions (-), 6 extractions (-), 10 extractions (-).

4.4.1.1 ^{1}H NMR, ^{13}C NMR and IR characterisation of ionic liquids [16a-b]

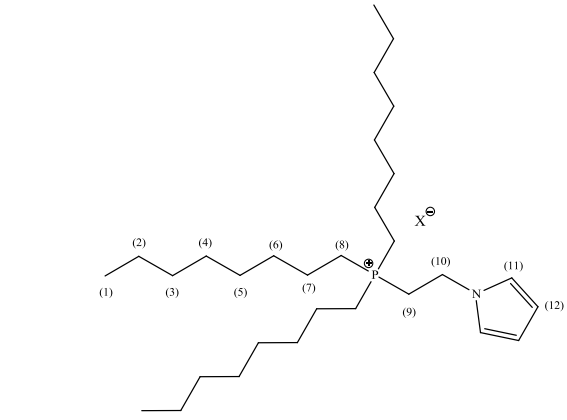

X =

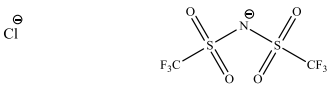

[16a] [16b]

Figure 4.24: Illustration of trioctyl(1-(pyrrol-1-yl)ethyl)phosphonium cation and its respective anions [16a-b].

Table 4.13: ^{1}H NMR assignment of ionic liquids [16a-b].

	[16a]	**[16b]**
H1	0.88 (*t*, 9H, *J* = 7.0)	0.88 (*t*, 9H, *J* = 7.0)
H2	1.26 - 1.49 (*m*, 36H)*	1.22 - 1.39 (*m*, 36H)*
H3	1.26 - 1.49 (*m*, 36H)*	1.22 - 1.39 (*m*, 36H)*
H4	1.26 - 1.49 (*m*, 36H)*	1.22 - 1.39 (*m*, 36H)*
H5	1.26 - 1.49 (*m*, 36H)*	1.22 - 1.39 (*m*, 36H)*
H6	1.26 - 1.49 (*m*, 36H)*	1.22 - 1.39 (*m*, 36H)*
H7	1.26 - 1.49 (*m*, 36H)*	1.22 - 1.39 (*m*, 36H)*
H8	2.17 (*m*, 6H)	1.88 (*m*, 6H)
H9	3.32 (*m*, 2H)	2.77 (*m*, 2H)
H10	4.41 - 4.51 (*dt*, 2H, *J* = 6.5, 18.4)	4.26 - 4.37 (*dt*, 2H, *J* = 6.5, 18.4)
H11	6.79 (*t*, 2H, *J* = 2.0)	6.69 (*t*, 2H, *J* = 2.0)
H12	6.16 (*t*, 2H, *J* = 2.0)	6.18 (*t*, 2H, *J* = 2.0)

Table 4.14: ^{13}C NMR assignment of ionic liquids [16a-b]

	[16a]	**[16b]**
Primary Carbons	12.1	13.0
Secondary Carbons	17.3 (*d*, *J* = 46) 19.9 (*d*, *J* = 4) 20.1 (*d*, *J* = 47) 20.6 26.9 27.0 28.7 (*d*, *J* = 15) 29.7 40.7 (*d*, *J* = 6)	17.1 (*d*, *J* = 46) 20.1 (*d*, *J* = 47) 20.5 (*d*, *J* = 4) 21.5 27.6 27.8 29.3 (*d*, *J* = 15) 30.6 41.1 (*d*, *J* = 6)
Tertiary Carbons	107.8 118.5	109.1 120.9
Quaternary Carbons	-	112.4 (*q*, *J* = 321)

Table 4.15: IR assignment of ionic liquids [16a-b].

	[16a]	**[16b]**
SO_2 (cm^{-1})	-	1351 1196

4.4.1.2 ^{1}H NMR characterisation of ionic liquids [16a-b]

From Figure 4.25 the characteristic coupling of the phosphorus is observed with the multiplet and doublet of triplets at 3.21 and 4.41 ppm respectively. These signals correspond to the hydrogen atoms of the ethyl linkage between the positive phosphorus centre and the pyrrole ring. Like the previous phosphonium salts, it can be seen that the anionic species has an effect on the chemical shifts of the ^{1}H NMR signals (Figure 4.25), in particular the signals for the H atoms directly adjacent to the positive centre and also that of the protons adjacent to the N atom. However, this effect does not appear to be as large as that of the alkyne ionic liquids in Section 4.3.2.2. When the chloride anion is exchange for the bis(triflimide) anion, chemical shifts of 2.17 - 1.98 ppm, 3.32 – 2.77 ppm, and 4.41 – 4.26 ppm for signals denoted as (9), (10), and (11) in Figure 4.24 are obtained demonstrating a shift upfield in the ^{1}H NMR spectra as the nucleophilicity of the anion decreases.

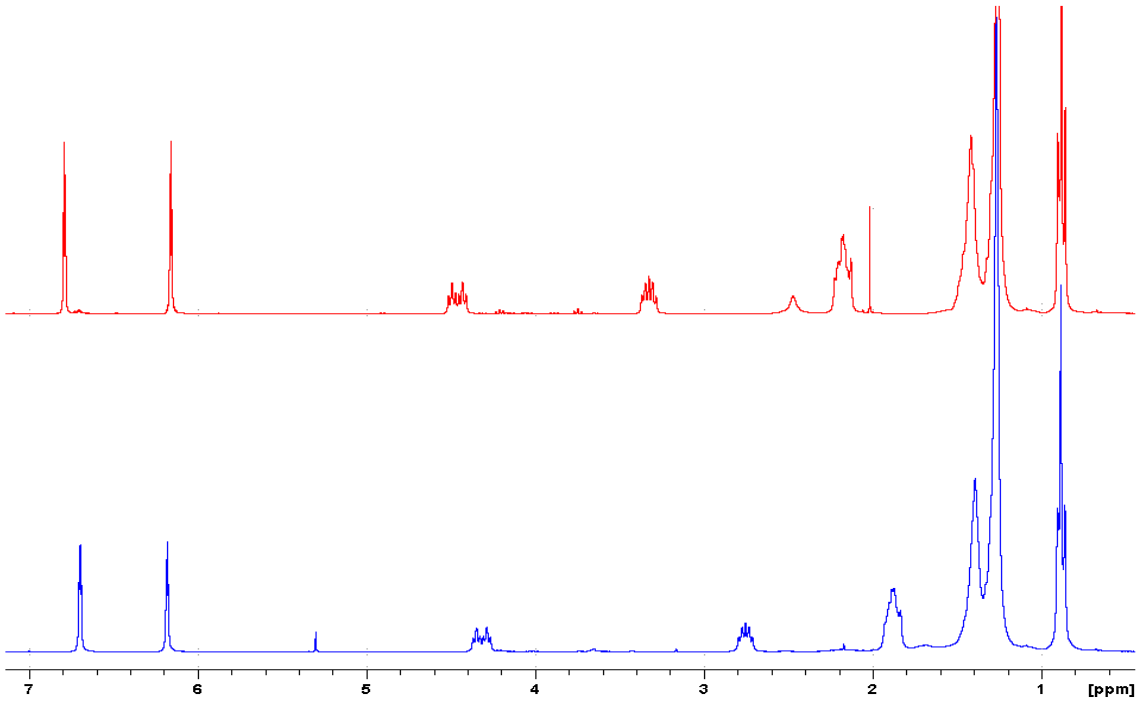

Figure 4.24: Anionic effect on the chemical shifts of the cationic protons using ionic liquids [16a] containing the chloride anion (-) and [16b] containing the bis(triflimide) anion.

4.4.1.3 ^{13}C NMR characterisation of ionic liquids [16a-b]

It can be seen that like the previous phosphonium ionic liquids mentioned in this chapter, the signals for carbon atoms which are three or more atoms away from the phosphorus centre are split into doublets. A representative ^{13}C NMR spectrum of [16a] is shown in Figure 5.26. One unusual feature that was observed was the difficulty in detecting the carbon signal of the ethyl chain directly adjacent to the phosphorus atom due to the low intensity compared to the octyl signals due to it being split and the relative abundance of the carbon atoms. This signal also tended to overlap with the signal denoted as (6) in Figure 4.24. Like the imidazolium ionic liquids and the previous phosphonium ionic liquids a minimal chemical shift is observed between anions, unlike that which is observed for their respective proton singles in the ^{1}H NMR.

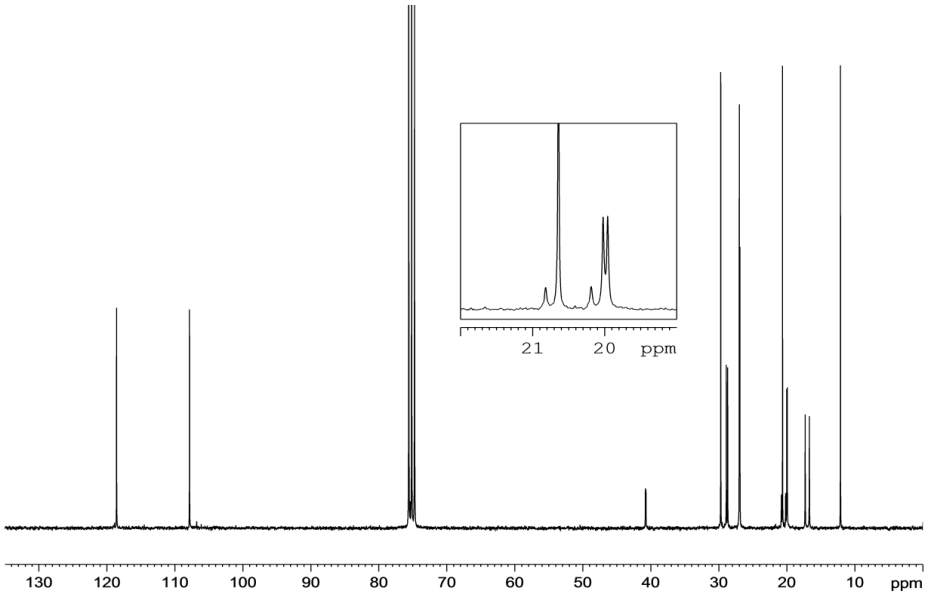

Figure 4.26: ^{13}C NMR spectrum of ionic liquid [16a] in $CDCl_3$.

4.4.2 Growth and characterisation pyrrole based ionic liquid polymers

Poly(pyrrole) is synthesised from a monomer pyrrole such as [16b] (scheme 4.5), whereby polymerisation occurs via the oxidation of the monomer. This oxidation results in the formation of a conjugated polymer chain with overlapping π-orbitals aswell as a positive charge along the backbone.[30] The poly(pyrrole) can be doped whereby an anion is incorporated into the polymer in order to balance the positively charged polymer backbone. This process includes the formation of polarons and bipolarons. A polaron (Scheme 4.5(a)) forms via the removal of an electron from the polymer backbone. When this process is allowed to further oxidise a bipolaron is formed

(Scheme 4.5(b)).[31,32] The formation of poly(pyrrole) can be performed both by the use of an oxidising agent or potentiostatically on an electrode surface.[26,28,33]

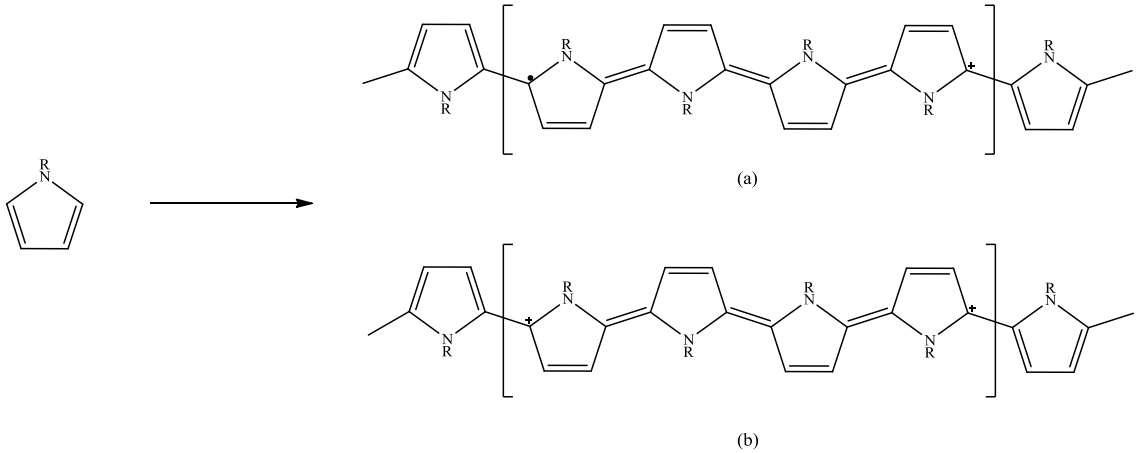

Scheme 4.5: Formation of functionalised poly(pyrrole) from functionalised pyrrole monomer with the polymer in (a) polaron form, (b) bipolaron form, where R = ionic liquid moiety.

The polymer of [16b] was grown potentiostatically by a colleague from the research group, Niall McGuinness, due to his experience in growing polypyrrole films on electrodes in organic media. Electrochemcial deposition of [16b] (0.02 M) was first attempted on a Au (4 mm) substrate using lithium perchlorate as the electrolyte (0.10 M) in anhydrous acetonitrile (2 cm^3). The reference electrode employed was a $Ag/AgNO_3$ which is equal to NHE (Normal Hydrogen Electrode) reference +0.544 V, while the counter electrode employed was a platinum (Pt) wire with a mesh attached. Argon (Ar) gas was bubbled through the solution for 15 min. The electroactivity of the monomer was first investigated using cyclic voltammetry and the peak oxidizing potential was determined to be 1.300 V vs. $Ag/AgNO_3$. So as to reduce the amount of over oxidation of the resulting polymer film, an oxidizing potential of 1.250 V vs. $Ag/AgNO_3$ was applied to the system. Overoxidation is common with the growth of polypyrrole films.[31,32] This potential was applied for 30 min until a charge density of 3.936 C cm^{-2} was obtained. An adherent film with complete coverage did not form on the Au substrate but polymer was observed to form at the electrode during polymerization. This brown/black polymer which formed at the electrode did not adhere to the substrate but remained floating in the electrochemical solution. The experiment was repeated utilizing a glassy carbon (4 mm) (GC) working electrode. A potential of 1.250 V vs. $Ag/AgNO_3$ was applied for 20 min until a charge density of 0.131 C cm^{-2} was consumed. No polymer was observed on the substrate and little polymer was formed in solution. Next electrochemcial deposition of [16b] (0.02

M) was attempted on a Au substrate using tetrabutylammonium hexafluorophosphate (0.10 M) as the electrolyte in anhydrous acetonitrile (2 cm^3). Argon gas was bubbled through the solution for 15 min. The electroactivity of the monomer was first investigated using cyclic voltammetry (Figure 4.27) and the peak oxidizing potential was determined to be 1.275 V vs. $Ag/AgNO_3$. So as not to overoxidize the film an oxidizing potential of 1.250 V vs. $Ag/AgNO_3$ was applied to the system. This potential was applied for 30 min until a charge density of 3.120 C cm^{-2} was obtained. An adherent film with good coverage was observed to form on the Au substrate. The growth of the polymer during the course of the experiment was monitored by recording the current formed as a function of time. The current-time plot is given in Figure 4.28(a). The trough and crest (current density maximum) at the beginning of the current-time plot (approximately t = 20 s) represent the nucleation of polymer sites on the electrode surface and the beginning of interference during diffusion of oligomer to the nucleation sites caused by the growth of the nucleation site.

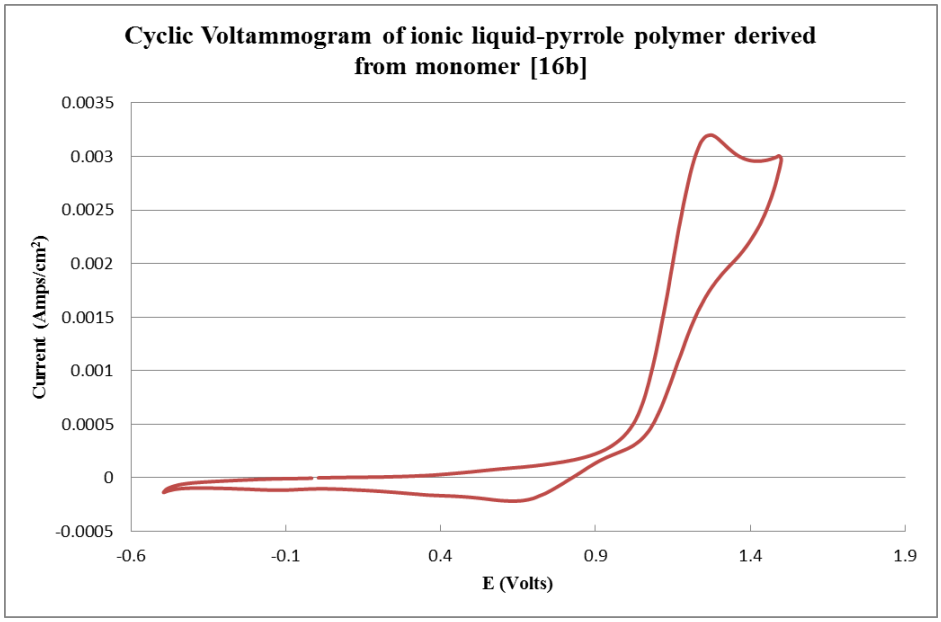

Figure 4.27: Cyclic voltammogram of an ionic liquid-pyrrole film electrosynthesised at 1.250 V vs. $Ag/AgNO_3$ from a monomer solution containing [16b] (0.02 M), tetrabutylammonium hexafluorophosphate (0.10 M) in anhydrous acetonitrile (2 cm^3) under bubbled Argon.

The growth of the polymer was confirmed by visual inspection of the electrodes surface on which a black polymer was observed to have formed. The resulting SEM micrographs of the surface are presented in Figure 4.28 (b) and (c). From these micrographs a clear difference in morphology can be observed than that observed in

unfunctionalised chloride doped pyrrole which displays typical "cauliflower" morphology. The pyrrole-ionic liquid polymer appears quite smooth with thin striations visible at higher magnifications.

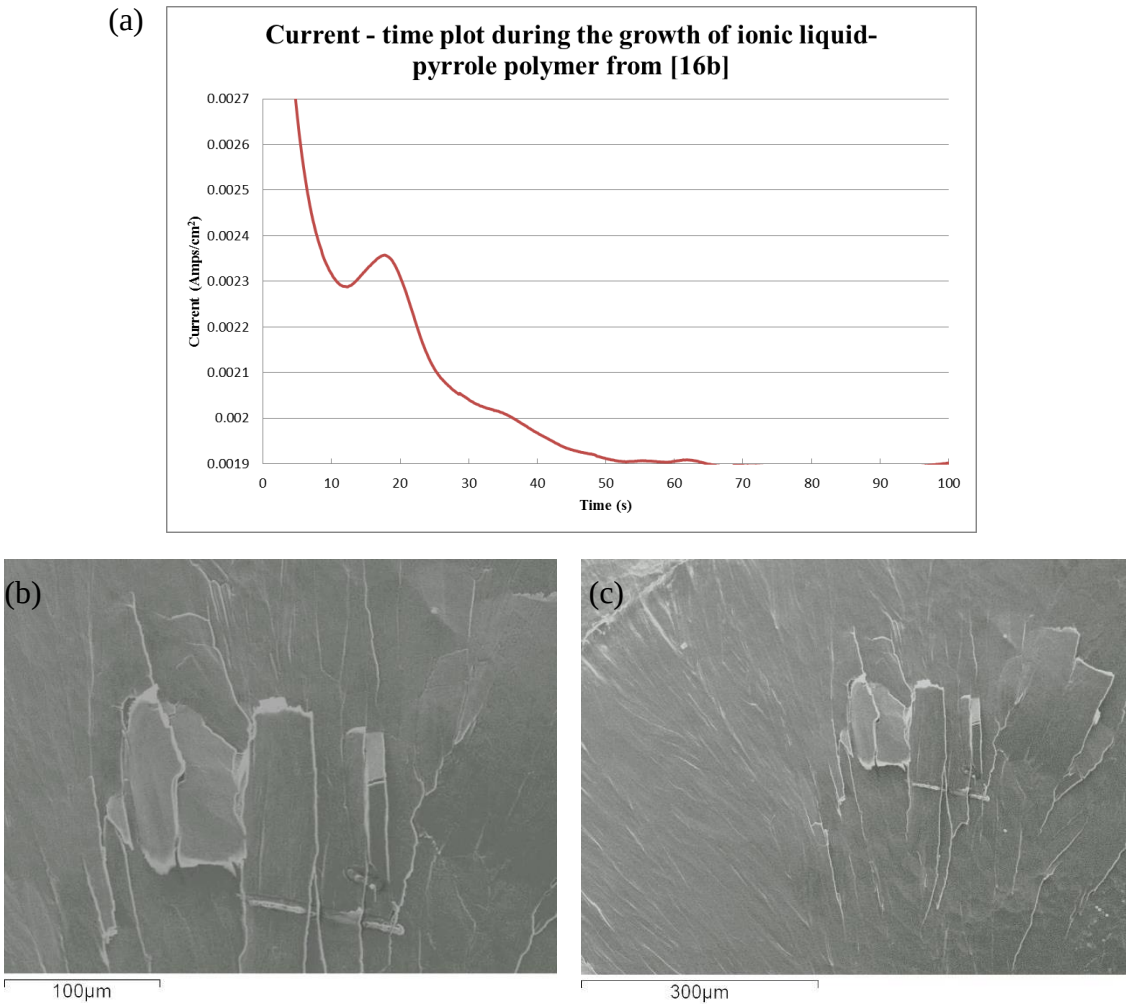

Figure 4.28: (a) Current time plot during the growth of an ionic liquid-pyrrole film electrosynthesised at 1.250 V vs. Ag/$AgNO_3$ from a monomer solution containing [16b] (0.02 M), tetrabutylammonium hexafluorophosphate (0.10 M) in anhydrous acetonitrile (2 cm^3) under bubbled Argon, (b) SEM micrographs of pyrrole-ionic liquid polymer doped with lithium hexafluorophosphates at × 350 magnification and (c) × 180 magnification.

4.5 Conclusions

The ionic liquids [12a] - [16b] were successfully synthesised and fully characterised using NMR, IR spectroscopy and mass spectrometry. The main issue that arose during the synthesis was the generation of the oxidised form of the trioctylphosphine which has been a problem encountered by several research groups and proved troublesome to remove. Although washes of the chloride precursors were successful at removing the

trioctylphosphine oxide, yield had to be sacrificed during this purification step. It was further found that extraction of the product using acetonitrile from warm hexane was also successful in the removal of the oxide without having a negative impact on yields.

Chemical shifts values for the signals relating to the hydrogen atoms near the phosphonium centre were shown to be dependant on the anion. In particular the position of the signals relating to the α hydrogens shifted upfield in the ^{1}H NMR as the cation anion interaction decreased in strength. This was observed with all five cations observed in Chapter 4. The phosphorus atom also resulted in splitting of both the hydrogen and carbon atoms signals in both the ^{1}H NMR and ^{13}C NMR where the distance between the atoms is no longer than 3 bond lengths.

Attempts to form phosphonium ionic liquids containing terminal azide based chains had limited success. Difficulties arose due to the inability to prevent quaternisation of the phosphonium at both ends of the di-halide chains resulting in a di-cationic species. While switching to a hetero-dihalide species, did result in the formation of some of the desired monoquaternised species, it was not possible to isolate the monoquaternised phosphonium salt to be isolated form the diquaternised species. On a more positive note incorporation of alkyne units onto the ionic liquids proved successful and as such could potentially be reacted with azide functionalised polymers.[34]

There was also success in generating polymers containing ionic liquids moieties. Generation of pyrrole monomers via functionalisation of the N site proved successful and was successfully polymerised onto an electrode. Polymerisation of this monomer could also be performed via chemical oxidation using $FeCl_3$. Chemical oxidation would enable the polymer to be produced on a much larger scale which potentially could be used in the area of gas absorption.

4.6 References

(1) Ramirez, R. E.; Sanchez, E. M. *Solar Energy Materials and Solar Cells* **2006**, *90*, 2384.

(2) Ferguson, L.; Scovazzo, P. *Industrial & Engineering Chemistry Research* **2007**, *46*, 1369.

(3) Zhang, Y.; Zhang, S.; Lu, X.; Zhou, Q.; Fan, W.; Zhang, X. *Chemistry-a European Journal* **2009**, *15*, 3003.

(4) Gurkan, B. E.; de la Fuente, J. C.; Mindrup, E. M.; Ficke, L. E.; Goodrich, B. F.; Price, E. A.; Schneider, W. F.; Brennecke, J. F. *Journal of the American Chemical Society* **2010**, *132*, 2116.

(5) Kagimoto, J.; Taguchi, S.; Fukumoto, K.; Ohno, H. *Journal of Molecular Liquids* **2010**, *153*, 133.

(6) Del Sesto, R. E.; Corley, C.; Robertson, A.; Wilkes, J. S. *Journal of Organometallic Chemistry* **2005**, *690*, 2536.

(7) Cieniecka-Roslonkiewicz, A.; Pernak, J.; Kubis-Feder, J.; Ramani, A.; Robertson, A. J.; Seddon, K. R. *Green Chemistry* **2005**, *7*, 855.

(8) Kosmulski, M.; Gustafsson, J.; Rosenholm, J. B. *Thermochimica Acta* **2004**, *412*, 47.

(9) Tsunashima, K.; Sugiya, M. *Electrochemistry Communications* **2007**, *9*, 2353.

(10) Esperanca, J.; Guedes, H. J. R.; Blesic, M.; Rebelo, L. P. N. *Journal of Chemical and Engineering Data* **2006**, *51*, 237.

(11) Adamova, G.; Gardas, R. L.; Nieuwenhuyzen, M.; Puga, A. V.; Rebelo, L. P. N.; Robertson, A. J.; Seddon, K. R. *Dalton Transactions* **2012**, *41*, 8316.

(12) Adamova, G.; Gardas, R. L.; Rebelo, L. P. N.; Robertson, A. J.; Seddon, K. R. *Dalton Transactions* **2011**, *40*, 12750.

(13) Zhang, J.; Zhang, S.; Dong, K.; Zhang, Y.; Shen, Y.; Lv, X. *Chemistry-a European Journal* **2006**, *12*, 4021.

(14) Myers, C.; Pennline, H.; Luebke, D.; Ilconich, J.; Dixon, J. K.; Maginn, E. J.; Brennecke, J. F. *Journal of Membrane Science* **2008**, *322*, 28.

(15) Liu, J.; Liu, H.; Wang, L. *Applied Organometallic Chemistry* **2010**, *24*, 386.

(16) Noack, K.; Schulz, P. S.; Paape, N.; Kiefer, J.; Wasserscheid, P.; Leipertz, A. *Physical Chemistry Chemical Physics* **2010**, *12*, 14153.

(17) Shah, S.; Protasiewicz, J. D. *Coordination Chemistry Reviews* **2000**, *210*, 181.

(18) Visser, A. E.; Swatloski, R. P.; Reichert, W. M.; Mayton, R.; Sheff, S.; Wierzbicki, A.; Davis, J. H.; Rogers, R. D. *Chemical Communications* **2001**, 135.

(19) Bates, E. D.; Mayton, R. D.; Ntai, I.; Davis, J. H. *Journal of the American Chemical Society* **2002**, *124*, 926.

(20) Hanioka, S.; Maruyama, T.; Sotani, T.; Teramoto, M.; Matsuyama, H.; Nakashima, K.; Hanaki, M.; Kubota, F.; Goto, M. *Journal of Membrane Science* **2008**, *314*, 1.

(21) McGuinness, N., NUI Maynooth, 2013.

(22) Negishi, E.; Boardman, L. D.; Sawada, H.; Bagheri, V.; Stoll, A. T.; Tour, J. M.; Rand, C. L. *Journal of the American Chemical Society* **1988**, *110*, 5383.

(23) Claridge, T. D. W. *High-Resolution NMR Techniques in Organic Chemistry*; Elsevier Science Serials, 1999.

(24) Anthony, J. L.; Anderson, J. L.; Maginn, E. J.; Brennecke, J. F. *Journal of Physical Chemistry B* **2005**, *109*, 6366.

(25) Goodrich, B. F.; de la Fuente, J. C.; Gurkan, B. E.; Lopez, Z. K.; Price, E. A.; Huang, Y.; Brennecke, J. F. *Journal of Physical Chemistry B* **2011**, *115*, 9140.

(26) Andreoli, E.; Rooney, D. A.; Redington, W.; Gunning, R.; Breslin, C. B. *Journal of Nanoscience and Nanotechnology* **2012**, *12*, 338.

(27) McCarthy, C. P.; McGuinness, N. B.; Alcock-Earley, B. E.; Breslin, C. B.; Rooney, A. D. *Electrochemistry Communications* **2012**, *20*, 79.

(28) McCarthy, C. P.; McGuinness, N. B.; Carolan, P. B.; Fox, C. M.; Alcock-Earley, B. E.; Breslin, C. B.; Rooney, A. D. *Macromolecules* **2013**, *46*, 1008.

(29) Ryan, E. M.; Breslin, C. B.; Moulton, S. E.; Wallace, G. G. *Electrochimica Acta* **2013**, *92*, 276.

(30) Heeger, A. J. *Synthetic Metals* **2001**, *125*, 23.

(31) Feast, W. J.; Tsibouklis, J.; Pouwer, K. L.; Groenendaal, L.; Meijer, E. W. *Polymer* **1996**, *37*, 5017.

(32) Toshima, N.; Hara, S. *Progress in Polymer Science* **1995**, *20*, 155.

(33) Benhaddad, L.; Bernard, M. C.; Deslouis, C.; Makhloufi, L.; Messaoudi, B.; Pailleret, A.; Takenouti, H. *Synthetic Metals* **2013**, *175*, 192.

(34) Chen, G.; Tao, L.; Mantovani, G.; Ladmiral, V.; Burt, D. P.; Macpherson, J. V.; Haddleton, D. M. *Soft Matter* **2007**, *3*, 732.

Chapter 5:

Investigation of Ionic Liquids as Carbon Dioxide Capture and Separating Materials

5.1 Introduction

In this chapter work will be presented on the potential of ionic liquids as CO_2 absorption and separation materials. Two differing approaches will be adapted to achieve each of these goals. In terms of the CO_2 sequestration studies, this will be achieved via the use of membranes which have been impregnated with ionic liquids through which CO_2 and N_2 gases will be passed using an "in house" custom built rig. The aim of this investigation is to determine if these gases permeate through these modified Supported Ionic Liquid Membranes (SILM) at different rates and thus, in principle facilitate the separation of these gases. The results of this comparative study will form the basis of the first part of this chapter.

Results presented in the second part of this chapter pertain to investigations into amino acid functionalised ionic liquids and the potential of these liquids as CO_2 sorbents. This was achieved via the impregnation of a mesoporous silica (MCM-41) with these ionic liquids which are capable of forming covalent bonds with CO_2 thus preventing it from entering the atmosphere. This CO_2 absorption was monitored using mass spectrometry using a rig built in the Materials and Surface Science Institute (MSSI) at the University of Limerick.

5.2 Supported ionic liquids membranes

The work presented in this section pertains to the study of the permeability of gases (CO_2 and N_2) through membranes impregnated with ionic liquids. This involves the impregnation of the pores in a solid support, such as a membrane with an ionic liquid. The use of "liquid membranes" in carbon sequestration technologies has been the focus of much investigation due to faster diffusion of a gas through a liquid than through a solid, thus increasing permeability values.[1-4] However many issues still arise from membrane technology such as fouling of the membrane, instability of the impregnated solvent under various environments, and elevated temperatures. To combat these problems, ionic liquid technology is currently being examined as a possible replacement for these solvents due to their favourable properties which are outlined in Chapter 1, such as negligible vapour pressure, and due to the large solubility of CO_2 in ionic liquids.[4-6]

This chapter contains various studies that influence the permeability of the gases through the supported ionic liquid membranes and attempts to optimise these values by

modification of the environment and supports. Approximate values for the permeability (Barrer) of CO_2 and N_2 through the SILMs were determined using Equation 5.1,[7]

$$P = \frac{(273 \times 10^7)Vl(\delta p/\delta t)}{76\Delta pAT} \qquad \text{(Equation 5.1)}$$

Where V is the permeate volume, l is the thickness of the membrane, (δp/δt) is the rate of change of pressure in the permeate vessel, Δp is the pressure difference over the membrane, A is the area of the membrane, T is the temperature applied to the membrane, and 1 Barrer = 10^{-10} cm^3(STP) cm cm^{-2} s^{-1} $cmHg^{-1}$. Using these data the selectivity of the gases was determined by obtaining a ratio of the permeabilities as shown in Equation 5.2.[7-10]

$$\alpha_{A/B} = \frac{P_A}{P_B} \qquad \text{(Equation 5.2)}$$

The diffusion coefficients of the gases were determined using the time lag data. The lag time was determined from the time intercept of the linear extrapolation of the steady state permeation data graph with the x-axis (time). The diffusion coefficients of gases were then calculated using Equation 5.3, known as the Daynes-Barrer equation where θ is the lag time, and l is the membrane thickness which assumes that the diffusion coefficient does not depend on the concentration of diffusant.[11]

$$D = l^2/6\theta \qquad \text{Equation (5.3)}$$

From this the solubility coefficient of the gases was determined due to their relationship as outlined in Equation 5.4, where P is the permeability, D is the diffusion coefficient, and S is the solubility coefficient.[11]

$$P = D.S \qquad \text{(Equation 5.4)}$$

Variation in the driving forces, membrane areas, or the size of the permeate vessel, would all have an effect on the gas permeability values.[9] From the literature it was found that several different values are reported for the permeability of CO_2 for [1c] which was the standard liquid used in this study, with values of 1344.3 and 500.0 Barrer reported.[12,13] In Figure 5.1, it is evident from work reported by Gan *et al.* that increases in pressure of the gas in the feed vessel result in dramatic increases in permeability of many gases.[14,15] This proves problematic due to the lack of reporting of the feed vessel

pressure which makes direct comparison between the system reported in this thesis and literature values difficult. As can be observed from Figure 5.1, permeability of CO_2 reduces significantly at low pressure differentials.[14] Therefore it might be expected that values of CO_2 and N_2 through the membranes in the present study might be expected to be low as the feed pressure was set at 1 bar.[14]

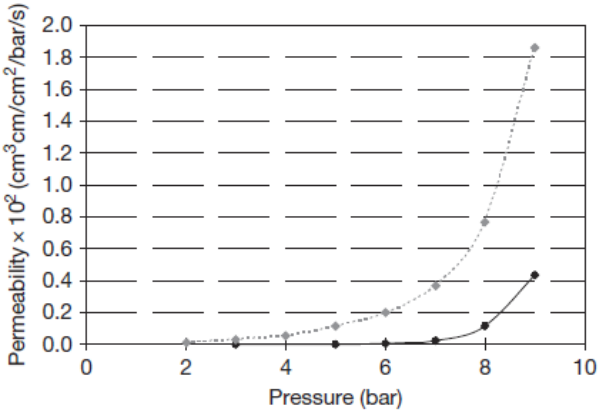

Figure 5.1: Effect of feed pressure on the permeability of CO_2 (dashed line) and N_2 (solid line) through BMIM Tf_2N [1c] supported ionic liquid membrane.[15]

5.2.1 Characterisation of supported ionic liquid membranes

In Chapter 2, it was mentioned that supported ionic liquid membranes (SILM) were fabricated via the application of ionic liquid onto a porous membrane with the excess blotted off to yield impregnated membrane.[16,17] The method is consistent with those outlined in the literature. PES was the support used for the majority of the study. The SILMs were characterised via a number of different methods such as IR, SEM, EDX, and membrane weight change. IR is by far the most useful technique due to the ease of identification of bands due to the functional groups associated with the ionic liquids from bands associated with the polymer. The infra-red spectra of the pristine PES modified membrane, neat ionic liquid [10a], and then the SILM are presented in Figure 5.2. The most distinguishable signals of the PES polymer support are the symmetric and asymmetric stretches of the sulfonyl groups at 1322 cm^{-1} and 1150 $cm^{-1}$and the C=C stretch due to the aromatic ring at 1577 cm^{-1} and 1486 cm^{-1}.[18] However, due to the presence of sulfonyl groups in the bis(triflimide) anion of some ionic liquids, it can be difficult to distinguish these from the bands of the sulfonyl groups of the PES membrane. When examining the ionic liquid IR spectrum, it is the signals due to the imidazole C-H stretch of the imidazole and other *N*-heterocylic rings signals present

from 2700-3300 cm^{-1} which are clearly distinguishable in comparison to the spectrum of PES. Therefore, when examining the spectra of the PES modified membranes these bands are clearly identifiable and it is evident that the ionic liquid is now incorporated into the pores of the PES polymer.

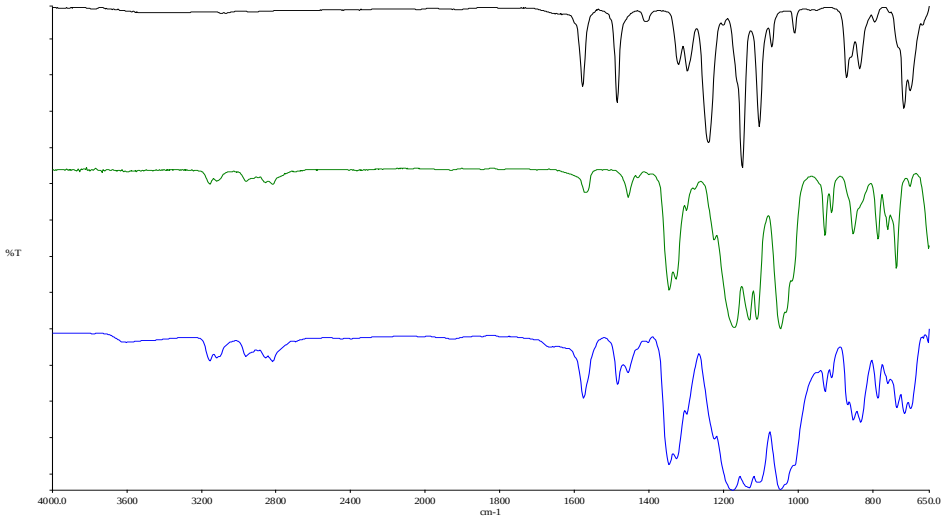

Figure 5.2: Infra-red spectra of polyethersulfone (-), ionic liquid 1-methyl-3-(morphol-4-yl)ethyl imidazolium bis(triflimide) (-), SILM(-).

The incorporation of the ionic liquid into the porous support can also be confirmed via the use of SEM and EDX. Due to the negligible vapour pressure of ionic liquids, it is possible to examine them under the SEM. There are stark differences when examining the morphology of both the pristine PES and SILM as highlighted in Figure 5.3. The pristine membrane clearly demonstrates a highly porous material, whereas in the case of the SILM, the ionic liquid [9a] can be clearly seen as it coats the membranes with a loss of porosity. There is also a lack of pore definition in the micrograph of the SILM when compared to that of the pristine membrane, indicating uptake of the liquid into the pores.

(a) (b)

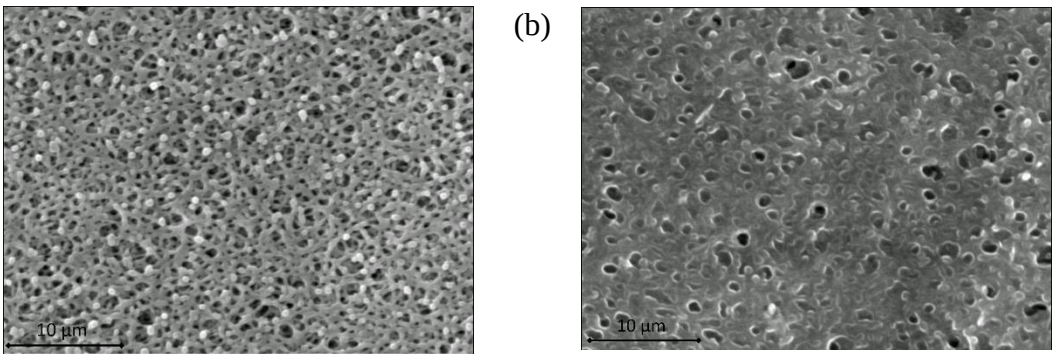

Figure 5.3: Scanning electron micrographs of (a) pristine PES membrane, and (b) a supported ionic liquid membrane modified with ionic liquid [9a].

EDX also proved quite useful when determining incorporation of the ionic liquid into the support. An obvious element to confirm incorporation of the ionic liquid is nitrogen in the EDX of the SILM, however this is extremely difficult due to the low atomic weight of nitrogen. Due to the presence of sulfur (S) atoms as part of the polymer support, it is also eliminated as a means of assessing incorporation of the liquid into the support. However, in the case of ionic liquids containing the Tf_2N^-, TFA^-, or $TFMS^-$ anion, EDX can be used to determine the presence of these ionic liquids due to the presence of the fluorine (F) atom which is easily detected due to its increased relative abundance in relation to the nitrogen atoms within each ionic liquid (Figure 5.4).[19]

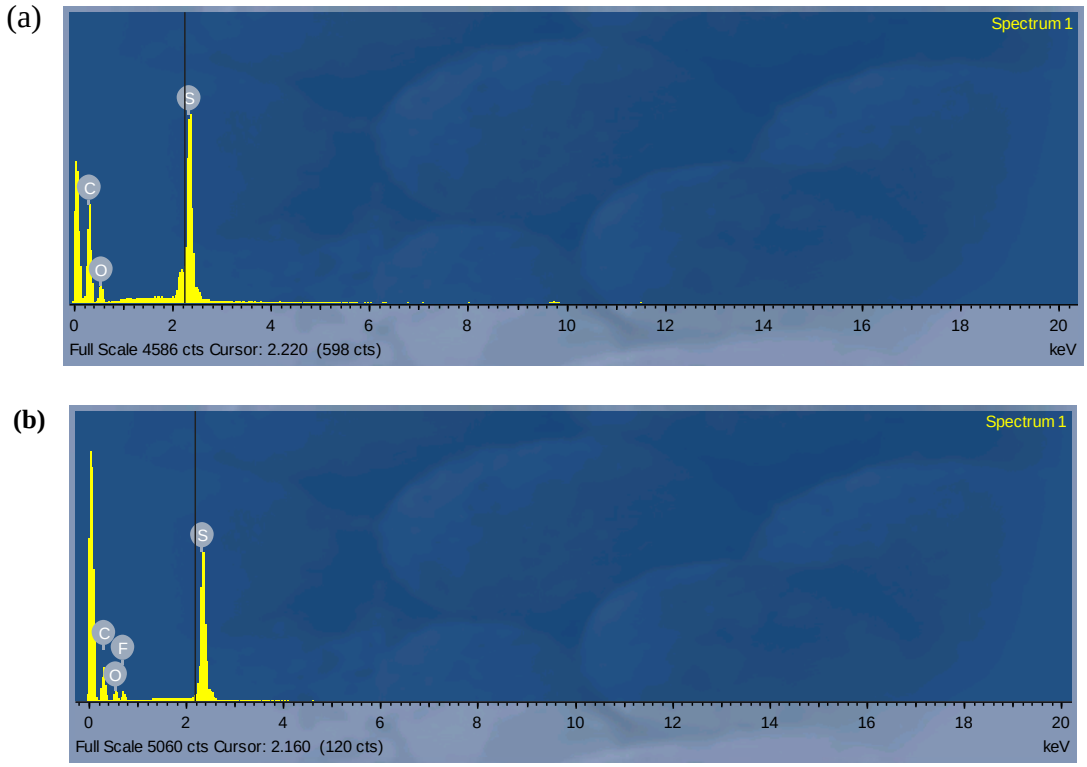

Figure 5.4: EDX spectrum of (a) pristine polyethersulfone membrane, and (b) polyethersulfone membrane impregnated with [9a].

5.3 Gas separation studies of ionic liquids

Presented in this section is the gas permeability studies of CO_2 and N_2 through PES membranes modified with ionic liquids [1c, 9a, 9c, 9d, 10a, and 11a] containing the bis(triflimide), dicyanamide, and trifluoroacetate anions. It is important to note that membranes tested in the absence of ionic liquids resulted in the immediate transfer of the gas to the permeate vessel, probably due to the microporous size pores of the membranes. This indicates that when the ionic liquid is present that it fills the pores of

the membrane which facilitates selective transport of the gas through the polymer. A standard ionic liquid [1c] was used to compare these results to literature reports. However for the rig that was built as part of the project, the permeability values for both CO_2 and N_2 for [1c] were approximately 10 times less than those reported for [1c] in the literature.[13] However due to both gases permeating slower by the same magnitude, CO_2/N_2 selectivity values matched those outlined in the literature and therefore this work focuses on the selectivity. These differences in permeability values most likely arise due to different pressure differentials or differences of the volume of the feed vessel, however due to the lack of reporting of these variables, a direct comparison with the literature values is not possible. Therefore the study presented is a preliminary screening investigation into the relative performance of the ionic liquids compared to each other. Selectivity (CO_2/N_2) values obtained do correspond well with the literature and as such these may be compared to previously published work. All SILMs were tested at 298 K and with a feed pressure differential of 1 bar unless otherwise stated.

5.3.1 Effect of anion variation on the permeability of CO_2 and N_2.

The effect of the anion on the permeability of both gases was determined utilising the 1-methyl-3-(piperid-1-yl)ethylimidazolium cation and the time lag method outlined in Chapter 2. The anions that were investigated as part of this study were the bis(triflimide) [9a], dicyanamide [9c], and trifluoroacetate [9d], each on a PES membrane (Figure 5.5). The saccharinate [9b] and trifluoromethanesulfonate [9e] anions were discounted due to the high viscosity experienced with [9b] and the formation of a low melting solid with [9e]. From the resulting experiments it was determined that the anion species had a significant effect on the permeability of CO_2 through the membranes. Significantly higher permeability values were obtained for [9a] which contains the bis(triflimide) anion, than those obtained for [9c] (dicyanamide anion) and [9d] (trifluoroacetate anion). The trend in these results was to be expected from reports of other ionic liquids in the literature. In a review presented by Scovazzo *et al.* whereby much of the research into gas permeabilities data were compiled,[13] variation of the anion in conjunction with the 1-ethyl-3-methylimidazolium cation resulted in the following general trend in CO_2 permeability, $Tf_2N^- > OTf^- \approx DCA^- > BF_4^-$, with values of 1702.4, 1171.4, 1237.0, and 968.5 Barrer, respectively.[13] This trend has also been observed in other research groups such as Jindaratsamee *et al.* where they observed the same effect using the BMIM cation with the BF_4^-, OTf^-, Tf_2N^-, DCA^-,

and PF_6^- anions on a polyvinylidene fluoride membrane support. This was also observed by Neves *et al.* using some of the ionic liquids investigated by Jindaratsamee *et al*.[6,20]

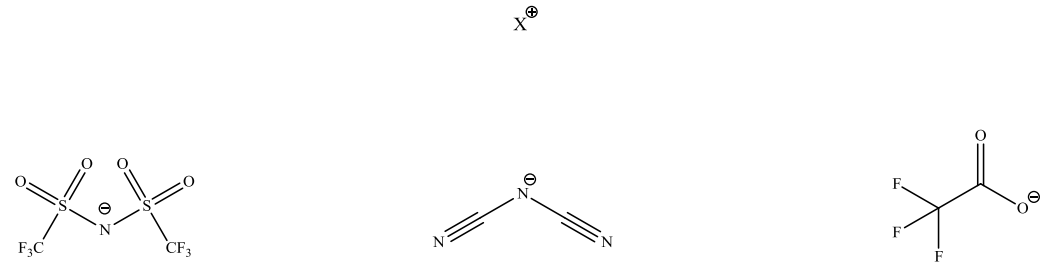

[9a] [9c] [9d]

Figure 5.5: Structures of the anions used as part of the SILM permeability studies, X = 1-methyl-3-(piperid-1-yl)ethylimidazolium cation.

From Figure 5.6(a), the values of the CO_2 permeabilities of [9a], [9c], and [9d], are determined to be 58.6, 10.1 and 7.4 Barrer at 298 K using a pressure differential of 1 bar. The higher CO_2 permeability of [9a] can be explained due to the presence of the sulfonyl groups on the anion which undergo weak Lewis acid Lewis base interactions therefore increasing the affinity of the liquid for CO_2.[21] The viscosity of the ionic liquids is also an important consideration when determining permeabilities, as an increase in viscosity generally tends to lead to a decrease in permeability. As discussed in Chapter 1, many of the physical and chemical properties of ionic liquids are anion dependent in the absence of a targeted functional group. The delocalisation of the charge density on the bis(triflimide) anion can result in lower melting points and it can have an effect on the viscosity producing less viscous liquids due to weaker cation – anion interactions.[22,23] Fluorination is also widely accepted to have a beneficial effect on CO_2 permeability although the exact cause of why this occurs is the source of much discussion.[24-26] One theory proposed by Cece *et al.* is that dipole-dipole interactions occur between the negatively charged fluorine, and the positively charged carbon atom of CO_2 resulting in an increase in solubility when compared to the corresponding non-polar hydrocarbon analogue.[26] It has also been observed that increasing the number of CF_3 groups on the anion results in increased CO_2 solubility in the ionic liquids which occurs in the bis(triflimide) anion.

(a)

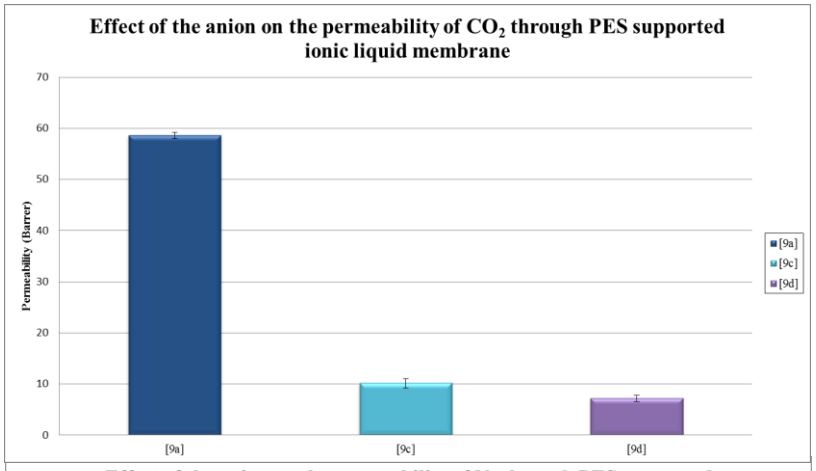

(b)

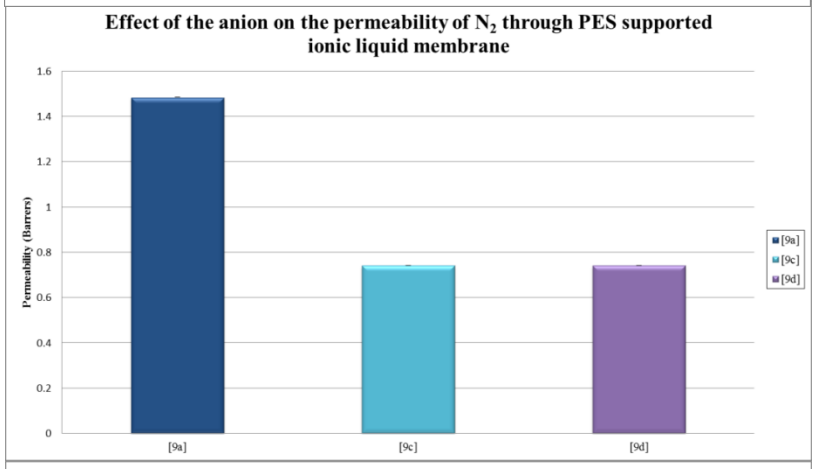

(c)

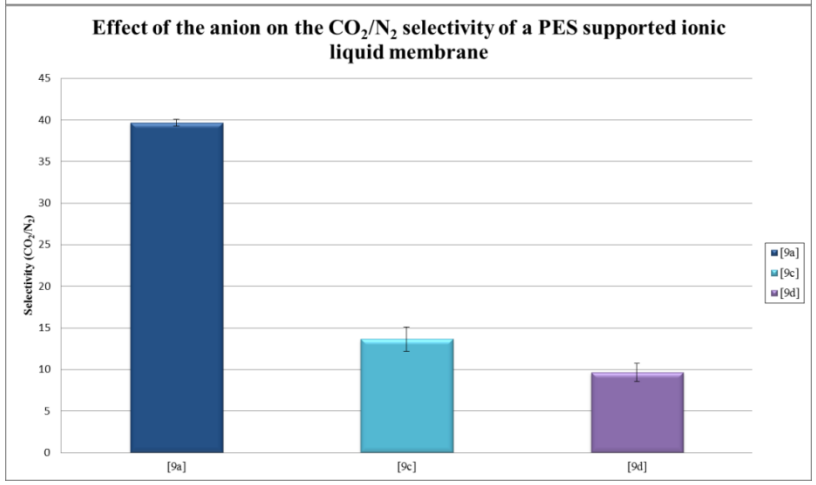

Figure 5.6: Effect of the anion species on (a) CO_2 permeability, (b) N_2 permeability, and (c) CO_2/N_2 selectivity of ionic liquids on PES support (n=3).

Permeability values for N_2 are widely reported to be quite low in comparison to CO_2 values in ionic liquids, which is an attractive property when looking at gas separation technology.[2,8,27-29] This trend was also seen with the ionic liquids investigated in this study, with the permeability values of the N_2 in all 3 ionic liquids significantly lower than the CO_2 as shown in Figure 5.6(b), with values of 1.4, 0.8 and 0.8 Barrer for liquids [9a], [9d], and [9e], respectively. These are as a result of a lack of favourable

interactions to aid in the dissolution of the inert, non-polar N_2 gas in the polar ionic liquids. A small anionic effect is evident which is most likely due to the lower viscosity of [9a] resulting in less resistance for the N_2 gas molecule to diffuse across the membrane.

It can be observed from examining Figure 5.6(c) that in this study that CO_2 permeability is the major contributing factor towards achieving good CO_2/N_2 selectivity with [9a] exhibiting both the largest CO_2 permeability and also the largest CO_2/N_2 separation value of 39, in comparison to values obtain for [9c] and [9d] of 13 and 9, at 298 K. These selectivity values again indicate that the anion has a large effect on the gas permeability properties of the ionic liquid and the ability to tune the ionic liquid for the specific task. In the report mentioned earlier by Scovazzo *at al.* giving data on the 1-ethyl-3-methylimidazolium cation, a different trend for CO_2/N_2 selectivity was observed than that of this study. Selectivity values of 23, 56, and 40 were reported using the bis(triflimide), dicyanamide, and trifluoroacetate anions.[13] This highlights that it is not simply one factor such as choice of anion which controls CO_2/N_2 selectivity. There are several reasons why a different CO_2/N_2 selectivity trend may occur. Firstly smaller alkyl chain lengths on the imidazolium cations can result in a much less viscous set of liquids. This would make CO_2 more permeable through the liquid which would help increase selectivity. Also, the cation used in our anionic study has a piperidine ring at the terminal carbon atom of an ethyl chain. Tertiary amines have been shown to reduce CO_2 permeability so this may account for the trends observed during this study.[10]

The results from the permeability studies can be further explained by examining the diffusion coefficients and solubility coefficients of the gases. It can be observed from Figure 5.7(a), that the anion had a significant effect on the diffusion coefficient of CO_2. Diffusion coefficients of CO_2 is greatest in ionic liquid [9a] with a value of 0.68×10^{-6} cm^2/s being observed, while significantly lower values of 0.37×10^{-6} cm^2/s and 0.37×10^{-6} cm^2/s were determined for [9c] and [9d], respectively, at 298 K. This can be partly explained by examining the viscosity of the ionic liquids. Ionic liquid [9a] exhibited one of the lowest viscosity values of the ionic liquids tested with a value of 115.0 mPa.s. This is consistent with literature reports that viscosity is related to the permeability of the gases.[30,31] Diffusivities of gases in solvents are determined by the Stokes – Einstein equation as shown in Equation 5.5, where T is absolute temperature, μ

is the viscosity of the solvent and V is the molar volume. From this is can be determined that diffusion of gases in ionic liquids is inversely proportional to ionic liquid viscosity. The Stokes-Einstein equations appears to be valid for use in ionic liquid systems due to the work reported by Ferguson *et al.* on phosphonium based ionic liquids.[32]

$$D \approx {}^{T}\Big/_{(\mu \bar{V}^{1/3})} \qquad \text{(Equation 5.5)}$$

However, it is clear from our results that viscosity is not the only factor in determining permeability of gases through the SILMs. CO_2 and N_2 permeability values were similar for [9c] and [9d] despite the large variation in viscosity with values of 91.3 mPa.s, and 3654.3 mPa.s observed for [9c] and [9d]. One consideration is highlighted in the work mentioned previously by Ferguson *et al.* in which they observed that the structure of the ionic liquid had a major impact on the diffusion of CO_2 through the ionic liquid.[32] Comparisons of the CO_2 permeability values using phosphonium and imidazolium ionic liquids of similar viscosities did not result in similar permeability values. This was attributed to the movement of aliphatic chains which create pockets allowing for more rapid diffusion of the gas through the phosphonium ionic liquid.[32]

Solubility of CO_2 in the ionic liquid would be expected to have a significant effect on its diffusion coefficients and permeability. From Figure 5.7(b), it is evident that variation of the anion has an effect on the solubility coefficient of CO_2 in the ionic liquid with values ranging from 0.085 cm^3(STP)/cm^3cmHg for [9a], to 0.020 cm^3(STP)/cm^3cmHg and 0.027 cm^3(STP)/cm^3cmHg for [9c] and [9d], respectively, at 298 K. This variation in solubility coefficients due to a change in anion species is a trend that has been widely documented in the literature.[20,33-35] As mentioned earlier in this section, the sulfonyl groups are known to increase the solubility of CO_2 in the ionic liquid but it can also be determined from the anionic study that fluorination did not achieve a major increase in CO_2 solubility coefficients. The liquid [9a] is both a fluoroalkyl and sulfonated anion, whereas [9d] is only a fluoroalkyl anion. CO_2 solubility cofficients in [9d] is 3.5 times less than [9a] thus indicating that the sulfonation of the anion has the larger effect. These results are consistent with the observation that weaker cation-anion based interactions result in higher CO_2 solubility values, as it is proposed in the literature these allow expansion of the lattice, producing more space to accommodate CO_2.[35,36]

(a)

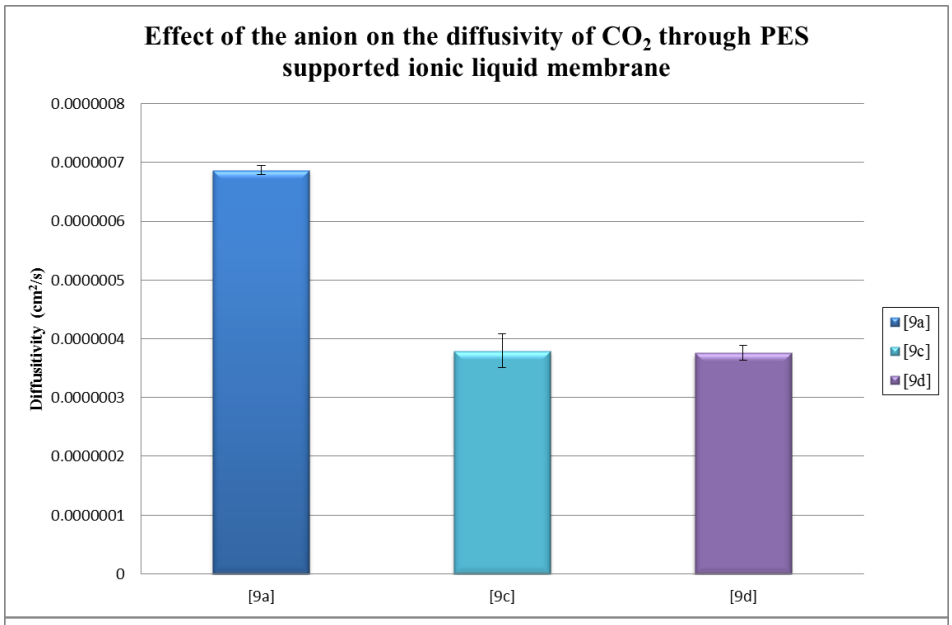

(b)

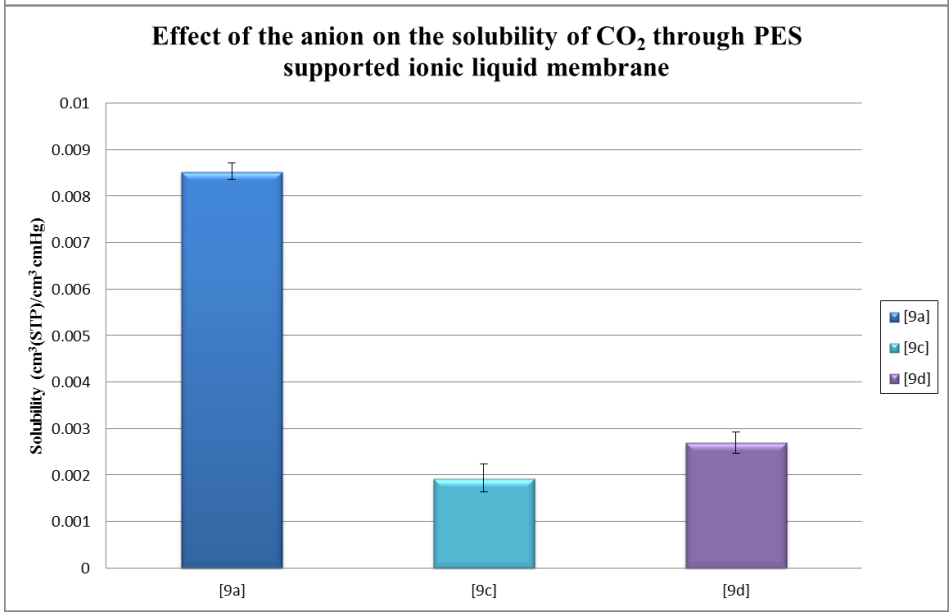

Figure 5.7: Effect of the anion on (a) the diffusion coefficients, and (b) the solubility coefficients of CO_2 in the ionic liquids at 298 K, (n = 3).

Unfortunately due to the slow permeation of N_2 through the membranes and the lack of a clearly defined lag phase, the diffusion coefficient of N_2 through the supported ionic liquid membrane, and in turn the solubility coefficient, could not be determined.[17] This problem has been reported in the literature and exists also for other slow permeating gases such as methane. Figure 5.8 compares the permeation profiles of CO_2 and N_2 in ionic liquid [10a].

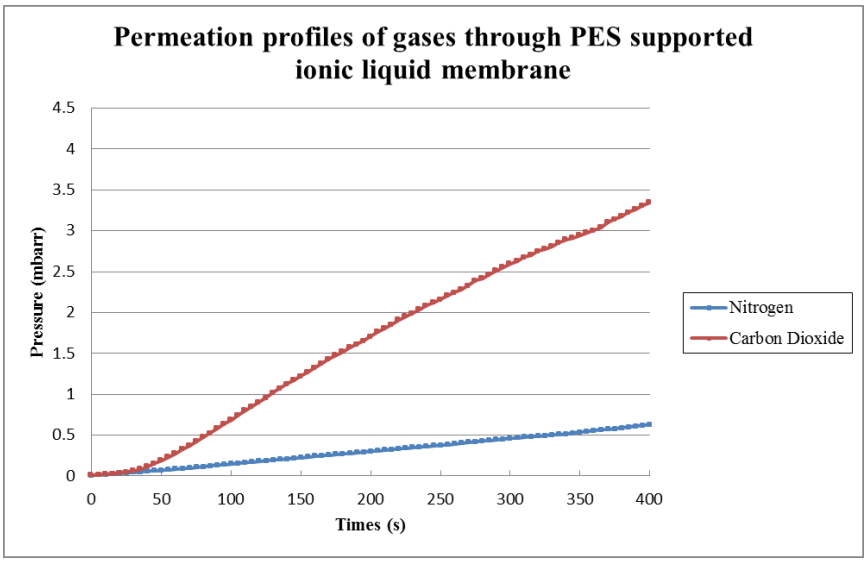

Figure 5.8: Permeation profiles of CO_2 and N_2 and the determination of the lag phase.

5.3.2 Effect of cation variation on the permeability of CO_2 and N_2.

The effect of the cation on the permeability of CO_2/N_2 through the SILM was determined via the use of three liquids all containing the bis(triflimide) anion with the following imidazolium based cations 1-butyl-3-methlimidazolium [1c], 1-methyl-3-(piperid-1-yl)ethylimidazolium [9a], 1-methyl-3-(morphol-4-y-l)ethylimidazolium [10a], and 1-methyl-3-(pyrrolid-1-yl)ethylimidazolium [11a] as shown in Figure 5.9.

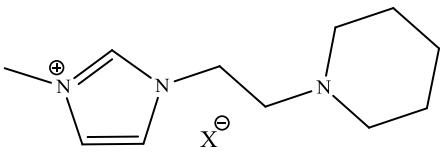

[9a]

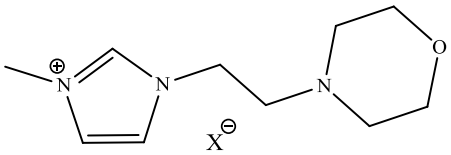

[10a]

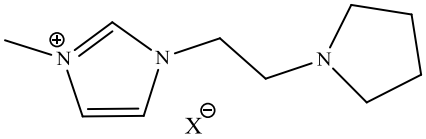

[11a]

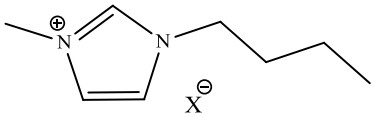

[1c]

Figure 5.9: Structures of the cations investigated as part of the permeability studies, X = Tf_2N^-.

In previous studies, it was demonstrated that variation of the cation had a small effect on the permeability of CO_2 through the ionic liquid.[13] These studies involved the ammonium based cations (Figure 5.10) and it was demonstrated that variation in the chain length had an effect on the permeability of CO_2 with a slight decrease in values observed until n > 8, thereafter values of CO_2 permeability decreased. The decrease at higher chain length was attributed to a reduction in the degrees of conformational freedom of the alkyl chain, increasing the ionic liquids viscosity and thus decreasing gas permeability values.[13] In these studies variation of the alkyl chain from 4-10 carbon atoms resulted in CO_2 permeability values of 830.4, 943.2 and 800.4 Barrer for the butyl, hexyl and decyl form respectively.[13,37]

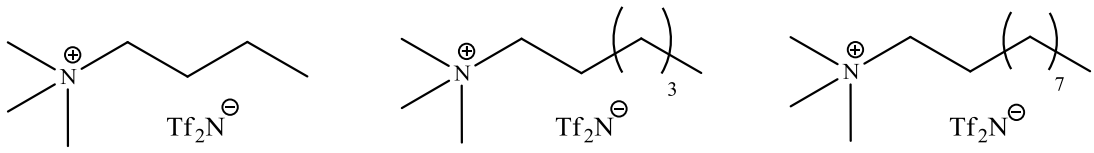

[N(4)111][Tf_2N] [N(6)111][Tf_2N] [N(10)111][Tf_2N]

Figure 5.10: Illustration of the ammonium ionic liquid cations used by Kilaru *et al.* in permeability studies.[37]

More recent work has focused on the tailoring of the ionic liquids towards gas separations via the use of polar groups and amines on the cation.[16] The use of a 1-(3-aminopropyl)-3-methylimidazolium cation (APMIM) on a nylon membrane at lower temperatures resulted in slower CO_2 permeability values.[16] At elevated temperatures (373 K) CO_2 permeability values were higher in APMIM than in the 1-hexyl-3-meythylimidazolium (HMIM) analogue. This incorporated amine resulted in higher viscosity values and lead to a much larger (CO_2/H_2) selectivity value at higher temperatures than that of the HMIM ionic liquid due to the NH_2 functionality aiding in the dissolution of CO_2. As is evident in Figure 5.9, modifications to the ionic liquid that formed part of this study were via the use of different *N*-heterocycles at the end of an ethyl chain. CO_2 permeability, N_2 permeability and CO_2/N_2 selectivity data for this series of SILMs are presented in Figure 5.11(a) – (c).

(a)

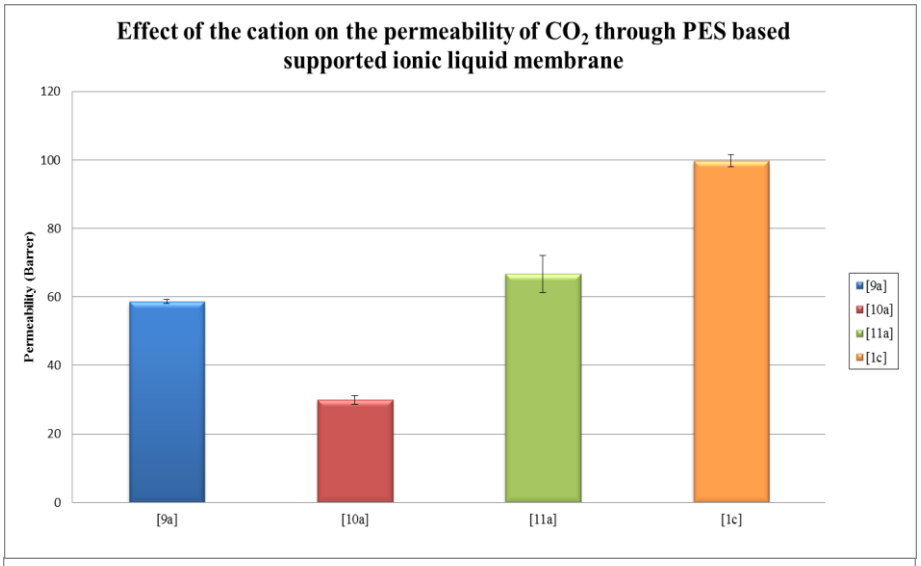

(b)

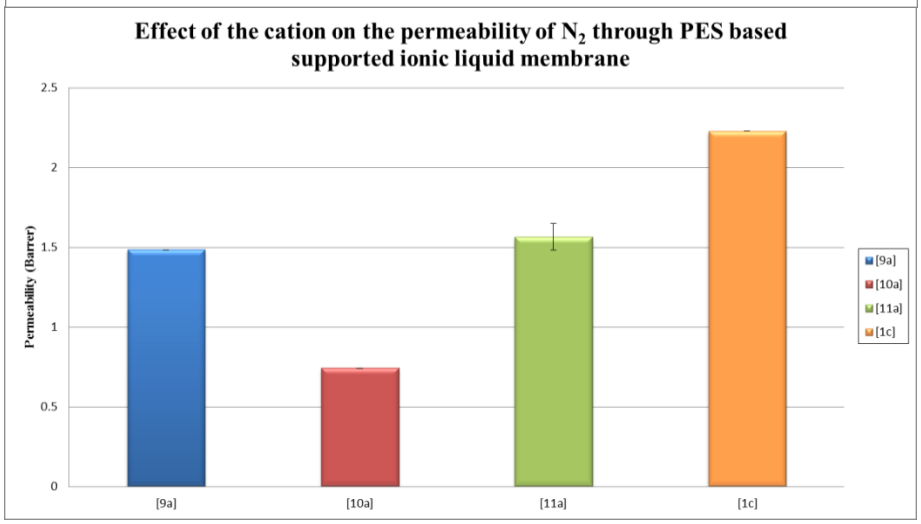

(c)

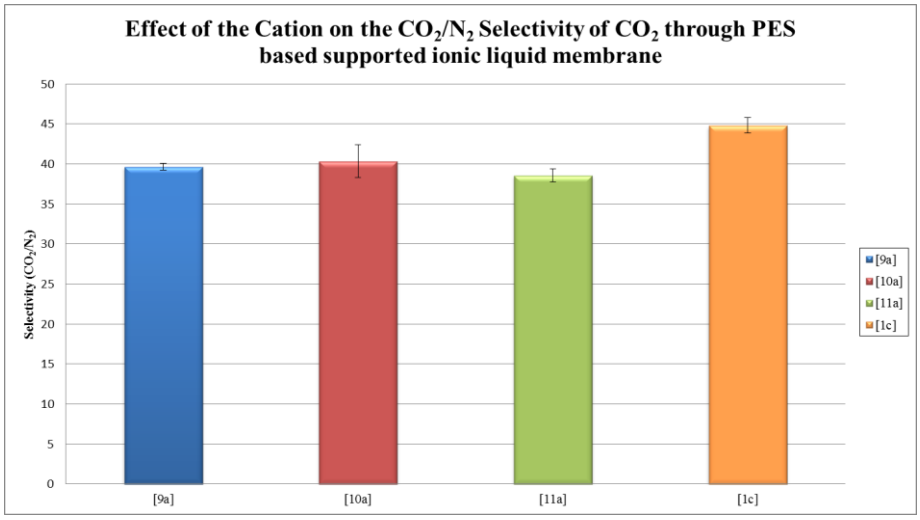

Figure 5.11 Effect of the cation species on (a) CO_2 permeability, (b) N_2 permeability, and (c) CO_2/N_2 selectivity of ionic liquids on PES support at 298 K, (n = 3).

Variation of the *N*-heterocyclic from the five carbon pyrrolidine ring to the six membered piperidine ring lead to no significant difference in the CO_2 permeability

values of 66.7 and 58.6 Barrer, respectively, at 298 K with a pressure differential of 1 bar. However the incorporation of the 6 membered morpholine ring resulted in a significant decrease in the CO_2 permeability with a value of 29.9 Barrer under the conditions described above, approximately half that observed with the other two cations. Incorporation of oxygen atoms in the cation of ionic liquids have previously been shown to increase the solubility and in turn decrease the permeability of CO_2 in ionic liquids.[8] Bara *et al.* synthesised oligo(ethylene glycol) functionalised ionic liquids (Figure 5.12) and measured gas solubilities.[8] They observed higher absorption values for these systems when compared to their alkyl counterparts. However, this is not a trend that was observed during the course of the current study as can be seen in Figure 5.13(a), with little change observed for the CO_2 solubility coefficients in [10a] 0.0078 (cm^3(STP)/cm^3 cmHg) compared to its counterparts [9a] 0.0085 (cm^3(STP)/cm^3 cmHg), and [11a] 0.0094 (cm^3(STP)/cm^3 cmHg). The lower CO_2 permeabilities values can be explained by examining the diffusion coefficient of the gas through the supported ionic liquid membrane as shown in Figure 5.13(b). The cation appears to have a much more pronounced effect on the diffusion coefficients than it has on the solubility coefficients of CO_2 with values of 0.68×10^{-6}, 0.38×10^{-6}, and 0.71×10^{-6} cm^2/s determined for ionic liquids [9a], [10a] and [11a] respectively. Due to the close similarity of the cations in terms of their structures, it is assumed that it is the presence of the oxygen atom which is affecting the diffusion coefficient of the gas.

(a)

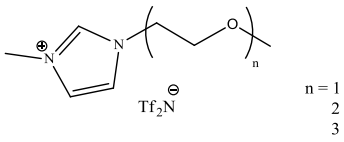

(b)

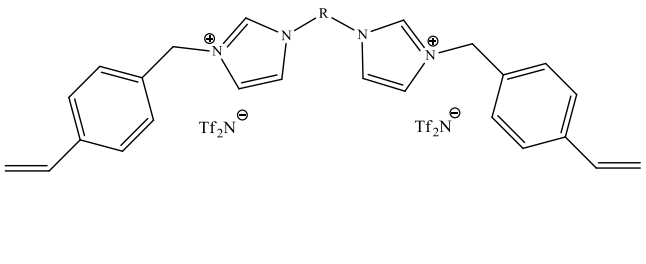

Figure 5.12: Illustration of (a) the ionic liquid cations and (b) ionic liquid polymer cations investigated using ether linkages.

(a)

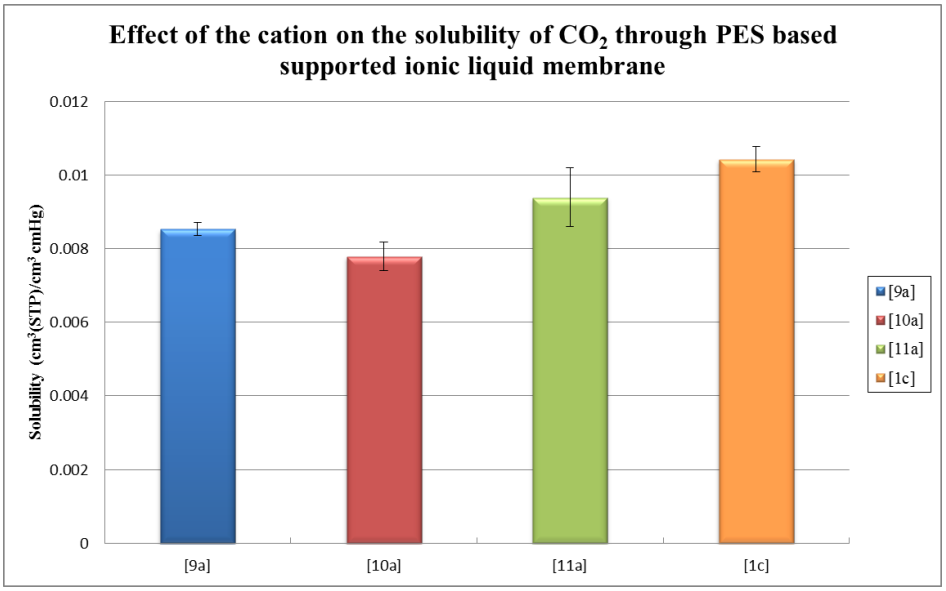

(b)

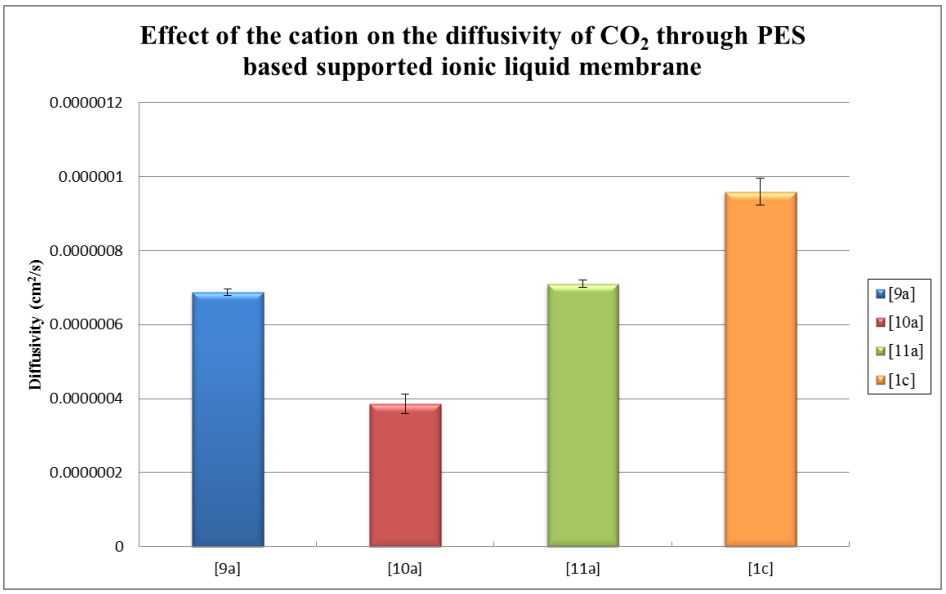

Figure 5.13: Effect of the cation on (a) the solubility, (b) the diffusion coefficients of CO_2 through supported ionic liquid membrane at 298 K, (n = 3).

Ether linkages in poly(ionic liquids) (Figure 5.12(a) and (b)) have been previously shown to affect CO_2 diffusion.[38] Varying the alkyl linkage to the analogous ether linkage resulted in CO_2 diffusion coefficient values of 1.2×10^{-8} (hexyl linkage), 0.83×10^{-8} (ethylene glycol linkage), and 0.78×10^{-8} cm^2/s (diethylene glycol linkage), a reduction of approximately 35%. This was attributed to the increased polarity of these salts (Figure 5.12) that would slow the diffusion of the CO_2 due to increased attraction. Furthermore, the presence of the ether linkages can restrict the degree of movement of the ether chains, resulting in a much more ordered packing of the ions and in-turn a denser liquid. An increase in density was observed in the case of the ether linked ionic

liquid polymers of 1.26 g/cm^3 for the $(CH_2)_6$ spacer to 1.49 g/cm^3 for that which contained the $((CH_2)_2O(CH_2)_2)$ linkage. From this, it is hypothesised that ionic liquid [10a] acts in a similar manner to those salts outlined from the literature above. There is a characteristic slow rate of diffusion and the reduced permeability of both CO_2 and N_2 through it, due to the presence morpholine ring on the cation increasing the polarity of the liquid.

The cation appeared to also have an effect on the permeability of N_2 through these systems. From Figure 5.11(b) we can see that ionic liquids [9a] and [11a] act in a similar manner with N_2 permeability values of 1.4 and 1.5 Barrer, respectively, at 298 K with a differential pressure of 1 bar. It is also evident that the permeability of N_2 in liquid [10a] is significantly reduced in comparison to the N_2 permeability values observed for the samples mentioned above, again following the trend observed during the CO_2 experiments. A value of 0.7 Barrer was observed for [10a] under the same conditions outlined above, half that observed for [9a] and [11a], respectively. This may be due to the increased polarity now exhibited by the cation by the presence of the oxygen atom on the morpholine ring. This is an opinion shared by Bara *et al.* whereby they propose that the presence of long ether linkages in any ionic liquids would aid in the uniform distribution of polar groups throughout the liquid resulting in a repelling effect in the presence of N_2.[8] As mentioned earlier oxygen containing groups have resulted in denser liquids, a trait that would also slow down the diffusion of any gas.[8,9] However due to the reasons outlined in Section 5.2, the diffusion coefficient of N_2 through the liquid was unable to be determined.

Variation of the cation seems to have a negligible effect on the CO_2/N_2 selectivity of the ionic liquids, in comparison to that observed during the anionic study, with recorded selectivity values for [9a], [10a], and [11a] of 39, 40, and 38 under the same conditions described previously. Although there was some variation of values recorded for the permeability of both gases through the ionic liquids, values for [10a] were reduced for both CO_2 and N_2, and resulted in CO_2/N_2 selectivity values which were comparative to the other bis(triflimide) samples tested (Figure 5.11(c)).

Experiments involving 1-butyl-3-methylimidazolium bis(triflimide) [1c] were also performed as a reference to the other novel samples tested. This was important due to

the discrepancy in literature values for the permeability values of N_2 and CO_2 in [1c]. From Figure 5.5(a), a permeability value of 99.7 Barrer was observed for CO_2 permeability of [1c].

There has been much discrepancy over N_2 permeability and in-turn CO_2/N_2 selectivity. From the literature it has been reported that ionic liquid [1c] has resulted in CO_2/N_2 selectivities of 19, 21, 31, 39, and 54.[6,13,20,30,39] Again as highlighted previously in Figure 5.1, it is easy to see how variances in feed pressure can result in vastly difference selectivity values due to the non-linear relationship between feed pressure and permeability. As well as that experimental conditions such as membrane area, thickness, and also the functionalities present of the membrane could all potentially have an effect, with supports employed in the studies varying from PES, to PVDF, nylon, and PTFE, all which contain functional groups that are known to help with CO_2 solubility.[16,17,31,40]

5.3.3 Effect of the membrane support on the permeability of CO_2 and N_2.

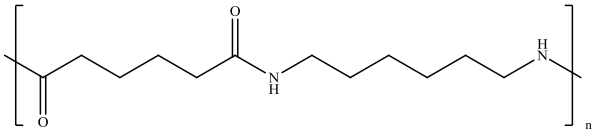

nylon 6,6

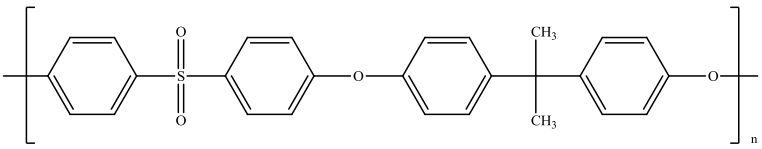

poly(ether sulfone)

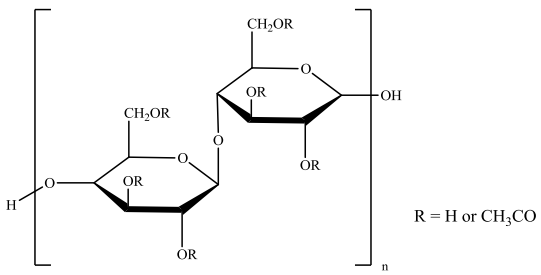

cellulose acetate

Figure 5.14: Illustration of the membrane supports investigated during the permeability studies.

As discussed in Section 5.3.1 and Section 5.3.2, the presence of certain functional groups can have a dramatic effect on the permeability of gases through the SILM due to physical properties associated with these functionalities, and interactions that occur between them and certain gases. To investigate the effect of the support on CO_2 permeability, nylon (ϕ = 0.2 μm), nylon (ϕ = 0.45 μm), PES (ϕ = 0.2 μm) and cellulose acetate (ϕ = 0.45 μm) membranes were impregnated with ionic liquid [9a]. PTFE was also investigated but due to the inability of the ionic liquid to fill the polymer pores, as shown in Figure 5.15, this membrane was discounted.

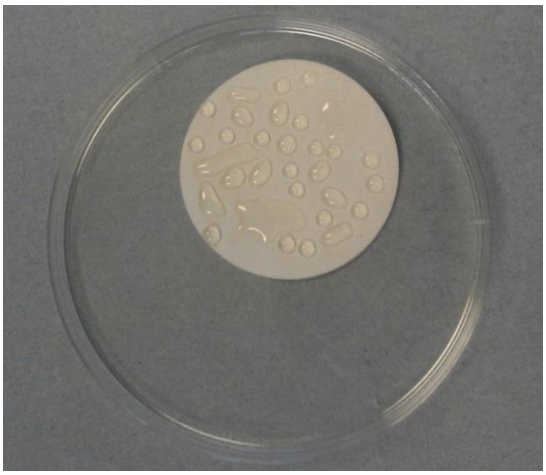

Figure 5.15: Attempted impregnation of PTFE membrane with ionic liquid [9a].

It has been shown that the presence of amines, sulfonates and fluoroalkyl groups can have a beneficial effect on permeability of CO_2 which can result in an increase in inter-gas selectivities.[20,41] Alternatively, a beneficial effect on selectivity can be achieved by impairing the permeability of a competing gas while keeping CO_2 permeability levels similar to those of unmodified ionic liquids, such as fluoro-alkyl groups promoting selectivity by reducing N_2 permeability.[8,10] While this is advantageous, excessive modification of the liquids can have undesirable consequences such as increased viscosity, which will compete with the beneficial modifications and can result in reduced diffusion and permeability through the liquid. Therefore the membrane support provides an ideal route to increase functionalities through which the gases in question must pass, without compromising the beneficial aspects of the ionic liquids. A wide plethora of supports have been employed such as poly(ionic liquids), alumina, zeolites, polyamides, poly(ether sulfonates), and fluoroalkyl membranes.[9,15,42,43] In the present study keeping experimental conditions constant with variation only in the supporting

membrane structure resulted in the determination of the contribution of the membrane towards gas permeability and selectivity (Figure 5.16(a-c)). [9a] was chosen for this study due to its high CO_2/N_2 selectivity values obtained during the cationic study.

(a)

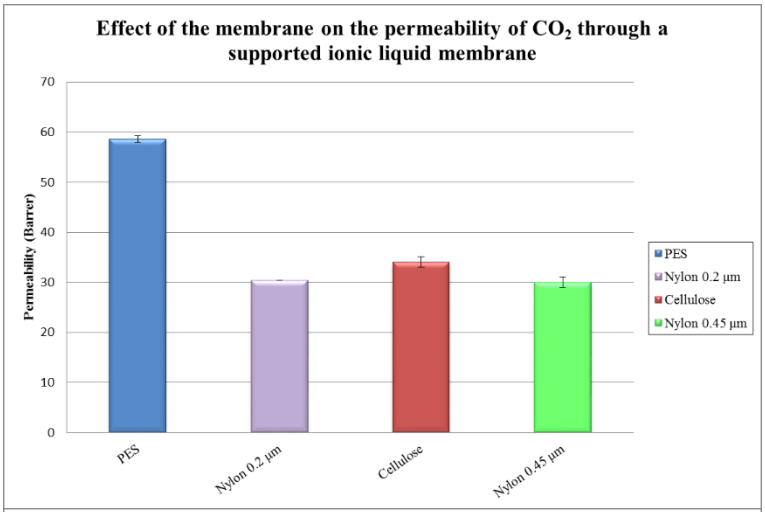

(b)

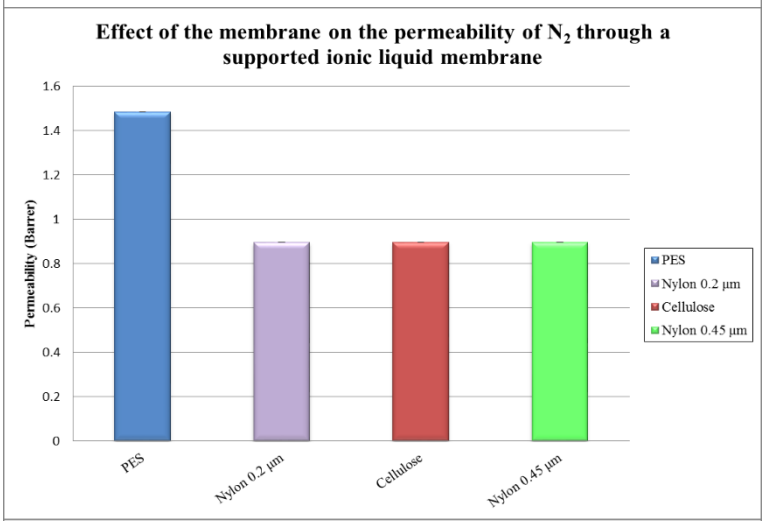

(c)

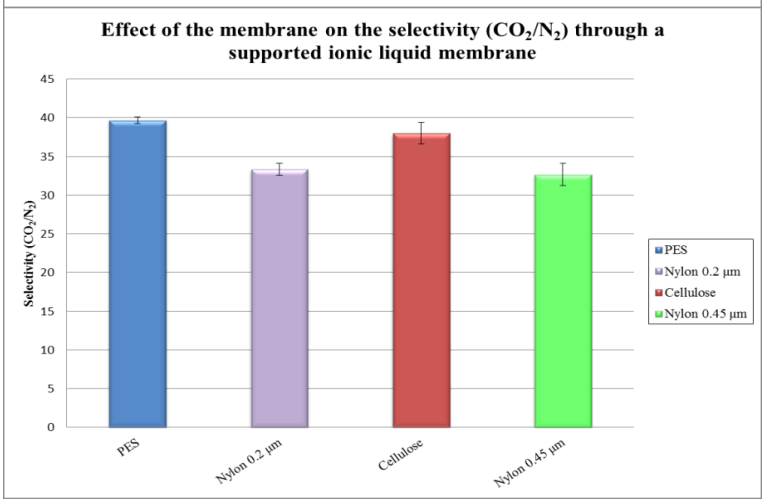

Figure 5.16: Effect of the membrane composition and pore size on the permeability of (a) CO_2, (b) N_2, and (c) CO_2/N_2 selectivity using ionic liquid [9a] at 323 K, (n = 3).

From Figure 5.16(a), a significance difference in the permeability of CO_2 through [9a] on the various supports at 323 K was observed, with values of 58.6, 30.4, 34.0, and 27.7 Barrer, respectively, for PES, nylon (ϕ = 0.20 μm), cellulose acetate, and nylon (ϕ = 0.45 μm). This difference indicates that membrane composition can have a huge impact on permeability values. As can be seen in Figure 5.14 the PES membrane contains the sulfonyl groups which was mentioned earlier, help increase CO_2 solubility, complementing the work performed by the liquid. However the trend seen in the CO_2 permeability studies is also repeated in Figure 5.16(b) during the N_2 studies with values of 1.4, 0.8, 0.8, and 0.8 Barrer respectively for PES, nylon (ϕ = 0.2 μm), cellulose acetate, and nylon (ϕ = 0.45 μm). Due to the membrane variation affecting both the permeability of CO_2 and N_2, it is unlikely that variation of the functional groups on the membrane supports would lead to different CO_2/N_2 selectivity values. This is shown by the similar selectivity values evident in Figure 5.16(c) clearly illustrating that the membrane support is having little effect.

Pore size was also an important consideration when investigating the SILM as it might be expected that larger pore size would equate to a faster permeability. However due to the size of the pores in relation to the size of the gas molecules in question and the blockage of these pores by the ionic liquid, this is not an issue. From Figure 5.16(a), CO_2 permeability using a nylon membrane of pore size 0.20 μm and 0.45 μm was investigated. The two membranes displayed negligible difference in the CO_2 permeability (≈ 3 Barrer) which indicates that no real difference was observed. The purpose of the ionic liquid is to fill or block the pores of the membranes. Regardless of the pore size, once filled the liquid should act in an identical manner to each other, a result which was observed.

Membrane swelling seems to be a determining factor of the gas permeability, in particular when examining the nylon and cellulose acetate based membranes. When PES was impregnated with the ionic liquids, no swelling of the membrane occurred. However, when the nylon and cellulose acetate membranes were impregnated, various degrees of swelling were observed via SEM analysis given in Figure 5.17 and Table 5.1. The excess ionic liquid was blotted off to leave that which was impregnated in the pores only. This swelling of the membranes when impregnated with the ionic liquid meant that a much larger amount of the 0.6 ml of the applied ionic liquid was present in the

polymer matrix of nylon and cellulose acetate membrane. The increased amounts of the ionic liquid in the polymer matrices results in both lower diffusion coefficients and solubility coefficients of CO_2 than in the PES counterpart as can be seen in Figure 5.18.

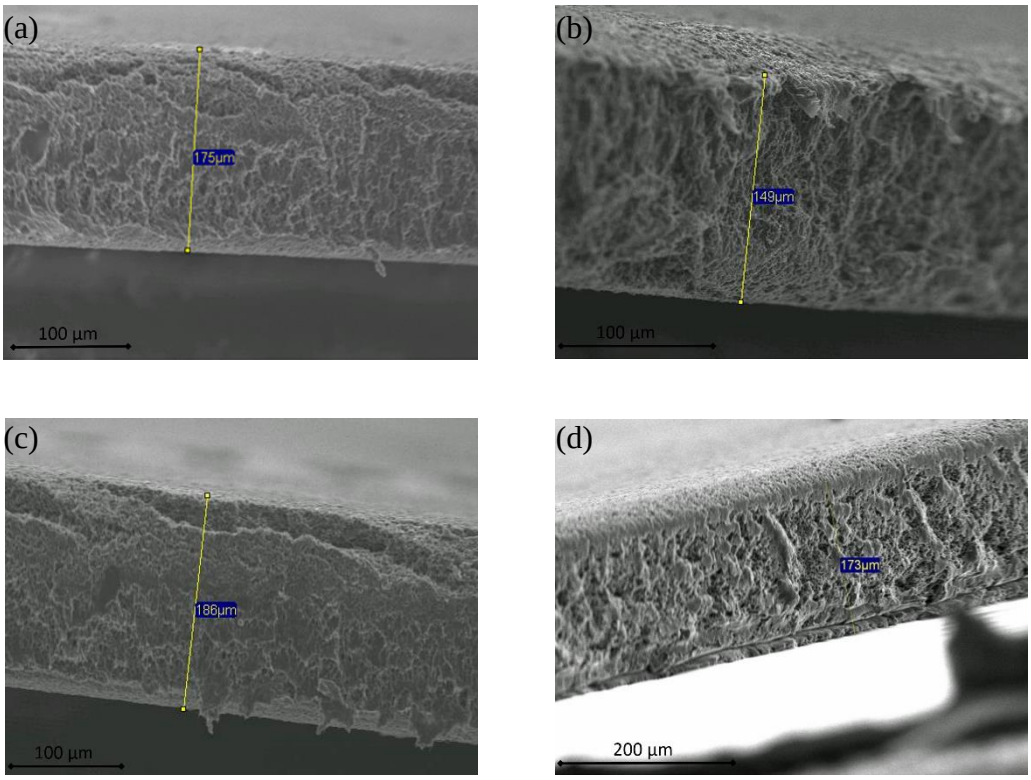

Figure 5.17: SEM micrographs of (a) nylon membrane (ϕ = 0.2 µm), PES membrane (ϕ = 0.2 µm), (c) nylon membrane (ϕ = 0.45 µm), and (d) cellulose acetate membrane (ϕ = 0.45 µm), with ionic liquid [9a].

Table 5.1: Effect of swelling on the various membranes employed as part of the permeability studies using ionic liquid [9a], (n=3).

Membrane	**Pore Size (µm)**	**Thickness (µm)**		**Diameter (mm)**	
		Before Impregnation	After Impregnation	Before Impregnation	After Impregnation
nylon 66	0.20	127	175	47	51
PES	0.20	145	149	47	47
Cellulose	0.45	127	173	47	53
Nylon 66	0.45	127	186	47	51

(a)

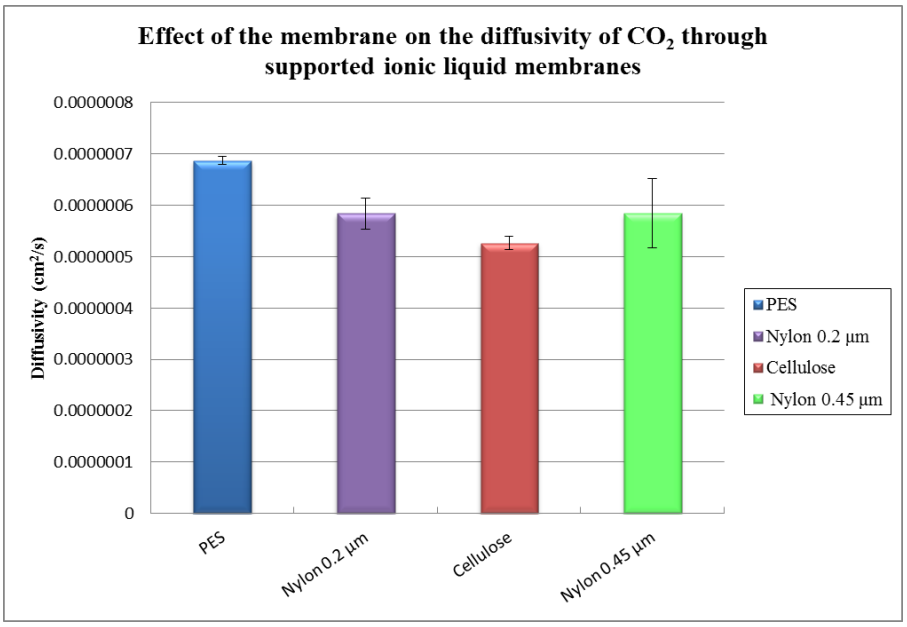

(b)

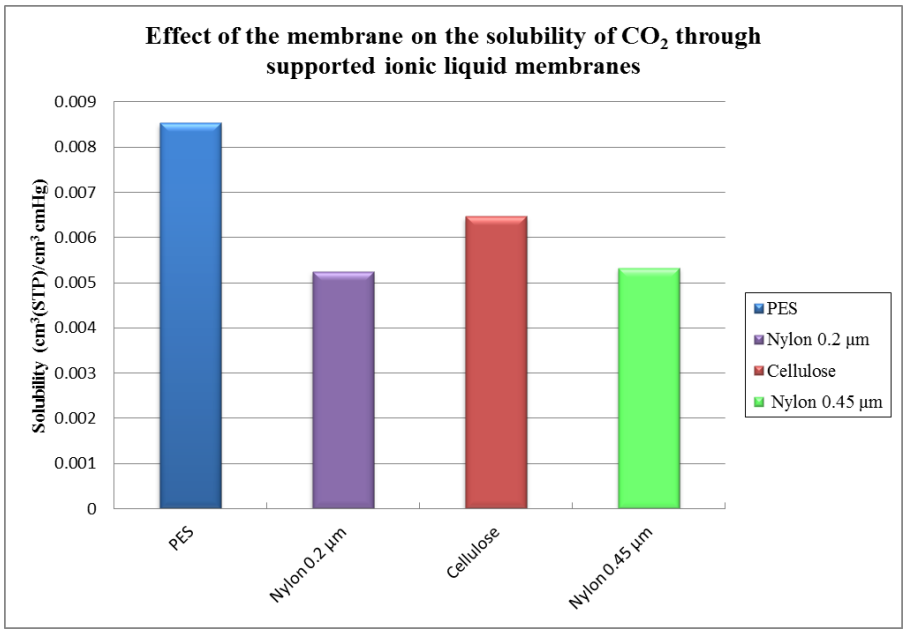

Figure 5.18: Effect of the supporting membrane on (a) the diffusion coefficient, and (b) the solubility coefficient of CO_2 through supported ionic liquid membranes at 323 K, (n=3).

From Figure 5.18(a), a decrease in the diffusion coefficient of CO_2 through the ionic liquid membrane was observed in the membranes tested when compared to values obtained using the PES membrane, with decreases of between 15-30% recorded. As mentioned earlier this membrane exhibited negligible swelling, whereas significant swelling was observed in all other cases and it is this that could be resulting in lower diffusion coefficients. However, more interestingly it can be seen that the membrane has an effect on the solubility coefficients of CO_2 in the ionic liquid. As mentioned earlier, when the nylon and cellulose acetate membranes were impregnated with the

ionic liquids an increase in ionic liquid uptake was observed when compared to the PES supports (Figure 5.19). With more ionic liquid present, the SILM takes on more bulk ionic liquid characteristics than when in the PES membrane, where a thinner layer of ionic liquid occurs. We would hypothesise that when a thicker layer of ionic liquid is present, the solubility of CO_2 is lowered due to the inaccessibility of more of the ionic liquid than if the ionic liquid was present as a thin film. Previous literature work demonstrated decreased solubility of gases with increased amount of ionic liquid present on the polymeric support.[43]

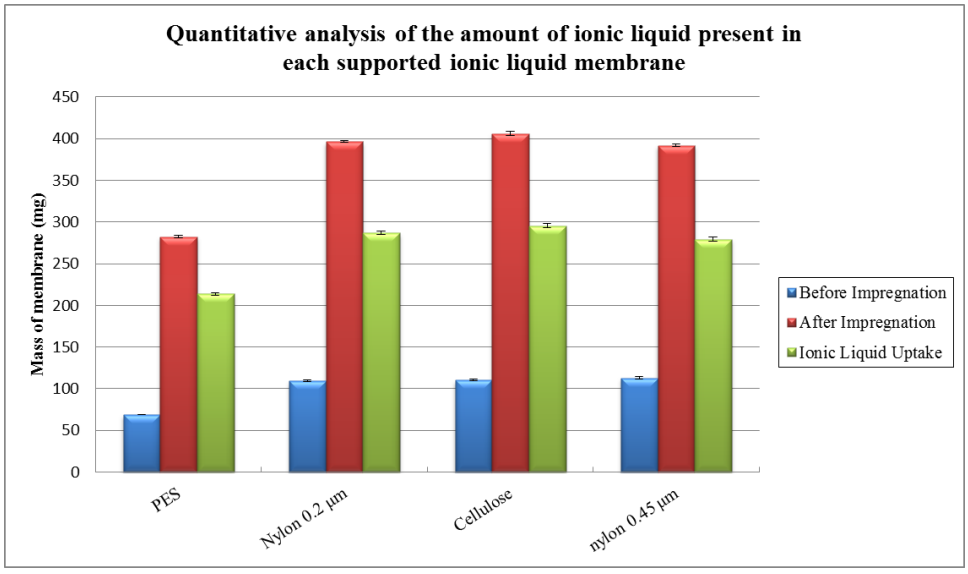

Figure 5.19: Quantitative analysis of the amount of ionic liquid present in various supported ionic liquid membranes using ionic liquid [9a], (n=3).

An important note that must be made is the degradation of the cellulose acetate membranes upon heating at elevated temperature. Work conducted on cellulose and ionic liquids have shown them to be useful materials for the breakdown of cellulose, and it appears that this also occurred with the cellulose acetate as can be seen from Figure 5.20.[44,45] Therefore due to this trait, cellulose membranes are an unsuitable material for CO_2 separation technology when used in conjunction with ionic liquids.

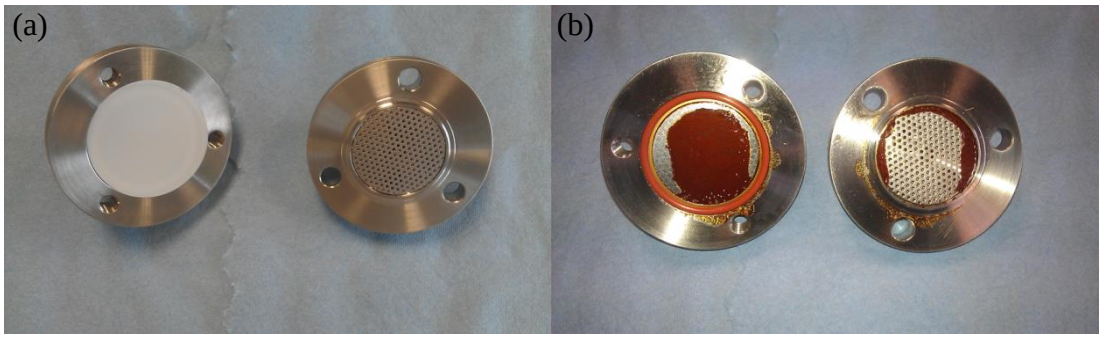

Figure 5.20: Cellulose acetate membranes in the gas permeation module (a) before and (b) after, examination of permeability at elevated temperatures.

5.3.4 Influence of temperature on the permeability of CO_2 and N_2.

Temperature is an important parameter that must be investigated during the course of these studies. Due to the elevated temperatures of flue gases, it is imperative that these systems can operate at these temperatures. Chillers can be employed to help drive down temperature to a more effective working range although these can result in a system which is less energy efficient, increasing costs. Amines have been investigated in this context before but due to their volatility at elevated temperatures regular replacement of solvent is essential.[3,42]

From Figure 5.21(a), it is evident that in general an increase in temperature generally results in an increase in CO_2 permeability, with values at elevated temperatures increasing from those achieved at 298 K. The increase in permeability with respect to temperature is widely reported in the literature.[16,46,47] In particular, in the case of liquids [9a] and [10a] we see temperature having the largest impact with CO_2 permeability increasing from 58.6 and 29.9 Barrer to values of 76.1 and 57.2 Barrer, respectively from 298 – 343 K. It is generally accepted that this increase in permeability is attributed to the decreasing viscosity of the liquids at higher temperatures, values for which can be found in Figure 5.22.[46] However, it was observed that [11a] and [1c] showed no dramatic change in CO_2 permeability (approximately 2-3 Barrer) with increasing temperatures despite both containing the same bis(triflimide) anion as [9a] and [10a].

(a)

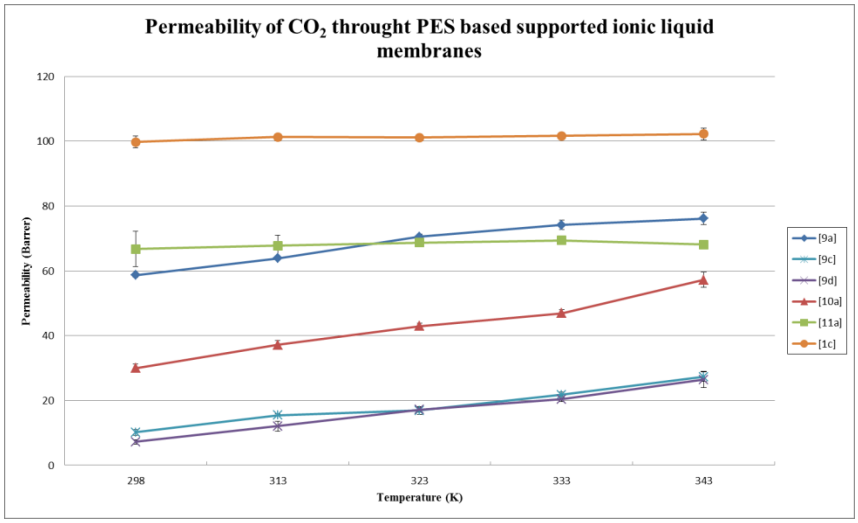

(b)

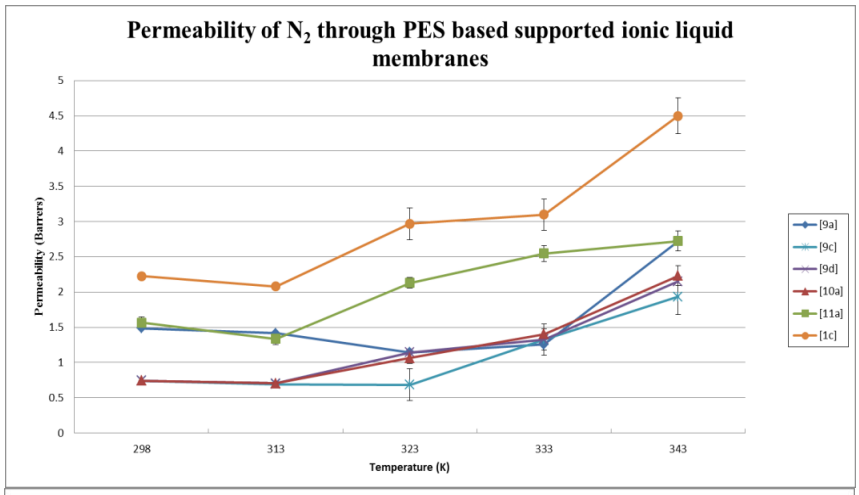

(c)

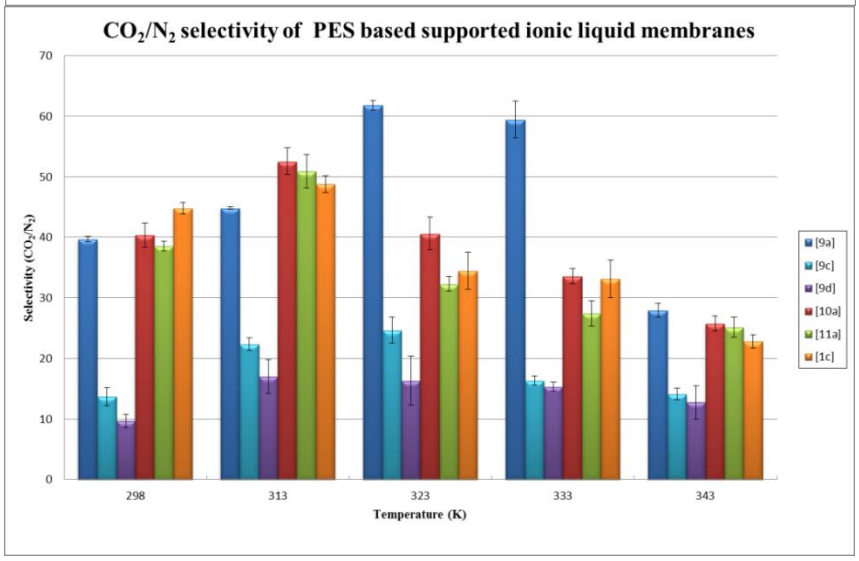

Figure 5.21: Effect of temperature on (a) CO_2 permeability, (b) N_2 permeability and (c) CO_2/N_2 selectivity on a PES supported ionic liquid membrane, (n = 3).

A comparison of the results for ionic liquids [9c] and [9d] showed that an increase in temperature does have an effect on the permeability of CO_2, with increases of approximately 100% observed in both cases at 343 K compared to those obtained at room temperature. It can be seen from Figure 5.22 that at 298 K, ionic liquid [9d] exhibits the highest viscosity values of 3654.3 mPa.s. As the temperature increases, an increase in both the CO_2 and N_2 permeability were observed although not to the levels observed with the bis(triflimide) ionic liquid [9a] despite the viscosities becoming more comparable (Figure 5.21). While this shows that viscosity can be important, it is not the only factor that influences permeability of gases. For example, the ionic liquid's functionalities are a key factor to permeability.[12,32] From Figure 5.22 it can be seen that [9c] has the lowest viscosity value out of the 5 novel liquids, but it does not result in the highest permeability, with values of 10.4 Barrer for [9c] compared to 66.7 Barrer exhibited by [11a] at 298 K.

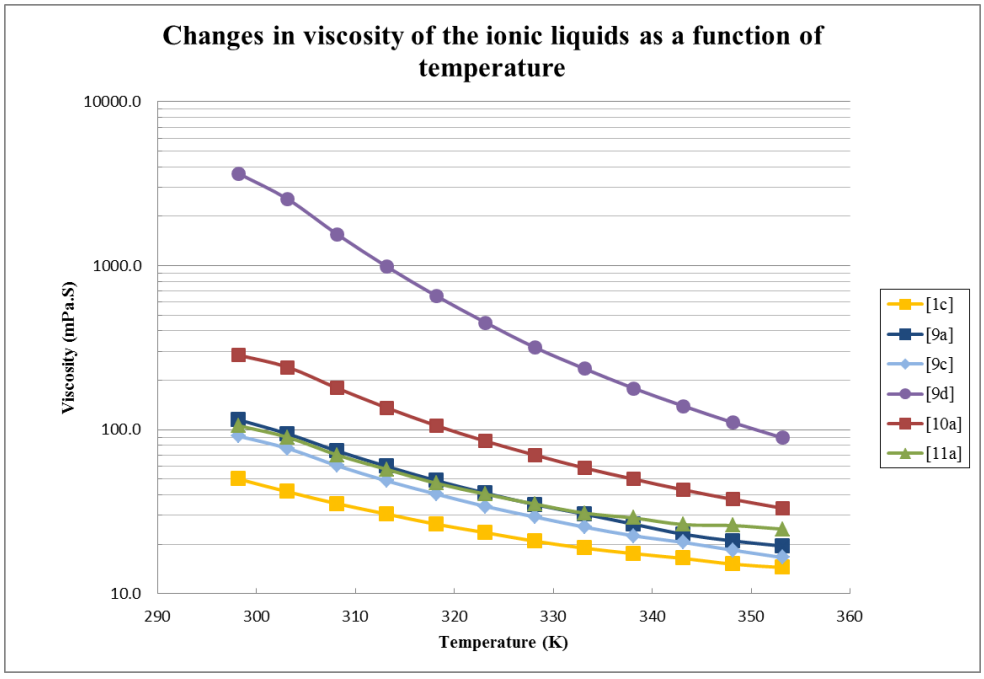

Figure 5.22: Change in viscosity of the ionic liquids as a function of temperature.

As with CO_2, permeability, it is evident from Figure 5.21(b) that N_2 permeability is also affected by increases in temperature due to the same reasons as outlined above. Although the magnitude of the N_2 permeability changes are small compared to the CO_2 permeability values, in terms of percentage difference, a significant effect was observed. An increase of over 200% was observed in [1c], and approximately 300% for liquids

[9c], [9d], and [10a], which as for the changes in CO_2 permeability is likely a result of decreasing viscosity.

CO_2/N_2 selectivity has been shown to decrease with increasing temperatures.[20,46,47] In work conducted by Jindaratsamee *et al*. it was noted that CO_2/N_2 selectivity using BMIM Tf_2N decreased from 56 to 42 over the 303 – 343 K temperature range.[20] This trend was also observed during the course of the permeability studies, although an initial increase was observed in most cases, as can be seen in Figure 5.21. This arose due to the increase in CO_2 permeability with no change in the N_2 permeability detected. However it is likely that changes did occur in the N_2 permeability studies but were below the detection limit of the apparatus. Typically the most optimum selectivity values were obtained over the temperature range of 313 - 323 K. Ionic liquid [9a] demonstrated the highest selectivity at 323 K with a value of 61. This is significantly higher than the optimum selectivity values obtained for the other bis(triflimide) based ionic liquids with values of 52, 50, and 48 for [10a], [11a], and [1c] respectively. This can be explained by examining the N_2 permeabilities in Figure 5.21(b). All four liquids exhibit no increase in N_2 permeability from 298 – 313 K, with similar selectivity values (Figure 5.21(c)) recorded for each. A further temperature increase of 10 K to 323 K resulted in increases in the N_2 permeability for ionic liquids [10a], [11a], and [1c]. This results in a CO_2/N_2 selectivity decrease, despite increasing CO_2 permeability values. The increase in N_2 permeability levels at 323 K does not occur in the presence of [9a] and as such the selectivity values continue to increase to a value of 61. Increasing temperature from this point led to decreases in selectivities due to increases in N_2 permeability values for all the ionic liquids. Ionic liquids [9c] and [9d] also exhibited maximum CO_2/N_2 selectivities at 323 K with values of 22 and 17, respectively. Although the values for N_2 permeability through [9c] and [9d] tended to be lower, so did those for CO_2 permeability and as such, negated the potential benefit that this could have created by the low N_2 permeability value.

Change in viscosity can be a factor when increasing permeability of all gases through the supported ionic liquid membranes. From Figure 5.23(a), it is clear that as temperature increased, the diffusion coefficients of CO_2 through the SILM also increased a result which was expected given Equation 5.5. This trend has been widely

reported in the literature with other ionic liquid systems.[32,46] It was mentioned earlier that the viscosity of the liquids was seen to decrease with increasing temperature. As a consequence, there is much less resistance for the gas to permeate through the membrane allowing for increases in the diffusion rate, a property exhibited by all the liquids tested. Diffusion coefficients for [9a] and [11a] were seen to increase from 0.68 × 10^{-6} cm^2/s to 1.50 × 10^{-6} cm^2/s, and 0.71 × 10^{-6} cm^2/s to 1.2 × 10^{-6} cm^2/s respectively. From Figure 5.23 it is clear that the diffusivity of CO_2 through the membrane was proportional to temperature and in turn the ionic liquids viscosity. A less rapid increase in diffusion coefficients of CO_2 through [10a], [9c], and [9d], can be observed from Figure 5.23(a).

(a)

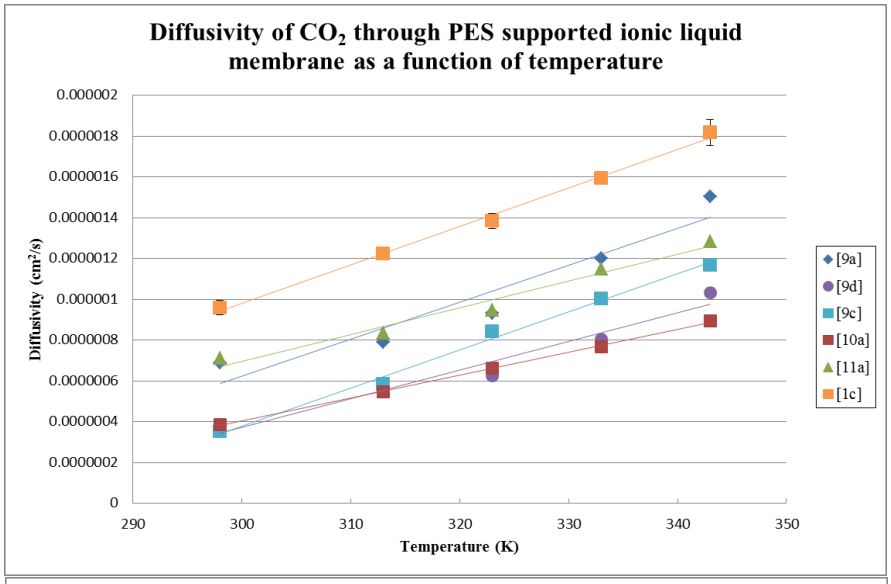

(b)

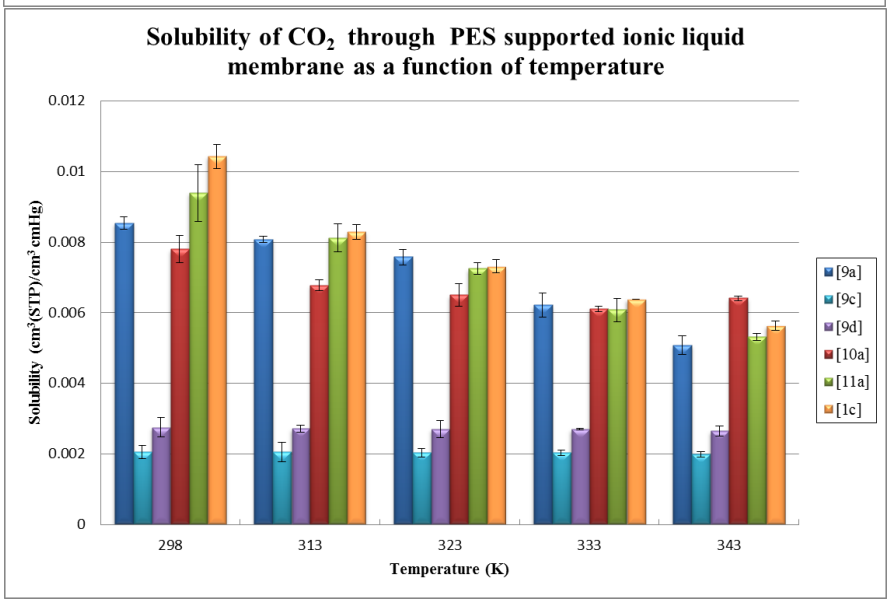

Figure 5.23: Effect of temperature on (a) the diffusion coefficients, and (b) the solubility coefficients of CO_2 through a supported ionic liquid membrane as a function of temperature, (n=3).

Looking at the optimum ionic liquid [9a] a decrease in the CO_2 solubility coefficients is observed from 0.0085 (cm^3(STP)/cm^3 cmHg) at 298 K, to 0.0050 (cm^3(STP)/cm^3 cmHg) at 343 K. The effect of temperature on the solubilty of CO_2 in the other bis(triflimide) salt was also significant with values only decreasing from 0.0104 and 0.0093 (cm^3(STP)/cm^3 cmHg) to 0.0056 and 0.0053 (cm^3(STP)/cm^3 cmHg) for [1c] and [11a], respectively over the same temperature range. However, temperature had a negligible effect on the solubility coefficients of CO_2 for [9c] and [9d] with solubility coefficients values changing from 0.0020 and 0.0027 (cm^3(STP)/cm^3 cmHg) to 0.0019 and 0.0026 (cm^3(STP)/cm^3 cmHg) respectively. Literature precedent shows that a decrease in CO_2 solubility in ionic liquids with increasing temperatures is to be expected.[30,31] Due to the functionalities already discussed in Section 5.3.1 reducing CO_2 solubility at room temperature, the temperature change plays a much less influential role for liquids [9c] and [9d].

5.3.5 Stability of supported ionic liquid membranes

Although these materials have proven effective at successfully separating CO_2 and N_2, in order for them to be a viable technology they must be able to withstand robust conditions and also be able for multiple uses. As mentioned in Chapter 1, one of the biggest problems concerning the use of supported liquid membranes in gas separation technologies has been their volatility, resulting in depletion of the liquid due to the high pressures and temperatures present.[5,12] To investigate the reusability of the materials, the optimum ionic liquid [9a] was subjected to several cycles of both gases and selectivity was monitored as shown in Figure 5.24. From this it is clearly evident that the permeability of both gases remains fairly constant over the 10 cycles of gases and in-turn results in good stability of the CO_2/N_2 selectivity of the supported ionic liquid membrane over this number of cycles. The good stability of the SILM is an unsurprising result considering literature precedent that has shown high stability for these systems.[14] Due to the low pressure differential across the membrane for the gas permeation rig used in the present research, removal of the liquid seems unlikely due to the negligible vapour pressure of the ionic liquids. During experiments performed by Gan *et al.* using nano-filtration membranes, it was determined that no discharge of ionic liquids was observed with a pressure differential of 10 bar across the membrane.[14] They

stated that the stability of the system was due to electrostatic interactions between the ionic liquid and functionalities on the membrane.

(a)

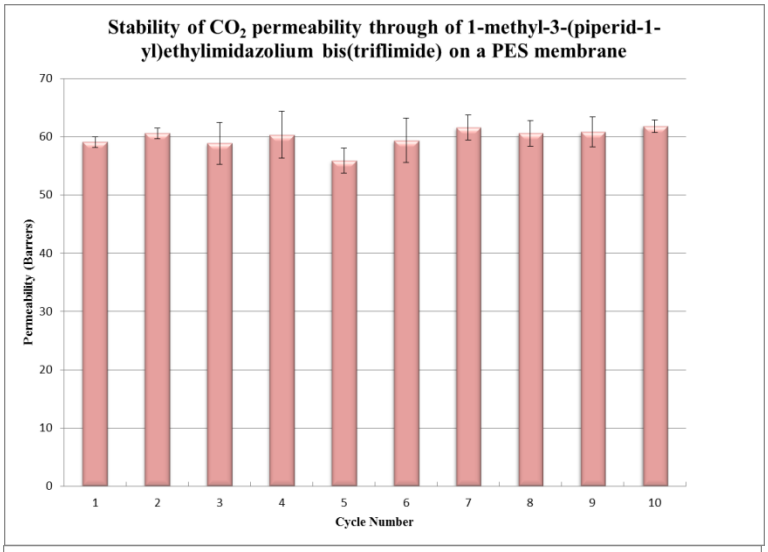

(b)

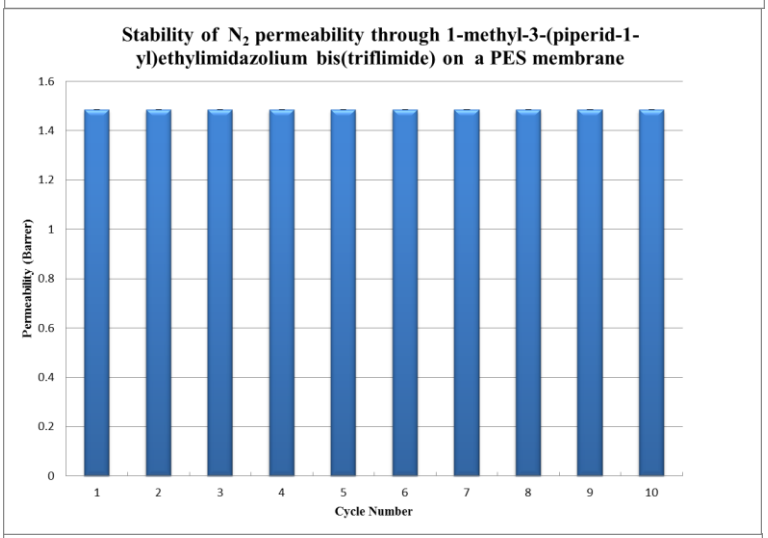

(c)

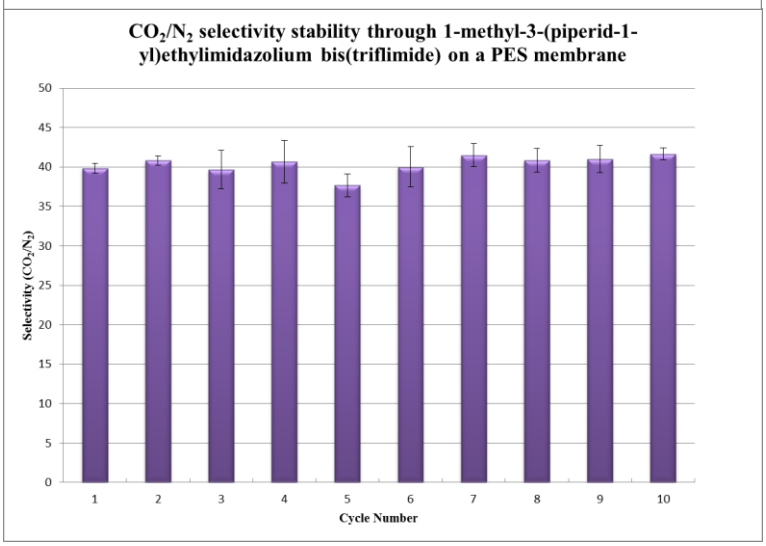

Figure 5.24: Investigating into the stability of the supported ionic liquid membranes containing ionic liquid [9c] over 10 cycles, (n=3).

5.3.6 Binary ionic liquid systems

As can be seen from work previously presented in this chapter it is clear that gas transport properties of the ionic liquids studied are different with respect to each other. Some have demonstrated higher CO_2 permeability values, while others have shown lower N_2 permeability values than others. Due to this an investigation was undertaken by which the incorporation of 2 different liquids into the same membrane was undertaken (Figure 5.25). While this would inevitably reduce CO_2 permeability, it was hoped that this would also reduce N_2 permeability and as such increase the membranes selectivity for the two gases. Two liquids were identified as the optimum ionic liquids, the standard [1c], and ionic liquid [9a] due to these exhibiting the highest CO_2/N_2 selectivity values of all ionic liquids tested in this study (Figure 5.21). In addition these ionic liquids were relatively easy to prepare in high yield and they exhibited high CO_2 permeability values. The binary systems were conducted by taking ionic liquids [9a] or [1c] and varying the loading (30%-50% (v/v)) of the other ionic liquids which demonstrated lower N_2 permeability values. The temperatures for the gas permeability studies were chosen based on where optimum CO_2/N_2 selectivity was obtained during the single liquid testing of [1c] or [9a].

In the case of ionic liquid [1c], four other liquids were mixed with [1c] before they were impregnated into the PES polymer matrix, which were [9a], [9c], [9d], and [10a]. The mixtures were visibly more viscous than the pure [1c]. Studies were carried out at 313 K, the temperature for which [1c] displayed the highest CO_2/N_2 selectivity. The results from the gas permeability studies are given in Figure 5.25.

(a)

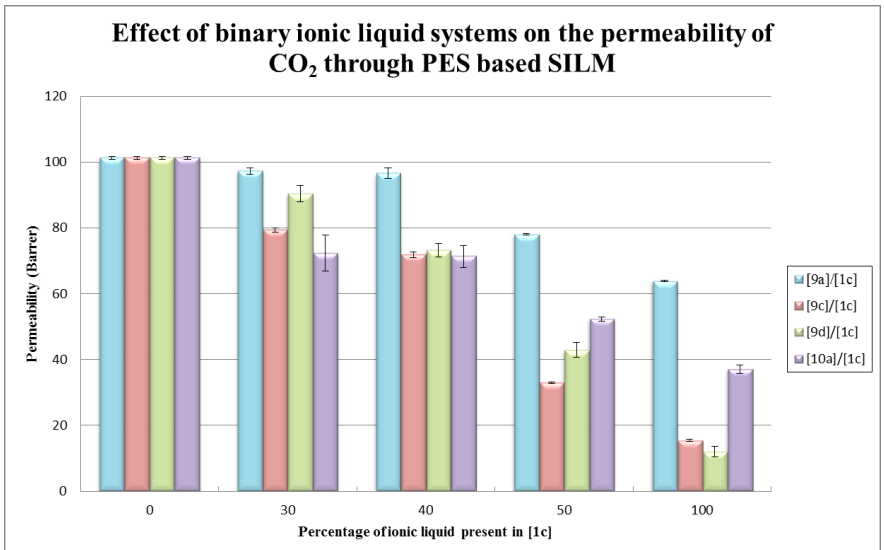

(b)

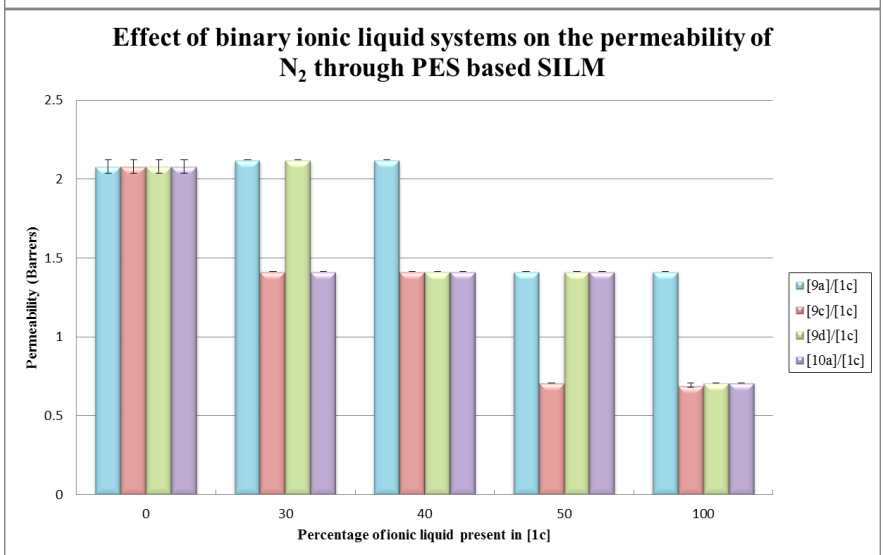

(c)

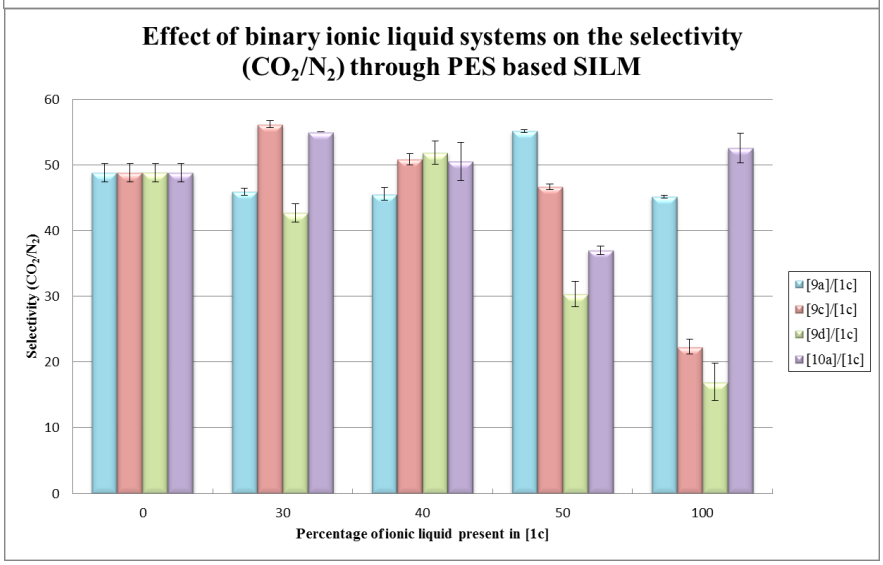

Figure 5.25: Effect of binary mixtures of ionic liquids with [1c] and (a) CO_2 permeability (b) N_2 permeability, and (c) CO_2/N_2 selectivity, (n=3).

From Figure 5.25 (a) and (b), it is clear that as the concentration of the ionic liquids [9c], [9d], and [10a], in the liquid [1c] increases, the permeability of CO_2 and N_2 decrease. As mentioned earlier these liquids have illustrated decreased CO_2 and N_2 permeability compared to [1c] so as the loading of these increase the binary system adopts more of that liquid's characteristics. Therefore the main focus of attention is on the CO_2/N_2 selectivity data. Over the loading range, it is evident that the selectivity fluctuates with no linear relationship between it and the ratio of the secondary ionic liquid. This is particularly evident in the case of the [10a]/[1c] 30/70 mixture, whereby addition of 30% (v/v) [10a] results in a slight increase in the selectivity of the gases compared to pure [1c] with a value of 55 being recorded which is due to the 33% decrease in N_2 permeability values. As the ratio of [10a] increases further, the selectivity begins to decrease due to N_2 permeability values remaining constant. However a secondary increase in selectivity is recorded when 100% of [10a] is present, a consequence of the low permeability of N_2 through the membrane. In all other cases, the loading at which a decrease of N_2 permeability occurs resulted in the increase in CO_2/N_2 selectivity. Of the four combinations tested, the highest selectivity recorded was for the [9c]/[1c] mixture at 30% (v/v) loading of [9c] which exhibited a selectivity of 56 compared to 48 for pure [1c], showing a small benefit of these dual systems.

The effect on the diffusion coefficients and solubility coefficients of CO_2 in these membranes was also determined. From Figure 5.26(a) it can be seen that the diffusion coefficient of CO_2 through the membrane decreases as the concentration of the secondary ionic liquid increases. As demonstrated previously these liquids have displayed significantly higher viscosity values that that of [1c] and due to the relationship between viscosity and diffusion coefficients. This is an unsurprising result as the mixture takes on the characteristics of the secondary ionic liquid as its concentration increases. It is also evident that [9a], due to its lower viscosity then [9c], [9d], and [10a], results in less of a decrease in the diffusion coefficient than its more viscous counterparts, with 30% (v/v) loading of [9a] in [1c] having a negligible effect on the diffusion coefficient of CO_2.

(a)

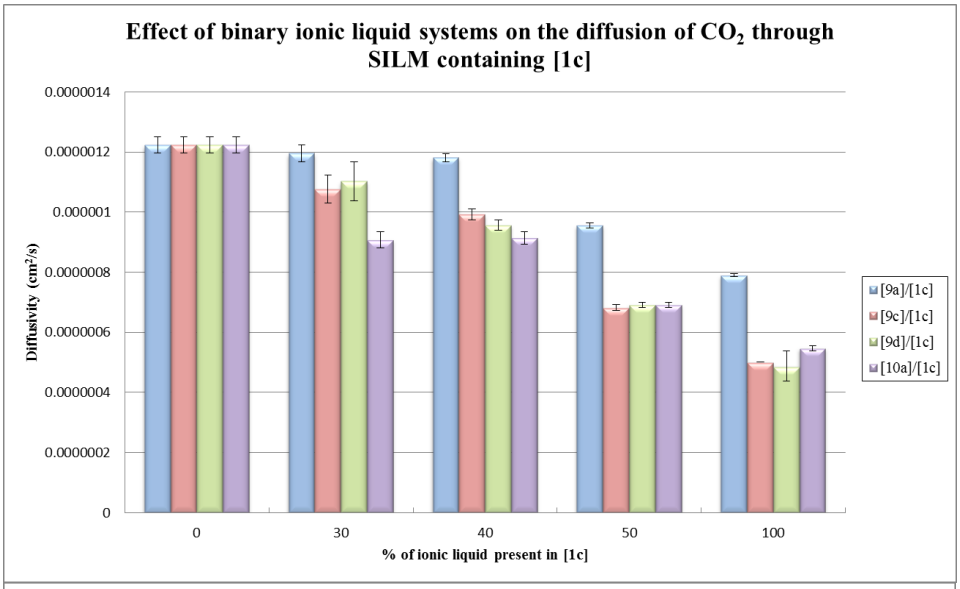

(b)

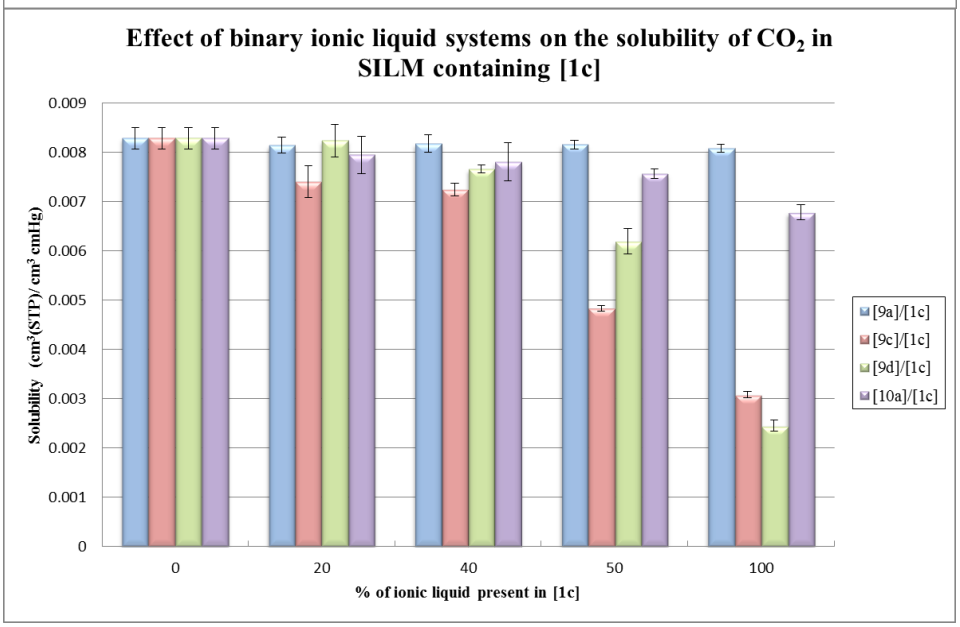

Figure 5.26: Effect of the binary ionic liquid systems on (a) the diffusion coefficients, and (b) the solubility coefficients of CO_2 in a PES membrane containing [1c], (n=3).

While similar trends in CO_2 permeability and diffusion coefficients occurred for all binary ionic liquid systems employed, it can be seen from Figure 5.26(b) that the effect of the binary mixtures on the solubility coefficients of the CO_2 is much more varied. In all cases a decrease in solubility coefficients is observed as the amount of secondary ionic liquid present increases, the magnitude of which is clearly related to the anion employed. In the case of the dicyanamide [9c] and trifluoroacetate [9d], a significant decrease is observed with decreases of 60 - 70% observed in both cases. When the bis(triflimide) anion is employed, it was observed that solubility coefficients of CO_2 in the ionic liquid does not decrease to the same extent as observed in the other anions. In

the case of [10a], this can be most likely attributed to the oxygen atom on the ring which as discussed earlier, increases the polarity of the liquid resulting in a stronger affinity for the gas. As seen earlier, [9a] had one of the lowest viscosity values, of the ionic liquids tested and as such results in a less pronounced change in the viscosity of the binary system when compared to pure [1c] and as such retains many of the favourable properties exhibited by [1c].

Due to the high selectivity value exhibited by [9a] at 323 K, and the small increase observed during the investigations of the binary systems containing liquid [1c], it was decided to employ the same binary studies but focus on [9a] as the optimum liquid and employ different ratios of ionic liquids [9c], [10d], and [10a] to determine if even greater CO_2/N_2 selectivity could be achieved. Unlike the previous binary system which operated at 313 K, this study was performed at 323 K to maximise the potential of the [9a] liquid. The ratio of the liquids was investigated at 30%, 40%, and 50% (v/v) loading of the ionic liquids compared to [9a]. From Figure 5.27(a) and (b), it is clearly evident that the permeability of CO_2 and N_2 follow the trends exhibited in the first binary study with increased amounts of the "secondary" ionic liquid resulting in decreased CO_2 permeability values due to an increasing viscosity. Again, it was observed that this effect was less pronounced on the bis(triflimide) anion due to sulfonyl groups which help increase the liquids affinity for CO_2.

In Figure 5.27(c), the CO_2/N_2 selectivity is presented and again like the previous binary system, there is a no general trend between the CO_2/N_2 selectivity and amount of "secondary" ionic liquid present for the three binary systems studied. In the case of [9c]/[9a] and [9d]/[9a] blends, it is evident that an increase in the amount of the "secondary" ionic liquids in the mixture resulted in a decrease in the permeability values, although not much change in selectivity occurred. However, in the case of the [10a]/[9a][blend, an initial decrease is observed before the selectivity increases sharply to 84 at a 40% (v/v) loading. This sudden increase is related to the decrease in N_2 permeability from 30 - 40%, whereby the permeability of N_2 is halved as the blend takes on characteristics associated with [10a] at the higher loadings. This selectivity value was the highest achieved throughout the study. The selectivity then decreases until 100% [10a] is present.

(a)

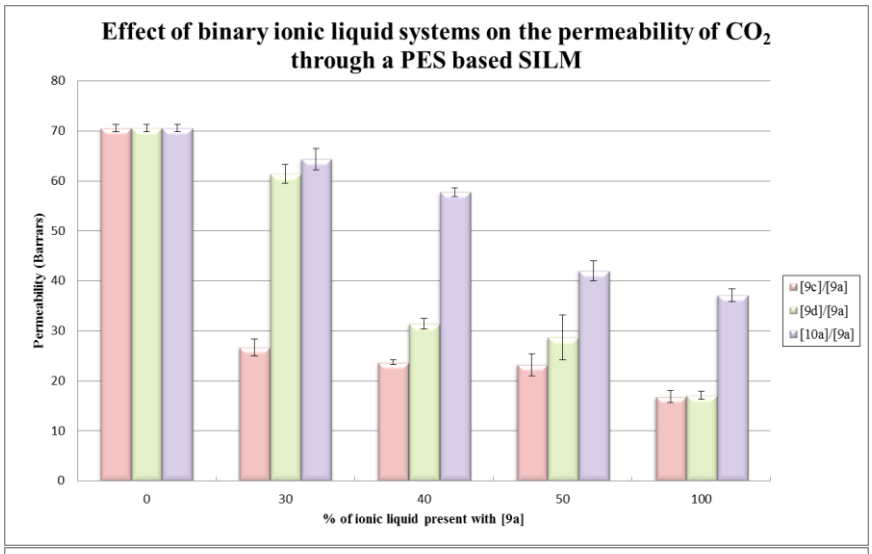

(b)

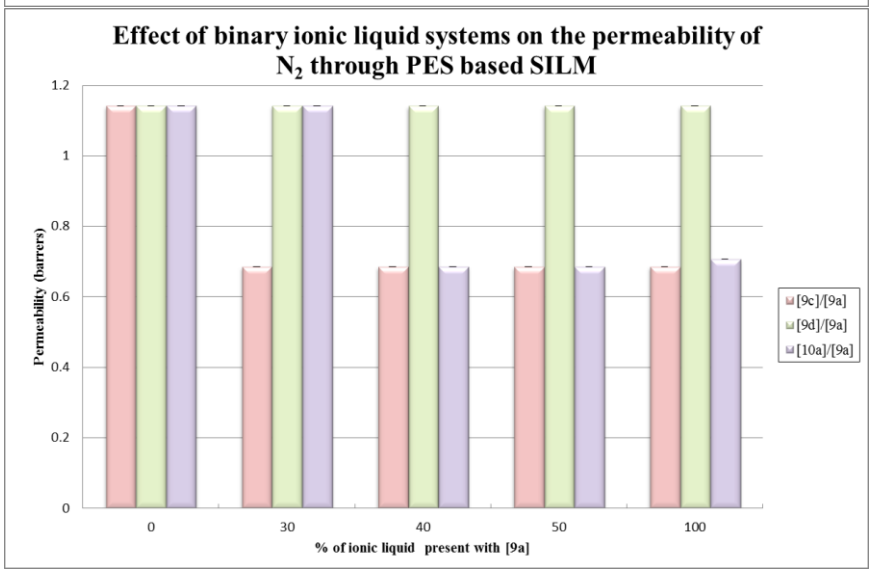

(c)

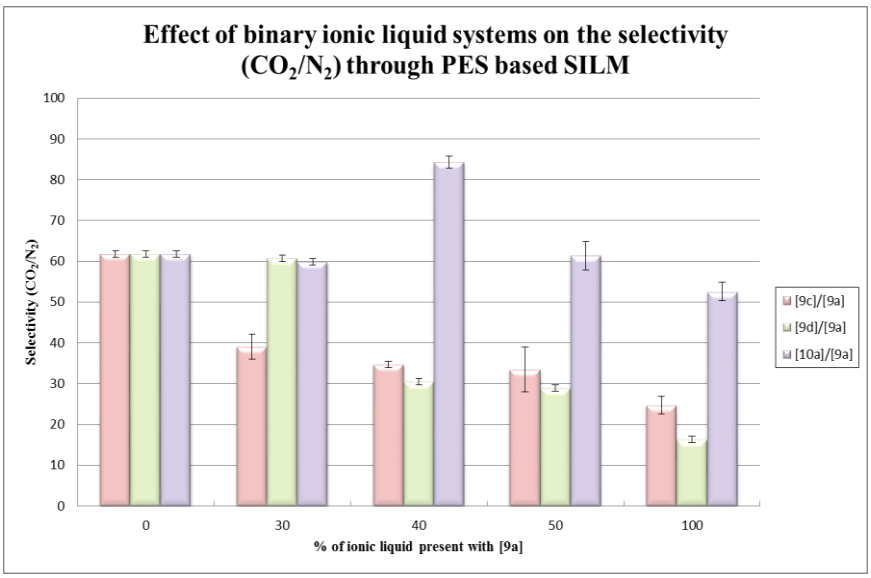

Figure 5.27: Effect of binary ionic liquid mixture with [9a] on (a) the permeability of CO_2, (b) the permeability of N_2, and (c) the CO_2/N_2 selectivity, (n=3).

The diffusion and solubility coefficients of CO_2 again follow similar trends to those observed during the binary ionic liquid study based on [1c], with all systems showing decreases in both diffusion and solubility coefficients as secondary ionic liquid content increases, illustrated in Figure 5.28(a) and (b). Again as was seen in the CO_2 permeability data, the [10a]/[9a] blend has less of a negative effect on the diffusion and solubility coefficients of CO_2 than the other two anions tested. Over the range of [10a]/[9a] mixture studied the solubility coefficients decreased by approximately 20% as opposed to the [9c] and [9d] based systems which showed over a 40% reduction in CO_2 solubility over the same range. This is most likely attributed to the bis(triflimide) anion and inclusion of the morpholine ring into the cation structure present in [10a].

(a)

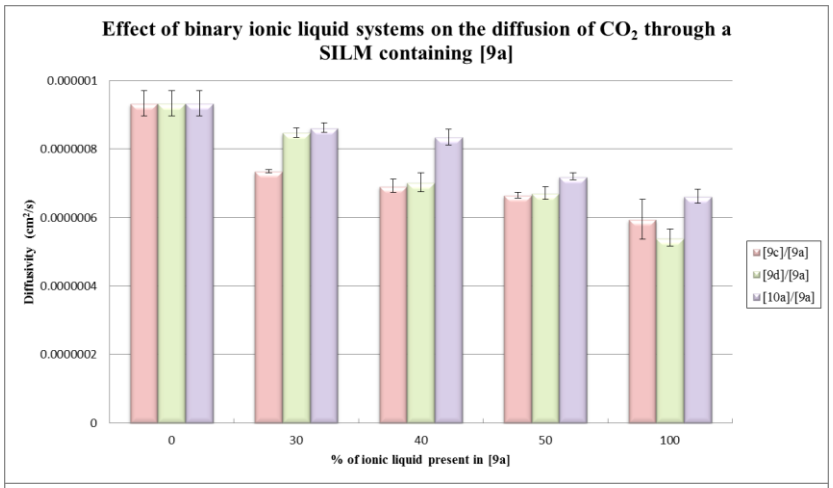

(b)

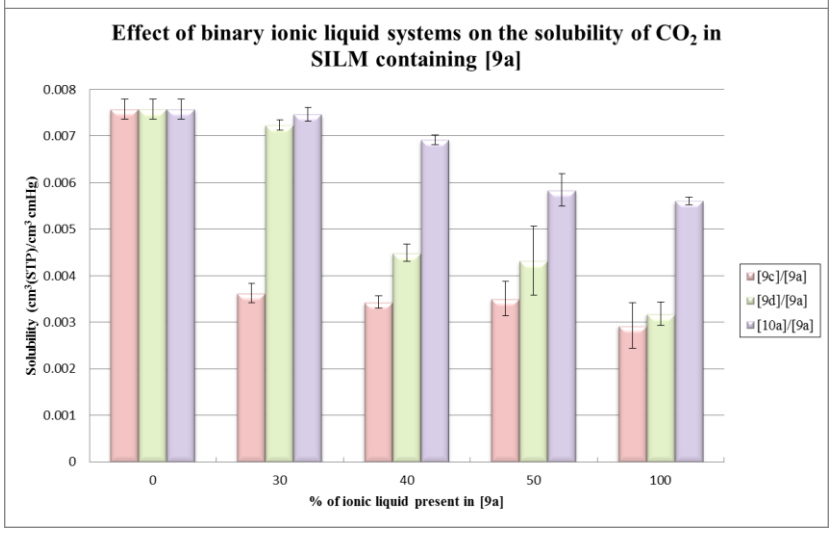

Figure 5.28: Effect of binary ionic liquid systems with [9a] on (a) the diffusion coefficient, and (b) the solubility coefficients of CO_2 in a SILM, (n=3).

5.4 CO_2 absorption studies of ionic liquids with amino acid ionic liquids

Work in this section pertains to investigations of ionic liquids incorporating primary amine functionality and their ability to absorb CO_2 via the reaction shown in Scheme 5.1 whereby the CO_2 is covalently attached to the nitrogen atom of the primary amine. This results in the formation of a new C – N bond with displacement of the H^+ ion which reacts with the amine moiety of a second mole of amine. All results in this section are obtained using a mesoporous silica (MCM-41) which is impregnated with the ionic liquid. The ionic liquids investigated in this section contained amino acid moieties as their anion and provide the source of the primary amine functionality. This method of CO_2 capture has been investigated previously by the use of organic amines, the most notable of which is monoethanolamine (MEA) which has been widely investigated.[48-51] A plethora of mesoporous supports have all been used, all of which have different pore size, functionalities, and surface area, all with the aim of increasing CO_2 absorption.[51,52] There are also several examples of CO_2 absorption studies utilising ionic liquids on these mesoporous silicas, with amino acid based ionic liquids also investigated albeit with alkylated phosphonium cations. These have demonstrated good stability and have undergone multiple CO_2 absorption/desorption cycles with little effect on their absorption capacity.[53] The CO_2 absorption studies were carried out in the University of Limerick.

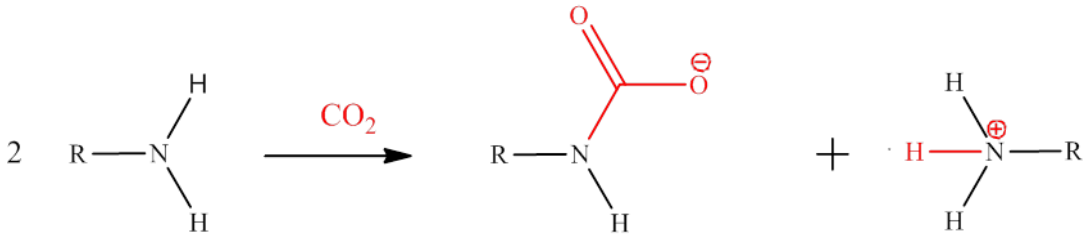

Scheme 5.1: Schematic of the role of amine functionality in the chemical absorption of CO_2.

5.4.1 Characterisation of impregnated MCM-41

Impregnated MCM-41 was the material used in the investigation into the potential use of ionic liquids as CO_2 sorbents. However, due to the use of amino acid based ionic liquids, it was not possible to determine the presence of the ionic liquids in the MCM-41 using EDX analysis, as was the case for the SILM discussed in Section 5.2, due to the absence of a signature element such as sulfur or fluorine in the amino acid. To determine the presence of the ionic liquid on the support, IR spectroscopy was used. From Figure 5.29, the presence of the MCM-41 and the ionic liquid can be clearly seen

that in the IR spectrum of the MCM-41 impregnated with [AAIL17] shown in blue. The peak at 3429 cm^{-1} is assigned as arising from the stretching vibrations of the terminal Si–OH group, and a broad peak 1068 cm^{-1} which corresponds to the internal and external asymmetric Si-O stretching modes of the mesoporous silica. The stretch at 1581 cm^{-1} corresponding to the C=O of the amino acid moiety of the ionic liquid as well as the C-H stretches of the imidazole ring at 2859 cm^{-1} and 2949 cm^{-1} also indicate the presence of the imidazole ring.[54,55]

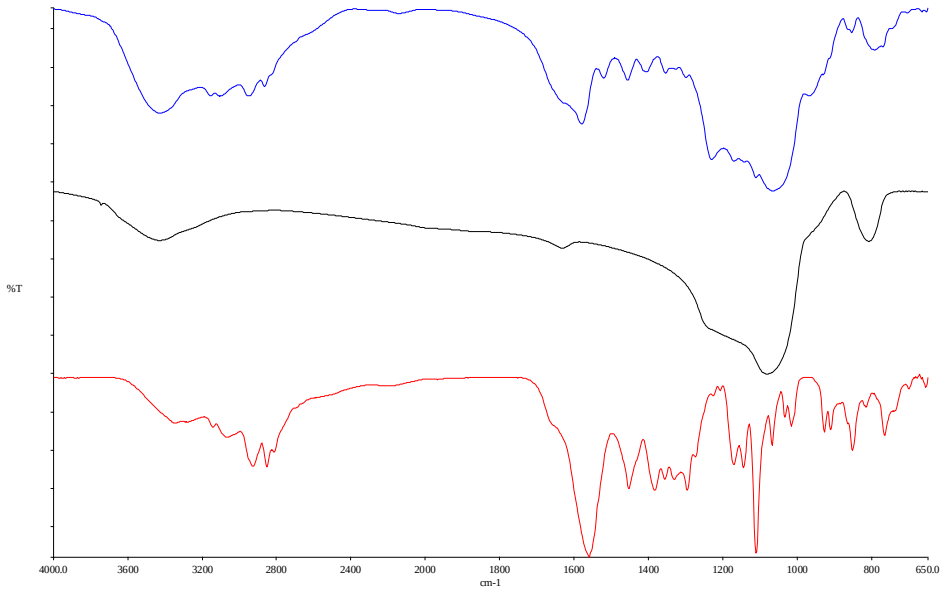

Figure 5.29: Infra-red Spectra of MCM-41 impregnated 1-methyl-3-(pyrrolid-1-yl)ethylimidazolium lysinate (-), MCM-41 (-), and 1-methyl-3-(pyrrolid-1-yl)ethylimidazolium lysinate (-).

5.4.2 Effect of anion variation on the CO_2 absorption

The permeation work presented earlier in this chapter has demonstrated that the anion has a major effect on the CO_2 permeability properties of the ionic liquids. To investigate CO_2 absorption, amino acid anions were employed due to them being naturally abundant, cheap, and a good source of primary amine functionality which have been shown to increase CO_2 absorption through a covalent interaction. This coupled with the potential lower desorption temperatures due to the steric hindrance imposed by the adjacent carbonyl group makes these systems potentially very interesting.[48] Work previously conducted on amino acid based ionic liquids have involved both the incorporation of the amino acid as both the cation by alkylation of the amine or, as the

approach adopted in this study, which involved the formation of the conjugate base which then becomes the anion.[56-60] Examples of these can be shown in Figure 5.30 (a). It would be expected that the cation based amino acid ionic liquids would be viewed as inferior with respect to CO_2 absorption due to the removal of the primary amine functionality thus removing chemical absorption potential of the liquids.

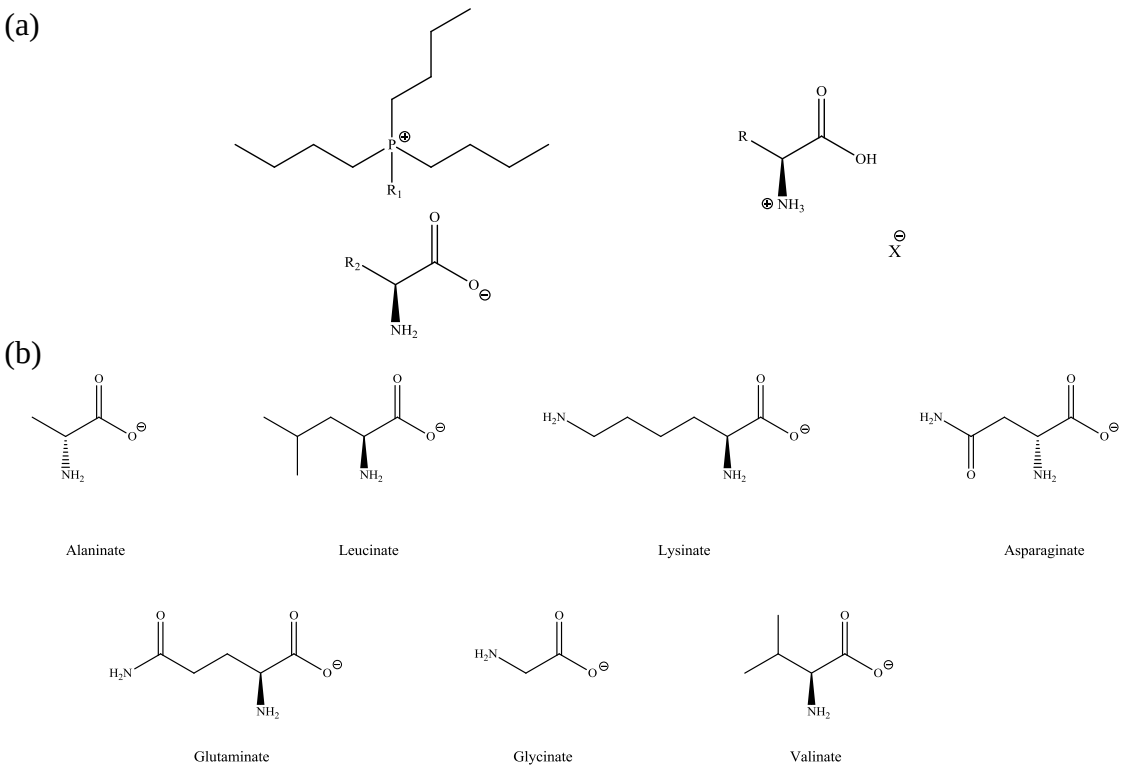

Figure 5.30: (a) Structure of ionic liquids synthesised previously utilising amino acid moieties, and (b) amino acid anions used in the CO_2 absorption studies presented in this thesis.

During this investigation of the anion, 7 ionic liquids, each containing a different amino acid anion (structures shown in Figure 5.30(b)) were tested once, as a preliminary screen to identify the optimum liquids. These were impregnated into the MCM-41 at a 50% weight loading and tested at an absorption temperature of 303 K over 1 cycle. The cation used was the 1-methyl-3-(pyrrolid-1-yl)ethylimidazolium cation due to its lower viscosity values that were identified in Chapter 3. The CO_2 absorption study values are presented in terms of mg/g solid tested whereby the solid represents the mass of the ionic liquid impregnated MCM-41 (Figure 5.31(a)-(c)). Neat MCM-41 has been shown in the literature to have a minor effect on CO_2 absorption with values of 9 mg/g solid tested found.[61] Control experiments conducted by David Madden on the MCM-41 support using the current rig in the University of Limerick found that 3 mg/g solid tested was observed.

(a)

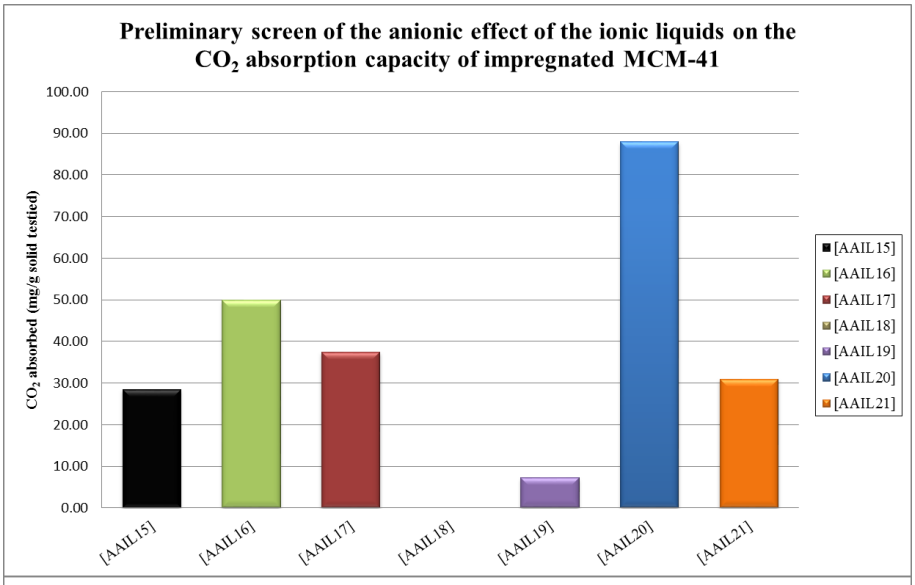

(b)

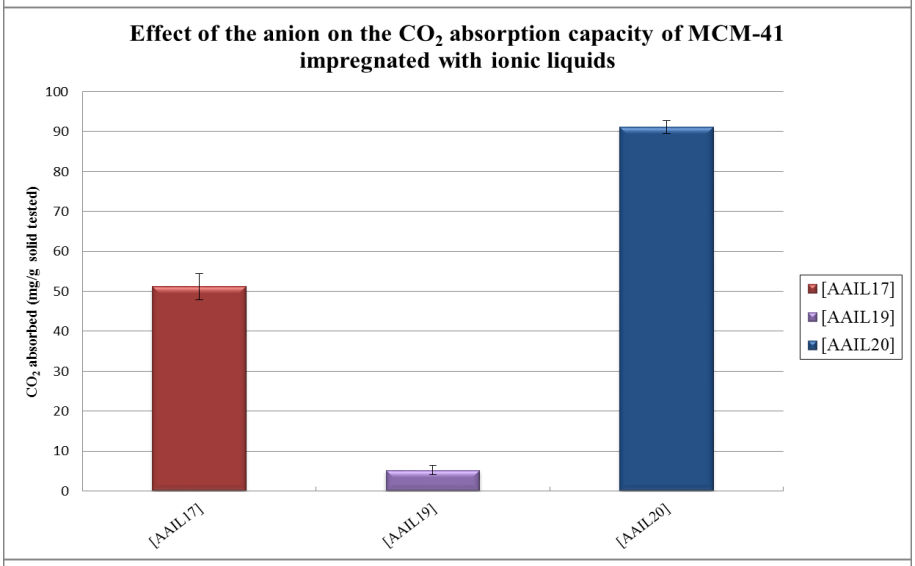

(c)

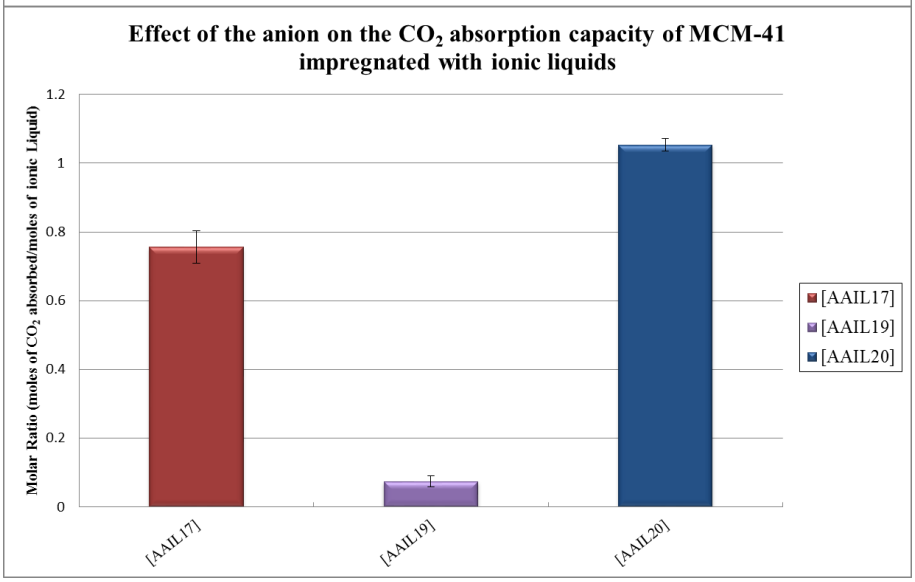

Figure 5.31: (a) Preliminary screen (n = 1), (b) study on 3 ionic liquid (n=3), and (c) molar ratio (n = 3), on the anionic effect for CO_2 absorption capacity at 303 K, pressure (1 bar), 15% CO_2 in He.

From Figure 5.31(a) and (b), it is evident that the choice of anion can have a significant effect on CO_2 absorption. The highest CO_2 absorption value of 88 mg/g solid tested was observed for [AAIL20] which contains the glycinate anion while [AAIL18] which contains the glutamate anion resulted in no uptake of CO_2. In the case of [AAIL17], [AAIL18], and [AAIL19] two amine groups are present on the anion and it was hoped that the incorporation of these units would increase CO_2 uptake but this appeared not to be the case with the [AAIL18] and [AAIL19] demonstrating the lowest CO_2 absorption capacity. The incorporation of these anions resulted in much more viscous ionic liquids due to the increase of hydrogen bonding due to the increased amine and carbonyl functionalities. It is proposed that more viscous ionic liquids result in lower absorption values due to the inability of the gas in question to access amine sites contained underneath the surface of the liquid hence the use of mesoporous silica supports to mitigate this problem.[53,61] In the majority of amino acid ionic liquid CO_2 absorption studies reported, glycinate anions tend to produce less viscous liquid thus making access to the amine sites of the ionic liquids much more probable.[59] In conjunction with that, the glycinate anion can interact with the CO_2 in a way that is not fully understood. Glycinate anions have been reported to undergo irreversible side reactions with CO_2 resulting in the formation of a precipitate which again would increase its potential to absorb CO_2 but limit its reusability.[62]

The mole ratio of CO_2 to ionic liquids are given in Figure 5.31 (c). In work presented by Goodrich *et al.* using the trihexyl(tetradecyl)phosphonium cation in conjunction with amino acid anions, similar molar ratio values of approximately 1.25 were reported for both the glycinate and the lysinate species.[62] The trend is different from results observed during this study. [AAIL20] achieved a molar ratio of greater than 1 with a value of 1.05 while [AAIL17] demonstrated a value of 0.75 at 1 bar. In the study presented in this thesis absorption was determined by heating the sample to 393 K to desorb the CO_2 that had been absorbed, which was monitored by mass spectrometry. It is possible that the temperature was too low to desorb more stable CO_2 which absorbed at the amine site at the end of the butyl chain of the lysinate anion and that the actual amount of CO_2 absorbed was not fully determined. This indeed is very plausible when looking at the optimal desorption profiles as shown in Figure 5.32. In the case of [AAIL20], the proximity of the carbonyl imports steric hindrance on the newly formed C-N bond. [AAIL17] contains the lysinate anion which has a free primary amine at the

end of a free alkyl chain. Chemically absorbed CO_2 as shown in amine technology is much more stable under these conditions and requires higher temperatures to ensure complete removal of the absorbed gas.[48] From Figure 5.32, it is evident that the peak maxima or optimal desorption for all the liquid occurs between 358-363 K temperature range, with the exception of [AAIL17] which contains the lysinate anion. The amount of CO_2 desorbing is still increasing above 373 K and as such has not been determined. As mentioned earlier this increasing stability is an indication of stronger C-N bonds involving the amine at the end of the alkyl chain.

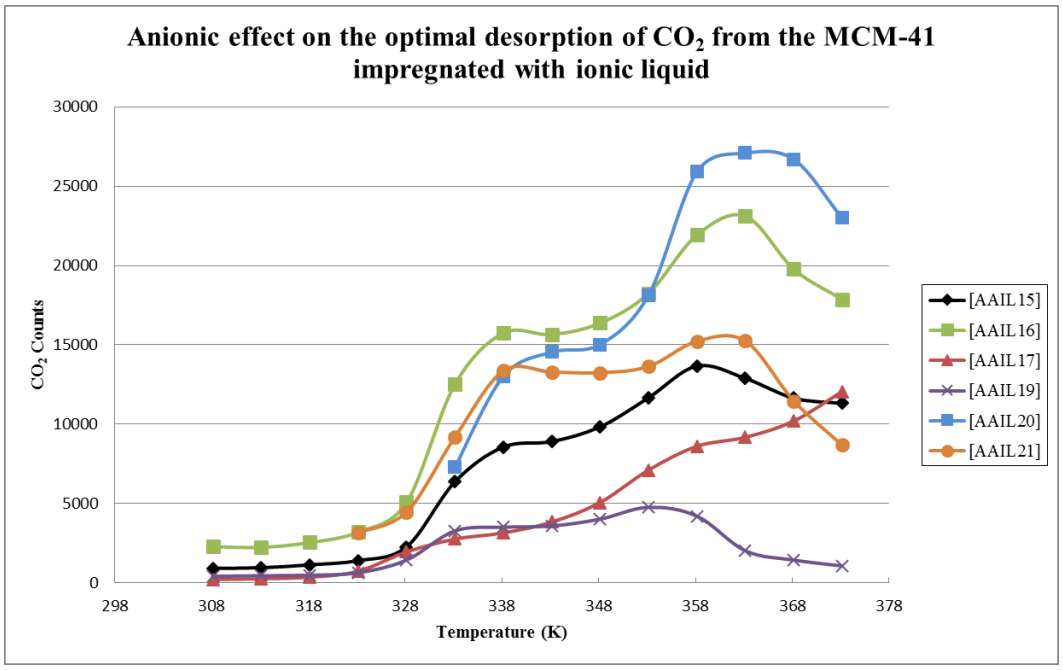

Figure 5.32: Anionic effect on the optimal desorption temperature of CO_2 from the amino acid ionic liquids (n = 1).

The shape of the desorption profiles is also quite interesting as in all cases there appears to be a minor maxima followed by a larger maximum at elevated temperatures except with [AAIL17] where it appears a further maximum may be present, although this seems to occur outside of the temperature range tested. These multiple maxima indicate different strengths of affinity between the ionic liquids and CO_2. Ionic liquids have been shown to absorb by both physical and chemicals means, with the physically absorbed ionic liquid held in place by weaker electrostatic interactions in comparison to the chemically bound CO_2. Therefore it is proposed that the maxima observed in Figure 5.32 are the optimal desorption temperatures of firstly the physically absorbed CO_2 at approximately 338 K and the chemically absorbed CO_2 at 363-368 K. Typical desorption temperatures for amine based technology range from 393 - 413 K and as

such required additional heat than the ionic liquids tested to recover the sample to continue absorbing.[63] This excess energy results in higher operating costs and thus makes the ionic liquid technology more desirable from an energy efficiency standpoint.

5.4.3 Effect of cation variation on CO_2 absorption

While it is widely regarded that the anion typically dictates the properties of ionic liquids, permeability results presented in Section 5.3.2 showed that the cation can also contribute to the diffusivity and solubility coefficients of CO_2.[64,65] Thus a preliminary screening was performed to investigate the effect that the cation might play on the CO_2 absorption characteristics. The cations examined (9a, 10a, 11a) were those illustrated in Figure 5.8 with the exception of [1c] under the same loading conditions (50% weight loading), temperature (313 K), and pressure (1 bar), that were used in the anionic study. The results of this study are presented in Figure 5.30(a) and (b). Due to the high CO_2 absorption values achieved with the glycinate anion, this was used in conjunction with all three cations.

From Figure 5.33(a) and (b) it is clear that the cation does have an effect on the CO_2 absorption capacity of the liquids albeit much less significantly than that exhibited during the anionic study. [AAIL6] shows the highest levels absorbed with 108 mg/g absorbed in comparison to 91 and 55 mg/g for [AAIL20] and [AAIL13], respectively. While [AAIL6] and [AAIL20] values are not too dissimilar, there is significantly less CO_2 absorbed by [AAIL13]. This can potentially be explained by the presence of the morpholine ring. As discussed previously in Section 5.3.2, the morpholine ring has been shown to increase the viscosity of the ionic liquids. This resulted in lower diffusion values during the permeation study and a similar effect may be occurring here. Visual inspection would indicate that the amino acid liquids are more viscous than any of the ionic liquids with the simple anions used during the permeation studies. The presence of the morpholine only serves to further increase the viscosity of the liquids and this probably inhibits movement of the CO_2 through the MCM-41 support, acting like a barrier between the incoming CO_2 and the amine sites in the liquid.

(a)

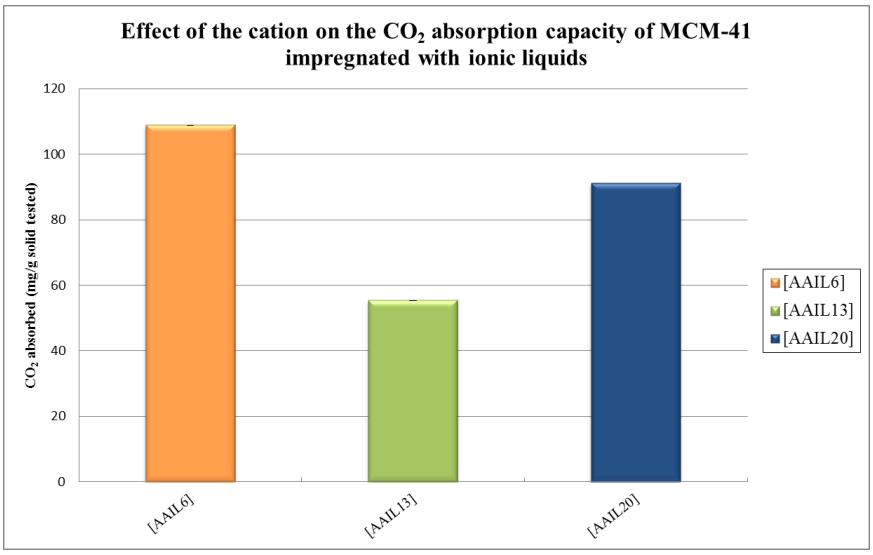

(b)

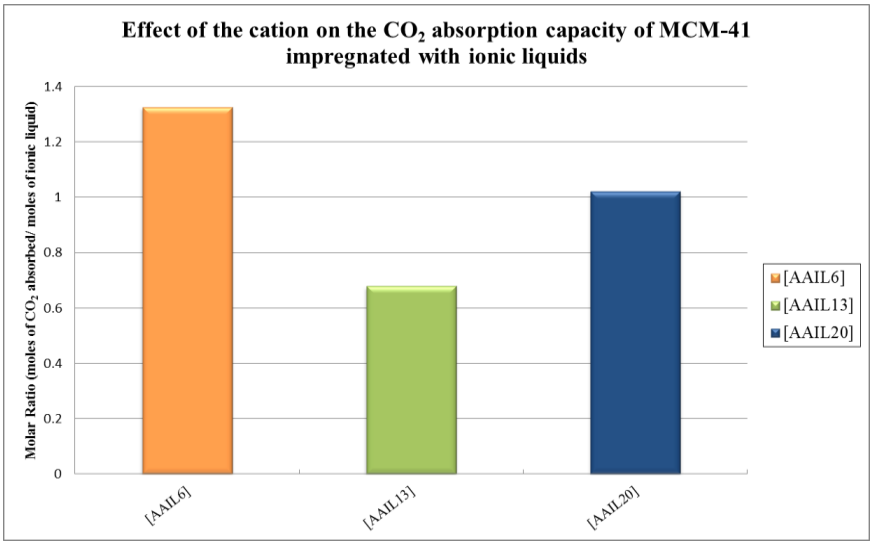

Figure 5.33: Preliminary screen of the effect of the cation on the CO_2 absorption capacity of the ionic liquids present in terms of (a) mg/g solid tested, and (b) molar ratio, (n = 1).

To examine in greater detail the CO_2 absorption capacity of the liquids, the molar ratios were examined as shown in Figure 5.33(b). From this it is clear that [AAIL6] is the superior liquid with a molar ratio of 1.33 in comparison to 1.02 and 0.68 for [AAIL13] and [AAIL20].

5.4.4 Effect of ionic liquid loading on CO_2 absorption capacity

Loading of the ionic liquid can also have an effect on the CO_2 absorption capacity. From the literature it can be seen that increased solvent loading onto a porous material such as silica does not automatically correspond to an increase in CO_2 absorption. [61,66,67] There are many factors that can affect the optimum loading capacity such as viscosity of the organic compound, porosity or surface area of the support, and pores size of the

support.[53,61,63] In work carried out by Goeppert *et al.* the CO_2 absorption as a function of polyethylenimines (PEI) content on a silica based support was investigated.[61] At 70 ^oC, it was found that CO_2 absorption increased as the loading was increased 10% - 50% PEI content, with approximately 35 mg of CO_2 absorbed/g solid tested increasing to 150 mg/g solid tested. Upon increasing the PEI content to 70%, a decrease in CO_2 absorption was observed, 140 mg CO_2 absorbed/g tested. This was attributed to the ease of dispersion of the PEI at the lower loading, allowing easier access of CO_2 to the amine sites. Upon increasing the amine content, several amine sites are now inaccessible to the incoming CO_2, resulting in a decrease in absorption capacity. It is due to this affect that an investigation into the loading was required to examine the potential of increasing the CO_2 absorption capabilities exhibited during the previous studies. During this study loading of the ionic liquid varied from 40-70% weight loading.

Presented in Figure 5.34(a) and (b) is the effect of loading of the ionic liquid onto the MCM-41 silica support utilising two ionic liquids [AAIL17] and [AAIL20]. From this we can see two very different profiles. [AAIL20] exhibits a continuous decrease in CO_2 absorption capacity as ionic liquid content increases, whereas with [AAIL17] an initial increase in CO_2 absorption levels as ionic liquid content increases from 40 – 60% can be seen, before a decrease in CO_2 absorption is observed at loadings higher than 60%. As can be seen from Figure 5.31(b), amine mole content is not a factor in the differences in CO_2 absorption observed for the two liquids. This graph demonstrates that despite similar number of moles of ionic liquid being present, [AAIL20] has a far greater absorption capacity despite two amine groups being present on [AAIL17] in comparison to [AAIL20] which has one. These decreases as mentioned previously are likely due to the amine sites of the ionic liquid becoming inaccessible to the incoming CO_2 gas at higher loadings as the ionic liquid blocks the pore decreasing surface area and pore volume. Due to limited resources surface area and pore volume (Table 5.2) of only the best performing system [AAIL20] was obtained via Brunauer–Emmett–Teller (BET) analysis which was conducted by Neal Leddy at Trinity College Dublin. A general decrease in the surface area was observed with 40% ionic liquid weight loading decreasing the surface area of the MCM-41 from 898.990 $m^{2/}g$ (neat) to 39.185 m^2/g before generally decreasing to 9.005 m^2/g as the ionic liquid content increases to 70% loading. An identical trend was also witnessed in the pore volume obtained via the

Barrett-Joyner-Halenda method with values of 0.468 cm^3/g obtained for neat MCM-41 before a gradual decrease to 0.010 cm^3/g was observed at 70% ionic liquid weight loading. Similar trends have been widely reported in the literature with amine loaded silica studies.[51,68,69]

(a)

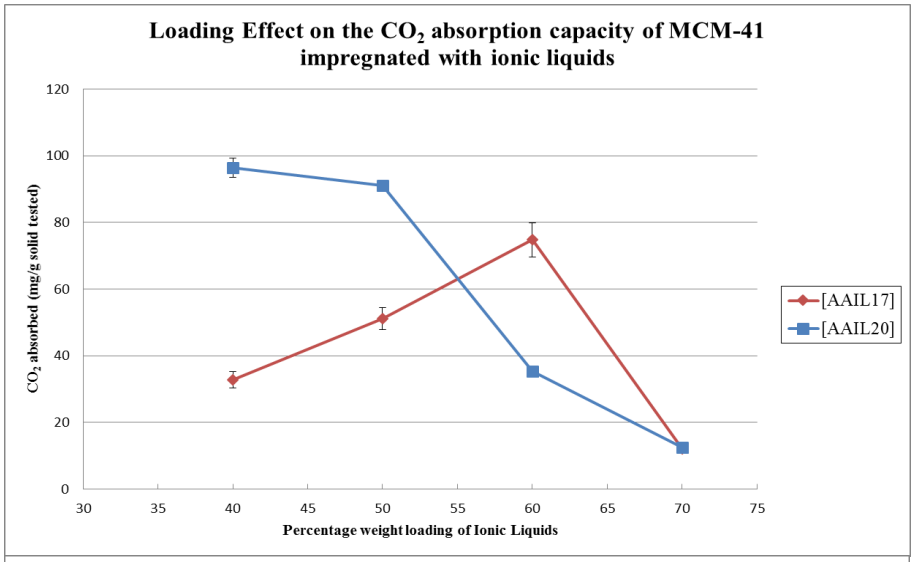

(b)

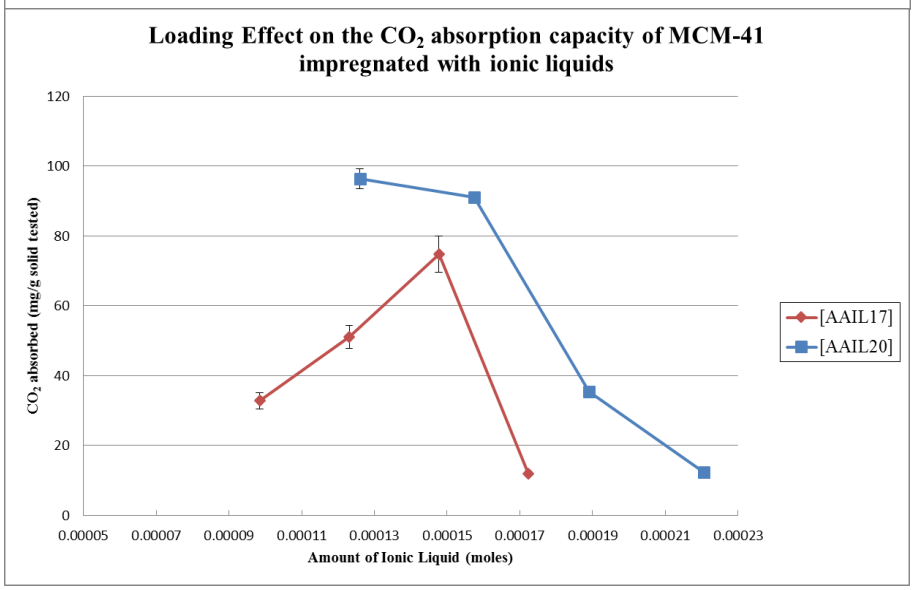

Figure 5.34: Effect of ionic liquid loading on the CO_2 absorption capability of the impregnated silica (n = 3).

Table 5.2: Surface area and pore size analysis of MCM-41 impregnated with [AAIL20].

Loading (%)	Surface Area (BET) (m^2/g)	Pore Volume (BJH) (cm^3/g)
0	898.990	0.468
40	39.185	0.082
50	9.682	0.052
60	30.866	0.035
70	9.005	0.010

5.4.5 Effect of temperature on CO_2 absorption temperature.

Variations in temperature can have a significant effect on the CO_2 absorption capability of sorbents.[61] Worked performed by Chen *et al.* using PEI impregnated in silica showed that absorption initially increased with temperature before a decrease was observed at higher temperatures.[70] This decrease coincided with the desorption temperature of their amine. This trend has also been reproduced in other reports in this area however, the temperature at which CO_2 absorption begins to decrease is dependent on the type of amine employed, with sterically hindered amines much more prone to desorb at lower temperatures.[48]

During the course of this study, the temperature of the silica was increased to mimic elevated temperature conditions that would be present with flue gases in a stripper system. The effect of this temperature change (303 – 333 K) was investigated using the two liquids examined in the loading study, [AAIL 17] containing the lysinate anion and [AAIL 20] containing the glycinate anion (Figure 5.34) at their optimal loadings. In the case of [AAIL 20], an initial increase in CO_2 absorption was observed from 303 – 318 K. It is known that the viscosity of ionic liquids generally decrease with increasing temperatures, a trend which was evident for the ionic liquids containing simple anions which were used in the permeability studies (Figure 5.22) . It is hypothesised that a similar trend occurs with the amino acid ionic liquids studied here. The viscosity of the amino acid ionic liquids were not determined due to time restraints concerning the smaller yields due to purification difficulties, which arose on the scaling up of synthesis, and the workability of the sample due to its "gum – like" appearance. This likely decrease in viscosity could result in greater ease of the gas to access more amine sites present in the ionic liquid as it would result in less resistance of the liquid against gas

penetration, thus increasing CO_2 absorption. From 318 – 333 K, a slight decrease in absorption was noted, 118 – 114 mg/g solid tested. At higher temperatures, absorption of CO_2 is competing with desorption of the CO_2 (Figure 5.35). At 333 K, the initial desorption was observed and this can explain the decrease in the CO_2 absorption in this temperature range despite decreasing viscosity.

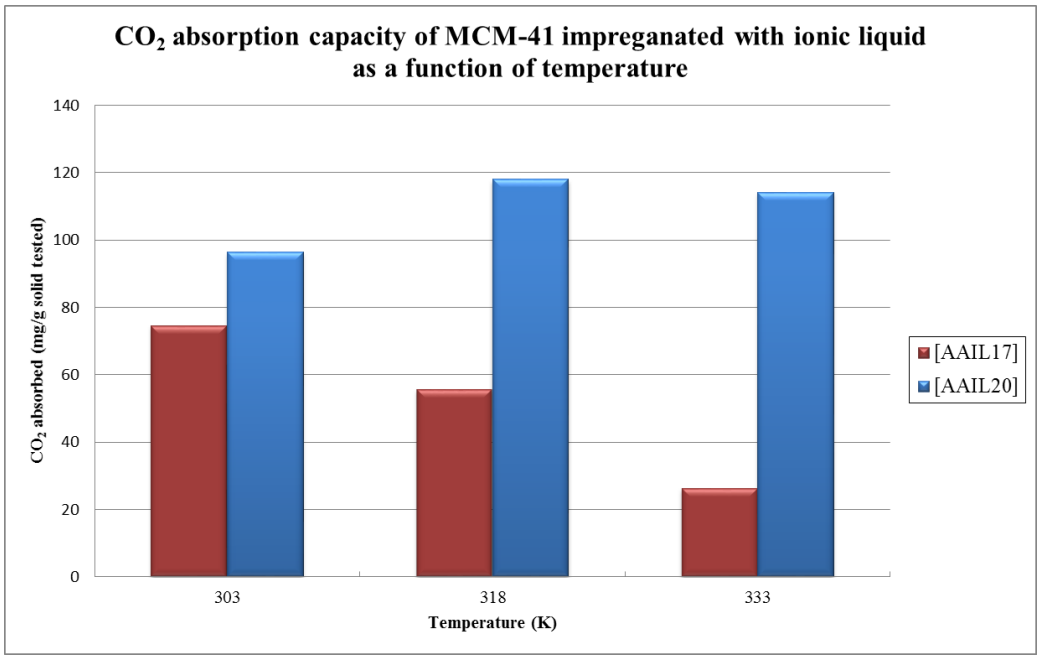

Figure 5.35: Effect of temperature on the CO_2 absorption capacity of the ionic liquids (n = 1).

It is clear from Figure 5.35 that [AAIL 17] (lysinate) acts significantly different to [AAIL 20] upon variation of temperature with a decrease in CO_2 absorption observed across the temperature range whereas with [AAIL 20] (glycinate) an increase in CO_2 absorption with increasing temperatures before a slight decrease is observed. As mentioned earlier the viscosity of these liquids were not obtained in the present study but it was clear from visual observations that the lysinate based is significantly more viscous than its glycinate counterpart and it is likely that this could explain the difference in behaviour. Although viscosity of the ionic liquid will decrease as the temperature increases, the viscosity of the lysinate ionic liquid is still high compared to the glycinate and leaves the amine sites inaccessible to the incoming CO_2 gas. In conjunction with this, upon examination of the structure of the anion, it is clear that the amine site adjacent to the carbonyl is more sterically hindered than its glycinate counterpart. As mentioned earlier in Section 5.4.2, this steric hindrance will result in weaker C–N bond strength and will be easier to break with increased temperature

(energy). At the same time desorption of CO_2 occurs and it is believed that this could be why a general decrease in CO_2 absorption occurs.

5.5 Conclusions

In this chapter a comparative preliminary study was carried out on the permeability of CO_2 and N_2 through SILMs and the absorption of CO_2 silica (MCM-41) impregnated with amino acid functionalised ionic liquids.

It is clear that several parameters affect the performance of CO_2 permeability through the supported ionic liquid membranes with the anion having the most dramatic effect on the permeability. For the range of ionic liquids studied, it was found that the incorporation of the bis(triflimide) anion resulted in the highest CO_2 permeability, diffusion and solubility coefficients. It also was the most effective anion at obtaining good CO_2/N_2 selectivity. It was also determined that cation choice played a role in the permeability of both gases. Incorporation of an oxygen atom in the cation resulted in a decrease in both the permeability and diffusion coefficients of CO_2 in the ionic liquid, however an increase in solubility coefficients was observed. This is likely due to the increased polarity of the ionic liquid, increasing the CO_2 affinity for the liquid resulting in lower diffusion coefficients and permeability values.

Temperature was shown to have an effect on the permeability of the ionic liquids, with all ionic liquids showing an increase in permeability for both gases upon heating. Diffusion coefficients were also shown to increase while decreases in solubility coefficients were observed for both gases. Selectivity (CO_2/N_2) values were shown to increase from room temperature to around 313 - 323 K before selectivity values decreased due to rising N_2 permeability at elevated temperatures. Viscosity was determined to be a major factor in affecting the permeability of both gases through the SILM. In terms of CO_2, increased diffusion coefficients and permeability measurements were observed with decreasing viscosity due to increasing temperatures. However viscosity was not the only factor influencing the permeability of CO_2. This was much more evident at elevated temperatures (approximately 343 K) whereby the majority of the ionic liquids displayed similar viscosity values, indicating that the

functionalities of the ionic liquids could also be affecting CO_2 and N_2 permeability values.

The supporting membrane was also shown to have an effect on the gas permeability properties. Membrane swelling was also observed in nylon and cellulose acetate membranes and we hypothesise that this was the cause of the decreases in permeability, solubility coefficients, and diffusion coefficients of CO_2 in comparison to that observed with the same liquid using the PES membrane. This may be due to the increased levels of ionic liquid present in the polymer matrix. The polymers also proved to be quite stable, with permeability and selectivity remaining constant over 10 cycles of measurements.

The investigation into the use of binary ionic liquid systems as CO_2 separation media has not been previously investigated to the best of our knowledge and yielded some promising results with CO_2/N_2 selectivity values increasing in some cases. For example, an increase was observed with the 40/60 (v/v) [10a]/[9a] blend demonstrating a selectivity value of 84 as opposed to 71 observed for the pure [9a] liquid at 323 K. These look even more favourable when compared to selectivity values of 23, 56, and 40 reported using the bis(triflimide), dicyanamide, and trifluoroacetate anions with the EMIM cation.[13] This illustrates the potential of these types of systems and opens a new avenue of investigation for ionic liquid systems.

When examining the amino acid functionalised ionic liquids as potential CO_2 absorption materials, similar trends were found to those observed in the gas permeability studies. While the cation was shown to have some effect on the CO_2 absorption capacity of the ionic liquid/silica, it was clear that the anion had the most dramatic effect. CO_2 absorption values ranged widely from 90 mg/g solid tested for [AAIL20] to 7 mg/g solid tested observed for [AAIL19] at 50% weight loading of the ionic liquid into the MCM-41 at 298 K. Although the viscosity values were not obtained in the current study, the literature suggests that viscosity differences of the ionic liquids are the most likely cause of these differences. The desorption profiles also suggest that two absorption process are occurring with the presence of two peak maxima at approximately 338 K and 363 K (Figure 5.32), and seem to indicate that both physical and chemical absorption of CO_2 into the ionic liquid/MCM-41 is occurring.

Loading of the ionic liquid into the silica was also examined and an effect was observed. The data obtained for [AAIL20] suggests a decrease in CO_2 absorption as the amount of ionic liquid in the silica increases, whereas in the case of [AAIL17] an increase in CO_2 absorption is observed over 40 – 60% ionic liquid weight loading before CO_2 absorption decreases over the 60 – 70% ionic liquid weight loading. It is hypothesised that these differences in trends may be as a result of the higher viscosity of [AAIL17] (visual observation), making it more difficult for the ionic liquid to evenly coat the silica surface at the 40% weight loading. It was shown from BET and BJH analysis that both surface area and pore volume of the MCM-41 decreased with increased [AAIL 20] loading. This should result in a reduction of amine sites accessible to the CO_2 gas and thus a decrease in CO_2 absorption. Temperature was also shown to have an effect on absorption of CO_2 with CO_2 absorption values increasing from 303 - 318 K before decreasing from 318 – 333K for [AAIL17], whereas for [AAIL20] a general decrease in CO_2 absorption was observed. The decrease in CO_2 absorption is a result of competing desorption process of the ionic liquids at elevated temperatures. The temperature at which the ionic liquid can be recycled (i.e. desorb CO_2 which has been absorbed to complete another cycle) was found to be lower than that of typical amines. MEA which has a typical desorption range of 393 – 413 K is significantly higher than that of the ionic liquids tested as part of this study (338 – 363 K). Therefore it requires less energy to regenerate the ionic liquid and thus, makes them attractive as CO_2 absorbents in this regard.[5,48,49,71,72]

5.6 References

(1) Yamasaki, A. *Journal of Chemical Engineering of Japan* **2003**, *36*, 361.

(2) Scovazzo, P.; Kieft, J.; Finan, D. A.; Koval, C.; DuBois, D.; Noble, R. *Journal of Membrane Science* **2004**, *238*, 57.

(3) Zou, J.; Ho, W. S. W. *Journal of Membrane Science* **2006**, *286*, 310.

(4) Yang, H.; Xu, Z.; Fan, M.; Gupta, R.; Slimane, R. B.; Bland, A. E.; Wright, I. *Journal of Environmental Sciences-China* **2008**, *20*, 14.

(5) Aaron, D.; Tsouris, C. *Separation Science and Technology* **2005**, *40*, 321.

(6) Neves, L. A.; Crespo, J. G.; Coelhoso, I. M. *Journal of Membrane Science* **2010**, *357*, 160.

(7) He, X.; Lie, J. A.; Sheridan, E.; Hagg, M.-B. *Industrial & Engineering Chemistry Research* **2011**, *50*, 2080.

(8) Bara, J. E.; Gabriel, C. J.; Lessmann, S.; Carlisle, T. K.; Finotello, A.; Gin, D. L.; Noble, R. D. *Industrial & Engineering Chemistry Research* **2007**, *46*, 5380.

(9) Bara, J. E.; Lessmann, S.; Gabriel, C. J.; Hatakeyama, E. S.; Noble, R. D.; Gin, D. L. *Industrial & Engineering Chemistry Research* **2007**, *46*, 5397.

(10) Bara, J. E.; Gabriel, C. J.; Hatakeyama, E. S.; Carlisle, T. K.; Lessmann, S.; Noble, R. D.; Gin, D. L. *Journal of Membrane Science* **2008**, *321*, 3.

(11) Erdni-Goryaev, E. M.; Alent'ev, A. Y.; Belov, N. A.; Ponkratov, D. O.; Shaplov, A. S.; Lozinskaya, E. I.; Vygodskii, Y. S. *Petroleum Chemistry* **2012**, *52*, 494.

(12) Hanioka, S.; Maruyama, T.; Sotani, T.; Teramoto, M.; Matsuyama, H.; Nakashima, K.; Hanaki, M.; Kubota, F.; Goto, M. *Journal of Membrane Science* **2008**, *314*, 1.

(13) Scovazzo, P. *Journal of Membrane Science* **2009**, *343*, 199.

(14) Gan, Q.; Rooney, D.; Xue, M.; Thompson, G.; Zou, Y. *Journal of Membrane Science* **2006**, *280*, 948.

(15) Gan, Q.; Rooney, D.; Zou, Y. *Desalination* **2006**, *199*, 535.

(16) Myers, C.; Pennline, H.; Luebke, D.; Ilconich, J.; Dixon, J. K.; Maginn, E. J.; Brennecke, J. F. *Journal of Membrane Science* **2008**, *322*, 28.

(17) Bara, J. E.; Gabriel, C. J.; Carlisle, T. K.; Camper, D. E.; Finotello, A.; Gin, D. L.; Noble, R. D. *Chemical Engineering Journal* **2009**, *147*, 43.

(18) Belfer, S.; Fainchtain, R.; Purinson, Y.; Kedem, O. *Journal of Membrane Science* **2000**, *172*, 113.

(19) de los Rios, A. P.; Hernandez-Fernandez, F. J.; Tomas-Alonso, F.; Palacios, J. M.; Gomez, D.; Rubio, M.; Villora, G. *Journal of Membrane Science* **2007**, *300*, 88.

(20) Jindaratsamee, P.; Shimoyama, Y.; Morizaki, H.; Ito, A. *Journal of Chemical Thermodynamics* **2011**, *43*, 311.

(21) Raveendran, P.; Wallen, S. L. *Journal of the American Chemical Society* **2002**, *124*, 12590.

(22) Bonhote, P.; Dias, A. P.; Papageorgiou, N.; Kalyanasundaram, K.; Gratzel, M. *Inorganic Chemistry* **1996**, *35*, 1168.

(23) Seddon, K. R.; Stark, A.; Torres, M. J. *Clean Solvents: Alternative Media for Chemical Reactions and Processing* **2002**, *819*, 34.

(24) Gomes, M. F. C.; Padua, A. A. H. *Journal of Physical Chemistry B* **2003**, *107*.

(25) Diep, P.; Jordan, K. D.; Johnson, J. K.; Beekman, E. J. *Journal of Physical Chemistry A* **1998**, *102*, 2231.

(26) Cece, A.; Jureller, S. H.; Kerschner, J. L.; Moschner, K. F. *Journal of Physical Chemistry* **1996**, *100*, 7435.

(27) Mahurin, S. M.; Dai, T.; Yeary, J. S.; Luo, H.; Dai, S. *Industrial & Engineering Chemistry Research* **2011**, *50*, 14061.

(28) Mahurin, S. M.; Hillesheim, P. C.; Yeary, J. S.; Jiang, D.-e.; Dai, S. *RSC Advances* **2012**, *2*, 11813.

(29) Scovazzo, P.; Havard, D.; McShea, M.; Mixon, S.; Morgan, D. *Journal of Membrane Science* **2009**, *327*, 41.

(30) Finotello, A.; Bara, J. E.; Camper, D.; Noble, R. D. *Industrial & Engineering Chemistry Research* **2008**, *47*, 3453.

(31) Bara, J. E.; Carlisle, T. K.; Gabriel, C. J.; Camper, D.; Finotello, A.; Gin, D. L.; Noble, R. D. *Industrial & Engineering Chemistry Research* **2009**, *48*, 2739.

(32) Ferguson, L.; Scovazzo, P. *Industrial & Engineering Chemistry Research* **2007**, *46*, 1369.

(33) Aki, S.; Mellein, B. R.; Saurer, E. M.; Brennecke, J. F. *Journal of Physical Chemistry B* **2004**, *108*, 20355.

(34) Anthony, J. L.; Anderson, J. L.; Maginn, E. J.; Brennecke, J. F. *Journal of Physical Chemistry B* **2005**, *109*, 6366.

(35) Sharma, P.; Park, S. D.; Baek, I. H.; Park, K. T.; Yoon, Y. I.; Jeong, S. K. *Fuel Processing Technology* **2012**, *100*, 55.

(36) Blanchard, L. A.; Gu, Z. Y.; Brennecke, J. F. *Journal of Physical Chemistry B* **2001**, *105*, 2437.

(37) Kilaru, P. K.; Scovazzo, P. *Industrial & Engineering Chemistry Research* **2008**, *47*, 910.

(38) Bara, J. E.; Hatakeyama, E. S.; Gabriel, C. J.; Zeng, X.; Lessmann, S.; Gin, D. L.; Noble, R. D. *Journal of Membrane Science* **2008**, *316*, 186.

(39) Jiang, Y.; Wu, Y.; Wang, W.; Li, L.; Zhou, Z.; Zhang, Z. *Chinese Journal of Chemical Engineering* **2009**, *17*, 594.

(40) Luis, P.; Neves, L. A.; Afonso, C. A. M.; Coelhoso, I. M.; Crespo, J. G.; Garea, A.; Irabien, A. *Desalination* **2009**, *245*, 485.

(41) Pereiro, A. B.; Tome, L. C.; Martinho, S.; Rebelo, L. P. N.; Marrucho, I. M. *Industrial & Engineering Chemistry Research* **2013**, *52*, 4994.

(42) Teramoto, M.; Nakai, K.; Ohnishi, N.; Huang, Q. F.; Watari, T.; Matsuyama, H. *Industrial & Engineering Chemistry Research* **1996**, *35*, 538.

(43) Park, Y.-I.; Kim, B.-S.; Byun, Y.-H.; Lee, S.-H.; Lee, E.-W.; Lee, J.-M. *Desalination* **2009**, *236*, 342.

(44) Swatloski, R. P.; Spear, S. K.; Holbrey, J. D.; Rogers, R. D. *Journal of the American Chemical Society* **2002**, *124*, 4974.

(45) Zhu, S. D.; Wu, Y. X.; Chen, Q. M.; Yu, Z. N.; Wang, C. W.; Jin, S. W.; Ding, Y. G.; Wu, G. *Green Chemistry* **2006**, *8*, 325.

(46) Barghi, S. H.; Adibi, M.; Rashtchian, D. *Journal of Membrane Science* **2010**, *362*, 346.

(47) Ilconich, J.; Myers, C.; Pennline, H.; Luebke, D. *Journal of Membrane Science* **2007**, *298*, 41.

(48) Sartori, G.; Savage, D. W. *Industrial & Engineering Chemistry Fundamentals* **1983**, *22*, 239.

(49) Filburn, T.; Helble, J. J.; Weiss, R. A. *Industrial & Engineering Chemistry Research* **2005**, *44*, 1542.

(50) Gray, M. L.; Hoffman, J. S.; Hreha, D. C.; Fauth, D. J.; Hedges, S. W.; Champagne, K. J.; Pennline, H. W. *Energy & Fuels* **2009**, *23*, 4840.

(51) Wei, J.; Liao, L.; Xiao, Y.; Zhang, P.; Shi, Y. *Journal of Environmental Sciences-China* **2010**, *22*, 1558.

(52) Hicks, J. C.; Drese, J. H.; Fauth, D. J.; Gray, M. L.; Qi, G.; Jones, C. W. *Journal of the American Chemical Society* **2008**, *130*, 2902.

(53) Zhang, J.; Zhang, S.; Dong, K.; Zhang, Y.; Shen, Y.; Lv, X. *Chemistry-a European Journal* **2006**, *12*, 4021.

(54) Bhoware, S. S.; Singh, A. P. *Journal of Molecular Catalysis a-Chemical* **2007**, *266*, 118.

(55) Selvaraj, M.; Pandurangan, A.; Seshadri, K. S.; Sinha, P. K.; Lal, K. B. *Applied Catalysis a-General* **2003**, *242*, 347.

(56) Tao, G.-h.; He, L.; Liu, W.-s.; Xu, L.; Xiong, W.; Wang, T.; Kou, Y. *Green Chemistry* **2006**, *8*, 639.

(57) Jiang, Y.-Y.; Wang, G.-N.; Zhou, Z.; Wu, Y.-T.; Geng, J.; Zhang, Z.-B. *Chemical Communications* **2008**, 505.

(58) He, L.; Tao, G.-H.; Parrish, D. A.; Shreeve, J. n. M. *Journal of Physical Chemistry B* **2009**, *113*, 15162.

(59) Zhang, Y.; Zhang, S.; Lu, X.; Zhou, Q.; Fan, W.; Zhang, X. *Chemistry-a European Journal* **2009**, *15*, 3003.

(60) Kagimoto, J.; Taguchi, S.; Fukumoto, K.; Ohno, H. *Journal of Molecular Liquids* **2010**, *153*, 133.

(61) Goeppert, A.; Meth, S.; Prakash, G. K. S.; Olah, G. A. *Energy & Environmental Science* **2010**, *3*, 1949.

(62) Goodrich, B. F.; de la Fuente, J. C.; Gurkan, B. E.; Lopez, Z. K.; Price, E. A.; Huang, Y.; Brennecke, J. F. *Journal of Physical Chemistry B* **2011**, *115*, 9140.

(63) Yu, C.-H.; Huang, C.-H.; Tan, C.-S. *Aerosol and Air Quality Research* **2012**, *12*, 745.

(64) Pringle, J. M.; Golding, J.; Baranyai, K.; Forsyth, C. M.; Deacon, G. B.; Scott, J. L.; MacFarlane, D. R. *New Journal of Chemistry* **2003**, *27*, 1504.

(65) Tokuda, H.; Hayamizu, K.; Ishii, K.; Abu Bin Hasan Susan, M.; Watanabe, M. *Journal of Physical Chemistry B* **2004**, *108*, 16593.

(66) Xu, X. C.; Song, C. S.; Andresen, J. M.; Miller, B. G.; Scaroni, A. W. *Energy & Fuels* **2002**, *16*, 1463.

(67) Yue, M. B.; Sun, L. B.; Cao, Y.; Wang, Z. J.; Wang, Y.; Yu, Q.; Zhu, J. H. *Microporous and Mesoporous Materials* **2008**, *114*, 74.

(68) Chen, C.; Yang, S.-T.; Ahn, W.-S.; Ryoo, R. *Chemical Communications* **2009**, 3627.

(69) Heydari-Gorji, A.; Belmabkhout, Y.; Sayari, A. *Langmuir* **2011**, *27*, 12411.

(70) Chen, C.; Son, W.-J.; You, K.-S.; Ahn, J.-W.; Ahn, W.-S. *Chemical Engineering Journal* **2010**, *161*, 46.

(71) Yeh, A. C.; Bai, H. L. *Science of the Total Environment* **1999**, *228*, 121.

(72) Zhou, S.; Wang, S.; Chen, C. *Industrial & Engineering Chemistry Research* **2012**, *51*, 2539.

Chapter 6:

Future Work

6.1 Introduction

As shown in Chapter 3 and 4, during the course of this study, ionic liquids containing both imidazolium and phosphonium cations were successfully synthesised incorporating several functionalities. All of which were characterised using IR, NMR spectroscopy, and Mass spectrometry. In some cases other characterisation was performed and T_{onset}, viscosity and refractive indices were obtained for those which were prioritised as part of the permeation studies, however these involve only a sample of all those ionic liquids which were synthesised. Therefore going forward it would be worthwhile completing the analysis of the physical properties of the remaining ionic liquids, in particular the amino acid ionic liquids whose viscosity for example were not determined due to their gum like nature and difficulty in transference from one vessel to another. As seen in Chapter 3, the determination of melting points using low tempertaure DSC proved difficult due to the lack of a clear sharp endothermic process which may be due to the T_m values being lower than the -50 ^oC to which the experiments were conducted, or also due to the rapid rate of cooling of the ionic liquids, forming glasses upon cooling resulting in the lack of a clearly defined melting point. It would be of interest to repeat the experiments at various cooling rates to investigate whether melting points could be resolved.

As seen in Chapter 4, pyrrole based ionic liquids monomers were successfully synthesised from which the corresponding polymers were grown electrochemically. This opens up an exciting new avenue of investigation with several applications possible in gas capture technology as well as others such as antimicrobial agents for which phosphonium salts have gained some attention.[1] Potentially one extension of the pyrrole ionic liquid polymers is via incorporation of the amino acid anions such as glycinate, the incorporation of which were successful during the imidazolium ionic liquids synthesis (Chapter 3). This would allow for polymers capable of physical fixation of CO_2 and as ionic liquids could be impregnated into the pores of the pyrrole ionic liquid polymer, a membrane could be produced that was capable of both physical and chemical absorption of CO_2.[2]

In terms of the gas permeability studies there are several future avenues of investigation which could progress this work significantly resulting in an even more comprehensive study. As shown from the binary ionic liquid systems, it was clearly evident that this

had a beneficial effect on the CO_2/N_2 separating ability of the supported ionic liquid membrane with results increasing from 60 for neat [9a] liquid, to 84 for 40/60 (v/v) [10a]/[9a] mixture. Therefore it is believed that these type of systems warrant further investigation, in particular using low viscosity ionic liquids as the main liquid present. From the literature a lot of data have been recorded using supported ionic liquids membranes whereby ionic liquid EMIM Tf_2N was used.[3] CO_2 permeability values were significantly higher when EMIM Tf_2N was used in comparison to those obtained with the BMIM Tf_2N, therefore loading of the ionic liquids presented in this thesis in different ratios with the EMIM Tf_2N is an avenue which could result in even greater selectivity values. Feed pressure could also play a crucial role in increased permeability and selectivity values for these gases. Increased pressures of gases can significantly increase the permeability and selectivity of the gases, which has been described in the literature.[4] Unfortunately due to limitations of the experimental set up, only feed pressure of 1 bar could be used, and thus these systems could be explored at elevated pressure over temperature ranges like those presented in Chapter 5, or using the different polymeric supports to establish the benefits that this may have on selectivity values.

The choice of gases presented in this work were limited with only CO_2 and N_2 in flue gases investigated. This of course is only a small sample of the gases which are present, with H_2S, SO_2, N_2O, O_2, and CH_4 among those also present, and these have been investigated with other systems.[5-8] Of those listed above the greatest of interest to researchers are those of SO_2 and CH_4. SO_2 behaves similarily to CO_2 and as such obtaining a material which can selectively separate CO_2 and SO_2 is difficult. Methane is of course another gas of interest but permeability of the gas through ionic liquids is typically slower than that of nitrogen which would prove problematic due to the proximity of the nitrogen data to the limit of the experimental set up when the leak rate is taken into account.[6] It is this which prevented investigations into methane on our rig in its current configuration and thus these investigations could be carried out on another rig. Another important consideration is the purity of the ionic liquids when investigating gas permeability. As seen in Section 1.9 impurities such as water and chlorides can have a large effect on the viscosity of these liquids which in turn affects the permeability. During the course of this study ionic liquids were considered free from chloride when they passed the silver nitrate test however traces may remain and as

such an extension of the current work would be to quantify the levels present using chloride sensors. Water content could also be determined using Karl Fisher titrations. Although as ionic liquids are hygroscopic, water content will change when they are exposed to the air

The CO_2 absorption studies of the ionic liquids demonstrated some promise, with the AAILs successfully capable of absorbing CO_2. However, it must be stressed that this is very much a preliminary study. For completeness in the future a more extensive study on the effect of the cation as well as temperature should be carried out. From Chapter 4, it was observed that temperature has a significant effect on the CO_2 absorption values however only 3 temperature points were examined with a difference of 15 K between each point. As with both ionic liquids tested, an increase followed by a decrease was observed. It is probable that investigation of the temperature range 313 – 328 K may result in increased CO_2 absorption values before the desorption process at elevated temperatures competes with the absorption. The largest omission from this work is the reusability of the materials as in an industrial setting the material would have to withstand constant absorption/desorption cycles. While all ionic liquids demonstrated good thermal stability (T_{onset}), the effect of constant elevated temperatures on a mesoporous silica support was not investigated and depending on the liquid in question this can result in gradual decomposition of the material. It should be noted that there is a temperature lag experienced with ionic liquids whereby the temperature recorded by the equipment may not be the temperature of the liquid. It would prove wise to conduct experiments involving multiple absorption/desorption cycles to investigate this stability, as well as TGA on neat ionic liquids and the ionic liquids on the solid support at various temperatures held for constant time lengths to monitor their thermal stability.

The effect of the silica support is also an area which was not investigated during the course this study. Blocking of the pores was observed by BET analysis of the MCM-41 impregnated with [AAIL20] by a decrease in both the surface area and pore volume values. Therefore it is clear that the support plays a crucial role in the gas capture properties and as such this may be manipulated to enhance CO_2 absorption via increase surface area, although this could potentially be negated due to the resulting decrease in pore volume. Our collaborators, Dr Teresa Curtin's research group (University of Limerick) have experience with mesoporous silicas, so expansion of the work presented

to incorporate supports such as SBA-15 and zeolites which tend to have larger pore size, is quite feasible.

Absorption studies should be carried out with realistic flue gas system whereby other gases such as those mentioned earlier are included into the CO_2 gas feed to fully assess the potential of these materials in a real CO_2 stripper unit. As evident from these experiments, the conditions used are "quite ideal" with no competing gases present as such a comparison investigation into levels of CO_2 absorbed in both ideal and mixed gas feels is most definitely of interest. In conjunction with this the presence of water vapour must be investigated due to its abundance in both flue gases and the atmosphere. Studies performed indicate that inclusion of water vapour can aid in CO_2 absorption however there is a threat that this may also reduce absorption levels due to the ionic liquids solubility towards water increasing the risk of the ionic liquid being removed from the silica's pores.[9]

6.2 References

(1) Cieniecka-Roslonkiewicz, A.; Pernak, J.; Kubis-Feder, J.; Ramani, A.; Robertson, A. J.; Seddon, K. R. *Green Chemistry* 2005, *7*, 855.

(2) Bara, J. E.; Lessmann, S.; Gabriel, C. J.; Hatakeyama, E. S.; Noble, R. D.; Gin, D. L. *Industrial & Engineering Chemistry Research* 2007, *46*, 5397.

(3) Scovazzo, P. *Journal of Membrane Science* 2009, *343*, 199.

(4) Gan, Q.; Rooney, D.; Zou, Y. *Desalination* 2006, *199*, 535.

(5) Shiflett, M. B.; Niehaus, A. M. S.; Yokozeki, A. *Journal of Physical Chemistry B* 2011, *115*, 3478.

(6) Bara, J. E.; Gabriel, C. J.; Lessmann, S.; Carlisle, T. K.; Finotello, A.; Gin, D. L.; Noble, R. D. *Industrial & Engineering Chemistry Research* 2007, *46*, 5380.

(7) Jiang, Y.; Wu, Y.; Wang, W.; Li, L.; Zhou, Z.; Zhang, Z. *Chinese Journal of Chemical Engineering* 2009, *17*, 594.

(8) Park, Y.-I.; Kim, B.-S.; Byun, Y.-H.; Lee, S.-H.; Lee, E.-W.; Lee, J.-M. *Desalination* 2009, *236*, 342.

(9) Wang, G.; Hou, W.; Xiao, F.; Geng, J.; Wu, Y.; Zhang, Z. *Journal of Chemical and Engineering Data* 2011, *56*, 1125.

Appendix

A1.1 Material presented at conferences

20th Irish Environmental Researchers' Colloquium (ENVIRON 2010), Limerick Institute of technology 17th - 19th February 2010. "*Development of imidazole based ionic liquids to capture and separate CO_2*". (poster)

Leuven Summer School on Ionic Liquids, Katholieke Universiteit Leuven, Belgium. 23rd -27th August 2010. *"Development and Characterisation of Task Specific Ionic Liquids, for the Capture and Separation of CO_2 gas"* (poster)

1st International Conference on Ionic Liquids in Separation and Purification Technology, Sitges, Spain. 4th - 7th September 2011. "*Ionic liquids containing amine functionalities: Potential materials for the capture and separation of carbon dioxide."* (poster)

22nd Irish Environmental Researchers Colloquium (ENVIRON 2012) University College Dublin (UCD). 7th-9th March. *"Novel Ionic Liquids for the Absorption and Sequestration of CO_2"* (Oral Presentation)

64th Irish Universities Chemistry Research Colloquium, University of Limerick, 14th – 15th June 2012. *"Novel Amino Acid based Ionic Liquids and their Potential use in the capture of Anthropogenic Carbon Dioxide"* (poster)

Green Chemistry in Ireland (II), Dublin City University (DCU) 12th July 2012. *"New Approaches, using Ionic Liquids Technology, to the Absorption and Sequestration of CO_2" (Oral Presentation)*

A1.2 Ionic Liquid Structures

Ionic Liquids [9a-11e]

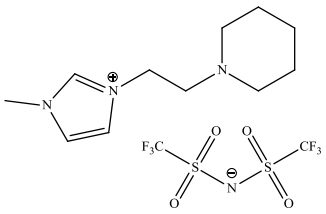

[9a]

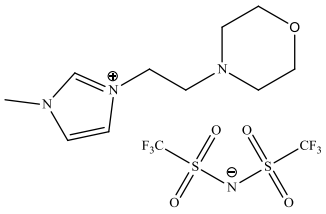

[10a]

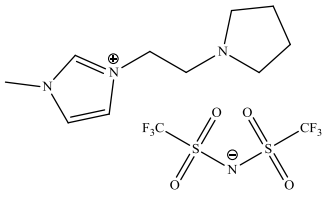

[11a]

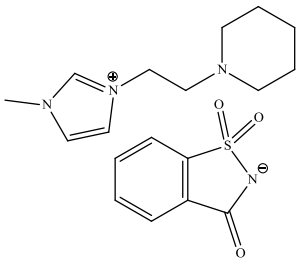

[9b]

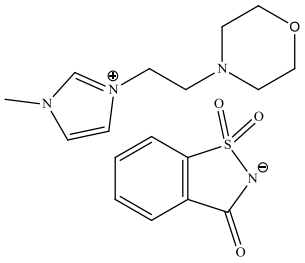

[10b]

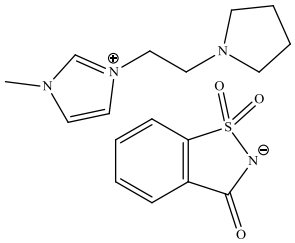

[11b]

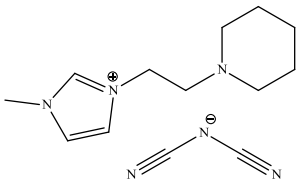

[9c]

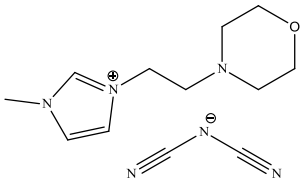

[10c]

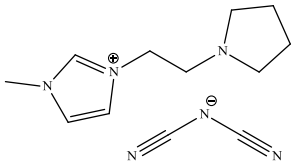

[11c]

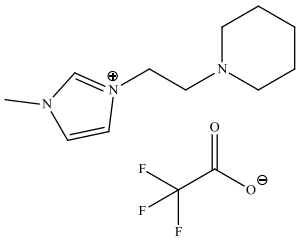

[9d]

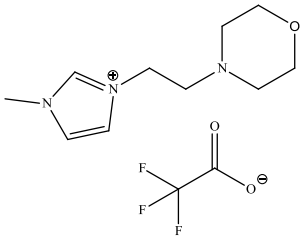

[10d]

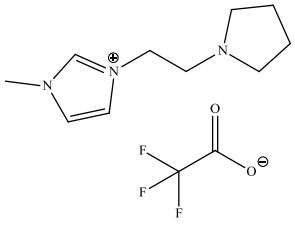

[11d]

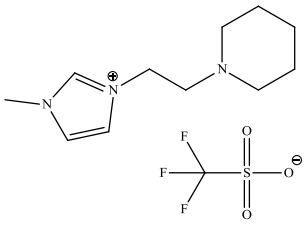

[9e]

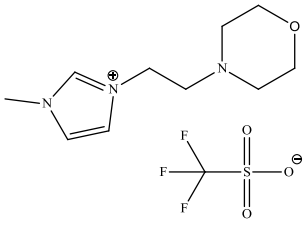

[10e]

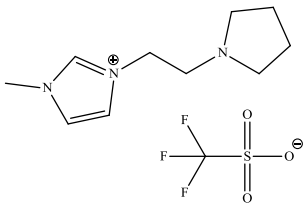

[11e]

Ionic Liquids [AAIL1]-[AAIL21]

[AAIL1] [AAIL2] [AAIL3] [AAIL4] [AAIL5] [AAIL6]

[AAIL7] [AAIL8] [AAIL9] [AAIL10] [AAIL11] [AAIL12]

[AAIL13] [AAIL14] [AAIL15] [AAIL16] [AAIL17] [AAIL18]

[AAIL19] [AAIL20] [AAIL21]